SOX11 interactome analysis: Implication in transcriptional control and neurogenesis

Dissertation

der Mathematisch-Naturwissenschaftlichen Fakultät

der Eberhard Karls Universität Tübingen

zur Erlangung des Grades eines

Doktors der Naturwissenschaften

(Dr. rer. nat.)

vorgelegt von

Birgit Heim, geb.Kick

aus Augsburg

Tübingen

2014

Gedruckt mit Genehmigung der Mathematisch-Naturwissenschaftlichen Fakultät der Eberhard Karls Universität Tübingen.

Tag der mündlichen Qualifikation:	12.02.2015
Dekan:	Prof. Dr. Wolfgang Rosenstiel
1. Berichterstatter:	Prof. Dr. Olaf Rieß
2. Berichterstatter:	Prof. Dr. Marius Ueffing

Für meine Familie

Table of contents

Summary

Somatic stem cells all over the body have the ability to self-renew by mitotic division, which enables the recovery of many tissues from injuries or infections. This is not the case within the adult mammalian brain, where the loss of post-mitotic neurons cannot be compensated. An exception to that is the sustained generation of new neurons from a pool of neural stem cells throughout the adult life. This process, referred to as adult neurogenesis, is restricted to only few areas of the post-natal brain, the neurogenic niches. It is regulated by a complex machinery of extrinsic and intrinsic mechanisms. The intracellular modulation of adult neurogenesis depends on tightly regulated processes, including the SOX family of transcription factors. Particularly, the SOXC factor SOX11 is critically required during neuronal fate commitment and the induction of a neuron-specific gene expression program. Current models suggest that both stem cell maintenance and neuronal differentiation are orchestrated by transcriptional core networks, comprised of biochemically interacting transcription factors, which cooperate on the maintenance and induction of developmental gene expression programs. According to this, the present study aimed to determine the regulatory transcriptional core program of late neuronal differentiation and maturation that defines early neuronal identity. Due to its relevance in neuronal differentiation and induction of immature neuronal gene programs, SOX11 was chosen as bait for the identification of the underlying transcriptional network.

As a prerequisite for the western blot analysis of the protein, SOX11-specific antibodies were established. The SOX11-centered network was obtained by determining SOX11-specific protein interactions in Neuro2a cells, using affinity-based purification coupled to quantitative mass spectrometry. The SOX11 interactome analysis revealed an enrichment of transcriptional modulators, involved in epigenetic mechanisms like chromatin remodelling, co-factors for transcriptional activation and silencing as well as transcription factors. Literature-based curation and GO term analysis yet identified several of the interacting proteins to participate in the regulation of neurogenesis, with respect to the maintenance of neural progenitor characteristics and the progression of neuronal differentiation. Data were further evaluated by establishing a SOX11-centered protein-protein interaction network using the experimentally derived dataset, matched with information from public mouse interaction databases. The network analysis revealed close connections between the single interactors as well as high connectivity and centrality of the

identified proteins. Selected SOX11 interacting proteins were further directed to functional characterisation by reporter assays on the SOX11-regulated immature neuronal markers DCX and Stathmin1. The promoter studies suggested a cooperative role for the SOX11 interacting transcription factors MYT1 and YY1 with SOX11 in the regulation of the investigated promoters. Finally, *in silico* promoter analysis on the regulatory fragments of DCX and Stathmin1 uncovered the presence of adjacent binding sites for MYT1 and SOX11 as well as for YY1 and SOX11 on the DCX promoter and for MYT1 and SOX11 in the Stathmin1 promoter, enabling a cooperative regulation of the early neuronal markers. The genome-wide binding profile revealed furthermore an enrichment of neurogenesis-related promoters in target sequences of MYT1 and SOX11.

Proteomic analysis of the SOX11-centered transcriptional network combined with functional promoter studies revealed new players in the intrinsic modulation of late neurogenesis and uncovered cooperative regulation of the transcription factors MYT1 and YY1 with SOX11 on early neuronal markers. Furthermore, a variety of new candidates for potential contribution in future reprogramming assays from somatic cells into functional neurons were identified.

Zusammenfassung

Somatische Stammzellen können sich durch mitotische Teilung vermehren, was eine Regeneration vieler Gewebe nach Verletzungen oder Infektion ermöglicht. Im adulten Säugerhirn kann der Verlust von post-mitotischen Neuronen jedoch nicht kompensiert werden. Eine Ausnahme bildet die das gesamte erwachsene Leben andauernde Differenzierung von Neuronen aus einem Pool von neuronalen Stammzellen. Dieser Prozess, bezeichnet als adulte Neurogenese, ist auf einige spezielle Bereiche des Gehirns, die neurogenen Nischen beschränkt. Dessen Regulierung unterliegt einer komplexen Maschinerie aus extrinsischen und intrinsischen Mechanismen. Bei den intrazellulären Prozessen der adulten Neurogenese spielen die Proteine aus der Familie der SOX Transkriptionsfaktoren eine entscheidende Rolle. Das SOXC Protein SOX11 stellt einen essentiellen Faktor während der Festlegung des neuronalen Schicksals von Vorläuferzellen und der Initiierung von frühen neuronalen Expressionsprogrammen dar. Aktuelle Modelle deuten darauf hin, dass sowohl die Erhaltung der Stammzelleigenschaften als auch die Differenzierung von zentralen Transkriptionsnetzwerken reguliert werden. Diese bestehen aus interagierenden Transkriptionsfaktoren, welche zusammen Genexpressionsprogramme kontrollieren. Aufgrund dieser Erkenntnisse, wurde die Studie darauf ausgelegt, regulatorische Prozesse der späten neuronalen Differenzierung und Reifung zu identifizieren, welche die frühe neuronale Identität innerhalb der unreifen Neuronen definieren. Durch seine zentrale Bedeutung für die neuronale Differenzierung und die Initiierung der Expression neuronaler Marker, wurde SOX11 als Ausgangspunkt für die Analyse des zu Grunde liegenden Transkriptionsnetzwerks gewählt.

SOX11-spezifische monoklonale Antikörper wurden zur Detektion des Proteins auf Western Blot Ebene generiert und validiert. Das SOX11-assoziierte Transkriptionsnetzwerk wurde durch die Bestimmung des SOX11-Interaktoms in Neuro2a Zellen mithilfe von Affinitätsaufreinigung und quantitativer Massenspektrometrie erstellt. Das identifizierte SOX11-spezifische Interaktom wies eine signifikante Anreicherung von Transkriptionsfaktoren und anderen Regulatoren auf Transkriptionsebene auf. Literaturrecherche und GO Term Analyse verifizierten 2009 #103" ¶ Khalfallah et al.,

bestimmten Daten mit Informationen aus öffentlichen Interaktionsdatenbanken

vervollständigt wurden, zeigt die Interaktionen zwischen den Proteinen, sowie die Konnektivität einzelner Faktoren. Ausgewählte SOX11 Interaktoren wurden mithilfe von Promotorstudien funktionell charakterisiert. Analysiert wurde der Einfluss auf die durch SOX11 aktivierten Promotoren von DCX und Stathmin1, zwei Markerproteine der frühen neuronalen Identität. Zwei Transkriptionsfaktoren, MYT1 und YY1, zeigten einen kooperativen Effekt mit SOX11 auf die Promotoren beider Gene. *In silico* Promotoranalysen für DCX und Stathmin1 ergaben benachbarte Bindungssequenzen sowohl für MYT1 und SOX11, als auch für YY1 und SOX11 innerhalb des DCX Promotors und für MYT1 und SOX11 innerhalb des Stathmin1 Promotors, durch welche die Kooperation der Transkriptionsfaktoren auf den Promotoren ermöglicht wird. Zudem ergab das Genom-weite Bindungsprofil von MYT1 und SOX11 eine Anreicherung von in die Neurogenese involvierten Genen.
Die proteomische Analyse des SOX11-Transkriptionsnetzwerks in Kombination mit funktionellen Promotorstudien identifizierte neue Faktoren, die eine Rolle bei der intrinsischen Modulierung der späten Neurogenese spielen und deckte die kooperative Aktivität von MYT1 und YY1 mit SOX11 in Bezug auf die Regulierung früher neuronaler Markern auf. Zusätzlich wurden einige Kandidaten identifiziert, die möglicherweise Strategien zur Reprogrammierung von somatischen Zellen in funktionelle Neuronen verbessern können und damit einen Beitrag zur regenerativen Medizin leisten.

1. Introduction

During the post-natal and adult life of mammals, somatic stem cells all over the body have the ability to proliferate and self-renew by mitotic division. In this way, many tissues are capable of maintaining function by regeneration to certain extend from injuries, infections, intoxications or environmental pollutions and loss of cells by physiological wear and tear. An exception to that are the neurons within both the central and peripheral nervous system. These regions are not able to recover from neuron loss, caused by genetic or metabolic disorders, inflammatory infections or injuries (Kim et al., 2006). In addition, aging and neurodegenerative diseases like Alzheimer's and Parkinson's disease represent major challenges to the adult central nervous system, as their progression implies neurodegenerative mechanisms in the brain (Bredesen et al., 2006). There are two regions within the post-natal mammalian brain, where different types of neurons are generated from a multipotent and self-renewing neural stem cell population throughout the adult life. The proliferation, migration and differentiation steps of this complex process, referred to as adult neurogenesis, are controlled by extrinsic and intrinsic mechanisms, including growth factors or signalling by neurotransmitters and a tightly regulated transcriptional network (Hsieh, 2012, Zhao et al., 2008). Understanding of the underlying regulatory machinery is of major importance, as the regenerative potential of the multipotent neural stem cell pool could serve as therapeutical basis with respect to the substitution of neurons, which are lost by neurodegenerative diseases or injuries.

1.1. Adult neurogenesis

1.1.1. Adult neural stem cells and neuronal precursor cells

In the post-natal nervous system of the mammalian brain, adult neural stem cells (NSCs) are multipotent, proliferating and self-renewing cells that are able to differentiate into cells of the neural lineage, including neurons, astrocytes and oligodendrocytes (Gage, 2000). While the glial cell population, comprised of astrocytes and oligodendrocytes, provides together with neurons the cellular basis for a functioning nervous system, neurons constitute the functional players that are responsible for signal transmission and formation of a complex, dense and functionally integrated neuronal network. A variety of models aimed to describe the identity and properties of the neural stem cells in the adult brain with different

outcome, suggesting the coexistence of several types of neural stem cells of distinct origins (Lugert et al., 2010). As the stemness of the NSCs has only been shown *in vitro*, but could not be assessed *in vivo* until the year 2011 (Bonaguidi et al., 2011), the term 'neural progenitors' was introduced to subsume proliferating cells that exhibit differentiation potential. These precursor cells can be localized to two distinct areas within the adult mammalian brain where neurogenesis occurs (Zhao et al., 2008). Adjacent to the lateral ventricle surrounding cell layer that consists of non-proliferating ependymal cells, lies the subventricular zone (SVZ) of the lateral ventricle which comprises three different types of progenitor cells, implicated in olfactory bulb-directed neurogenesis (see figure 1A) (Consiglio et al., 2004): type A migrating neuroblasts (Doetsch et al., 1999), type B glial fibrillary acidic protein (GFAP)-positive progenitors and type C transit amplifying cells (Merkle et al., 2007). The second neurogenic area, the subgranular zone (SGZ) of the hippocampal dentate gyrus, includes two types of neural stem cells, exhibiting different molecular markers and cell morphologies (see figure 1B). Quiescent radial glia-like type I precursors feature a long radial process, which traverses the granule cell layer and branches when it reaches the molecular layer. They express Nestin, SRY-related 2 (SOX2) and GFAP. (Fukuda et al., 2003, Garcia et al., 2004, Suh et al., 2007). The second progenitor cell type, which potentially originates from type I cells, displays short dendrites, expresses Nestin and SOX2, but lacks GFAP expression. It is not known, if the three different neural cell types, neurons, astrocytes and oligodendrocytes, arise from the same type of NSCs or from divergent unipotent progenitors, and at which point in time fate decisions are made. Furthermore, it is not clear whether single precursor cells display both self-renewal features and differentiation capacity at the same time. Additionally, the question arises, to what extent the NSCs of the distinct regions SVZ and SGZ exhibit the same intrinsic properties and reveal their diverse characteristics due to their different localisation (Ming and Song, 2011).

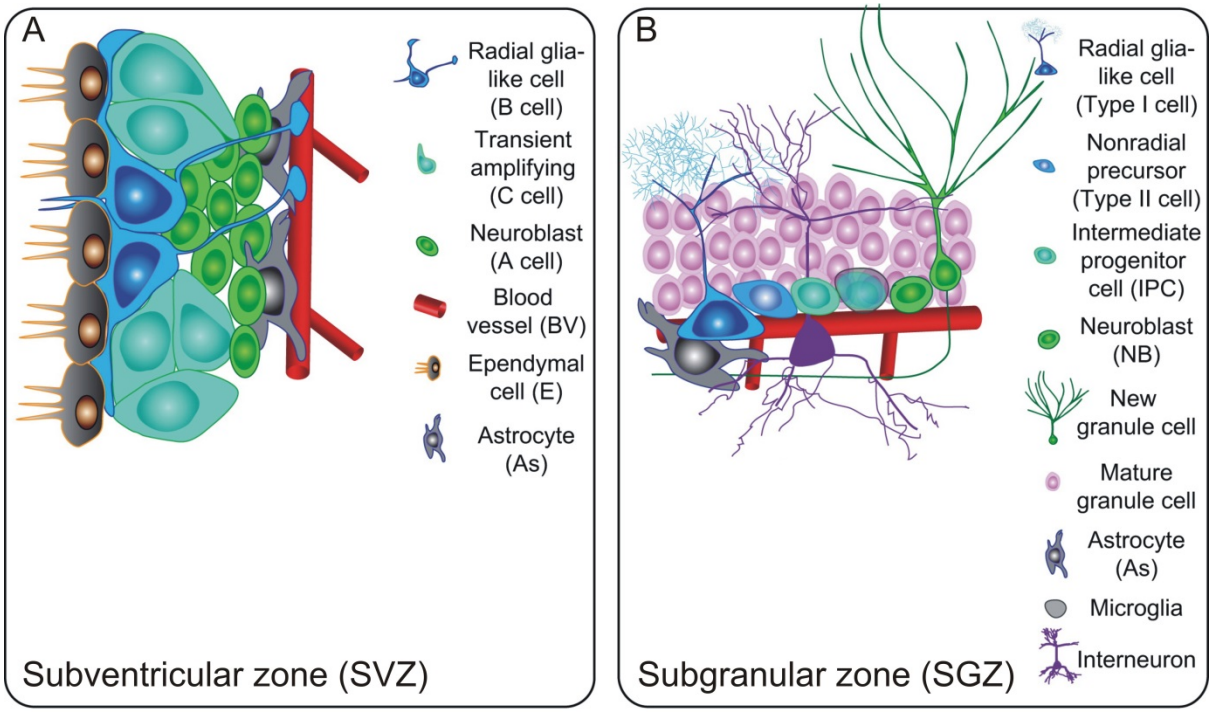

Figure 1: Cell type composition of the subventricular zone and subgranular zone
(A) The subventricular zone (SVZ) is located next to ependymal cells around the lateral ventricle and is composed of type B radial glia-like cells which give rise to type C transient amplifying progenitors that differentiate to type A neuroblasts. They are under the influence of blood vessel- and astrocyte-released factors. (B) In the subgranular zone (SGZ) of the hippocampal dentate gyrus the type I radial glia-like cells and type II nonradial precursors are situated beneath the granule cell layer and are under the control of astrocytes, interneurons, microglia and blood vessels. They differentiate and maturate via the stage of intermediate progenitor cells and neuroblasts into granule neurons.
(Modified and reprinted from Neuron, Volume 70/ Issue 4, Guo-li Ming, Hongjun Song, Adult Neurogenesis in the Mammalian Brain: Significant Answers and Significant Questions, Pages 687–702, Copyright © 2011, with permission from Elsevier)

1.1.2. Neurogenic niches

Microenvironments of the mammalian brain, where the sustained generation of new functional neurons takes place throughout adult life, are referred to as neurogenic niches. Both the subgranular zone (SGZ) of the hippocampal dentate gyrus and the subventricular zone (SVZ) of the lateral ventricle are defined as neurogenic niches, as they possess the essential conditions for the constant differentiation and maturation of neurons from neural stem cells (Doetsch, 2003, Morrison and Spradling, 2008, Palmer et al., 1997) (see figure 2). The generation of adult new-born neurons is restricted to the SVZ and SGZ in the brain. Progenitor cells of the SVZ are situated next to the ependymal cell layer of the lateral ventricles. Neurons originated from the SVZ migrate directly along the rostral migratory stream and are subsequently integrated into the olfactory bulb as granule neurons in the granule cell layer or as periglomerular neurons in the glomerular layer (see figure 2) (Zhao et al.,

2008). Within the SGZ, neuronal precursor cells are located beneath the granule layer, which is composed of mature neurons as well as of new immature neurons. Also astrocytes, oligodendrocytes and different types of mature neurons are located in this area. Hippocampal astrocytes support the differentiation of adult neural stem cells and enable functional integration of the new-born neurons *in vitro* (Song et al., 2002, Zhao et al., 2008).

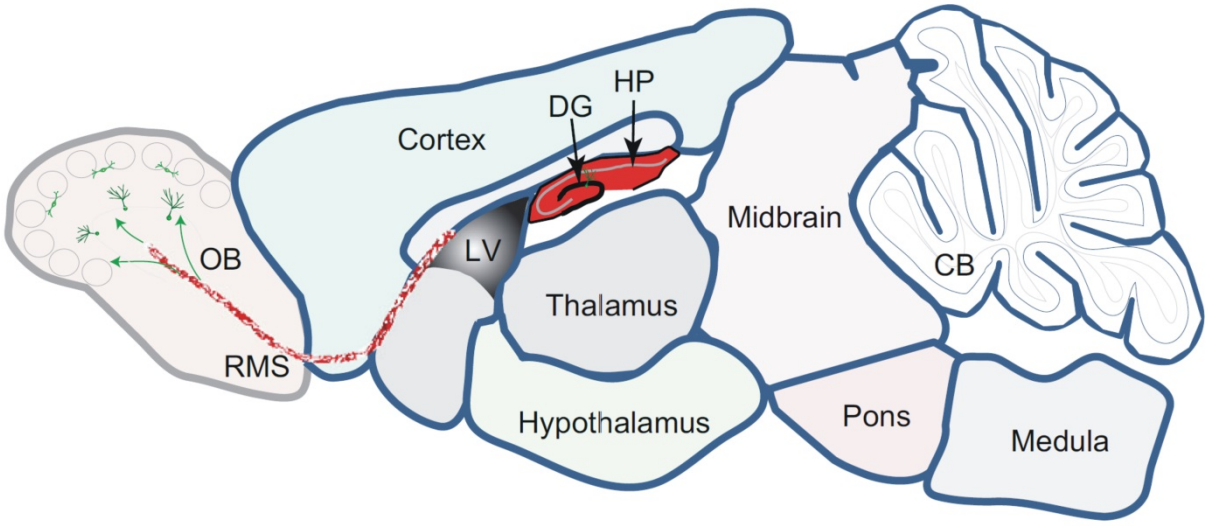

Figure 2:Neurogenic niches in the adult rodent brain
Adult neurogenesis takes places in two neurogenic niches of the rodent brain, the subgranular zone of the dentate gyrus (DG) within the hippocampal formation (HP) and the subventricular zone of the lateral ventricle (LV). Subventricular zone-derived neurons migrate along the rostral migratory stream (RMS) (in red) and are integrated into the olfactory bulb (OB).
(Reprinted from Neuron, Volume 70/ Issue 4, Guo-li Ming, Hongjun Song, Adult Neurogenesis in the Mammalian Brain: Significant Answers and Significant Questions, Pages 687–702, Copyright © 2011, with permission from Elsevier)

1.1.3. Regulation of adult neurogenesis

1.1.3.1. Extrinsic mechanisms

The complex machinery of adult neurogenesis is regulated by a combination of extrinsic and intrinsic signals. Two excellent reviews describe the regulatory processes in detail (Ming and Song, 2011, Zhao et al., 2008). In extracellular signalling, neurotransmitters transferred through the dense integrated neuronal network around the NSCs play an important role. Signals can be received by synaptic contacts directly by the neural progenitors or indirectly by the local surrounding cells (Deisseroth et al., 2004, Nacher and McEwen, 2006, Tozuka et al., 2005). Additionally, growth factors are involved in the extrinsic regulation of

neurogenesis. Well studied examples are epidermal growth factor (EGF) and fibroblast growth factor 2 (FGF2) (Kuhn et al., 1997, Zhao et al., 2007). Furthermore, there are other NPC-influencing mechanisms, including the neurotrophin brain-derived neurotrophic factor (BDNF), which seems to enhance SGZ neurogenesis and to play a role in the survival of new neurons (Duman and Monteggia, 2006). Moreover, adult neurogenesis is mediated by different signalling pathways. Well studied regulatory pathways that are involved are Notch signalling (Imayoshi et al., 2010, Pierfelice et al., 2011) sonic hedgehog (Shh) (Ahn and Joyner, 2005) and Wnt signalling (Lie et al., 2005, Song et al., 2002). Furthermore, several receptors modulate the progression of adult neurogenesis, such as Toll-like receptors (TLR) (Rolls et al., 2007) and receptors of the proinflammatory cytokine Tumor necrosis factor-alpha (TNF-α) (Iosif et al., 2006).

1.1.3.2. Intrinsic mechanisms

The major players in the intracellular regulation of adult neurogenesis are transcription factors and proteins involved in cell cycle control.

Cell cycle inhibitors like p16, p21 and p53 ensure the quiescence of adult neural precursors, thus maintaining the stem cell pool of slowly dividing cells, which is indispensable for sustained neurogenesis throughout lifetime (Gil-Perotin et al., 2006, Kippin et al., 2005, Molofsky et al., 2006).

The intrinsic regulatory mechanisms of both self-renewal maintenance and neuronal differentiation are based on a variety of transcription factors, which are connected in regulatory networks to control gene expression programs. The regulation is dependent on the distinct spatiotemporal expression of the particular transcriptional modulators, which is important for their sequential action (see expression in grey boxes in figure 3 and 4). Furthermore, the activity of transcription factors is based on the interaction with other factors. There is rising evidence that both stem cell maintenance and neuronal differentiation are orchestrated by transcriptional core networks, comprised of biochemically interacting transcription factors, which cooperate on the maintenance and induction of developmental gene expression programs (Chen et al., 2008, Hobert, 2011). Nevertheless, the underlying mechanisms remain to be fully elucidated.

The orphan nuclear receptor TLX, which is expressed in many areas of the adult brain, is implicated in sustaining the undifferentiated state and proliferation capacity

of neural precursors (Shi et al., 2004). SOX2 is a key regulator in maintaining the progenitor pool of NPCs, including multipotency and self-renewal properties (Suh et al., 2007), mediated by the Notch/RBPJK signalling pathway (Ehm et al., 2010). This transcription factor seems to modulate also Shh signalling, which is critically required for NPC maintenance (Favaro et al., 2009). Additionally, SOX2 is involved in the regulation of TLX expression (Shimozaki et al., 2011). Moreover, the transcription factors of the FOXO family (Paik et al., 2009) as well as OLIG2 (Hack et al., 2005) and the RE1 silencing transcription factor (REST), which is responsible for silencing of neuronal gene expression in ES cells (Ballas et al., 2005, Gao et al., 2011) are involved in the preservation of the undifferentiated state and maintenance of the quiescent NSC pool.

Another central mechanism to be regulated during adult neurogenesis is the neuronal fate commitment of NPCs, followed by the differentiation and maturation into functional neurons. This implicates a variety of transcription factors, including paired box protein PAX6 and homeobox protein DLX-2 (Doetsch et al., 2002, Hack et al., 2005).

The maturation and survival of newborn neurons is controlled by other factors, such as the transcription factor cAMP response element-binding protein CREB (Jagasia et al., 2009), forkhead box protein G1 (FOXG1) (Shen et al., 2006) as well as the maturation promoting proteins homeobox factor PROX1 (Karalay et al., 2011, Lavado et al., 2010) and Kruppel-like factor 9 (KLF-9) (Scobie et al., 2009).

Moreover, proneural basic helix-loop-helix transcription (bHLH) factors have important roles in the modulation of neurogenesis, like Neurogenin2 (NGN2) that is expressed in amplifying progenitors and is involved in fate specification (Ozen et al., 2007, Roybon et al., 2010). Neurogenic differentiation factor 1 (NEUROD1) controls late maturation and survival of new-born neurons (Gao et al., 2009)

Critically required for the control of neural differentiation are the SOXC transcription factors SOX4 and SOX11. They are expressed in progenitors within neurogenic niches during early neural fate commitment and promote neuronal differentiation of NPCs *in vitro*. Furthermore, they induce the activation of neuron-specific expression programs (Bergsland et al., 2006, Haslinger et al., 2009, Mu et al., 2012).

Also other intrinsic mechanisms can influence the early events of neural differentiation, as LINE-1 transposons are found to insert into neuronal precursor

cells, resulting in an expression change in neural genes and neuronal somatic mosaicism (Muotri et al., 2005).

1.1.3.3. Epigenetic regulation

In addition to the molecular players, also epigenetic regulation is implicated in the modulation of adult neurogenesis, including the following different mechanisms: DNA methylation and histone modification through the Polycomb (PcG) and Trithorax (TrxG) complexes, ATP-dependent chromatin remodelling, histone deacetylation and acetylation, neuron-restrictive silencing factor (NRSF/REST)-mediated gene regulation and non-coding RNAs (Sun et al., 2011). A prominent example is methyl-CpG-binding domain protein 1 (MBD1), a modulator of DNA methylation that is involved in FGF signalling by regulating the FGF2 promoter, a growth factor supporting adult neurogenesis in NPCs. Thus it controls the balance between proliferation and differentiation (Li et al., 2008). The H3K4 methyltransferase mixed-lineage leukemia 1 (MLL1), a member of the TrxG chromatin remodelling complex, regulates DLX2 expression and in this way induces neuronal differentiation (Lim et al., 2009). Also the PcG complex modulates adult neurogenesis as its component BMI-1 maintains precursor cell properties through the cell cycle inhibitor p16 (Molofsky et al., 2005). In multipotent NPCs, the promoters of NGN2, NEUROD1, NEUROD2, SOX4, and SOX11 are silenced through PcG-mediated repression. In later stages, during neuronal differentiation and maturation, by contrast, SOX2 expression is impaired epigenetically by PcG (Mohn et al., 2008). Notably, Methyl-CpG-binding protein 2 (MECP2) binds and represses the activity of the Brain-derived neurotrophic factor (BNDF) promoter, which plays a role in NPC self-renewal control (Martinowich et al., 2003). Additionally, some microRNAs contribute to the fine-tuning of adult neurogenesis. MiR137 for example is co-regulated by MECP2 and SOX2 and exerts influence on the proliferation and differentiation of NPCs (Szulwach et al., 2010).

1.1.4. Development and functional integration of new-born neurons

In the neurogenic SVZ of the adult rodent brain, the quiescent periventricular astrocytes or radial glia-like cells (B cells) get activated to divide into transit amplifying cells (C cells), which in turn differentiate into neuroblasts (A cells) (Doetsch et al., 1999). These immature neurons migrate towards the olfactory bulb through the rostral migratory stream (RMS) (see figure 3). They are not guided by radial glia or axon fibers like in the developing brain, but migrate tangentially in chains associated with each other, also referred to as chain migration, bordered by a structural network of specialised astrocytes (Lois et al., 1996). When they reach the olfactory bulb, after migration for up to 5mm along the RMS, the neuroblasts turn radially away from the path to enter the adjacent cell layers, where they differentiate into two different types of interneurons, namely granule neurons and periglomerular neurons (Alvarez-Buylla and Garcia-Verdugo, 2002) (see figure 3).

Chain migration is based on cell-cell adhesion, dependent on the polysialated neural cell adhesion molecule (PSA-NCAM) (Bonfanti and Theodosis, 1994, Hu et al., 1996). It is additionally mediated by Slit/Robo-signalling, with SLIT 1 and SLIT2 being expressed in the SVZ and the septum and repel the neuroblasts (Wu et al., 1999). The Ephrin-B family of proteins, Beta 1 integrins and receptor tyrosine kinase ERBB4, are also involved in the direction of new-born neurons to their destination (Anton et al., 2004, Conover et al., 2000, Jacques et al., 1998). Besides, the extracellular matrix protein Reelin is crucial for the coordination of chain migrating neuroblasts (Zhao et al., 2007).

As they reach their final destination, the maturating cells integrate into existing circuits. Initially they receive GABA inputs, before they form glutamate receptors and dendritic spines. (Saghatelyan et al., 2005).

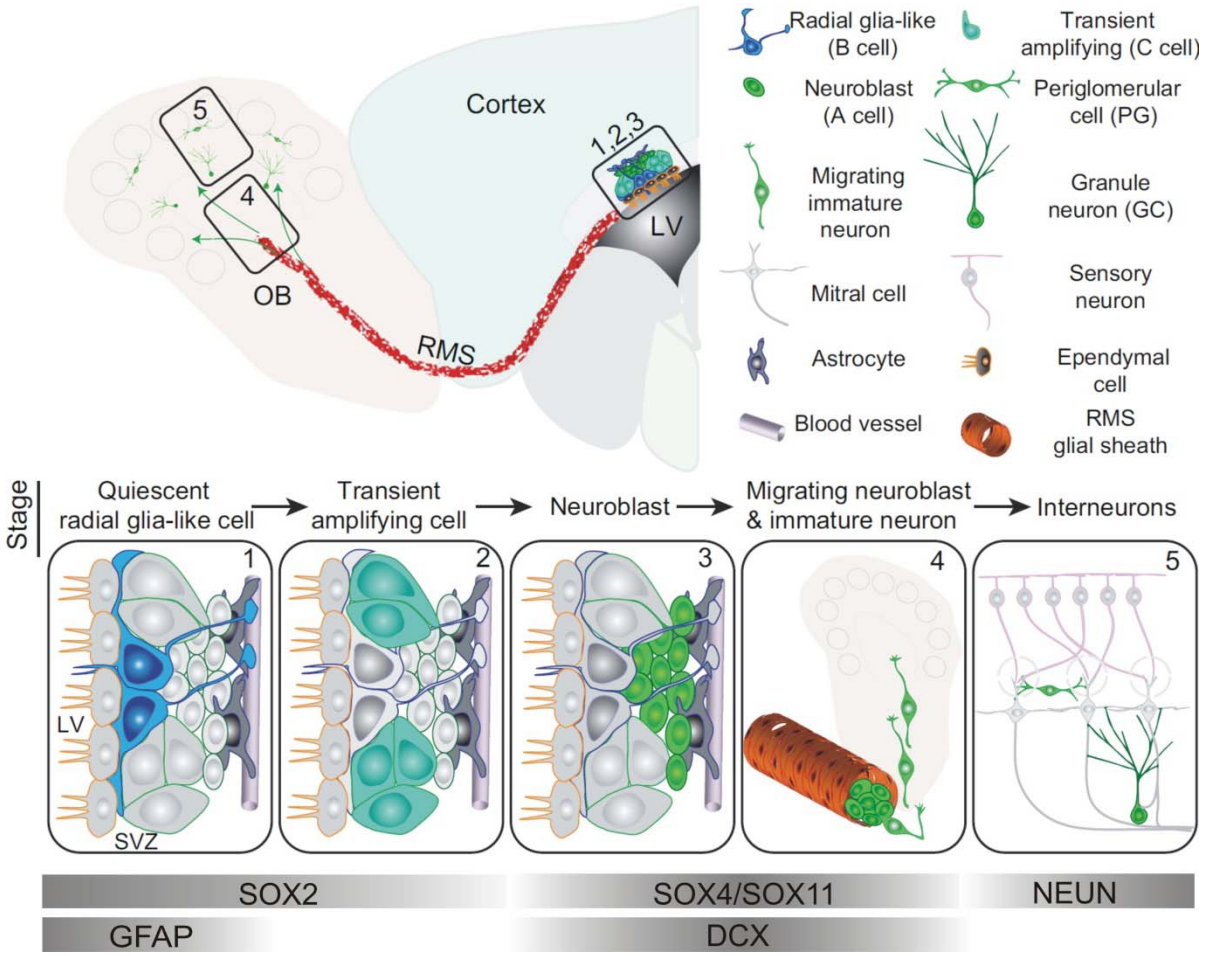

Figure 3:Neurogenesis in the subventricular zone and migration towards the olfactory bulb
Rarely dividing glia-like precursor cells (1) give rise to transient amplifying cells (2) which differentiate into neuroblasts (3). These in turn migrate along the rostral migratory stream (RMS) towards the olfactory bulb (OB) (4), where they differentiate into the distinct interneurons granule cells and periglomerular cells (5). The temporal expression of major intrinsic regulatory transcription factors is depicted in grey boxes.
(Modified and reprinted from Neuron, Volume 70/ Issue 4, Guo-li Ming, Hongjun Song, Adult Neurogenesis in the Mammalian Brain: Significant Answers and Significant Questions, Pages 687–702, Copyright © 2011, with permission from Elsevier)

In the hippocampal SGZ of the dentate gyrus, quiescent neural stem cells get activated to rapidly proliferating progenitors that are committed to neuronal fate and maturate via neuroblasts and immature neurons into granule neurons. In the course of this, they migrate from the SGZ the short range into the granular zone, project their dendrites into the molecular layer and integrate into the existing neuronal circuity (see figure 4) (Zhao et al., 2006). Disrupted-in-schizophrenia (DISC1) may be involved in directing the new-born neurons, as decreased levels of DISC1 result in mispositioning to other cell layers (Duan et al., 2007). Other guidance molecules may additionally regulate the migration, like the Reelin pathway that seems to direct not only SVZ-derived neuroblasts, but also hippocampal neuronal migration (Gong et al., 2007).

Initially, the new-born neurons become depolarised in response to GABA. The depolarisation switches to hyperpolarisation after 2-4 weeks, at the same time dendritic spines develop and glutamatergic responses are initiated. Long-term potentiation can be induced more easily at this stage, than in mature neurons. These mechanisms facilitate synaptic plasticity, which may play a role in the formation of new memories (Ge et al., 2007, Schmidt-Hieber et al., 2004). The maturation is not finished yet, even if the cells already possess many characteristics of mature neurons (Zhao et al., 2006). At the age of 4 weeks they are more likely to be integrated into circuits that support spatial memory, than existing granule neurons (Kee et al., 2007, Marin-Burgin et al., 2012). After 8 weeks, the density of mushroom shaped spines increase. Spine formation and integration into the neuronal network is under the control of DISC1 (Duan et al., 2007). Now, the maturating neurons receive comparable glutamatergic and GABAergic input as mature granule cells do (Laplagne et al., 2007).

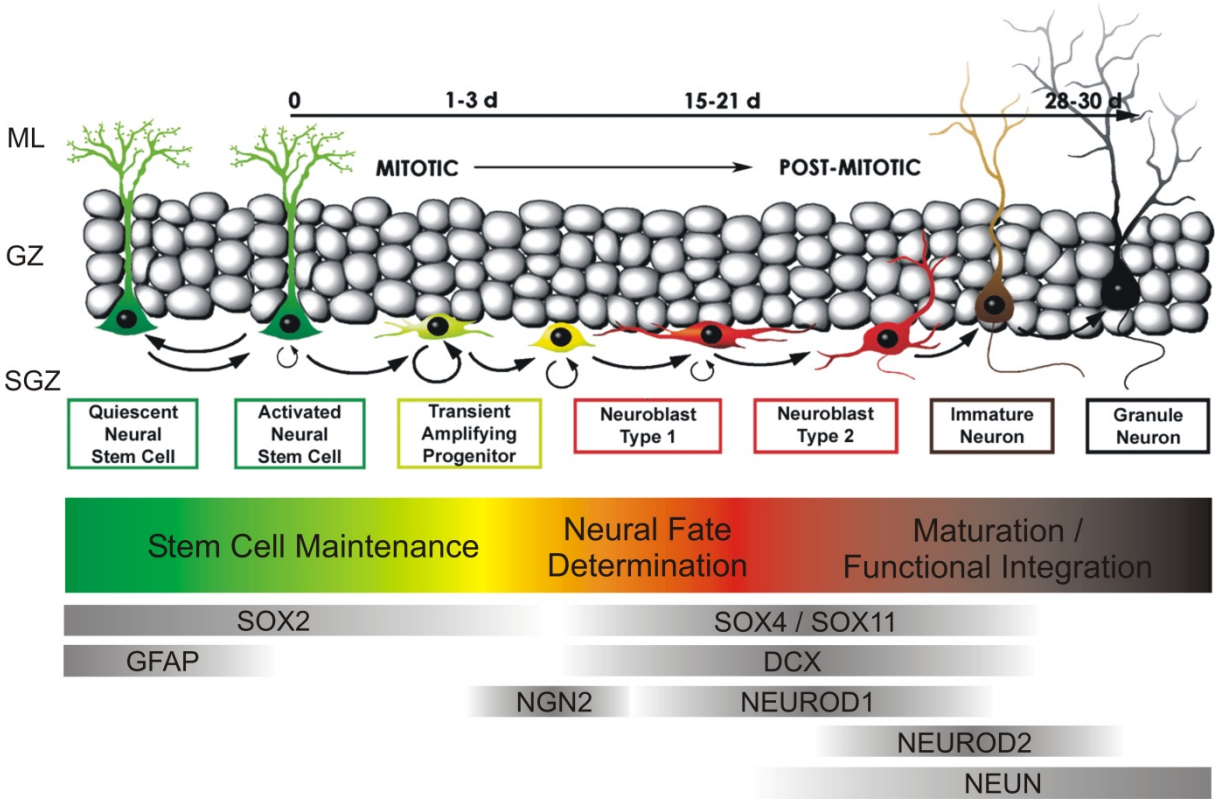

Figure 4:Adult neurogenesis in the hippocampal dentate gyrus
Rarely dividing neural stem cells (type-I cells) get activated to rapidly proliferating progenitors (type-II cells) and are committed to neuronal fate. While migrating from the subgranular zone (SGZ) of the dentate gyrus to the granular zone (GZ), they develop into mature neurons and project their dendrites into the molecular layer (ML). The temporal expression of major intrinsic regulatory transcription factors is depicted in grey boxes.
(Modified from Encinas et al., 2006, Fluoxetine targets early progenitor cells in the adult brain, Proc Natl Acad Sci USA 103 (21), 8233-8238 (Encinas et al., 2006) reprinted with permission of PNAS. Copyright (2006) National Academy of Sciences, U.S.A.

1.1.5. Function of adult neurogenesis

1.1.5.1. SVZ-derived neurons and olfaction

Subventricular neurogenesis is supposed to play a role in olfaction, as the newly generated neurons migrate to the olfactory bulb. This is supported by the fact that several mechanisms implicated in the regulation of SVZ neuronal differentiation and migration are associated with the olfactory sensory system. It was found, that olfactory experience of animals modulates adult neurogenesis. Odour deprivation inhibits maturation in terms of reduced spine length and density as well as survival of new-born neurons in the olfactory bulb. Moreover, for 2-4 week old neurons, sensory activity is a crucial factor for their survival (Petreanu and Alvarez-Buylla, 2002). A reduced population of new-born interneurons results in turn in a loss of odour discrimination (Gheusi et al., 2000). In coincidence with that, mice that learned an odour discrimination task, exhibited more 3 week old interneurons (Alonso et al., 2006). Additionally, enriched odour exposure increases the number of newly generated neurons from the SVZ and enhances olfactory memory (Rochefort et al., 2002). Also the diminished SVZ neurogenesis in aging mice, which results in impaired odour fine discrimination, supports the implication of the olfactory bulb new-born neurons in olfaction (Enwere et al., 2004).

1.1.5.2. Hippocampal neurogenesis and learning and memory, stress and depression

Due to the differential connectivity of the hippocampus along the dorsal-ventral axis, it is functionally divided into two sub regions. The dorsal hippocampus is supposed to play a crucial role in learning and memory, especially spatial learning, whereas the ventral hippocampus may be implicated in emotional regulation like anxiety-related behaviours (Bannerman et al., 2004). Notably, hippocampus-mediated learning events are key regulators of hippocampal neurogenesis as they enhance the differentiation into new neurons (Gould et al., 1999). In more detail, spatial navigation learning ensures survival of 1 week old SGZ-derived immature neurons that already formed GABAergic synapses with the surrounding neuronal network. They enter the hyper-excitable stage, which enables their implication in memory formation, whereas more immature neurons are subjected to cell death and precursor cell proliferation is induced (Dupret et al., 2007). This suggests a selective control by the process of

learning concerning the survival and removal of distinct mature neurons, dependent on the required functions. In general, exposure to an enriched environment increases the rate of neurogenesis and survival of new-born neurons of certain maturities (Tashiro et al., 2007). Additionally, it improves ability of learning and long-term memory as well as object recognition (Bruel-Jungerman et al., 2005). There is rising evidence, that physical exercises like running supports cognition and other brain functions (Hillman et al., 2008). In coincidence with that, voluntary running is found to enhance proliferation of hippocampal NPCs and increases the success in learning tasks (van Praag et al., 1999).

Moreover, hippocampal adult neurogenesis is influenced by stress and depression. In the brain, psychosocial stress initiates the release of hypothalamic corticotropin-releasing factor (CRF) that results in secretion of adrenocorticotropic hormone (ACTH). ACTH is turn induces the release of glucocorticoids, which implicate a reduced hippocampal volume as well as impaired dendritic arborisation and neurogenesis (Dranovsky and Hen, 2006, McEwen, 2001). Furthermore, major depressive disorder (MDD) is associated with reduced hippocampus size, supporting the influence of depression on adult SGZ neurogenesis (Videbech and Ravnkilde, 2004). In coincidence with that, the treatment with different antidepressants, such as serotonin reuptake inhibitors (SRI), tricyclic antidepressants (TCAs), monoamine oxidase inhibitors and electroconvulsive therapy (ECT) increases hippocampal neurogenesis (reviewed in (Duman, 2004))

1.1.6. Influence on CNS disorders

Compared to rodents, in humans, adult neurogenesis takes place in the SGZ and potentially in the SVZ (Curtis et al., 2007, Eriksson et al., 1998, Spalding et al., 2013). A magnetic resonance spectroscopy-based method was developed to enable the observation of neural progenitors and developing neurons in the living human brain (Manganas et al., 2007). Thus, human patients and mouse models contribute to the understanding of the implication of adult neurogenesis in disorders affecting the central nervous system.

Seizure, being the hallmark of epilepsy, is known to induce neurogenesis in both neurogenic niches, the SVZ and SGZ. As the disorder leads to cognitive effects, the focus is laid on hippocampal neurogenesis. Up to 5 weeks lasts the seizure-

dependent elevation of SGZ neurogenesis until it declines to a normal level, which induces proliferation of both progenitors and neuroblasts. Seizure-induced neurons display abnormal dendrite morphology and migration. Even neurons born before seizure activity are influenced to develop mossy fibre sprouting. The aberrant neurons yet integrate functionally into the neuronal circuity, despite their abnormal morphology. Seizure-induced neurogenesis can be inhibited by the antiepileptic drug VPA, which also increases the performance of rats in learning tasks (Jessberger et al., 2007, Walter et al., 2007). Nevertheless, the role of seizure-dependent abnormal neurogenesis in epilepsy is not completely understood until now.

In animal models, it was shown that after ischemic stroke neurogenesis is promoted in the germinal niches SVZ and SGZ. As a consequence, new-born neurons are recruited and migrate to the site of injury, guided by blood vessels. The mobilised neurons express the neuronal markers of the cells destroyed in the injured region and thus contribute to the self-repair of the brain after stroke insult (Arvidsson et al., 2002). However, the positive restorative effect of the new-born neurons is not sufficient to completely restore brain damage due to a limited number of generated neurons, the transient migration to the injury and an insufficient integration into the local circuities (Thored et al., 2007). Moreover, a portion of the stroke-induced new neurons display morphological abnormalities and integrate aberrantly into the neuronal network (Niv et al., 2012). The injection of NPCs from the adult brain into stroke-damaged regions already helped to restore brain function in mice (Bacigaluppi et al., 2009). The adaption of the cells to the microenvironment, their integration and positive influence on the homeostasis by secretion of specific factors and impact on the immune response (Pluchino and Cossetti, 2013) renders them to promising candidates for the regenerative therapy after stroke.

The implication of adult neurogenesis in neurodegenerative diseases is to date not fully elucidated. Mouse models overexpressing wildtype α-Synuclein, a protein that accumulates in Parkinson's disease, dementia with Lewy bodies and multiple system atrophy, demonstrated a reduced survival of new neurons from the SVZ and SGZ, but proliferation was not altered. In contrast, mutant α-Synuclein led to decreased proliferation of NPCs in the SVZ (Winner et al., 2008). Alzheimer's disease is an age-related disorder, characterised by a damage of brain regions involved in learning and memory (Price et al., 1986). As the hippocampus plays an important role in these aspects and ageing is known to be associated with a markedly decreased level of

adult neurogenesis (Kuhn et al., 1996), the decline of new-born neurons may be implicated in the pathogenesis of Alzheimer's disease. One of the disorder's hallmarks is the formation of senile plaques, containing amyloid-β (Aβ) peptide (Price et al., 1986). Mouse models, overexpressing variants of this protein were generated, which resulted in the amyloid pathology phenotype. Interestingly, the short-term proliferation and differentiation of hippocampal NPCs was not affected, but the long-term survival of the new-born neurons was severely impaired. In consequence, the diminished regeneration of neurons caused by the protein plaques during adult life might contribute to the disease progression (Verret et al., 2007). Furthermore, Aβ-induced imbalances in GABA- and glutamatergic neurotransmission may play a role in the reduction of hippocampal neurogenesis (Li et al., 2009, Sun et al., 2009).

1.2. Immature neuronal markers DCX and STMN1

The microtubule-associated protein Doublecortin (DCX) is involved in the stabilization of microtubules and induces their bundling (Horesh et al., 1999). Initially, DCX was identified through its association with X-linked lissencephaly, a severe brain malformation, affecting mainly males, which is characterised by abnormal cortical lamination and classified as a neuronal migration disorder, which is caused by mutations in the DCX gene (Barth, 1987, des Portes et al., 1998, des Portes et al., 1997). Additionally, mutant DCX was found to be the major cause of another cortical disorder, subcortical laminar heterotopia (SCLH), marked by a heterotopic layer of misplaced neurons (des Portes et al., 1998, Pinard et al., 1994).

The protein was identified to be expressed during corticogenesis in cell bodies and leading processes of migrating neurons as well as in axons of differentiating neurons (Francis et al., 1999). DCX expression was furthermore identified in neuronally committed progenitors and early new-born neuroblasts, aroused from the adult SVZ and SGZ that decreases upon the occurrence of mature neuronal markers. Based on its expression profile, the microtubule-associated protein is considered as one of the earliest markers for immature neurons that are generated in the neurogenic niches of the lateral ventricle and dentate gyrus during adult neurogenesis (Brown et al., 2003). Also on the genetic level, the marker protein was studied. The *DCX*-regulatory region, composed of a 3.5-kb fragment upstream of the ATG start codon was identified. This fragment displayed activity in cultured neuronal precursor cells that

overlapped with endogenous DCX expression as well as with the early neuronal markers βIII-tubulin and microtubule-related MAP2. However, neurogenesis-associated growth factors didn't appear to influence the regulatory region. The regulators of the *DCX* promoter, which comprises binding sites for various transcription factors related to neurogenesis, like the proneural factor NEUROD1, thus remained unknown (Karl et al., 2005). Recently, the promoter has been shown to be under the control of the SOXC proteins SOX11 and SOX4 in reporter assays using the above-mentioned *DCX* regulatory element coupled to luciferase as reporter gene (Mu et al., 2012).

Microtubule dynamics are known to play a role in neuronal differentiation (Poulain and Sobel, 2010) and migration during cortical development (Jaglin and Chelly, 2009). This importance in the regulation of neurogenesis is furthermore underlined by the characteristics of another microtubule-associated protein, Stathmin1 (STMN1). The complete Stathmin family of microtubule-binding proteins is expressed in the early postnatal developing brain (Amat et al., 1991, Curmi et al., 1999). Whereas Stathmin2-4 are continuously down-regulated during development, Stathmin1 is still present in the adult brain. Considerable high expression levels of the protein are detected in the neurogenic niches of the lateral ventricle and hippocampal dentate gyrus as well as in migration pathways (Camoletto et al., 2001, Jin et al., 2004). The expression pattern resembles the presence of DCX in these niches. Knockout of either Stathmin1 or DCX in rats led to an inhibition of the neuronal chain migration of neuroblasts generated in the SVZ along the rostral migratory stream towards the olfactory bulb, indicating pivotal roles for both microtubule-associated proteins in the migration of new-born neurons to their final destination regions (Jin et al., 2004). Also in the SGZ of the dentate gyrus, Stathmin1 is expressed in neuroblasts and immature granule neurons, pointing to its relevance as early neuronal marker. It might be involved in the migration of new-born neurons as well as in the regulation of neural precursor differentiation into young neurons and maintenance of neuronal cell types (Boekhoorn et al., 2014). Moreover, Stathmin1 was recently identified as putative direct transcriptional target of the transcription factor SOX11 (K. Doberauer, J. v. Wittgenstein, D.C. Lie, unpublished data).

1.3. The SOX transcription factors

1.3.1. Characteristics of SOX proteins

The large SOX (SRY-related HMG box) family of proteins are transcription factors, which contain a specific DNA binding domain, called high mobility group (HMG) box (Laudet et al., 1993). The superordinated HMG box superfamily is divided into 2 subgroups. Members of the TCF/SOX/MATA group comprise single sequence-specific HMG domains while members of the HMG/UBF consist of multiple HMG domains that possess a general affinity for the binding to DNA sequences. Through their special way of binding, where the three alpha helices of the HMG box attach to the minor groove of the DNA, the members of the TCF/SOX/MATA group induce a bending of the DNA of 80° to 135°. As this brings regulatory regions on the DNA into close proximity and enables gene activation by interaction of bound transcription factors, the SOX proteins are designated as architectural transcription factors (Connor et al., 1994, Grosschedl et al., 1994, van de Wetering and Clevers, 1992). The SOX family name giving Sex-determining region Y (SRY) gene, which is responsible for male sex determination, was the first identified and characterised member of the family (Gubbay et al., 1990). The HMG box amino acid composition of each SOX family member is supposed to be at least 50% identical to the corresponding domain of the SRY protein. The 20 until now identified SOX proteins are development-regulating transcription factors, divided into subgroups A-H, according to the similarity of their HMG box regions (see figure 5) (Bowles et al., 2000, Schepers et al., 2002). Due to their binding to only slightly differing DNA consensus sequences, the SOX proteins have to be specifically activated by the interaction with other proteins, that enable the discrimination of their targets and lead to cooperative regulation of cell-specific gene expression programs (Kamachi et al., 2000). Additional to their DNA-binding domain, the transcription factors comprise subtype-specific domain structures (see figure 5).

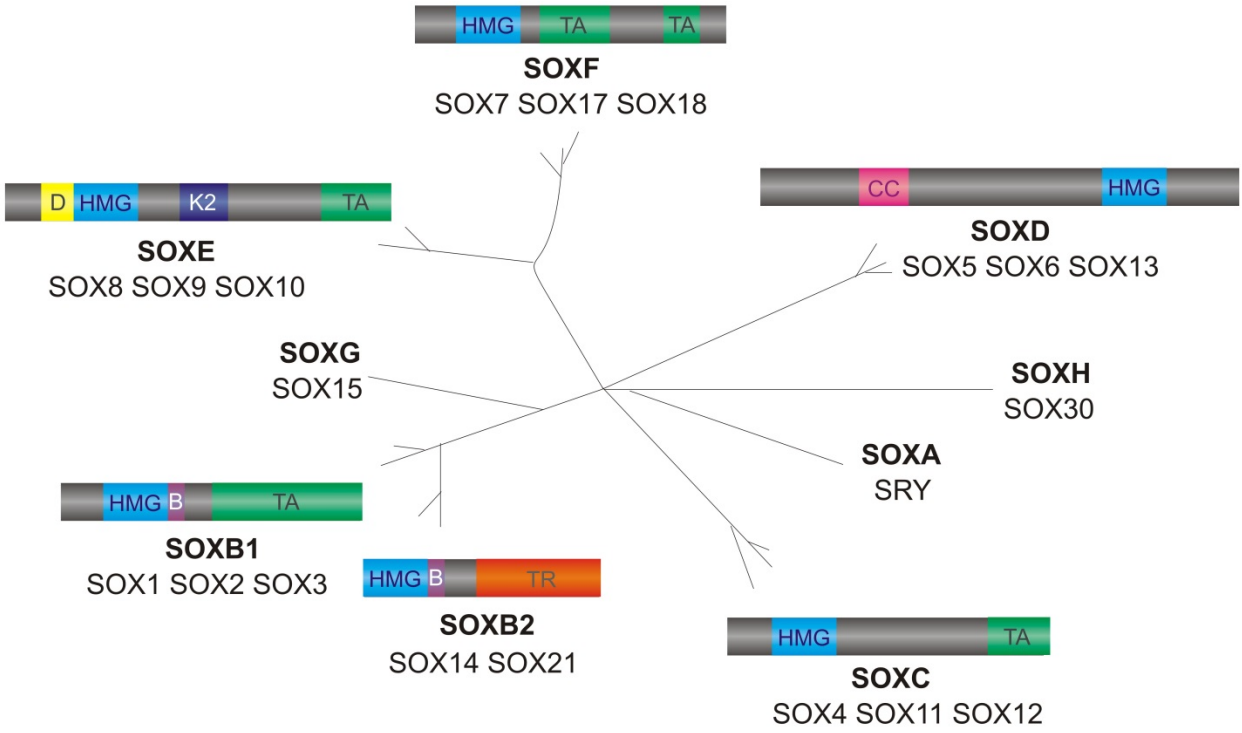

Figure 5:Phylogenetic relationship and domain structure of SOX subgroups
SOX subgroups A-H, classified by the similarity of their HMG box region and domain structure, are illustrated as a tree. The different groups possess specific trans-activation (TA), trans-repression (TR), coiled-coil (CC), dimerization (D), protein-interaction (K2) or group B homology domains.

SRY is the only member of the SOXA group. The SOXB subgroup comprises a characteristic group B homology domain directly after the HMG box. Based on the modulating effect of the C-terminal protein domain on gene expression, this group is further subdivided. The SOXB1 proteins SOX1, SOX2 and SOX3 possess trans-activating function whereas the subgroup SOXB2, with the members SOX14 and SOX21, reveal trans-repressing function (Sandberg et al., 2005). A C-terminal trans-activation domain is the characteristic of the SOXC subgroup that consists of SOX4, SOX11 and SOX12. (Dy et al., 2008, Hoser et al., 2008). The SOXD members SOX5, SOX6 and SOX13 homo- or heterodimerise with other SOXD proteins through their coiled-coil domain (Lefebvre, 2010). SOX8, SOX9 and SOX10 represent the group of SOXE proteins and share an N-terminal dimerization domain prior to the HMG box, which enables cooperative DNA-binding. Members of this subgroup exhibit furthermore a protein-protein interaction domain and a C-terminal trans-activation domain (Wegner, 1999). Interestingly, they bind as monomers or dimers to DNA sequences depending on different cellular contexts (Schlierf et al., 2002). The SOXF group, composed of SOX7, SOX17 and SOX18, includes two domains responsible for trans-activation (Francois et al., 2010). SOXG and H have with SOX15 or SOX30 only one subgroup member.

1.3.2. Functional implications of SOX proteins in the nervous system

1.3.2.1. Functions in the peripheral nervous system

Besides the functions of SOX transcription factors within the nervous system, they also exert influence on other developmental mechanisms. These include sex determination (Connor et al., 1995, Gubbay et al., 1990, Hacker et al., 1995, Kent et al., 1996, Koopman et al., 1990, Morais da Silva et al., 1996), lens development (Kamachi et al., 1998, Nishiguchi et al., 1998), chondrogenesis (Lefebvre, 2010, Smits et al., 2001, Wagner et al., 1994) and haematopoiesis (Dumitriu et al., 2006, Lefebvre, 2010, Liber et al., 2010, Schilham et al., 1997, Urbanek et al., 1994, Yi et al., 2006).

The best investigated system, where different SOX transcription factors have various functions, is the nervous system. Besides the central nervous system (CNS), some of the proteins are implicated in the development of the peripheral nervous system (PNS). Peripheral ganglia of the autonomous nervous system are derived from neural crest cells. SOX10 is expressed in these neural crest cells from the beginning of their appearance and is also present in sensory, sympathetic and enteric ganglia as well as along nerves of the Schwann cell lineage. Whereas the expression in the enteric system is temporary, the other parts of the peripheral nervous system express the transcription factor until the adult stage, where it is then limited to macroglia (Kuhlbrodt et al., 1998). Mutations in SOX10, rendering the protein functionally inactive, lead to a neural crest phenotype, accompanied by neuron and glia loss in the PNS as well as the complete absence of the enteric nervous system, classifying the transcription factor as indispensable for the PNS development (Southard-Smith et al., 1998). Heterozygous mutations of SOX10 are also detected in patients suffering from Waardenburg-Hirschsprung disease, characterised by a congenital aganglionic megacolon combined with distinct pigmentation defects and deafness (Kuhlbrodt et al., 1998, Pingault et al., 1998). In summary, this points to a role for SOX10 in early neural crest development. Also proteins of the SOXC subgroup are involved in the sympathetic nervous system formation. SOX11 promotes the proliferation of tyrosine hydroxylase expressing cells in sympathetic ganglia, whereas SOX4 is required for the cells' survival. Knockout studies in mice confirmed this, as they revealed deficiencies in proliferation and survival in the sympathetic ganglia upon SOX4/11 depletion (Potzner et al., 2010). In addition,

SOX11 knockout leads to impaired survival of sensory neurons in trigeminal and sensory ganglia (Lin et al., 2011). In *Xenopus laevis* and *Petromyzon marinus*, the implication of the SOXC proteins even in early neural crest differentiation is shown (Uy et al., 2014). SOX11 is also implicated in nerve regeneration in the PNS, through activation of the regeneration-associated SPRR1A (Jing et al., 2011).

1.3.2.2. Functions in the central nervous system

1.3.2.2.1. Embryonic neurogenesis

One characteristic of ES cells is the open chromatin state with a loose association of DNA to histones. This is mediated by the chromatin remodelling factor CHD1 and enables low expression levels of genes that are specifically expressed in defined tissues in later stages (Gaspar-Maia et al., 2009, Guenther et al., 2007, Meshorer et al., 2006). Enhancers and promoters of these genes are positioned in non-methylated accessible parts of the DNA and feature a bivalent structure. This includes active chromatin modification marks, like H3K4me3 (H3 lysine 4 tri-methylation), and repressive marks, like H3K27me3 (H3 lysine 27 tri-methylation), in dependence of the occupancy and activity of Polycomb complexes PRC1 and PCR2 on the histones (Ku et al., 2008, Mikkelsen et al., 2007). Pioneer transcription factors bind to these regions and through their action ensure the ES cell characteristics. Upon differentiation, they may be replaced by other lineage specific transcription factors (Smale, 2010). These regulators exert their functions through biochemical interaction with other transcription factors. They assemble to core transcriptional networks that coordinate stem cell maintenance and differentiation by the synergistic sustainment and induction of developmental gene expression programs (Chen et al., 2008, Hobert, 2011).

SOX2 plays an important role in the maintenance of stem cell properties. Its action of is dosage-dependent and requires the cooperation with OCT-3/4 and Nanog to form a transcriptional network defining ES identity, which maintains pluripotency and inhibits differentiation (Boyer et al., 2005, Chen et al., 2008). Moreover, SOX2 is involved in the differentiation of pluripotent ES cells towards the early neuronal lineage. It supports the neuroectodermal development by silencing of mesendodermal fate expression programs (Thomson et al., 2011, Wang et al., 2012). Also *in vivo*, SOX2 promotes the differentiation of bipotential axial stem cells into a

neural tube fate, which later develop to the CNS and not to paraxial mesoderm, as the transcription factor TBX6 promotes (Takemoto et al., 2011). Recently, SOX9 was found to induce differentiation of ES cells into all three germ layers by repressing SOX2 expression through enhanced formation of p21, capable of silencing the SOX2 enhancer (Yamamizu et al., 2014). All of the three SOXB1 proteins SOX1, SOX2 and SOX3 are expressed in the majority of multipotent neuronal progenitors in both the developing and the adult CNS. Studies in mouse and chicken embryos revealed a redundant function in the maintenance of progenitor characteristics and repression of neural differentiation (Bylund et al., 2003, Favaro et al., 2009, Graham et al., 2003). However, ablation of SOX2 in mice results in a more severe phenotype, than deletion of SOX1 or 3, characterised by the complete loss of NSCs and neurogenesis in the early postnatal hippocampus and dentate gyrus hypoplasia in embryonic mice (Favaro et al., 2009). The SOX2-dependent regulation of NSC properties functions partly through Shh and Notch signalling pathways (Favaro et al., 2009, Taranova et al., 2006). The SOXB1 factors have to be down-regulated upon neural differentiation, as they are no more present in post-mitotic neuroblasts. Proneural transcription factors of the basic helix-loop-helix (bHLH) class commit NPCs neural fate and induce progression of neurogenesis by supressing the expression of SOX1-3 (Bylund et al., 2003). They furthermore promote the expression of SOX21. Studies in chicken embryos proposed a model where SOX21 counteracts SOX1-3 and induces neurogenesis potentially by repressing the SOXB1 factors target genes (Sandberg et al., 2005).

Proneural bHLH proteins also induce the expression of SOXC genes SOX4 and SOX11 during differentiation of NPCs (Bergsland et al., 2006). The third protein of the subgroup, SOX12, may be induced as well, but its function is supposed to be less dominant as is seems to possess a weak activation capacity, compared to the other SOXC factors. Moreover, SOX4 and SOX11 can easily compensate its loss (Hoser et al., 2008). Also SOX4 and SOX11 function redundantly, as deletion of one of the factors has only little effect on neurogenesis (Cheung et al., 2000, Sock et al., 2004). In agreement with this assumption, a depletion of both SOX4 and SOX11 leads to a massive cell death mainly in immature neurons of the developing nervous system (Bhattaram et al., 2010, Thein et al., 2010). The SOXC factors are critically required for the survival of neural progenitors and activate mediators of the Hippo signalling pathway (Bhattaram et al., 2010). In contrast to the SOXB1 factors, both SOXC

proteins promote neural fate commitment and maturation, as they induce the expression of early neuronal markers β-tubulin III and MAP2 (Bergsland et al., 2006). Transcriptional profiling in embryonic and adult neural stem cells linked SOX4 and SOX11 to both stem cell differentiation and neurogenesis (Miller et al., 2013). Moreover, epigenetic mechanisms promote neuronal differentiation by regulation of SOX4 and SOX11 expression (Feng et al., 2013, Ninkovic et al., 2013).

In general, these findings suggest a crucial role for several SOX proteins in the progression of neurogenesis, with a defined temporal order of their expression and activity. SOX2, which is already expressed in ES cells is accompanied by SOX1 and SOX3 during the NPC state, followed by the SOX21-dependent exit of the precursor cell state and the induction of neuronal differentiation by SOX4 and SOX11. A genome-wide-binding pattern analysis of SOX2, SOX3 and SOX11 by chromatin immunoprecipitation (ChIP) analysis combined with ChIP sequencing in ES cell-derived neural precursors and immature neurons revealed an overlap of 96% for SOX2 and SOX3 binding in NPCs (Bergsland et al., 2011). This confirms the assumption of functional redundancy between SOXB1 proteins. Moreover, SOX3 and the p300 co-activator showed many common target sites related to brain-specific regulatory regions, mostly enhancer rather than promoter sequences. SOX2 binds to ES-specific regions that are not occupied by SOX3 in NPCs. The overlapping sequences of SOX2 and SOX3 are situated near neural genes, partly already known as SOXB1 targets. Many of them are also associated with the bivalent histone modification marks H3K4me3 and H3K27me3. These findings identified SOX2 as a pioneer factor binding to neural genes in ES cells and preselecting them for activation by sub sequential expressed transcription factors that drive neural development. Notably, the genome-wide-binding profile of SOX3 in NPCs and SOX11 in early neurons also revealed a high overlap. 30% of the SOX3 targets are not bound by SOX11 and only 8% of the SOX11 targets are not recognised by SOX3. Genes occupied by only one of the factors are predominantly expressed in mature neurons and glia, pointing to a re-occurrence of SOX3 in later stages of neuronal maturation, as described before (Bergsland et al., 2011, Ferri et al., 2004, Malas et al., 2003). In contrast, targets of both factors are expressed either in NPCs or immature neurons, where SOX3 strongly activates the genes in NPCs and SOX11 induces expression of neuron-specific markers. This hints at an implication of SOX3 not only in the activation of NPC-specific genes, but also suggests a function as

pioneer factor for neuronal enhancers that are activated by SOX11 in later stages. That is supported by the active H3K4me3 mark of SOX3- activated genes in NPCS and both active H3K4me3 and repressive H3K27me3 histone marks of genes that are preselected, but not activated by SOX3. Neuronal genes in immature neurons are specifically marked by the active form H3K4me3 (Bergsland et al., 2011). Finally, a model has been established, where neurogenesis is regulated by the sequential action of SOXB1 and SOXC factors. Here, the pioneer factor SOX2 preselects neural genes in the state of ES cells and accomplishes along with other joining SOXB1 proteins their conversion to NPCs. Besides, NPC-specific genes get activated. At this stage, SOX3 additionally primes neuronal genes and thus promotes their active transcription by the SOXC proteins SOX4 and SOX11 during differentiation into neurons (illustrated in figure 6) (Bergsland et al., 2011).

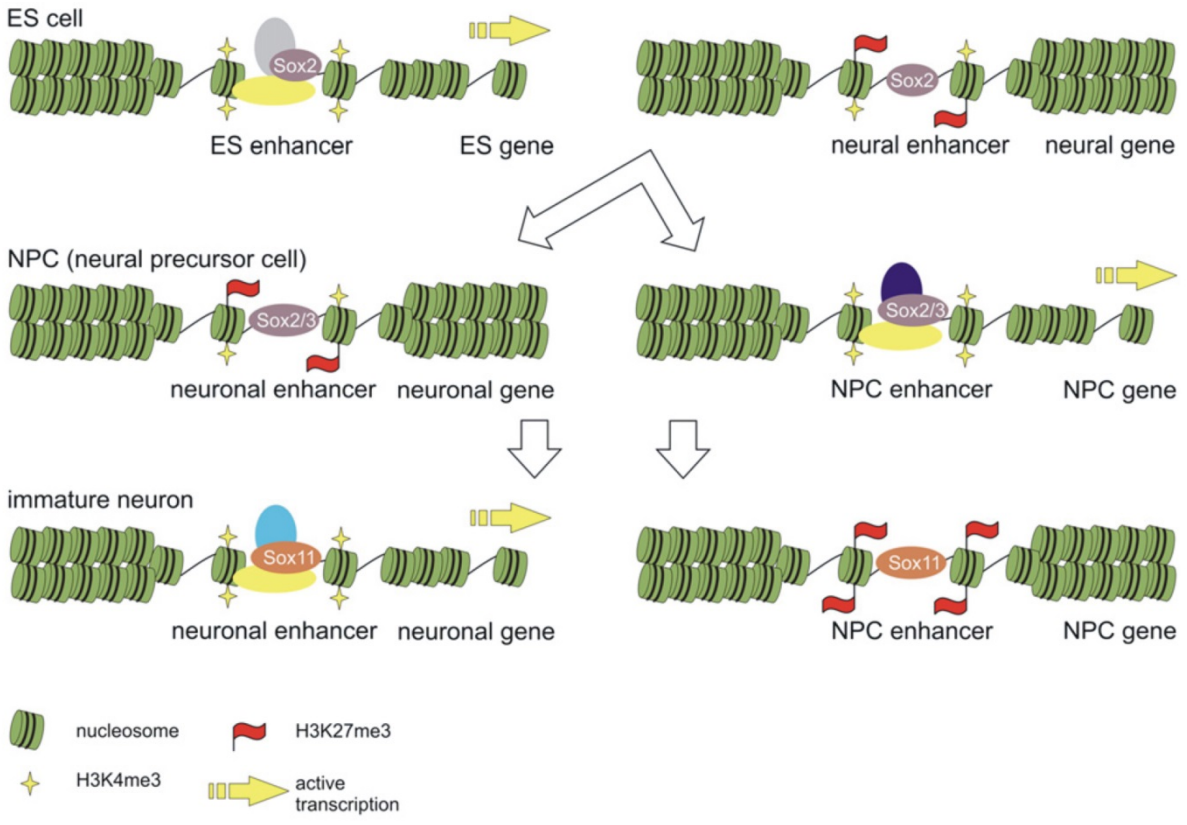

Figure 6:Sequential action of SOX transcription factors during neurogenesis
SOX2 binds to ES enhancers in ES cells marked with H3K4me3 and activates gene transcription and binds to neural enhancers with both H3K4me3 and H3K27me3, which remain silent. Upon differentiation to NPCs, SOX2 gets joined by SOX3 to activate NPC enhancers with the active histone mark H3K4me3 and to bind the silent neuronal enhancers, carrying both marks. During maturation to early neurons, SOX11 activates neuronal gene transcription by occupying neuronal enhancers with active histone marks and binds to NPC enhancers marked with the repressive H3K27me3.
(Modified from Wegner et al. 2011, reprinted with permission of Genes & Development)

1.3.2.2.2. The role of SOXB1 in adult neurogenesis

The regulation of neurogenesis within the adult brain requires to some extent the same SOX transcription factors that are already involved in the neuronal development of the embryonic brain. The multipotency regulator SOX2 is found to be expressed in the neurogenic niches of the adult mouse brain. Within the SGZ of the hippocampal dentate gyrus it is expressed in quiescent radial glia-like type-1 stem cells and rapidly proliferating type-2 precursor cells and astrocytes (see figure 4). Upon neural fate commitment, SOX2 becomes down-regulated, coinciding with the expression of early neuronal markers (Steiner et al., 2006). In adult neural stem cells, it is a key regulator for the maintenance of multipotency and self-renewal capacities of the proliferating progenitor pool. *In vitro*, precursor cells isolated from the adult hippocampal dentate gyrus exhibited self-renewing properties. In addition, they showed the ability to differentiate into cells of the neuronal lineage in an *in vitro* GFP reporter assay using a SOX2 promoter (Suh et al., 2007). Deletion of SOX2 in adult mice results in NPC loss and deprivation of hippocampal neurogenesis (Ferri et al., 2004). Furthermore, the transcription factor seems to modulate Shh signalling, which is critically required for the NPC maintenance through activation of the Shh promoter (Favaro et al., 2009). The Notch/RBPJK signalling pathway was identified to regulate SOX2 expression through binding of both Notch and RBPJK to the SOX2 promoter (Ehm et al., 2010). Moreover, SOX2 is implicated in the regulation of TLX, a factor expressed in many parts of the adult brain, which plays a crucial role in the maintenance of NSC properties (Shi et al., 2004, Shimozaki et al., 2011). Notably, SOX2 also actively counteracts neuronal differentiation through inhibition of Wnt signalling-dependent activation of the proneural bHLH factor NEUROD1 (Kuwabara et al., 2009, Lie et al., 2005).

Also the SOXB1 member SOX3 is found to be expressed in the SVZ of the lateral ventricle and the SGZ of the dentate gyrus in the adult brain. Proliferating progenitor cells display high expression levels of the transcription factor, which decline in the course of neuronal differentiation. This points to a similar role to that in embryonic brain development, where SOX3 joins SOX2 to maintain the pool of proliferating precursors and occupy silent neuronal genes to prime them for later activation (Wang et al., 2006).

1.3.2.2.3. The role of SOX11 in adult neurogenesis

The SOXC factor SOX11 plays a major role in the regulation of both embryonic and adult neurogenesis. Its significance for an accurately controlled CNS development is demonstrated by the recently discovered fact that SOX11 deletion and mutations are linked to CNS malformation. This includes severe mental retardation and Coffin-Siris syndrome, a congenital disorder which is associated with intellectual disability and microcephaly (Lo-Castro et al., 2009; Tsurusaki et al., 2014). A genome-wide binding profile of the postnatal and adult mammalian brain revealed association of SOX4 and SOX11 with stem cell differentiation and neurogenesis (Miller et al., 2013). Additionally, a large number of neuronal lineage specific genes were identified as SOX11 targets in ES cell derived immature neurons (Bergsland et al., 2011). The SOX4 and SOX11 loci are modified by crucial epigenetic regulators, implicated in neural stem cell differentiation adult neurogenesis (Feng et al., 2013, Ninkovic et al., 2013).

In the adult mouse brain, SOX11 is prominently expressed in the two neurogenic niches subgranular zone of the dentate gyrus and the subventricular zone of the lateral ventricle as well as in the rostral migratory stream, which directs neuroblasts to the olfactory bulb. Furthermore, it is transiently present in neuronally committed progenitors and immature new-born neurons, but not in SOX2-expressing NPCs (Haslinger et al., 2009).

Moreover, SOX11 was shown to promote neuron-specific gene programs in both embryonic and adult neurogenesis. In the developing brain, SOX11 as well as SOX4 were discovered to promote late neural fate commitment and neuronal differentiation, by activating the expression of a subset of early neuronal markers like β-tubulin III and MAP2 (Bergsland et al., 2006), as well as the F-actin binding protein Drebrin (Song et al., 2008, Wang et al., 2010). Notably, the SOX11 expression in the adult brain overlaps with DCX expression, another early neuronal marker protein.

In neural stem cells isolated from the SVZ, SOX11 overexpression was capable of inducing neuronal differentiation, which was monitored by the neuronal proteins DCX and MAP2 (Haslinger et al., 2009). These findings suggest a stage-specific role for SOX11 in the regulation of adult neurogenesis. More recently, it was found that SOX4 and SOX11 display overlapping expression patterns in the hippocampal neurogenic lineage and that not only SOX11, but also SOX4 over-expression induces neurogenesis from NSCs *in vitro*. Additionally, the depletion of both SOXC factors

inhibits *in vitro* and *in vivo* neuronal differentiation from adult neuronal precursors. Conditional removal of Sox11 from embryonic and adult neural stem cells blocks precursor cell proliferation (Wang, Lin, Lai, Parada, & Lei, 2013).

Furthermore, SOX4 and SOX11 were found to activate the immature neuronal marker DCX in reporter assays using NPCs (Mu et al., 2012). DCX expression is also modulated by the proneural proteins NEUROD1 and PROX1 (Lavado et al., 2010, Seo et al., 2007), which are under the control of the Wnt-signalling pathway (Karalay et al., 2011, Kuwabara et al., 2009). Regarding the fact that SOXC proteins are involved in the modulation of Wnt-signalling (Lee et al., 2011, Sinner et al., 2007), a cooperation of SOXC pathways and Wnt-signalling combined with the downstream operators NEUROD1 and PROX1 in the organisation of neural fate commitment, neuronal differentiation and maturation to new-born granule neurons is easily conceivable.

The regulation of adult neurogenesis underlies the temporal expression and sequential action of transcriptional modulators. Furthermore it is based on the cooperation of a variety transcription factors that are connected in transcriptional networks. For other SOX proteins, like SOX2, several interaction partners are identified so far, exemplified by the collaborating transcription factors OCT3/4 and Nanog (Boyer et al., 2005, Chen et al., 2008). Despite this fact, to date, the information about proteins that act together with SOX11 on gene activation is very rare. Previously, Sox11 was found to cooperate with POU3f3 and POU3f2, two members of the neurogenesis related POU-III class of transcription factors in reporter assays (Kuhlbrodt et al., 1998). Additionally, the differentiation efficiency of neural stem cells induced by SOXC proteins was found to be significantly enhanced by the over-expression of POU transcription factors. Furthermore, a motif composed of a combination of pro-neurogenic transcription factor and SOXC binding sites was identified to be enriched in regulatory regions of neuronal fate determination genes (Ninkovic et al., 2013). Somatic cells can be converted into neurons by these pro-neurogenic factors, whereby efficiency is increased by expression of SOXC proteins (Liu et al., 2013, Mu et al., 2012, Ninkovic et al., 2013). Nonetheless, the identification of SOX11 interaction partners that cooperate on the induction of neuronal gene programs would provide crucial insights into the regulation of neurogenesis and remains to be further elucidated.

1.3.3. Involvement of SOX proteins in reprogramming assays

The reprogramming of somatic cells into neurons provides a powerful tool for regenerative medicine, enabling the exploration of diseases and generating new targets, which can be used for therapy development, like drug screening. Furthermore, potential cell-based therapies for disease intervention are of special importance, aiming at the substitution of neurons lost in neurodegenerative disorders like Alzheimer's disease or Parkinson's disease. Initial studies demonstrated that the trans-differentiation of somatic cells into other lineages is dependent on epigenetic mechanisms (Taylor and Jones, 1979). They revealed moreover, transcription factors as the underlying intrinsic determinants for the cell conversion (Davis et al., 1987, Lassar et al., 1986). The cell fate switch between closely related cell types was obtained easier than among unrelated lineages, probably due to similar epigenetic marks (Nerlov and Graf, 1998, Xie et al., 2004). The discovery that proteins, commonly used to identify ES cells are responsible for the maintenance of the cell's properties, led to a large screen using multiple ES cell-specific markers for the reprogramming of mouse fibroblasts into pluripotent cells. A reduction to the minimal number of indispensable factors for pluripotency induction, enabled the generation of the newly discovered induced pluripotent stem cells (iPS cells). The four defined factors necessary for reconversion of fibroblasts into iPS cells were OCT3/4, SOX2, KLF4 and c-MYC (Takahashi and Yamanaka, 2006). By a procedure called directed differentiation, the iPS cells can subsequently be differentiated into cell types of all three germ layers by defined factors. The generation of neuronal cells from iPS cells can be directed by several mechanisms like treatment with the BMP inhibitor Noggin (Chambers et al., 2009, Smith and Harland, 1992), co-cultures with murine PA6 stromal cells (Pomp et al., 2008) or neural induction by different factor combinations like FGF8A, WNT1, retinoic acid and SHH (Cooper et al., 2010). Although the iPS cell technology provides several advantages for the progress of stem cell biology, the application of iPS cell-derived neurons in practical clinical trials is difficult, due to the low efficiencies, the time consuming procedure and obstacles concerning potential tumour induction from the pluripotent cells. To overcome this, an alternative method was introduced, based on the generation of neuronal cells directly from adult somatic cells. The first successful direct reprogramming of fibroblasts into induced neuronal cells was achieved in 2010. The combination of the defined factors ASCL1, BRN2

(also called POU3F2) and MYT1L was sufficient to convert mouse fibroblasts into functional neurons without the pluripotent state in between (Vierbuchen et al., 2010). This exemplifies the possibility of trans-conversion even between cells of different germ layers. Of special interest is the practicability of this direct trans-differentiation method in regenerative medicine, which is based on the faster procedure without the necessity of the pluripotent step. Additionally, the process may enable direct *in situ* conversion in patients in the future. The applied somatic fibroblasts are, furthermore, ubiquitously available and can be used in an autologous fashion. Until now, several combinations of transcription factors have successfully been applied for the direct reprogramming of both fibroblasts and astrocytes into different types of induced neurons. Mouse fibroblasts were trans-differentiated to dopaminergic neurons (Caiazzo et al., 2011), to motor neurons (Son et al., 2011) and to neuronal precursor cells (Lujan et al., 2012) by different combinations of factors. Also striatal astrocytes were converted into neurons *in vivo* (Torper et al., 2013). Interestingly, after brain injury within the cerebral cortex, NEUROD induced the *in vivo* generation of reactive glial cells into neurons (Guo et al., 2014). Also human fibroblasts were reprogrammed into glutamatergic neurons by different combinations of transcription factors and microRNAs (Ambasudhan et al., 2011, Pang et al., 2011, Yoo et al., 2011). Dopaminergic neurons were differentiated from human fibroblasts (Caiazzo et al., 2011, Pfisterer et al., 2011). Moreover, another combination of transcription factors was sufficient to induce conversion of human fibroblasts into motor neurons (Son et al., 2011).

NGN2 is one of the bHLH transcription factors that initiate the progression of neurogenesis (Bertrand et al., 2002). Moreover, it was found to act upstream of SOXC proteins and is involved in the activation of SOXC factor expression (Bergsland et al., 2006). The bHLH factor is sufficient for the direct conversion of human fibroblasts into neurons, but forced expression of SOX11 is required to enhance the efficiency (Liu et al., 2013). Also astrocytes can be reprogrammed into glutamatergic neurons by NGN2 (Berninger et al., 2007, Heinrich et al., 2010). However, the efficiency is heavily enhanced upon addition of SOXC factors, whereas depletion of the proteins from astrocytes strongly impairs the ability of the cells to convert into neurons (Mu et al., 2012). Additionally, SOX11 was applied together with NFIB and POU3F4 to successfully trans-differentiate glial cells into neurons (Ninkovic et al., 2013). Taken together, these findings underline the essential role of SOX

transcription factors, especially SOX2 and SOXC proteins in the reprogramming of somatic cells into iPS cells as well as in the direct conversion into neuronal precursor cells and neurons, respectively.

2. Aim of the study

The family of SOX transcription factors plays a pivotal role during embryonic and adult neurogenesis in both maintenance of the proliferating multipotent neural stem cell pool and commitment of the precursor cells to a neuronal fate as well as in the progression of differentiation into functional neurons. Recently, SOX11 was identified as a crucial regulator during neural fate commitment and the induction of a neuron-specific gene expression program. The importance of SOX11 for a coordinated CNS development is illustrated by the discovery that SOX11 deletion and mutations are associated with CNS malformation and Coffin-Siris syndrome, a congenital disorder characterised by intellectual disability and microcephaly (Lo-Castro et al., 2009, Tsurusaki et al., 2014). Current models indicate that stem cell maintenance and differentiation are coordinated by core transcriptional networks, which are composed of various transcription factors that physically interact, thereby maintaining and inducing developmental gene expression programs in a synergistic fashion (Chen et al., 2008, Hobert, 2011).

According to this previous knowledge, the present study aimed to determine the regulatory transcriptional core program of late neuronal differentiation and maturation that defines early neuronal identity. Due to its relevance in neuronal differentiation and induction of immature neuronal gene programs, SOX11 was chosen as bait for the identification of the underlying transcriptional network. To this end, several objectives were addressed within this study.

I. <u>Generation of SOX11-specific monoclonal antibodies</u>

At the beginning of the study, only few antibodies recognising SOX11 in Western Blotting and Immunoprecipitation were commercially available. They were polyclonal and differed batch-to-batch in specificity and signal intensity. The establishment of monoclonal anti-SOX11 antibodies enables the specific and robust detection of the murine SOX11 protein, which is essential for the further analysis of the transcription factor.

To that end, protein-specific monoclonal antibodies were produced. Their suitability on western blot level and immunoprecipitation was tested and protocols were optimised.

II. Determination of a SOX11-centered transcriptional network

The interaction partners of the transcription factor SOX11 serve as potential co-regulators in the modulation of targets on the transcriptional level. Their identification could provide insights into assembled transcription factor complexes and networks orchestrating the regulation of neurogenesis and determining early neuronal identity. The set-up of a protein-protein interaction network can further illustrate the relationship between the identified proteins and integrate the dataset into a biological context by evaluation of literature-based knowledge.

The establishment of a proteomic SOX11-centered transcriptional interaction dataset was realised by the determination of the SOX11 interactome in the mouse neuroblastoma cell line Neuro2a using SILAC labelling in affinity based purifications and quantitative proteomic approaches. The SOX11-centered protein-protein interaction network was assembled by matching the obtained interaction data with prevalidated protein interaction data from public databases.

III. Functional promoter studies of interacting candidate proteins

The functional evaluation of identified SOX11 interaction partners on different promoters reveals their relevance in the regulation of particular cellular processes like neurogenesis. Furthermore potential cooperation of transcription factors on the modulation of transcriptional programs can be uncovered.

The promoter studies were carried out by the use of interacting proteins in reporter assays on SOX11-regulated immature neuronal markers DCX and Stathmin1, combined with co-expression of SOX11 and knockdown of selected candidates.

IV. *In silico* modelling of selected candidate proteins

A powerful tool for the determination of binding sites on regulatory regions of the DNA is represented by *in silico* promoter analysis. Genome-wide as well as promoter-specific binding profiles of selected interactors and models including SOX11 and other transcription factors from the SOX11 interactome can provide useful information about possible binding to transcriptional target sequences and cooperative action on promoters.

In silico promoter modelling was accomplished by the use of the Genomatix software. The analysis included determination of binding profiles of single

transcription factors, the construction of models and their overrepresentation in selected and genome-wide promoter regions.

3. Material and Methods

3.1. Material

3.1.1. Equipment

Analytical balance ABJ 120-4M	Kern, Balingen,Germany
Autoclave DX-150	Systec, Wettenberg, Germany
Berthold Mitras LB 940 Microplate Reader	Berthold, Bad Wildbad, Germany
CO_2-Incubator HeraCell 150i	Heraeus, Hanau, Germany
Compartment dryer T20	Heraeus, Hanau, Germany
Developer Curix 60	Agfa, Mortsel, Belgium
Freezer (-80°C) Forma 900 Series	Thermo Fisher Scientific, Waltham, MA, USA
Freezer Liebherr Comfort	Liebherr, Bulle, Switzerland
Geldocumentation device Easy RH	Herolab, Wiesloch, Germany
Ice machine AF200	Scotsman, Vernon hills, IL, USA
Incubator INB 300 for bacteria	Memmert, Schwabach, Germany
Infrared lamp model 2580	Kindermann, Eibelstadt, Germany
IntelliMixer	NeoLab, Heidelberg, Germany
Laboratory balance S72	Kern, Balingen,Germany
Laboratory hood model 854006.1	Wesemann, Syke, Germany
Laminar flow HeraSafe HS 12	Heraeus, Hanau, Germany
Laminar flow MSC 12	Thermo Fisher Scientific, Waltham, MA, USA
Light table Prolite 5000	Kaiser, Buchen, Germany
Lightcycler® 480	Roche, Penzberg, Germany
Magnetic stirrer and heater MR Hei-Standard	Heidolph, Schwabach, Germany
Megafuge 16	Heraeus, Hanau, Germany
Microscope PrimoVert	Zeiss, Göttingen, Germany
Microwave	Siemens, München, Germany
Multifuge X3R	Heraeus, Hanau, Germany
Neubauer counting chamber	Marienfeld, Lauda-Königshofen, Germany
pH meter PB-11	Sartorius, Göttingen, Germany
Platform shaker Duomax 1030	Heidolph, Schwabach, Germany
Power Supply Consort	Consort, turnhout, Belgium
Power Supply PowerPak Basic	Bio-Rad, Hercules, CA, USA
Refrigerator	Liebherr, Bulle, Switzerland
Refrigerator Vapor Trap RVT400-230	Thermo Fisher Scientific, Waltham, MA, USA
Roller mixer RM5	Assistent, Sondheim, Germany
Rotating incubator Infors HAT	Ecotron, Bruckmühl, Germany
Sonificator Sonopuls HD70	Bandelin, Berlin, Germany
Speedvac Concentrator SPD111V-230	Thermo Fisher Scientific, Waltham, MA, USA
Table top centrifuge 5415D	Eppendorf, Hamburg, Germany
Table top centrifuge Fresco17, refrigerated	Heraeus, Hanau, Germany
Table top centrifuge Pico21	Heraeus, Hanau, Germany
Thermoblock MBT 250	ETG, Ilmenau, Germany

Thermocycler Primus	MWG-Biotech, Ebersberg, Germany
Thermocycler Primus 96 Plus	MWG-Biotech, Ebersberg, Germany
Thermomixer Comfort	Eppendorf, Hamburg, Germany
Thermomixer Univortemp	Universal Labortechnik, Leipzig, Germany
Transluminator Fluo Link (312 nm)	Bachofer Laboratoriumsgeräte, Reutlingen, Germany
Ultrapure water purification system Nanopure	Thermo Fisher Scientific, Waltham, MA, USA
Ultrasonic bath Sonorex Digitec	Bandelin, Berlin, Germany
UV/VIS Spectrometer T70	PG Instruments Limited, Lutterworth, United Kingdom
Vacuum pump 2522Z-02	Welch, Niles, IL, USA
Vortex Mixer	NeoLab, Heidelberg, Germany
Waterbath WNB 14 and shaker SV1422	Memmert, Schwabach, Germany

3.1.2. Consumables and Labware

96 well plate, white, flat bottom, non-binding	Greiner bio-one, Kremsmünster, Austria
Accu-jet® pro pipetting aid	Brand, Wertheim, Germany
Amersham Hyperfilm ECL	GE Healthcare, Waukesha, WI, USA
ART™ Barrier pipette tips 1000µl	Thermo Fisher Scientific, Waltham, MA, USA
ART™ Barrier pipette tips 10µl	Thermo Fisher Scientific, Waltham, MA, USA
ART™ Barrier pipette tips 20µl	Thermo Fisher Scientific, Waltham, MA, USA
ART™ Barrier pipette tips 200µl	Thermo Fisher Scientific, Waltham, MA, USA
Baffled flask 250ml	Neolab, Heidelberg, Germany
Baffled flask 500ml	Neolab, Heidelberg, Germany
Blue Rack für 6xTubes	GLW Storing Systems, Würzburg, Germany
Blue Rack für 6xTubes	GLW Storing Systems, Würzburg, Germany
Box for 15 ml Centr. Tube	Neolab, Heidelberg, Germany
Box for 50 ml Centr. Tube	Neolab, Heidelberg, Germany
Box for Pipette Tips (Gilson)	Gilson, Middleton, WI, USA
Canula	Neolab, Heidelberg, Germany
Cell scraper	Sarstedt, Nümbrecht, Germany
Centrifugation tubes 15ml	Greiner bio-one, Kremsmünster, Austria
Centrifugation tubes 50ml	Greiner bio-one, Kremsmünster, Austria
Comb 10 well for 0.75 mm gels	Bio-Rad, Hercules, CA, USA
Cryo Tube Rack	Nunc, Rochester, NY, USA
Cryobox 0.5 ml tubes	Carl-Roth, Karlsruhe, Germany
Cryobox 1.5 / 2.0 ml tubes	Carl-Roth, Karlsruhe, Germany
Cryotubes, 1.8 ml Innengewinde	Nunc, Rochester, NY, USA
Culture tube 14ml	BD Biosciences, Franklin Lakes, NJ, USA
Cuvette 1,5ml	Sarstedt, Nümbrecht, Germany
Drigalski spatula	Carl-Roth, Karlsruhe, Germany
Filtersystem 0.22 µm	Corning, Corning, NY, USA
Flea, 1 to 8 cm	Neolab, Heidelberg, Germany
Gel loading tips	Carl-Roth, Karlsruhe, Germany
Glas plate with 0.75mm spacer	Bio-Rad, Hercules, CA, USA

Gloves purple nitrile	Kimberly-Clark, Irving, TX, USA
Gloves soft nitrile	Paul Hartmann, Heidenheim, Germany
Graduated measuring glass	Duran Group, Wertheim, Germany
Hybond-P PVDF Transfer membrane	GE Healthcare, Waukesha, WI, USA
Hypercassette	GE Healthcare, Waukesha, WI, USA
Hyperscreen	GE Healthcare, Waukesha, WI, USA
Icebath	Neolab, Heidelberg, Germany
Inlays for Cryobox 0.5 ml tubes	Carl-Roth, Karlsruhe, Germany
Inlays for Cryobox 1.5 / 2ml tubes	Carl-Roth, Karlsruhe, Germany
Inoculation loop	Carl-Roth, Karlsruhe, Germany
Kimwipes Lite	Kimberly-Clark, Irving, TX, USA
Laboratory bottle, 50-2000ml	Neolab, Heidelberg, Germany
MicroSpin Columns	GE Healthcare, Waukesha, WI, USA
Multiwell plates, 96 wells	Greiner bio-one, Kremsmünster, Austria
Parafilm sealing foil	Brand, Wertheim, Germany
Pasteur capillary pipette	VWR International, West Chester, PA, USA
Pasteur-Pipette PP	VWR International, West Chester, PA, USA
PCR rack	Carl-Roth, Karlsruhe, Germany
Petridish 90x14.2 mm	VWR International, West Chester, PA, USA
pH Indicator sticks	Carl-Roth, Karlsruhe, Germany
Pipette 10µl	Gilson, Middleton, WI, USA
Pipette 100µl	Gilson, Middleton, WI, USA
Pipette 1000µl	Gilson, Middleton, WI, USA
Pipette 2µl	Gilson, Middleton, WI, USA
Pipette 20µl	Gilson, Middleton, WI, USA
Pipette 200µl	Gilson, Middleton, WI, USA
Pipette tips 101-1000µl	Sarstedt, Nümbrecht, Germany
Pipette tips 1-10µl	Sarstedt, Nümbrecht, Germany
Pipette tips 1-200µl	Sarstedt, Nümbrecht, Germany
Pipette tips; D1000	Gilson, Middleton, WI, USA
Pipette tips; D200	Gilson, Middleton, WI, USA
Pipette tips; DL10	Gilson, Middleton, WI, USA
Pipettes, serological, 10ml, sterile	BD Biosciences, Franklin Lakes, NJ, USA
Pipettes, serological, 25ml, sterile	BD Biosciences, Franklin Lakes, NJ, USA
Pipettes, serological, 2ml, sterile	BD Biosciences, Franklin Lakes, NJ, USA
Pipettes, serological, 50ml, sterile	BD Biosciences, Franklin Lakes, NJ, USA
Pipettes, serological, 5ml, sterile	BD Biosciences, Franklin Lakes, NJ, USA
Polypropylen insert with bottom spring	Sigma-Aldrich, St. Louis, MO, USA
Reaction tube 0.2ml	Sarstedt, Nümbrecht, Germany
Reaction tube 0.5ml, safe-lock	Eppendorf, Hamburg, Germany
Reaction tube 1.5ml, safe-lock	Eppendorf, Hamburg, Germany
Reaction tube 15ml	Sarstedt, Nümbrecht, Germany
Reaction tube 2ml, safe-lock	Eppendorf, Hamburg, Germany
Reaction tube 50ml	BD Biosciences, Franklin Lakes, NJ, USA
Scalpell	VWR International, West Chester, PA, USA

Short plate	Bio-Rad, Hercules, CA, USA
Slide-A-Lyzer Dialysis cassette, 10MWCO, 3ml	Thermo Fisher Scientific, Waltham, MA, USA
Spin Columns, 5MWCO	Neolab, Heidelberg, Germany
Stage Tips C-18, 200 µl	Thermo Fisher Scientific, Waltham, MA, USA
Sterilfilter Millex 0,22 µm (Millex)	Merck, Darmstadt, Germany
Syringes	BD Biosciences, Franklin Lakes, NJ, USA
Tissue Dishes, 10cm, Nunclon Surface	Nunc, Rochester, NY, USA
Tissue Dishes, 14cm, Nunclon Surface	Nunc, Rochester, NY, USA
Water bath stabiliser, AKASOLV Aqua Care	Carl-Roth, Karlsruhe, Germany
Whatman chromatohrapy paper	GE Healthcare, Waukesha, WI, USA

3.1.3. Chemicals

1,4-Dithiothreitol (DTT)	Merck, Darmstadt, Germany
2-Iodacetamide (IAA)	Merck, Darmstadt, Germany
2-Mercaptoethanol	Sigma-Aldrich, St. Louis, MO, USA
2-Propanol p.a.	Merck, Darmstadt, Germany
Acetonitrile LC-MS CHROMASOLV®, ≥99.9%	Sigma-Aldrich, St. Louis, MO, USA
Agar-Agar	Carl-Roth, Karlsruhe, Germany
Agarose	Lonza, Basel, Switzlerland
Ammonium Bicarbonate	Sigma-Aldrich, St. Louis, MO, USA
Ammonium Hydroxide p.a.	Sigma-Aldrich, St. Louis, MO, USA
Ammonium Persulfate	Sigma-Aldrich, St. Louis, MO, USA
Ampicillin Sodium Chrystalline	Carl-Roth, Karlsruhe, Germany
Bis-Acrylamid/Acrylamid; 37,5:1; 30%	Serva Elektrophoresis, Heidelberg, Germany
Bromophenolblue	Sigma-Aldrich, St. Louis, MO, USA
Chloramphenicol	Carl-Roth, Karlsruhe, Germany
Chloroform p.a.	Merck, Darmstadt, Germany
Dimethyl Sulfoxide	Applichem, Darmstadt, Germany
EDTA Disodium Salt Dihydrate	Applichem, Darmstadt, Germany
EGTA	Sigma-Aldrich, St. Louis, MO, USA
Ethanol 99%, denatured MEK/BIT	SAV liquid production, Flintsbach, Germany
Ethanol p.a.	Merck, Darmstadt, Germany
Ethidiumbromide	Applichem, Darmstadt, Germany
Ficoll 400	Sigma-Aldrich, St. Louis, MO, USA
G418	Merck, Darmstadt, Germany
Glacial Acetic Acid p.a.	Merck, Darmstadt, Germany
Glycerin	Carl-Roth, Karlsruhe, Germany
Glycin	Carl-Roth, Karlsruhe, Germany
HEPES	Sigma-Aldrich, St. Louis, MO, USA
Hydrochloric Acid p.a.	Merck, Darmstadt, Germany
Imidazole	Sigma-Aldrich, St. Louis, MO, USA
IPTG	Fermentas, Burlington, Canada
Isopropanol LC grade	Merck, Darmstadt, Germany
Kanamycin Sulfate	Carl-Roth, Karlsruhe, Germany

Lysozyme	Sigma-Aldrich, St. Louis, MO, USA
Magnesiumchloride	Sigma-Aldrich, St. Louis, MO, USA
Methanol LC-MS grade	Merck, Darmstadt, Germany
Methanol LC-MS grade	VWR International, West Chester, PA, USA
Methanol p.a.	Merck, Darmstadt, Germany
Monopotassium Phosphate p.a.	Carl-Roth, Karlsruhe, Germany
Na2-EGTA	Sigma-Aldrich, St. Louis, MO, USA
Nonident P40	Roche, Penzberg, Germany
OrangeG	Sigma-Aldrich, St. Louis, MO, USA
Phenylmethanesulfonyl fluoride (PMSF)	Sigma-Aldrich, St. Louis, MO, USA
Polyethylenimine, Linear (MW 25,000)	Polysciences, Warrington, PA, USA
Ponceau S	Sigma-Aldrich, St. Louis, MO, USA
Potassium Chloride p.a.	Carl-Roth, Karlsruhe, Germany
RapiGest SF Surfactant	Waters, Milford, MA, USA
Sodium Chloride p.a.	Merck, Darmstadt, Germany
Sodium Hydroxide pellet p.a.	Carl-Roth, Karlsruhe, Germany
Sodium phosphate dibasic (Na2HPO4)	Sigma-Aldrich, St. Louis, MO, USA
Sodium phosphate monobasic (NaH2PO4)	Sigma-Aldrich, St. Louis, MO, USA
Spectinomycin dihydrochloride pentahydrate	Sigma-Aldrich, St. Louis, MO, USA
TEMED p.a.; 100 ml (Merck, Darmstadt, Germany)	Merck, Darmstadt, Germany
Trifluoracetic Acid, for protein seq.	Merck, Darmstadt, Germany
Tris(hydroxymethyl) Aminomethane (Tris ultrapure)	Sigma-Aldrich, St. Louis, MO, USA
Trypsin from porcine pancreas; proteomics grade	Sigma-Aldrich, St. Louis, MO, USA
Tryptone/Peptone from Casein	Carl-Roth, Karlsruhe, Germany
Tween® 20	Sigma-Aldrich, St. Louis, MO, USA
Urea	Carl-Roth, Karlsruhe, Germany
Water, HPLC grade	VWR International, West Chester, PA, USA
Water, HPLC grade	Merck, Darmstadt, Germany
Yeast Extract	Carl-Roth, Karlsruhe, Germany

3.1.4. Special reagents

$12C_6$, $^{14}N_2$ lysine	Silantes, München, Germany
$^{12}C_6$,$^{14}N_4$ arginine	Silantes, München, Germany
$^{13}C_6$,$^{14}N_4$-L-arginine	Silantes, München, Germany
4.4.5.5-D_4-L-lysine	Silantes, München, Germany
Adenosin 5'-Diphosphate (ADP)	Sigma-Aldrich, St. Louis, MO, USA
AGFA Developer G153	Röntgen Bender, Baden-Baden, Germany
AGFA Fixer G354	Röntgen Bender, Baden-Baden, Germany
Anti-FLAG-M2-agarose	Sigma-Aldrich, St. Louis, MO, USA
Blotting Grade Blocker, nonfat dry	Bio-Rad, Hercules, CA, USA
BSA	PAA, Pasching, Austria
Coomassie Brilliant Blue	Merck, Darmstadt, Germany
Dialysed FBS	Sigma-Aldrich, St. Louis, MO, USA
Didesoxyadenosine 5′-triphosphate (ATP)	Sigma-Aldrich, St. Louis, MO, USA

dNTP Mix; 40µM (10 mM each nt)	New England Biolabs, Ipswich, MA, USA
Dulbecco's Modified Eagle Medium	Sigma-Aldrich, St. Louis, MO, USA
Dulbecco's PBS	Sigma-Aldrich, St. Louis, MO, USA
ECL plus Western Blotting Substrate	Thermo Fisher Scientific, Waltham, MA, USA
ECL Western Blotting Substrate	Thermo Fisher Scientific, Waltham, MA, USA
Effectene transfection reagent	Qiagen, Hilden, Germany
Fetal bovine serum (FBS)	Sigma-Aldrich, St. Louis, MO, USA
Flag peptide	Sigma-Aldrich, St. Louis, MO, USA
GeneRuler^{TM} 1kb Plus DNA ladder	Thermo Fisher Scientific, Waltham, MA, USA
L-Glutamine, 200mM	Life Technologies, Carlsbad, CA, USA
Magnesiumchloride (50mM)	Thermo Fisher Scientific, Waltham, MA, USA
Ni-NTA Superflow (50% suspension)	Qiagen, Hilden, Germany
PageRuler Plus; 250kDa; prestained	Fermentas, Burlington, Canada
PageRuler; 170kDa; prestained	Fermentas, Burlington, Canada
Penicillin/Streptomycin	Life Technologies, Carlsbad, CA, USA
Phosphatase Inhibitor Cocktail 2	Sigma-Aldrich, St. Louis, MO, USA
Phosphatase Inhibitor Cocktail 3	Sigma-Aldrich, St. Louis, MO, USA
Phusion HF Reaction buffer	Thermo Fisher Scientific, Waltham, MA, USA
Phusion High-Fidelity DNA Polymerase	Fermentas, Burlington, Canada
Proline	Silantes, München, Germany
Protease Inhibitor Cocktail Complete	Roche, Penzberg, Germany
Protein Assay Dye Reagent	Bio-Rad, Hercules, CA, USA
Protein G PLUS-Agarose	Santa Cruz, Santa Cruz, CA, USA
SILAC DMEM	Thermo Fisher Scientific
Strep Tactin Superflow (50% suspension)	IBA, Göttingen, Germany
Strep-Tag Elution Buffer with D-Desthiobiotin	IBA, Göttingen, Germany
Trypsin EDTA	Life Technologies, Carlsbad, CA, USA

3.1.5. Buffers, Solutions and Media

In this study dH_20 describes deionised water and ddH_20 is referred to ultra-pure water (Thermo Fisher Scientific, Waltham, MA, USA).

3.1.5.1. Cell culture

Growth Medium	Dulbecco's Modified Eagle Medium 10% FBS 0.5% Penicillin/Streptomycin
SILAC Medium Light	SILAC DMEM 10% dialysed FBS 2% L-Glutamine

	0.5% Penicillin/Streptomycin 2mM Proline 0.55mM $^{12}C_6$, $^{14}N_2$ Lysine 0.4mM $^{12}C_6$,$^{14}N_4$ Arginine
SILAC Medium Heavy	SILAC DMEM 10% dialysed FBS 2% L-Glutamine 0.5% Penicillin/Streptomycin 2mM Proline 0.55mM 4.4.5.5-D_4-L-lysine 0.4mM $^{13}C_6$,$^{14}N_4$-L-arginine
Cryo Medium	90% FBS 10% DMSO
PEI Transfection Reagent	1mg/ml Polyethylenimine (PEI) dH_20 dissolve with stirring at 80°C, cool down to RT adjust pH to 7.8 using HCL

3.1.5.2. E.coli culture

LB- Medium	1% (w/v) Tryptone/Peptone from Casein 0.5% (w/v) Yeast Extract 1% (w/v) NaCl adjust pH to 7.0 using NaOH dH_20
LB-Agar	1% (w/v) Tryptone/Peptone from Casein 0.5% (w/v) Yeast Extract 1% (w/v) NaCl 1% (w/v) Agar agar dH_20

3.1.5.3. Nickel-NTA Purification

Na-phosphate buffer 1	50mM Na_2HPO_4 300mM NaCl 10 mM Imidazole
Na-phosphate buffer 2	50mM NaH_2PO_4 300mM NaCl 10 mM Imidazole
Na-phosphate buffer	Titrate Na-phosphate buffer 1 and 2 to pH 8.0
Lysis buffer	Na-phosphate buffer 1mM DTT 0.5 mg/ml Lysozyme
Urea buffer	Na-phosphate buffer 8M Urea
Wash buffer	Na-phosphate buffer 20mM Imidazole
Elution buffer 1-4	Na-phosphate buffer 50mM, 100mM, 150mM, 250mM Imidazole

3.1.5.4. Agarose Gels

TAE-buffer (50x)	2M Tris 50mM EDTA 1M Acetic Acid dH20
OrangeG loading buffer (6x)	250mg/ml Ficoll 400 0.5% (w/v) SDS 50mM EDTA 1 spatula tip OrangeG ddH20

3.1.5.5. Nuclear extraction and affinity purification

Nuclear extraction buffer A	10mM HEPES 1mM EDTA 0.1mM EGTA 10mM KC 1mM PMSF 1µg/ml phosphatase inhibitor cocktail 2 and 3 1mM DTT 1µg/ml complete protease inhibitor
Nuclear extraction buffer C	20mM HEPES 0.2 mM EDTA 0.1mM EGTA 25% glycerol 420mM NaCl 1.5mM MgCl2 1mM PMSF 1µg/ml phosphatase inhibitor cocktail 2 and 3 1mM DTT 1µg/ml complete protease inhibitor
TBS (10x)	300mM Tris 1.5M NaCl dH_20 adjust pH to 7.4 using HCL
Washing buffer	0.1% NP40 1µg/ml phosphatase inhibitor cocktail 2 and 3 1µg/ml complete protease inhibitor TBS (1x)

3.1.5.6. SDS-PAGE, Coomassie staining and Western blot analysis

Laemmli buffer (5x)	250mM Tris-HCl pH 6.8 5% SDS 50% Glycerol 500mM 2-Mercaptoethanol 0.05% (w/v) Bromophenol Blue
Running buffer (10x)	20M Glycin 2.47M Tris 1% (w/v) SDS dH_20
Western buffer (10x)	1.92M Glycin 250mM Tris dH_20
Western buffer (1x)	Dilute Westernbuffer (10x) 1:10 with dH20 and apply 20% MeOH
TBS-T (10x)	300mM Tris 1.5M NaCl 1% Tween® 20 dH_20 adjust pH to 7.4 using HCL
Blocking Solution	5% Blotting Grade Blocker TBS-T (1x)
Coomassie Staining Solution	0.4% (w/v) Coomassie brilliant blue dH_20
Fixer Solution	50% MeOH 12% Acetic Acid dH_20

3.1.6. Kits

Dual-Luciferase® Reporter Assay System Kit	Promega, Fitchburg, WI, USA
EndoFree Plasmid Maxi Kit	Qiagen, Hilden, Germany
Gel Extraction Kit	Fermentas, Burlington, Canada
GeneJET™ Plasmid Miniprep Kit	Fermentas, Burlington, Canada
Omniscript® Reverse Transcription Kit	Qiagen, Hilden, Germany
PCR Purification Kit	Fermentas, Burlington, Canada
peqGOLD Total RNA Kit	Peqlab Biotechnologie, Erlangen, Germany
PureYield Plasmid Midiprep Kit	Promega, Fitchburg, WI, USA
SsoAdvanced™ Universal SYBR® Green Supermix	Bio-Rad, Hercules, CA, USA
TOPO TA Cloning Kit	Invitrogen, Carlsbad, CA, USA

3.1.7. Enzymes

BamHI-HF	New England Biolabs, Ipswich, MA, USA
Benzonase nuclease	Merck, Darmstadt, Germany
BglII	New England Biolabs, Ipswich, MA, USA
BP Clonase II Enzyme Mix, with proteinase K	Invitrogen, Carlsbad, CA, USA
ClaI	New England Biolabs, Ipswich, MA, USA
HindIII	New England Biolabs, Ipswich, MA, USA
Hpa I	New England Biolabs, Ipswich, MA, USA
LR Clonase II Enzyme Mix, with proteinase K	Invitrogen, Carlsbad, CA, USA
Phusion High-Fidelity DNA Polymerase, HF Reaction buffer (5x) and $MgCl_2$ (50mM)	Thermo Fisher Scientific, Waltham, MA, USA
PmeI	New England Biolabs, Ipswich, MA, USA
SfiI	New England Biolabs, Ipswich, MA, USA
T4 DNA Ligase and Reaction buffer (10x)	Roche, Penzberg, Germany
T4 Polynucleotide Kinase and Reaction buffer (10x)	Roche, Penzberg, Germany
Taq DNA Polymerase and Reaction buffer (10x)	Fermentas, Burlington, Canada

3.1.8. Oligonucleotides

.

Table 1: Oligonucleotides for shRNA-mediated knockdown

The shRNA target sequences are depicted in normal capital letters. Bold capital letters indicate flanking regions including italicised pseudo-ClaI sites at the 5' end of reverse oligonucleotides. The loop sequence is denoted as lower case letters.shRNA sequences are from Mission® shRNA Sigma-Aldrich.

Oligo name	Sequence 5'-3'
Tcf4_f_1	**CCGG**GCTGAGTGATTTACTGGATTTctcgagAAATCCAGTAAATCACTCAGC**TTTTT**
Tcf4_r_1	***CG*AAAAA**GCTGAGTGATTTACTGGATTTctcgagAAATCCAGTAAATCACTCAGC**CCGG**
Tcf4_f_2	**CCGG**CCCAGTACTATCAGTATTCAActcgagTTGAATACTGATAGTACTGGG**TTTTT**
Tcf4_r_2	***CG*AAAAA**CCCAGTACTATCAGTATTCAActcgagTTGAATACTGATAGTACTGGG**CCGG**
Znf24_f_1	**CCGG**TCCTACAGTCAGAGCTCAAACctcgagGTTTGAGCTCTGACTGTAGGA**TTTTTG**
Znf24_r_1	***CG*CAAAAA**TCCTACAGTCAGAGCTCAAACctcgagGTTTGAGCTCTGACTGTAGGA**CCGG**

Znf24_f_2	**CCGG**GTTCTGTGGTTCTACTATTTActcgagTAAATAGTAGAACCACAGAAC**TTTTTG**
Znf24_r_2	***CG*CAAAAA**GTTCTGTGGTTCTACTATTTActcgagTAAATAGTAGAACCACAGAAC**CCGG**
Yy1_f_1	**CCGG**ACATCTTAACACACGCTAAAGctcgagCTTTAGCGTGTGTTAAGATGT**TTTTTG**
Yy1_r_1	***CG*CAAAAA**ACATCTTAACACACGCTAAAGctcgagCTTTAGCGTGTGTTAAGATGT**CCGG**
Yy1_f_2	**CCGG**CCCTAAGCAACTGGCAGAATTctcgagAATTCTGCCAGTTGCTTAGGG**TTTTTG**
Yy1_r_2	***CG*CAAAAA**CCCTAAGCAACTGGCAGAATTctcgagAATTCTGCCAGTTGCTTAGGG**CCGG**
Myt1_f_1	**CCGG**AGGAGGAAGATGAAGAGGAAGctcgagCTTCCTCTTCATCTTCCTCCTT**TTTTTG**
Myt1_r_1	***CG*CAAAAA**AAGGAGGAAGATGAAGAGGAAGctcgagCTTCCTCTTCATCTTCCTCCT**CCGG**
Myt1_f_2	**CCGG**AGGAGAAGAAGAAGAGGAGGActcgagTCCTCCTCTTCTTCTTCTCCTT**TTTTTG**
Myt1_r_2	***CG*CAAAAA**AAGGAGAAGAAGAAGAGGAGGActcgagTCCTCCTCTTCTTCTTCTCCT**CCGG**
Myt1_f_3	**CCGG**GAAGAAGAAGAGGATGAGGAGctcgagCTCCTCATCCTCTTCTTCTTCT**TTTTTG**
Myt1_r_3	***CG*CAAAAA**AGAAGAAGAAGAGGATGAGGAGctcgagCTCCTCATCCTCTTCTTCTTC**CCGG**
Myt1_f_4	**CCGG**AGGAGGAGGAAGAAGATGAAGctcgagCTTCATCTTCTTCCTCCTCCTT**TTTTTG**
Myt1_r_4	***CG*CAAAAA**AAGGAGGAGGAAGAAGATGAAGctcgagCTTCATCTTCTTCCTCCTCCT**CCGG**
Myt1_f_5	**CCGG**AGGAAGAAGAGGAGGAGGAAGctcgagCTTCCTCCTCCTCTTCTTCCTT**TTTTTG**
Myt1_r_5	***CG*CAAAAA**AAGGAAGAAGAGGAGGAGGAAGctcgagCTTCCTCCTCCTCTTCTTCCT**CCGG**
neg.ctrl_f	**CCGG**CAACAAGATGAAGAGCACCAActcgagTTGGTGCTCTTCATCTTGTTG**TTTTT**
neg.ctrl_r	***CG*AAAAA**CAACAAGATGAAGAGCACCAActcgagTTGGTGCTCTTCATCTTGTTG**CCGG**

Table 2: Primer

Primer name	Sequence 5'-3'	Application
Oligo-d(T)	ttttttttttttttt	cDNA synthesis
C-SF_f_Sfi	aataggcctcctaggccgctcggatccactagtaa	Direct cloning
C-SF_r_PmeI	tattgtttaaactgatcagcgagctctagcat	Direct cloning
U6_for	aatagatatcgatccgacgccgccatctc	Direct cloning
U6_rev	aataaagcttgttaacaaacaaggcttttctccaagg	Direct cloning
H1_for	aatagatatcgaacgctgacgtcatcaacc	Direct cloning
H1_rev	aataaagcttgttaacgtggtctcatacagaactta	Direct cloning
attB1	ggggacaagtttgtacaaaaaagcaggct	Gateway cloning
attB2	ggggaccactttgtacaagaaagctgggt	Gateway cloning
Sox11_NGW_f	aaaagcaggcttcgtgcagcaggccgagagc	Gateway cloning
Sox11_NGW_nterm_r	aagaaagctgggtgctcgaggctgtccttcagcatcttcc	Gateway cloning
Yy1_qRT_f	gatgatgctccaagaacaatagc	qRT-PCR
Yy1_qRT_r	ctttgccacactctgcacag	qRT-PCR
Myt1_qRT_f4	ttcatcacccacagacagct	qRT-PCR
Myt1_qRT_r4	gggaagttgcaatgatcccc	qRT-PCR
Tcf4_qRT_f3	cagggatcttgggtcacatg	qRT-PCR
Tcf4_qRT_r3	gtggcaaccctgaacgtt	qRT-PCR
Znf24_qRT_f2	acttgggttcgagagcatca	qRT-PCR
Znf24_qRT_r2	acaagcacttcccgtttctg	qRT-PCR
Pdhb_qRT_f	gtagaggacacgggcaagat	qRT-PCR
Pdhb_qRT_r	tgaaaacgcctcttcagca	qRT-PCR
CAG_IRES_GFP_rev	gacaaacgcacaccggcctt	Sequencing
C-SF_IRES_GFP_for	atggtaatcgtgcgagag	Sequencing

(TOPO)M13 for	caggaaacagctatgacc	Sequencing
(TOPO)M13 rev	tgtaaaacgacggccagt	Sequencing
PWX1_f	tgttaccactcccttaag	Sequencing
PWX1_r	ttaaaggtgccgtctcgc	Sequencing
pENTattL1for	tcgcgttaacgctagcatggatctc	Sequencing
pENTattL2rev	acatcagagattttgagacacgggc	Sequencing

3.1.9. Plasmids

Table 3: Vectors

Vector name	Vector type	Tag	Resistance
(C)SF-TAP pDEST	Destination Vector	(C)-SF-TAP	Ampicillin, Chloramphenicol, Neomycin
(N)SF-TAP pDEST	Destination Vector	(N)-SF-TAP	Ampicillin, Chloramphenicol, Neomycin
CAG-(C)SF-IRES-GFP	Destination Vector	(C)-SF-TAP	Ampicillin
CAG-IRES-GFP	Expression Vector		Ampicillin
Gateway® pDONR™221	Donor Vector		Kanamycin
Gateway® pENTR223	Entry Vector		Spectinomycin
pCR™4-TOPO® TA	TOPO Cloning Vector		Kanamycin, Ampicillin
pETM30	Expression Vector	6xHIS-GST	Kanamycin
PWX1_H1 (human promoter)	Knockdown Vector		Ampicillin
PWX1_U6 (mouse promoter)	Knockdown Vector		Ampicillin

Table 4: Constructs

Construct name	cDNA	Vector	Clone number (PlasmID)
(C)-SF-TAP pDEST-CBX6	CBX6	(C)-SF-TAP pDEST	
(C)-SF-TAP pDEST-MYT1	MYT1	(C)-SF-TAP pDEST	
(C)-SF-TAP pDEST-TCF4	TCF4	(C)-SF-TAP pDEST	
(C)-SF-TAP pDEST-TIF1b	TIF1b	(C)-SF-TAP pDEST	
(C)-SF-TAP pDEST-YY1	YY1	(C)-SF-TAP pDEST	
(C)-SF-TAP pDEST-ZNF24	ZNF24	(C)-SF-TAP pDEST	
(N)-SF-TAP pDEST-Sox11	Sox11	(N)-SF-TAP pDEST	
CAG-(C)-SF-IRES-GFP-CBX6	CBX6	CAG-(C)-SF-IRES-GFP	
CAG-(C)-SF-IRES-GFP-MYT1	MYT1	CAG-(C)-SF-IRES-GFP	
CAG-(C)-SF-IRES-GFP-TCF4	TCF4	CAG-(C)-SF-IRES-GFP	
CAG-(C)-SF-IRES-GFP-TIF1b	TIF1b	CAG-(C)-SF-IRES-GFP	
CAG-(C)-SF-IRES-GFP-YY1	YY1	CAG-(C)-SF-IRES-GFP	
CAG-(C)-SF-IRES-GFP-ZNF24	ZNF24	CAG-(C)-SF-IRES-GFP	
CAG-IRES-GFP-Sox11	Sox11	CAG-IRES-GFP	
pDONR221-Sox11	Sox11	pDONR221	
pDONR221-YY1	YY1	pDONR221	HsCD00076053
pENTR223-CBX6	CBX6	pENTR223	HsCD00372584
pENTR223-MYT1	MYT1	pENTR223	HsCD00370176
pENTR223-TCF4	TCF4	pENTR223	HsCD00365172

pENTR223-TIF1b	TIF1b	pENTR223	HsCD00378889
pENTR223-ZNF24	ZNF24	pENTR223	HsCD00399501
pETM30-Sox11	Sox11	pETM30	
PWX1_H1-Myt1_1	Myt1	PWX1_H1	
PWX1_H1-Myt1_2	Myt1	PWX1_H1	
PWX1_H1-Myt1_3	Myt1	PWX1_H1	
PWX1_H1-Myt1_4	Myt1	PWX1_H1	
PWX1_H1-Myt1_5	Myt1	PWX1_H1	
PWX1_H1-Tcf4_1	Tcf4	PWX1_H1	
PWX1_H1-Tcf4_2	Tcf4	PWX1_H1	
PWX1_H1-Yy1_1	Yy1	PWX1_H1	
PWX1_H1-Yy1_2	Yy1	PWX1_H1	
PWX1_H1-Znf24_1	Znf24	PWX1_H1	
PWX1_H1-Znf24_2	Znf24	PWX1_H1	
PWX1_U6-Myt1_1	Myt1	PWX1_U6	
PWX1_U6-Myt1_2	Myt1	PWX1_U6	
PWX1_U6-Myt1_3	Myt1	PWX1_U6	
PWX1_U6-Myt1_4	Myt1	PWX1_U6	
PWX1_U6-Myt1_5	Myt1	PWX1_U6	
PWX1_U6-Tcf4_1	Tcf4	PWX1_U6	
PWX1_U6-Tcf4_2	Tcf4	PWX1_U6	
PWX1_U6-Yy1_1	Yy1	PWX1_U6	
PWX1_U6-Yy1_2	Yy1	PWX1_U6	
PWX1_U6-Znf24_1	Znf24	PWX1_U6	
PWX1_U6-Znf24_2	Znf24	PWX1_U6	

3.1.10. *E.coli* strains

Library Efficiency® DH5a	Invitrogen, Carlsbad, CA, USA
One Shot® BL21(DE3)	Invitrogen, Carlsbad, CA, USA
One Shot® *ccd*B Survival™ 2 T1R	Invitrogen, Carlsbad, CA, USA

3.1.11. Antibodies

Table 5: Commercial antibodies for Western blot analysis

Antibody	Species	Dilution	Company
Anti-Actb	mouse monoclonal	1:10000	Sigma-Aldrich, St. Louis, MO, USA
Anti-FLAG® M2-Peroxidase (HRP)	mouse monoclonal	1:1000	Sigma-Aldrich, St. Louis, MO, USA
Anti-Gapdh	mouse monoclonal	1:10000	Merck, Darmstadt, Germany
Anti-GFP	rabbit polyclonal	1:5000	Invitrogen, Carlsbad, CA, USA
Anti-Myt1	rabbit polyclonal	1:1000	LifeSpan Biosciences, Seattle, WA, USA
Anti-Phox2b	rabbit polyclonal	1:1000	Acris Antibodies, Herford, Germany

Anti-Sox11	rabbit polyclonal	1:1000	Sigma-Aldrich, St. Louis, MO, USA
Anti-Tcf4	rabbit polyclonal	1:1000	Abcam, Cambridge, UK
Anti-Tif1b	rabbit polyclonal	1:1000	Cell Signaling, Danvers, MA, USA
Anti-Yy1	rabbit polyclonal	1:1000	Cell Signaling, Danvers, MA, USA
Anti-Znf24	rabbit polyclonal	1:5000	Novus Biological, Littleton, CO, USA

Table 6: In house produced anti-SOX11 protein specific monoclonal antibodies

Clone number	Species	IgG subtype	Clone number	Species	IgG subtype
7E2	rat	G1+2a	12D3	rat	2b
19B2	rat	2a	12D9	rat	2a
24F8	rat	G1+2a+2b	12D10	rat	2a
20A4	rat	G1	12G3	rat	2b
10D10	rat	G1	12G8	rat	2a
18C12	rat	2a+2b	13C6	rat	2a
20E12	rat	G1	13C11	rat	G1
18F10	rat	2b	14D9	rat	2a
10F12	rat	G1	14D11	rat	2a
12B11	rat	G1	14G8	rat	2c
12B3	rat	2b	14G9	rat	G1+2a
13G2	rat	G1+2a+2b+2c	14H1	rat	2b
17E1	rat	G1	15B12	rat	2a
17E6	rat	2a	15D12	rat	2a
13F2	rat	G1+2a	15 E3	rat	2a+2b
1D5	rat	G1	15 E8	rat	2a
5B7	rat	G1+2a+2b+2c	15G6	rat	2c
8G10	rat	G1	15G11	rat	2a
8H10	rat	G1	17B5	rat	G1
4H7	rat	2a	17C1	rat	G1
11F8	rat	2b	17 E2	rat	2b
4A4	rat	G1	17 E3	rat	2a
4H9	rat	G1	17 G1	rat	2a
2A12	rat	2b	18B1	rat	G1
8F4	rat	G1+2a+2b	18F11	rat	G1
1C9	rat	2c	19C3	rat	2a
1 E10	rat	2b	19G8	rat	2a
1H2	rat	2a	20B5	rat	2b
2 E7	rat	2a	20C5	rat	2a
2 E8	rat	2a	20 E7	rat	G1
2H6	rat	2a	21D9	rat	2a
3G9	rat	2b	21C1	rat	G1
3H7	rat	G1	21F5	rat	2a+2b
4H6	rat	G1	22A4	rat	G1

5F11	rat	2b	22B7	rat	2a
5G5	rat	2a	23A6	rat	2a
6A8	rat	2b	23D1	rat	2b
6B6	rat	2b	23D5	rat	2a
6D6	rat	2a	23F8	rat	2a
6H7	rat	2a	24A5	rat	G1
7H3	rat	G1+2a	24B2	rat	2a
8F1	rat	2b	24D11	rat	2a
8G7	rat	2b	6E4	mouse	2a
8F4	rat	G1	7C10	mouse	2a+2b
9 E12	rat	2a	6E2	mouse	2a
9H4	rat	G1	5E12	mouse	2a
10C5	rat	2a	1C3	mouse	2a+2b
10D6	rat	2a	4A11	mouse	2b
10 E10	rat	2a+2b	4E8	mouse	2a
10G2	rat	2b	4E7	mouse	2a
10G4	rat	2a+2b	6C2	mouse	2a
11A3	rat	2a	5B11	mouse	2b
11C1	rat	2a	2H5	mouse	2a
11C9	rat	2a	2A8	mouse	2b
11G11	rat	2a	5E3	mouse	2b

Table 7: Secondary antibodies, HRP-conjugated

Antibody	Species	Dilution	Distributor
anti-mouse IgG	goat polyclonal	1:15000	Jackson Immunoresearch, West Grove, PA, USA
ranti-rabbit IgG	goat polyclonal	1:15000	Jackson Immunoresearch, West Grove, PA, USA
anti-rat IgG	goat polyclonal	1:15000	Jackson Immunoresearch, West Grove, PA, USA
anti-rat IgG2a	mouse	1:8000	E. Kremmer
anti-rat IgG2b	mouse	1:4000	E. Kremmer
anti-rat IgG2c	mouse	1:4000	E. Kremmer
anti-rat IgG1	mouse	1:8000	E. Kremmer
anti-mouse IgG2a	rat	1:1000	E. Kremmer
anti-mouse IgG2b	rat	1:1000	E. Kremmer

3.1.12. Mass spectrometry

LTQ Orbitrap Velos	Thermo Fisher Scientific, Waltham, MA, USA
Q Exactive plus	Thermo Fisher Scientific, Waltham, MA, USA
Ultimate 3000 Nano-LC	Thermo Fisher Scientific, Waltham, MA, USA

3.1.13. Software and databases

3.1.13.1. Software

Corel Draw V.11.633	Corel Corporation, Ottawa, Canada
Cytoscape V.2.8.3	Cytoscape Consortium (http://www.cytoscape.org/index.html)
EndNote 9	Thomson Reuters, New York, NY, USA
Genomatix Software Suite V.3.2	Genomatix Software GmbH, München, Germany
ImageJ 1.41	W. Rasband, National Institutes of Health (NIH), Bethesda, MA, USA (http://www.hhs.gov)
Lightcycler® 480 software release 1.5.0 SP1 V.1.5.0.39	Roche, Penzberg, Germany
Mascot V.2.4.0	Matrix Science, Boston, MA, USA
MaxQuant V.1.5.0.30	J. Cox, M. Mann, Max-Planck Institute for Biochemistry, Martinsried, Germany (http://www.maxquant.org)
MS Office 2010 (Word, Excel, PowerPoint)	Microsoft, Redmond, WA, USA
Scaffold V.4.3.4	Proteome Software Inc., Portland, OR, USA (http://www.proteomesoftware.com/products/scaffold/)
Vector NTI Suite 9.0	Invitrogen, Carlsbad, CA, USA
XCalibur V. 2.07	Thermo Fisher Scientific, Waltham, MA, USA

3.1.13.2. Databases

Biogrid	http://www.thebiogrid.org/
Ensembl Genome Browser	http://www.ensembl.org/
GEO	http://www.ncbi.nlm.nih.gov/geo/
I2D	http://ophid.utoronto.ca/ophidv2.204/
NCBI	http://www.ncbi.nlm.nih.gov/
NCBI Blast	http://blast.ncbi.nlm.nih.gov/Blast.cgi
NCBI Nucleotide	http://www.ncbi.nlm.nih.gov/sites/entrez?db=nuccore
NCBI Protein	http://www.ncbi.nlm.nih.gov/sites/entrez?db=protein
NCBI PubMed	http://www.ncbi.nlm.nih.gov/sites/entrez
Pathway Commons	www.pathwaycommons.org/
Primer 3	http://primer3.ut.ee/
Swiss-Prot	http://www.expasy.ch/sprot/
ToppGene Suite	Cincinnati Children's Hospital Medical Center, Cincinnati, OH, USA (https://toppgene.cchmc.org/)
UniProt	http://www.uniprot.org/

3.2. Methods

3.2.1. Cell culture

3.2.1.1. Maintenance and growth of cells

Neuro2a cells and HEK-T cells were grown at 37°C in a humidified atmosphere containing 5% CO_2 in Dulbecco's Eagle Medium supplemented with 0.5% Penicillin/Streptomycin and 10% FBS (see 3.1.5.1.) until they reached confluency (3-4 days). At that time, the cells were washed with 5ml prewarmed dPBS, detached by incubation with 1ml Trypsin/EDTA for 3 minutes at 37°C, resuspended in fresh prewarmed growth medium and plated on new medium filled dishes in a ratio of 1:10 and 1:20 for HEK-T cells and Neuro2a cells, respectively.

3.2.1.2. Cryopreservation and thawing of cells

For the generation of cryoconservation stocks, cells of one 10cm plate were washed with dPBS, detached using Trypsin/EDTA and resuspended in growth medium, followed by centrifugation for 3min at 500xg. Subsequently the cell pellet was dissolved in cryo medium (see 3.1.5.1.) and distributed into five cryopreservation tubes. To avoid intracellular ice formation, a slow freezing procedure was applied. Therefore the aliquots were incubated for 20min at 4°, 1h at -20°C and overnight at -80°C before they were transferred to liquid nitrogen for long term storage. When thawing the cells again, they were defreezed quickly in a waterbath at 37°C to prevent them from DMSO-mediated cytotoxicity and resuspended in prewarmed growth medium. The next day, when cells had already adhered to the dish, the medium was exchanged to remove residual cryo medium and cell debris.

3.2.1.3. Transient transfection

Cells were seeded one day before transfection, enabling implementation of transient transfection at 50-60% confluency.

3.2.1.3.1. Effectene

Transient transfection using Effectene transfection reagent was performed in 6-well plates using 400ng DNA according to the manufacturer's manual.

3.2.1.3.2. PEI

PEI transfection reagent (1mg/ml) (see 3.1.5.1.) was added drop wise to the DNA in a ratio of 1:4 (1µg DNA corresponds to 4 µl PEI solution), mixed carefully and incubated for 15min at room temperature in order to allow complex formation. Meanwhile, the growth medium of the cells was exchanged with fresh prewarmed medium. 500µl medium (for 6 wells) was added to the PEI-DNA complexes and incubated for additional 10min. After that, the mixture was added drop wise onto the cells that were subsequently cultured for further 2 days post transfection.

3.2.1.4. Stable isotope labelling of amino acids in cell culture (SILAC)

Stable isotope labelling of amino acids in cell culture (SILAC) is a common approach used for quantitative mass spectrometry (Ong et al., 2002). It is based on the integration of heavy or light isotope-labelled amino acids into the proteome of cells. In this way, two conditions can be combined in one sample for proteomic analysis, enabling quantification by the formation of ratios. As the heavy labelling results in a specific peptide mass shift, specific binders can be distinguished from unspecific ones after tandem mass spectrometry, as it is shown in figure 7. Lysine and arginine are the most common selected amino acids for labelling, which ensures the presence of at least one labelled amino acid for tryptic peptides after LC-MS/MS analysis. Essential amino acids are chosen and dialysed serum is used to guarantee proper integration of the correct amino acids. The selected heavy arginine results in a mass shift of 6Da compared to the light form, whereas peptides comprising the heavy labelled lysine are 4Da heavier than the ones with the light lysine incorporated.
As described earlier (Boldt et al., 2014), for SILAC labelling cells were cultured in SILAC DMEM lacking L-lysine and L-arginine, complemented with 0.5% Penicillin/Streptomycin, 10% dialysed FBS, 2% L-glutamine, 2mM proline 0.55mM lysine and 0.4mM arginine (see 3.1.5.1.). Proline was added in order to prevent arginine to proline conversion (Bendall et al., 2008). Light labelled medium was supplemented with the amino acids $^{12}C_6$, $^{14}N_2$ -L-lysine and $^{12}C_6$, $^{14}N_4$ -L-arginine whereas heavy labelled medium was supplemented with 4.4.5.5-D_4-L-lysine and $^{13}C_6$, $^{14}N_4$-L-arginine. After approximately 4 cell doublings, meaning about 2 weeks, the labelled aminoacids were integrated into the proteins and experiments could be performed.

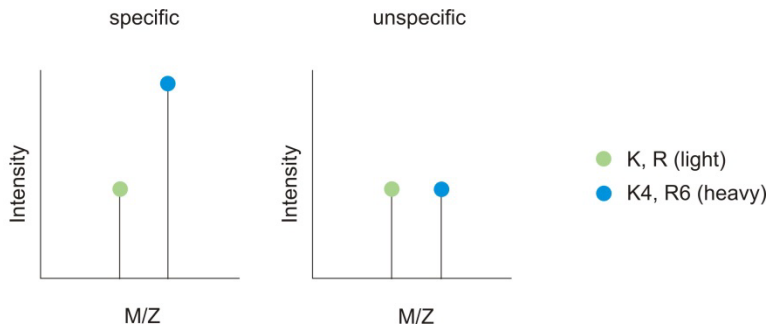

Figure 7:SILAC quantification after LC-MS/MS
SILAC labelling of cells results in a mass shift in the peaks after tandem mass spectrometry analysis. This allows the discrimination of specific or unspecific binders and the quantification by generation of ratios.

3.2.1.5. Generation and maintenance of stable expression cell lines

Neuro2a cells were transfected in 10cm dishes using 3.2 µg DNA of either (N)-SF-TAP pDEST-Sox11 or empty vector control by application of PEI transfection reagent. After two days, they were splitted in a ratio of 1:100 on 10cm plates. From that step on, the growth medium was supplemented with 500µl/ml G418, which selects the plasmid carrying cells from the others due to the neomycin resistance of the vector. Every other day the medium was exchanged. After 19 days, clones formed by the surviving cells were picked under microscope control into 24-well plates, one clone per well with each well containing 1ml growth medium complemented with 750µg/ml G418. When the cells were confluent, they were expanded stepwise to 6-wells and 10cm dishes. The stable expression level was determined by western blot analysis of nuclear extracts and Strep affinity purification followed by mass spectrometry.

3.2.2. Molecular biology

3.2.2.1. Enzymatic DNA treatments

3.2.2.1.1. DNA restriction

Restriction enzymes cut double stranded DNA at or next to specific recognition sites, resulting in blunt or sticky ends, depending on the type of enzyme.
DNA was digested via restriction enzymes using the corresponding buffers and reaction conditions provided by NEB on the website (http://www.neb.com). 2000 units of restriction enzyme were applied for the digestion of 1µg DNA. Usually 5µg of target

cDNA containing plasmid and 5µg of the destination vector were incubated with the same restriction endonucleases for 2h. When double digestion was performed, the reaction buffer with the best reactivity for both enzymes was selected. In some cases this was not possible, that's why a sequential restriction procedure was applied with a purification step after the first step using PCR purification kit according to the manufacturer's instructions. The reaction was stopped by incubation on ice and the cut fragments were purified from agarose gels using the gel extraction kit according to the manufacturer's instructions.

3.2.2.1.2. A-tailing of DNA fragments

A-tailing implies the addition of a dATP to the 3' end of blunt ending dsDNA which results in A overhangs. DNA fragments carrying this modifcation can be used for TA cloning, where T and A overhangs anneal without the further need of restriction enzymes. For the A-tailing 20µl of a blunt end PCR product, obtained with the Phusion polymerase was incubated with 0.1µl Taq polymerase, 5µl Taq reaction buffer (10x), 5µl dATP (2mM) and 1.25µl $MgCl_2$ (50mM) in a total reaction volume of 50µl for 15min at 72°C. After termination of the reaction on ice, the product was purified via PCR purification kit.

3.2.2.1.3. Annealing of DNA fragments

Single stranded DNA molecules anneal through the formation of hydrogen bonds between the complementary nucleobases A/T and G/C which results in basepairs, leading to the generation of double stranded DNA sequences.
Oligonucleotides were annealed using 2µl of each of the complementary fragments in a total reaction volume of 20µl obtained by addition of 16µl nuclease free water. The reaction was incubated in a Thermocycler for 4min at 94° to linearize the ssDNA and subsequently the fragments were annealed at 70°C for 10min, followed by slow cool down to prevent the Oligos from denaturing.

3.2.2.1.4. Phosphorylation of DNA fragments

Blunt ended double stranded DNA fragments have to be phosphorylated at the 5' OH group to enable ligation with restricted plasmid vectors.
Therefore, 5µl of annealed Oligonucleotides were incubated with 1µl polynucleotide kinase (PNK), 0.1µl ATP (10mM) and 1µl PNK reaction buffer (10x) in a total volume of 10µl with nuclease free water for 90min at 37°C. Subsequently the reaction was terminated by cool down on ice.

3.2.2.1.5. Ligation

DNA fragments that were cut by restriction endonucleases can be joined by the formation of phosphodiester bonds between the 3'OH group and the phosphorylated 5' OH group of both molecules, enzymatically catalysed by T4 DNA Ligase.
For the ligation of a DNA fragment with the vector backbone, a three times greater amount of the insert in terms of molarities compared to the vector was incubated together with the backbone, complemented with 1µl of T4 DNA Ligase and 1µl T4 DNA Ligase reaction buffer (10x) in a total reaction volume of 10µl at 15°C overnight.

3.2.2.2. E.coli culture and plating

Bacteria were grown in LB-medium (see 3.1.5.2) supplemented with special antibiotics as selection markers. Depending on the plasmid coded antibiotica resistance, Ampicillin (100µg/ml), Kanamycin (50µg/ml), Chloramphenicol (30µg/ml) and Spectinomycin (100µg/ml) were applied. The *E.coli* were cultured in volumes of 5ml or 100ml according to the following experiments. Following bacterial transformation, *E.coli* were spread out on LB-agar plates (see 3.1.5.2), also complemented with selection antibiotics in the above-mentioned concentrations.

3.2.2.3. Transformation and cryoconservation of E.coli

Transformation is referred to the uptake of pure DNA into the bacterium. Plasmid DNA constructs were transformed into *E.coli* by application of the heat shock method. In this technique chemically competent bacteria are heated to 42°C to make the cell wall permeable by the induction of pore formation, that enable the uptake of supercoiled plasmid DNA into the cells.

To transform vectors into the competent cells, 50µl of library efficient DH5α, one aliquot of one shot BL21 or one shot *ccd*B survival strain respectively were incubated with 1µl (100ng/µl) plasmid DNA or 5µl of a ligation reaction for 1h on ice, followed by heat shock at 42°C for 30s, 2min cool down on ice and incubation with 250µl SOC medium for 1h at 37°C in the shaking bacteria incubator to initiate bacterial growth. After that, 30-200µl were spread out on LB-agar plates containing selection antibiotics specific for the transformed vector, in order to prevent unspecific bacteria contamination and the plates were incubated at 37°C overnight. Formed colonies were transferred into 5ml of LB-medium supplemented with the corresponding selection antibiotics and cultured overnight. The day after, cryoconservation stocks could be prepared. Therefore 500µl of the bacterial culture was mixed thoroughly with 500µl sterile 80% glycerol and was thereafter stored at -80°C. DNA could be purified from the remaining culture. When the *E.coli* were thawed again, a small amount of the frozen cryo stock was transferred into 5ml LB-medium containing the corresponding antibiotics using an inoculation loop and the bacteria were grown at 37°C overnight.

3.2.2.4. DNA isolation from E.coli

DNA was purified from bacterial cultures using the GeneJET™ Plasmid Miniprep Kit for 5ml cultures and PureYield Plasmid Midiprep Kit or EndoFree Plasmid Maxi Kit for 100ml cultures according to the manufacturer's instructions.
The yield was determined in 1:100 dilutions by photometric measurement of the absorbance at 260nm and 280nm and subsequent automatic calculation of the DNA concentration according to the following formula:

DNA concentration [ng/µl] = OD_{260} x 50 x dilution factor

Additionally, the ratio of OD_{260}/OD_{280} was determined, indicating the purity of DNA, which is best at a ratio of 1.8.

3.2.2.5. Polymerase chain reactions

Polymerase chain reactions enable the fast and effective amplification of DNA fragments. At the first step, the dsDNA is denatured to single strands at 98°C for 5min (Initial denaturation), before several cycles (30-35) of the following three steps are performed to ensure a great yield of PCR product. At the beginning of every cycle, the DNA is denatured at 98°C for 1min (Denaturation), then forward and reverse primers bind to their complementary sequences each on one strand at a specific temperature (Annealing), before the amplification of both strands takes place at 72°C, catalysed through Phusion High-Fidelity DNA Polymerase (see 3.1.7) (Elongation). Thereafter, a final extension step is performed at 72°C for 10min, before the reaction is terminated by cool down to 4°C. The following PCR program is adjusted for every PCR, as the template length differs, which results in the variation of elongation time. Also the annealing temperature has to be calculated freshly for each primer pair according to the melting temperatures (T_m) of the primers.

Initial denaturation	98°C	5min	
Denaturation	98°C	1min	35x
Annealing	55°C *(55°C-71°C)*	1min	
Elongation	72°C	30s *(1min per 1kb)*	
Final extension	72°C	10min	
Cool down	4°C	∞	

Usually, 60ng of genomic DNA and 1ng of plasmid DNA respectively were utilised as template. 1µl dNTP mix (10mM of each nucleotide), 10µl Phusion HF reaction buffer (5x), 1.5µl $MgCl_2$ (50mM), 2.5µl of each primer (10µM), 0.5µl Phusion Polymerase (2U/µl) and nuclease free water were added to the DNA in a final reaction volume of 50µl.

3.2.2.6. Cloning of plasmid expression vectors

3.2.2.6.1. Classical cloning

Classical cloning is referred to the insertion of a target DNA fragment into a vector backbone by the use of corresponding restriction endonucleases that create matching overhangs, which can be ligated together. For the generation of expression vectors using classical cloning, two procedures were applied. In the first approach the target sequence was cut out of an existing plasmid vector (5µg) with the same restriction enzymes the destination vector (5µg) was cut, both digestions were purified from an agarose gel using a gel extraction kit (see 3.1.6) and then the fragments were ligated using T4 DNA ligase at 15°C overnight (see 3.2.2.1.5). The other method includes the amplification of the fragment using PCR primers carrying the corresponding restriction sites at the ends. The PCR product was digested with the required restriction enzymes, purified from an agarose gel and ligated with the vector backbone. The success of the cloning was determined via transformation, DNA isolation followed by restriction digestion or sequencing.

3.2.2.6.2. TOPO cloning

If there was no successful ligation of the PCR product with the plasmid, TOPO cloning using the TOPO TA Cloning Kit (see 3.1.6) was applied. Therefore 3' adenine overhangs were added to the undigested PCR fragment via A-tailing (see 3.2.2.1.3), allowing the integration of the product into the TOPO vector via TA cloning (annealing of A and T overhangs of the insert and vector) according to the manufacturer's instructions. Once the TOPO reaction was transformed into *E.coli* and DNA was isolated, the vector was cut with the pair of restriction enzymes that had been incorporated into the PCR primers and the fragment could be ligated with the appropriate digested destination vector.

3.2.2.6.3. Gateway cloning

Gateway cloning is a highly efficient and universal cloning method from Invitrogen, that is based on site specific recombination of attachment (*att*) sites of bacteriophage lambda into *E.coli* (Landy, 1989). It enables cloning where no suitable restriction sites are available and simplifies the transfer of cDNA between different destination vectors. The first reaction (BP-reaction) is mediated by the lysogenic pathway, where

recombination of an *att*B-flanked PCR product with an *att*P-donor vector creates an *att*L-comprising entry clone and an *att*R-containing by-product. This is catalysed by the bacteriophage λ Integrase (Int) and *E.coli* Integration Host Factor (IHF) proteins (BP Clonase™ enzyme mix) (see figure 8). The reaction is transformed into *E.coli* under kanamycine selection as the entry clone carries the resistance. Both by-product and pDONR vector comprising bacteria die because of the cytotoxic *ccd*B gene they carry. The LR-reaction is part of the lytic pathway, where the *att*L sites of the entry vector recombinate with *att*R sites of the destination vector, which results in an *att*B site carrying expression clone and a by-product comprised of *att*P1 sites. The reaction is mediated by the bacteriophage λ Int and Excisionase (Xis) proteins and the E. coli Integration Host Factor (IHF) protein (LR Clonase™ enzyme mix). The selection of the expression clone with ampicillin results in the loss of all bacteria carrying the *ccd*B gene (destination vector and by product) and the entry vector (no ampicillin resistance).

At the beginning of the gateway cloning procedure, the PCR product of the gene of interest was generated (see 3.2.2.5). Thereafter, the *att*B sites were linked to the PCR fragment during another PCR, using the *att*B Primers (see table 2). Subsequently the BP-reaction was performed by incubating 3µl of the *att*B carrying PCR product with 1µl pDONR vector (90ng/µl) and 1µl BP-clonase II mix (see 3.1.7) for 4h at 25°C. The reaction was terminated by incubation with 0.5µl proteinase K for 10min at 37°C. After transformation and selection via kanamycin, DNA was isolated, followed by LR-reaction. Therefore, 1µl of the DNA (100ng/µl) were incubated with 1µl pDEST vector (100ng/µl), 2µl Miniprep elution buffer and 1µl LR clonase II mix (see 3.1.7) for additional 4h at 25°C. Thereafter, 0.5µl proteinase K was added and the reaction was incubated at 37°C for 10min. Subsequently the complete LR-reaction was transformed into *E.coli*.

Figure 8:Gateway BP- and LR-Reaction
The BP clonase II enzyme mix mediates the recombination of the *att*B sites of the PCR product with the *att*P sites of the pDONR vector, which results in an *att*L site containing entry clone and an *att*R site carrying by-product. The *att*L sites of entry vector recombinate with the *att*R sites of the destination vector, catalysed by the LR clonase II enzyme mix which results in the *att*B site comprising expression clone and an *att*P1 containing by-product.

3.2.2.7. Induction of protein expression in BL-21 cells

The induction of protein expression in the *E.coli* strain BL21 is possible through the use of expression vectors comprising the gene of interest under the control of a T7 promoter, which itself gets activated by T7 RNA polymerase, which is produced by the BL21 cells under the control of the lacUV5 promoter. This promoter can be induced by IPTG, resulting in expression of the protein of interest.

For this purpose, the gene of interest carrying pETM30 vector was transformed into competent BL21 cells and an overnight grown culture was divided 1:100 into 2 100ml cultures that were cultured until OD_{600} reached values between 0.5 and 0.7. Subsequently the expression was induced by incubation with 0.5mM IPTG for 4h at 22°C under shaking. Thereafter, the cells were pelleted at 5000xg for 10 min and stored at -20°C.

3.2.2.8. Nickel-NTA purification

Recombinant proteins carrying a His tag can be easily purified using nickel chelate affinity chromatography. Nickel-NTA agarose filled columns bind the His tag via Nickel ions while other proteins pass through leading to purification of the tagged proteins. After washing, the elution is performed stepwise using increasing Imidazole concentrations.

Protein expression was induced in BL21 cells. The pelleted cells of 200ml culture volume were resuspended in 4ml lysis buffer (see 3.1.5.3) and lysed by application of 8 ultrasonic intervals of 15s duration and 15s breaks in between. After the subsequent centrifugation at 14000xg at 4°C for 30min, the supernatant was transferred to a Ni-NTA matrix filled column (500ml 50% suspension), that had been washed with 5ml HPLC water and equilibrated with 2.5ml lysis buffer beforehand. The column was rotated for 1h at 4°C, followed by collection of the flowthrough and 3 proximate 5min washing steps with 5ml wash buffer (see 3.1.5.3). Finally, the recombinant protein was eluted in 5 steps with increasing imidazole concentrations, using 0.5ml elution buffers 1 (50mM), 2 (100mM), 3 (150mM) and twice 4 (250mM) (see 3.1.5.3). The matrix was regenerated by incubation with 5ml 0.5M NaOH for 30min and washed with 1ml 30% EtOH, before it was stored at 4°C in a 50%-slurry with 30% EtOH.

3.2.2.9. Dialysis

Dialysis provides a possibility to remove toxic reagents by the exchange of buffers. Here, purified proteins were dialysed against PBS using the slide-a-lyser system. The chamber was hydrated in PBS, loaded with the protein suspension and dialysis was performed in a PBS filled beaker on a magnetic stirrer for 2 times 90min and finally overnight at 4°C. In between the incubation steps the buffer was exchanged with fresh PBS. The dialysed suspension was subsequently removed from the chamber.

3.2.3. Gene expression analysis

3.2.3.1. Isolation of total RNA

Total RNA was purified from Neuro2a cells using the peqGOLD Total RNA Kit according to the manufacturer's instructions applying biopure reaction tubes and barrier tips. The RNA was kept on ice until concentration was determined, thereafter stored at -80°C.

3.2.3.2. Qualitative and quantitative evaluation of RNA

Quantification and qualitative analysis of isolated RNA was performed by photometric measurement at 260nm and 280nm. The purity and quality was assessed by the ratio of OD_{260}/OD_{280} which has his optimum for RNA at a value of 2. A higher ratio indicates degradation, whereas a lower ratio points to contamination with DNA. The concentration of purified RNA was calculated according to the following formula.

RNA concentration [ng/µl] = OD_{260} x 40 x dilution factor

3.2.3.3. cDNA synthesis

Reverse transcription of mRNA into cDNA was performed by application of the Omniscript Reverse Transcription Kit (see 3.1.6) using Oligo-d(T) primer (see table 2) according to the manufacturer's instructions in RNAse free reaction tubes. A RT-control, a mixture of RNA samples to that no reverse transcriptase was added, was also implemented.

3.2.3.4. Quantitative Real-Time PCR

Real-time PCR provides a powerful tool for the relative quantification of gene expression levels. The fluorescent dye SYBR green incorporates into double stranded DNA, which allows the monitoring of DNA amplification in real-time starting from the beginning of the elongation phase. The lower the initial amount of DNA present in the reaction, the more cycles it takes until fluorescence is detectable. As the amount of fluorescence is proportional to the quantity of PCR product, the cycle number when the signal rises above the background fluorescence and becomes detectable at the early exponential phase can be calculated. This time point is named

the crossing point (C_p) and is used for the quantification of the original DNA level. The C_P values are compared to the crossing points of reference genes that have to be ubiquitously expressed in stable levels, to enable relative quantification. The theoretical efficiency of each amplification step has a value of 2, as the amount of PCR product doubles in every cycle, but in reality it is mostly lower, leading to the need of efficiency calculation for each PCR product. To this end a standard curve using serial dilution of a cDNA-mix (1:10, 1:50, 1:250, 1:1250) was integrated in every run, as the efficiency (E) can be calculated according to the slope of the standard's regression line, exemplified by the following formula.

$$E = 10^{\left(\frac{-1}{-slope}\right)}$$

The relative expression (R) was calculated considering the $\Delta\Delta C_P$ method introduced by Pfaffl in 2001 (Pfaffl, 2001), integrating the efficiency of target and reference gene, as well as ΔC_P values of control and sample, as illustrated by the following formula.

$$R = \frac{E_{target}^{\Delta C_{P\ target}^{(control-sample)}}}{E_{reference}^{\Delta C_{P\ reference}^{(control-sample)}}}$$

The quantitative real-time PCR was performed on a Lightcycler480 (Roche) in biological triplicates of sample and controls whereas standards were measured in duplicates. Data were normalised to pyruvate dehydrogenase beta (Pdhb) as reference gene. Melting curve analysis was applied to ensure specific amplification of the desired PCR product.

3.2.4. Protein chemistry

3.2.4.1. Extraction of nuclear lysates

Nuclear extraction provides an efficient method for the enrichment of nuclear proteins such as transcription factors and transcriptional modulators.
To this end, confluent cells were washed with 10ml dPBS and harvested in 2.5ml dPBS per 14cm plate using cellscrapers. Thereafter, cells were pelleted at 500xg for 5min, resuspended in 1ml dPBS and pelleted again at 500xg for 5min at 4°C. Subsequently the cytoplasmic fraction was collected by resuspending the cells in 3 times volume according to pellet size in buffer A (see 3.1.5.5). After 15 min of incubation 0.1% NP40 was added for 2min in order to break the cell membrane. Following centrifugation at 10000xg for 5min at 4°C the supernatant was removed (cytoplasmic fraction) and the nuclei were harshly resuspended in 2 times volume according to pellet size buffer C (see 3.1.5.5) and rotated on an intellimixer for 20 min at 4°C. After centrifugation at 10000xg for 5min at 4°C the supernatant containing nuclear proteins was collected.

3.2.4.2. Quantification of protein concentration

Protein concentration was determined using the Bradford assay. It is based on the complex formation of the dye Coomassie brilliant blue with proteins under acid conditions. The maximum of absorption of the dye which is at 465nm without proteins is shifted to 595nm in the presence of protein-dye complexes. The concentration can be calculated by applying a standard curve using BSA as standard protein (Bradford, 1976). The determination of protein concentration was performed in triplicates. Therefore, standards with BSA concentrations of 0, 0.2, 0.4, 0.6, 0.8 and 1mg/ml were prepared, 20µl of the standards or 1µl of each sample were mixed with 1ml of Bradford protein assay dye reagent (1x) and subsequently the absorbance was assessed by photometric measurement at 595nm.

3.2.4.3. SDS-polyacrylamide electrophoresis (SDS-PAGE)

The SDS-PAGE enables the separation of proteins according to their molecular weight. SDS forms complexes with the proteins, prevents in this way protein interactions, masks their intrinsic charge and creates anions. The presence of β-Mercaptoethanol in the loading buffer impedes formation of secondary structures as it destroys disulphide bonds. Additionally the samples can be further denatured by incubation at 96°C for 3min. These steps allow the fractionation of proteins only by their size. While proteins pass the stacking gel (pH 6.8, 4% acrylamide) chloride ions move in front of them. Uncharged Glycin ions follow the protein-SDS complexes and overtake them as the ions get negatively charged due to the pH change at the border to the separation gel (pH 8.8, 10% acrylamide) and concentrate the proteins to a sharp line, allowing the start of separation, with smaller proteins faster migrating than bigger ones (Schagger and von Jagow, 1987).

Gels were casted using the Mini-Protean 3 system chambers and 0.75mm spacers. The separation gel was prepared (see table 9), filled between the glass plates and was covered with isopropanol. After polymerisation of the acrylamide/bisacrylamide matrix, that was started by ammonium peroxodisulfate (APS) and catalysed by N,N,N',N'-tetramethylethylenediamine (TEMED), isopropanol was removed and the stacking gel (see table 8) was added. Finally, combs with the desired well number were inserted. The gels were placed into the gel chambers which were filled with running buffer exactly like the buffer chambers. The combs were removed and the wells rinsed with running buffer to remove residual gel pieces.

The nuclear lysates were mixed with 5x Laemmli buffer at defined protein amounts (10-60µg) in a total volume of 15-20µl, denatured for 3min at 96°C, cooled down and loaded onto the stacking gel. 6µl of PageRuler (170kDa) was used as size standard. The gels were run at 80V until the proteins entered the separation gel, then 120V were applied until the bromophenol blue line reached the bottom of the separation gel.

Table 8: Stacking gel solution

Reagent	Volume [ml]
1.5M Tris-HCl pH 6.8	0.7
30% (w/v) Bis-Acrylamid/Acrylamid (37,5:1)	0.7
ddH_2O	3.5
10% (w/v) SDS	0.05
Bromophenol blue	0.005
TEMED	0.02
10% (w/v) APS	0.05

Table 9: Separation gel solution

Reagent	Volume [ml]
1.5M Tris-HCl pH 8.8	2.5
30% (w/v) Bis-Acrylamid/Acrylamid (37,5:1)	3.3
ddH_2O	4
10% (w/v) SDS	0.1
TEMED	0.02
10% (w/v) APS	0.05

3.2.4.4. Coomassie Staining of SDS-gels

Polyacrylamid gels were first stained with Coomassie brilliant blue in 1965 (Meyer and Lamberts, 1965). The dye forms stable non-covalent complexes with proteins, on the basis of Van der Waals forces and electrostatic interactions.
Gels were subjected to Coomassie staining in order to estimate protein concentration after affinity purification or to determine purity of proteins after purification of proteins. To this end, the proteins run on the polyacrylamide gels were fixed by incubation for 3 times 10min in fixer solution (see 3.1.5.6) and subsequently stained with Coomassie staining solution (see 3.1.5.6) for 30s-2min. Thereafter, the gels were destained by 3 times incubation for 10min in fixer solution, until only the protein bands were visible.

3.2.4.5. Western blot analysis and detection

Proteins can be easily immobilised, as they are transferred from SDS-polyacrylamid gels to nitrocellulose or PVDF membranes without loss of resolution. Antibodies can be bound and the signals are detectable via autoradiography (Towbin et al., 1979).
Here, proteins were transferred to polyvinylidene difluoride membranes (PVDF) using the tank blotting system Mini Trans-Blot® Cell from Biorad. Foam pad and whatman

papers were equilibrated in Western buffer (see 3.1.5.6) The black side of the gel holder cassette was covered with a wetted foam pad and 2 whatman papers. Then the gel was placed on the paper, followed by the PVDF membrane that was activated in methanol for 1min before. 2 more whatman papers and one foam pad were placed on top of the membrane. Between each step air bubbles were removed using a blot roller. The cassette was closed and placed into the blotting module in the tank with the black sides facing each other, which was filled with western buffer and one ice pack. The blotting was performed in a cold room at 90V for 90min. Thereafter, the membrane was incubated for 1h in blocking solution (see 3.1.5.6) in a falcon under rolling, followed by overnight incubation with a protein specific primary antibody (see 3.1.11). After three 10min washing steps with TBS-T the secondary HRP-coupled antibody (see 3.1.11) which recognised the species of the primary antibody was applied for 1h, before the membrane was washed additionally three times for 10min. Thereafter, the detection was carried out using the ECL or ECLplus system according to the manufacturer's instructions. Subsequently, the chemiluminescence signals that were generated through the reaction of the horseradish peroxidase from the secondary antibody with the luminol of the ECL reagent were detected on hyperfilms in a developer machine.

3.2.5. Analysis of protein-protein interactions

3.2.5.1. Co-Immunoprecipitation

Co-Immunoprecipitation (Co-IP) is a suitable method for the analysis of protein interactome analysis. Specific antibodys for a chosen bait protein are bound to a matrix which is coupled to an immunoglobulin binding protein, in most cases one of the Streptococcal proteins G or A, which are capable of binding to antibodys with different specificities to various species and immunoglobulin subtypes. By addition of cell lysate, the bait protein is captured by the coupled bait-specific antibody and can be pulled down upon elution. Contemporarily, interaction partners that are bound to the bait protein at that time, also referred to as preys, are co-precipitated. The interaction partners can subsequently be determined by mass spectrometric or western blot analysis.

In this study, 500µg nuclear lysate was incubated with 1ml of antibody from hybridoma supernatant (0.02µg/µl) with addition of 1ml nuclear extraction buffer C

(see3.1.5.5) or 1µg of commercial antibody in a minimal reaction volume of 500µl, filled up with nuclear extraction buffer C on an intellimixer at 4°C overnight in order to enable antibody-bait binding. The day after, 10µl of the packed Protein G PLUS-Agarose beads (see 3.1.4) were washed three times with PBS and pelleted at 1000xg for 1min and were directly added to the antibody-nuclear lysate suspension and incubated for additional 3 hours at 4°C on the end-over-end shaker to couple the antibody to the matrix. Thereafter, the solution was transferred to microspin columns and the beads were washed three times using nuclear extraction buffer C and pelleted at 100xg for 5s. Subsequently, the proteins were eluted by addition of 20µl 2x Laemmli buffer and incubation for 30min at 37°C under shaking or by a 2 step elution with incubation of 2 times 200µl 100mM glycine, pH 2.5 for 5min at room temperature, followed by neutralisation with 2M Tris.

3.2.5.2. Strep affinity purification

The Strep affinity purification is an efficient tool for the co-immunoprecipitation of proteins coupled to a tandem Strep-tag II allowing protein complex analysis. This one-step purification method is part of the Strep FLAG tandem affinity purification strategy (SF-TAP) published before (Gloeckner et al., 2007). To that end, over-expressed proteins are linked to a SF-TAP tag, comprised of a tandem Strep-tag II and a FLAG-tag with a molecular weight of 4.6kDa in total (see figure 9). The Strep tag is able to bind to a Strep Tactin matrix and can be eluted via D-Desthiobiotin.

Figure 9:Strep FLAG tandem affinity purification tag (SF-TAP)
The structure of (N) SF-TAP starts with the FLAG tag at the N-terminus, followed by a tandem Strep-tagII, whereas the (C) SF TAP begins with the tandem Strep-tagII at the N-terminal end and possesses the FLAG tag at the C-terminus.

Nuclear lysates were incubated with 25µl packed Strep Tactin Superflow (see 3.1.4) beads per 14 cm dish for 1h with addition of 300U benzonase nuclease per mg nuclear extract to exclude DNA-mediated interactions between proteins. Thereafter,

the suspension was transferred into spin columns and washed three times with washing buffer (see 3.1.5.5), centrifuged at 100xg for 5s and eluted with 400µl Strep elution buffer (1x) containing D-Desthiobiotin for 10min on an end-over-end shaker at 4°C, followed by centrifugation at 1000xg for 1min at 4°C.

3.2.5.3. FLAG affinity purification

The one-step FLAG affinity purification is a suitable method for the analysis of protein-protein interactions. It is based on the pulldown of proteins linked to a FLAG tag via the affinity of the tag to anti-FLAG-M2-agarose. The protein complexes are eluted by replacement using FLAG octapeptide. The affinity of the FLAG system is higher than the Strep affinity purification method. This tool is the second part of the Strep FLAG tandem affinity purification strategy (SF-TAP) (Gloeckner et al., 2007) but can also be performed as one-step purification. The same SF-TAP tag (see figure 9) as for Strep affinity purification is used.
Nuclear extracts were incubated in micro spin columns with 12.5µl packed anti-FLAG-M2-agarose beads per 14cm dish for 1h on a rotating intellimixer at 4°C, with the beads washed before 3 times in nuclear extraction buffer C at 5000xg for 1min. 300U benzonase nuclease was added per mg lysate in order to eliminate DNA-dependent interactions of the bait protein with other proteins. Thereafter, the matrix was washed 3 times using washing buffer (see 3.1.5.5) by gentle centrifugation at 100xg for 5s to prevent the beads from running dry. Subsequently, 200µl FLAG peptide (0.2µg/µl in 1x TBS) elution buffer was added to the agarose and rotated for 10min at 4°C, followed by centrifugation at 1000xg for 1min at 4°C.

3.2.5.4. Methanol-Chloroform precipitation

The precipitation of proteins in solution is possible through methanol-chloroform precipitation according to the protocol published by Wessel and Flügge in 1984, which allows the efficient precipitation of proteins even in the presence of salt, detergents or ß-mercaptoethanol (Wessel and Flugge, 1984). To one part of sample, 4 parts methanol and one part chloroform is added. The addition of 3 parts water results in phase separation, leading to the precipitation of proteins in the interphase of methanol-chloroform-water. The removal of the upper phase and further addition of methanol results in pelleted proteins after centrifugation.

To that end, to 200µl aliquots of protein solutions 800µl methanol was added, mixed by vortexing and centrifuged at 9000xg for 30s. Thereafter, 200µl chloroform was added, mixed again by vortexing and centrifuged at 9000xg for 30s. Following the addition of 600µl HPLC water, vortexing and centrifugation at 9000xg for 2min, two phases were visible, with the precipitated proteins present in the interphase. The upper aqueous phase was removed carefully and discarded, additional 600µl methanol were applied to the sample and mixed briefly. Subsequent centrifugation at 16000xg for 2min revealed a protein pellet that was dried under air flow after removal of the supernatant.

3.2.5.5. In-solution tryptic proteolysis

The tryptic cleavage of proteins in-solution was carried out according to a protocol published before (Gloeckner et al., 2009). Trypsin is a serine protease from the pancreas that hydrolises peptide bonds at the carboxyl end of the amino acids arginine and lysine, when the next following amino acid is no proline. This tryptic digestion of peptide chains leads to small peptide fragments that are suitable for mass spectrometry analysis. The surfactant RapiGest is added to the reaction in order to facilitate the solubilisation of the precipitated proteins (Yu et al., 2003). The addition of Dithiothreitol (DTT) prevents cysteine-rich peptides from random oxidation and reduces disulfide bonds, whereas 2-iodoacetamide (IAA) is used for the alkylation of the cysteine residues.

The precipitated proteins (10-20µg) were dissolved in 30µl ammonium bicarbonate (50mM) with the addition of 4µl RapiGest surfactant (2%) by vortexing strongly. After that, 1µl DTT (100mM) was added, mixed and incubated at 60°C for 10min. Subsequently, the samples were cooled down to room temperature and incubated with 1µl IAA (300mM) for 30min at room temperature in darkness, as IAA is heat- and light-sensitive. The peptides were digested using 2µl trypsin solution (1µg/µl trypsin in 1mM HCl) overnight. The next day, 1.9µl trifluoroactetic acid (TFA) (100%) was added to a final concentration of 5% to quench the enzymatic digestion. The reaction was transferred to polypropylene inserts in reaction tubes, was incubated for 10min at room temperature, followed by centrifugation at 16000xg for 10min and finally the peptide solution between the pellet and the upper oleic phase was regained.

3.2.5.6. In-gel pre-fractionation

The in-gel pre-fractionation and tryptic cleavage of samples prior to LC-MS/MS analysis was performed according to a protocol published before (Gloeckner et al., 2009). The protein lysate was subjected to SDS-PAGE, but the electrophoresis was stopped when the sample had run approximately 1cm in the separation gel. Thereafter, the gel was stained by Coomassie brilliant blue (see 3.2.4.4) and incubated in ddH_20 for 1min. Subsequently, the sample was cut into 6 slices on a glass plate that were again sliced in 4 pieces, before they were transferred into 6 HPLC H_20-filled wells of a 96 well plate on a rocking plate shaker. The gel pieces were destained by washing twice for 5min with 100µl 40% acetonitrile after the water was removed. Then they were incubated for 2min in 100µl 100% acetonitrile for dehydratation. After removal of the supernatant, the pieces were dried for 10min. Subsequently, 100µl DTT (5mM) solution was applied and incubated for 10min at 60°C. Alkylation with 100µl IAA (25mM) for 45min in darkness followed after discarding the supernatant. Subsequently the liquid was removed and the slices were washed again twice for 10min in 100µl 40% acetonitrile and for 2min in 100µl 100% acetonitrile, before they were dried once more. Thereafter, 40µl trypsin solution (10ng/µl) was applied and incubated overnight at 37°C. The next day, the reaction was stopped by 10µl 2.5% TFA solution for 15min. The supernatant of each well was transferred into a reaction tube, to which the supernatants of the next steps were added. The gel pieces were incubated in 80µl 50/0.5 solution (50% acetonitrile in 0.5% TFA) for 15min, supernatant was pooled to the solution of the step before and 80 µl 100/0.5 solution (100% acetonitrile in 0.5% TFA) was applied for another 15min. Thereafter the supernatant was added to the pooled fractions and the volume of thecomplete sample was reduced in a SpeedVac to 2-5µl. Following resuspension in 0.5% TFA to a volume of 10-20µl, the samples could directly be measured by LC-MS/MS.

3.2.5.7. Desalting via stop and go extraction tips

Digested peptide mixtures that have been prepared for mass spectrometry analysis have to be desalted prior to the measurement, in order to remove interfering agents like detergents, salts or other contaminants that may affect the analysis. Furthermore, proteins are concentrated by this step. In this study, stop and go extraction tips (StageTips), pipette tips that are filled with a C18 matrix and possess a

binding capacity of 10µg, were used (Rappsilber et al., 2003). Peptides bind to the C18 material, while salt and other contaminants pass through. After washing, the peptides can be eluted using organic solvents.

The StageTips had to be equilibrated with 20µl 80/5 solution (80% acetonitrile in 5% TFA) and washed once with 20µl 0/5 solution (5% TFA) prior to loading of the acidified peptide mixture (see 3.2.5.5). Thereafter, the matrix was washed again using 20µl 0/5 solution, followed by a two-step elution by application of an acetonitrile gradient with the first elution step using 20µl 50/5 solution (50% acetonitrile in 5% TFA) and the final elution with 20µl 80/5 solution, thus enabling also the recovery of the more hydrophobic peptides. The volume of the concentrated and purified peptide solution was subsequently reduced in a SpeedVac to 2-5µl. Following resuspension in 0.5% TFA to a volume of 10-20µl, the samples could directly be measured by LC-MS/MS.

3.2.5.8. LC-MS/MS analysis

LC-MS/MS analysis is an efficient and sensitive method for the identification of peptides and finally proteins by database alignment. In principle, the enzymatically cleaved and desalted peptide mixtures are separated using reversed-phase liquid chromatography (LC) before they are directed to mass spectrometry analysis. The first step is the transfer of the polar, non-volatile and thermally unstable peptides into the gas phase without degradation (Mann et al., 2001). To that end, soft ionisation techniques are used. The electrospray ionisation (ESI) was developed by Fenn in 1989 (Fenn et al., 1989). A high voltage is applied to the analytes that are in solution, resulting in an electrospray of small droplets that transfer their charge onto the analyte molecules. The spray, which leads to the generation of multiply charged ions can be stabilised by the use of nebulizer gases. Each mass spectrometer usually comprises the following parts: the ion source and optics, a mass analyser and a detector. There are many different types of mass analysers available. Basically, the mass to charge ratio (m/z) of analytes is measured, allowing the identification and quantification by the comparison of known masses with experimentally identified masses and fragmentation patterns. (Mann et al., 2001, Yates et al., 2009). For the structural analysis of peptides, like peptide sequencing, tandem mass spectrometry has to be applied. Thereto, mass to charge ratios are measured in the first mass analyser, then precursor ions are selected for fragmentation, resulting in the fragment

ions that are detected in the second mass analyser (Gstaiger and Aebersold, 2009). The orbitrap mass analyser has a high mass accuracy and resolution. It is an ion trap, where ions are trapped in an electrostatic field. The electrostatic attraction of the ions towards a central electrode is counteracted by a centrifugal force based on the tangential velocity of the ions. This results in spiral movements of the ions around the electrode and an image current that can be detected by an outer electrode. After a Fourier transform m/z ratios can be determined from oscillation frequencies of ions (Scigelova and Makarov, 2006). This technique achieves a mass accuracy of less than 2 ppm in peptide mixtures with high complexity (Yates et al., 2006). The resolving power has its maximum at 100000 at m/z 400, decreasing with an increasing m/z ratio of the ion. In the LTQ-Orbitrap system, the orbitrap is linked to a linear ion trap for the determination of m/z values from peptide fragments, which is characterised by a high sensitivity, but low mass accuracy and resolution. The trapped ions are directed to the C-trap, where they are fragmented by collision induced dissociation (CID) or higher-energy collisional dissociation (HCD) when a HCD-cell is added, and stored until they are transferred to the orbitrap. The LTQ-Orbitrap displays sensitivity in the femtomole region, a dynamic range of $1e^4$ combined with a moderate scan rate (Olsen et al., 2009, Yates et al., 2009). In the Q Exactive system, a quadrupole mass filter and a HCD-cell are coupled to the Orbitrap. A quadrupole comprises four rods that are able to select for certain masses by the application of an oscillating electric field. This enables the implementation of quantification by targeted mass spectrometry. By using the selected ion monitoring (SIM) method one can select for a specific precursor ion mass in a known retention time window that is subsequently fragmented. This leads to more specific results than with a full scan method, where only the most abundant peaks are detected. In selected reaction monitoring (SRM), also referred to as multiple reaction monitoring (MRM) one single fragment ion can be selected and monitored, resulting in only one peak for quantification. The Q Exactive displays a resolution of 140000 at m/z 200 combined with less than 1 ppm mass accuracy (Michalski et al., 2011, Yocum and Chinnaiyan, 2009).

Quantitative mass spectrometry for SILAC experiments was carried out using an Ultimate 3000 Nano-RSLC liquid chromatography system combined with a LTQ-OrbiTrap Velos mass spectrometer by a nano spray ion source. The tryptic peptides were resuspended in 10-20µl 0.5% TFA and automatically injected and eluted after

5min from the Nano trap column (75μm i.d. × 2cm, packed with Acclaim PepMap100 (C18, 3μm, 100Å) onto the analytical column (75μm i.d. × 25cm, Acclaim PepMap RSLC) and separated using an acetonitrile gradient from 2 to 35% of buffer B (80% ACN and 0.08% formic acid in HPLC-grade water) in buffer A (2% ACN and 0.1% formic acid in HPLC-grade water) at a flow rate of 300nl/min over 145min followed by a short washing step of 5min from 35% B to 95% B in buffer A and equilibration for 5min with 2% buffer B in buffer A. The eluted peptides were analysed by a LTQ-Orbitrap Velos mass spectrometer. From a high-resolution mass spectrometry pre scan with a masse range of 300-1500, the 10 most intense peptide peaks were selected for collision induced dissociation (CID) fragmentation in the linear ion trap if they exceeded an intensity of at minimum 200 counts and if they were at least doubly charged. The fragmentation was performed with normalised collision energy of 35 and the fragments were detected in the linear ion trap with normal resolution. Every fragmented ion was excluded for 20s by dynamic exclusion. The lock mass with a value of value of 445.12002 was activated (Olsen et al., 2005).

The targeted approaches were also pre-fractionated on an Ultimate 3000 Nano-RSLC liquid chromatography system coupled to a Q Exactive plus mass spectrometer for analysis by a nano spray ion source. The tryptic peptides were automatically injected and eluted after 5min from the Nano trap column (75μm i.d. × 2cm, packed with Acclaim PepMap100 (C18, 3μm, 100Å) onto the analytical column (75μm i.d. × 25cm, Acclaim PepMap RSLC) and separated using an acetonitrile gradient from 2 to 35% of buffer B (80% ACN and 0.08% formic acid in HPLC-grade water) in buffer A (2% ACN and 0.1% formic acid in HPLC-grade water) at a flow rate of 300nl/min over 80min followed by a short washing step of 5min from 35% B to 95% B in buffer A and equilibration for 5min with 2% buffer B in buffer A. The emitted peptides were analysed using single reaction monitoring (SIM) on a Q Exactive plus mass spectrometer. Inclusion lists containing precursor ion masses (m/z), charge (z) and retention time windows of 10min were applied. The resolution for SIM scans was set to 70000 and maximum fill time was defined to 100ms (AGC target value $5x10^4$), resolution for HCD spectra was set to 7500 and a maximum fill time of 500ms was determined (AGC target value $1x10^5$). Normalised collision energy was set to 26 and the underfill ratio was fixed to 10%.

3.2.5.9. Data analysis

For SILAC labelling all raw data acquired by tandem mass spectrometry on the LTQ-Orbitrap Velos were analysed by MaxQuant Software version 1.5.0.30 (Cox and Mann, 2008) using the SwissProt/UniProt mouse database (2014_04, 16,669 entries) as described (Tyanova et al., 2014) and in house R-scripts for filtering. For MaxQuant analysis, multiplicity was set to 2, carbamylation was set as fixed modification, glutamine/asparagine deamination, methionine oxidation and protein N-terminal acetylation were included as variable modifications. Trypsin was selected as enzyme in specific digestion mode, 2 missed cleavages were allowed at maximum. Min ratio count was set to 1. Only protein IDs found in a minimum of one forward and one reverse experiment with a minimum of 1 unique peptide were considered for the final dataset. Significance A and B were calculated according to Cox and Mann (Cox and Mann, 2008) by application of in house R-scripts. Contaminants were excluded and proteins were considered as significant with a H/L ratio of at least a value of 2.
SIM scan data from the Q Exactive were analysed with Skyline version 2.5.0.6157. The software was used to detect and select fragment ions for the quantification. Raw data were quantified by building ratios of the peak areas intensities from specific fragment ions of the corresponding samples.

3.2.5.10. Protein-protein interaction network and GO term analysis

Network visualisation was achieved by matching data from FLAG affinity purifications with interaction databases. Besides Sox11 TCF4, MYT1, TRIM28, ZNF24, YY1 and CBX6 served as baits. To create the network, Cytoscape version 2.8.3 (Shannon et al., 2003) was applied. Already described interactions were integrated into the experimental dataset using the GeneMANIA plugin (Montojo et al., 2010) that acquires data from the interaction databases Biogrid, GEO, I2D and Pathway Commons. We included physical interactions, with at least one experimental validation (in vivo, in vitro or yeast two-hybrid) generated by pull-down, affinity purifications or affinity chromatography.
The term gene ontology (GO term) was introduced by the Gene Ontology Consortium that aims to support biological relevant annotation of genes and gene products in many organisms. It supplies a systematic language for the assignment of gene's and gene product's attributes into three key biological domains all organisms have in

common, namely molecular function, biological process an cellular component (Gene Ontology, 2008).
GO term analysis was carried out using the dataset of significant Sox11 interacting proteins that were identified by R-script from MaxQuant analysis, by application of the ToppGene suite tool ToppFun (Chen et al., 2009). Bonferroni correction and a cut-off of 0.05 were adapted to the data.

3.2.6. Functional characterisation

3.2.6.1. Reporter assay

Reporter gene assays are used to characterise regulatory elements, like promoters. They are linked to a reporter gene that is transcribed once the promoter gets activated, and finally translated into the reporter protein. As they serve as markers for the regulation of the promoter activity, usually reporter proteins possess chemiluminescent or bioluminescent activity, to generate an easy detection system (see figure 10). In this study a dual luciferase assay was applied using firefly luciferase from the firefly as a reporter gene and renilla luciferase from the sea pansy (Renilla reniformis) under the control of a constitutively active promoter as a normalisation control to level out variations in transfection efficiency. The firefly luciferase catalyses in the presence of Mg^{2+} ions the reaction of ATP, firefly luciferin and O_2 to oxyluciferin, AMP, CO_2, diphosphate and light (560nm). The Renilla luciferase catalyses the reaction of coelenterazine and O_2 to coelenteramide, CO_2 and light (482nm) (Bronstein et al., 1994). The bioluminescence is detected in a luminometer and firefly signals are subsequently normalised to renilla signals.

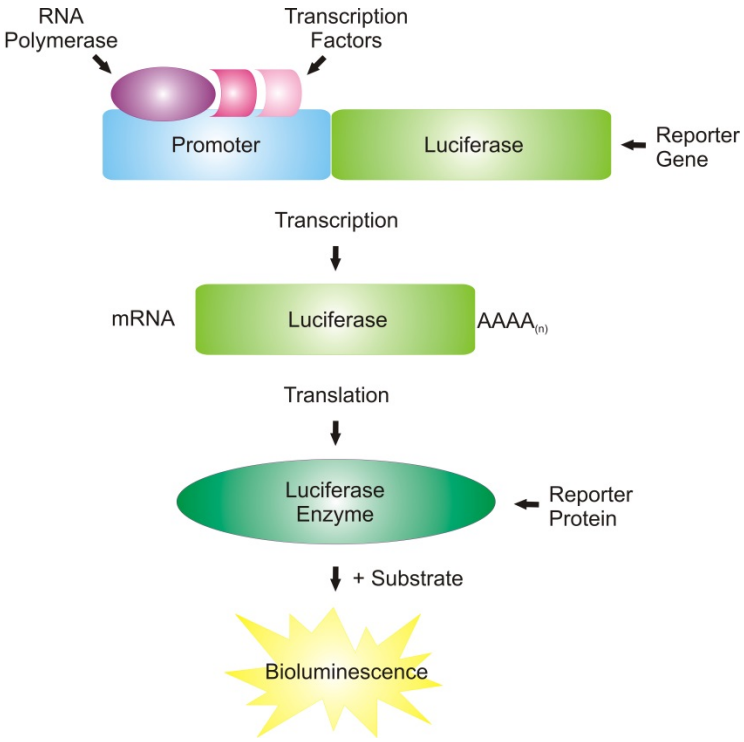

Figure 10:Scheme of a luciferase reporter assay
A promoter of interes is coupled to a luciferase, which serves as reporter gene. Upon promoter activation the gene is transcribed and translated into the luciferase enzyme, the reporter protein. The addition of the luciferase specific substrate results in bioluminescence that can be measured and confirms promoter activity.

For the assay, cells were seeded on 6 well plates in a density of $23x10^4$ cells per well for HEK-T and $15x10^4$ cells for Neuro2a cells. The plasmids Sox11 (N)SF-TAP pDEST (190ng) , MYT1 (C)SF-TAP pDEST (1500ng), TCF4 (C)SF-TAP pDEST (740ng), YY1 (C)SF-TAP pDEST (740ng), ZNF24 (C)SF-TAP pDEST (1500ng) and shRNA knockdown constructs Myt1 PWX1-H1, Tcf4 PWX1-H1, Yy1 PWX1-H1, Znf24 PWX1-H1 (1500ng) were co-transfected after 24h of cellular growth using PEI (see 3.2.1.3.2) with a human DCX-promoter luciferase reporter construct (740ng) (Karl et al., 2005) and a human Stmn1-promoter luciferase reporter construct (740ng) (Benlhabib and Herrera, 2006), respectively together with Renilla–luciferase under the control of the human elongation factor 1 promoter (74ng) for normalisation (Lie et al., 2005). Harvest and reporter luciferase assay was performed 48h post transfection using the Promega dual luciferase assay kit according to the manufacturer's manual and a Mithras LB 940 Multimode Microplate Reader. Each measurement was accomplished at least three times in 3 biological replicates.

3.2.6.2. In silico promoter analysis

In silico promoter analysis provides a tool for the theoretical alignment of transcription factor binding sites and promoter sequence information. The potential binding of single or multiple transcription factors on neighbouring consensus sequences can be determined as well as the distribution of binding sites on selected promoters.
Specific binding sites on DNA that are recognised by common transcription factors were determined using the Genomatix Software Suite Version 3.2. The analysis was performed for Sox11, Myt1 and Yy1. Genomatix graphically generated consensus sequence logos using a previously described algorithm (Crooks et al., 2004, Schneider and Stephens, 1990). Nucleotides in capital letters depict the core sequence, which is defined as highest conserved, consecutive positions of the consensus, nucleotides in bold exhibit a degree of conservation above 60%. Models including Sox11 and Myt1 respectively Sox11 and Yy1 were generated by applying the Fast M tool from Genomatix. The Model Inspector tool was used for the detection of adjacent binding sites of the previously defined models in the promoter sequences within a set distance from 5 to 700 basepairs.

4. Results

4.1. Experimental workflow

The need for new candidates in reprogramming strategies of somatic cells into functional neurons and the involvement of Sox11 in the neural fate determination and induction of neuronal expression programs gave rise to the question of early neuronal identity and the underlying transcriptional modulation, which led to the determination of a Sox11-centred transcriptional core network by proteomic analysis.

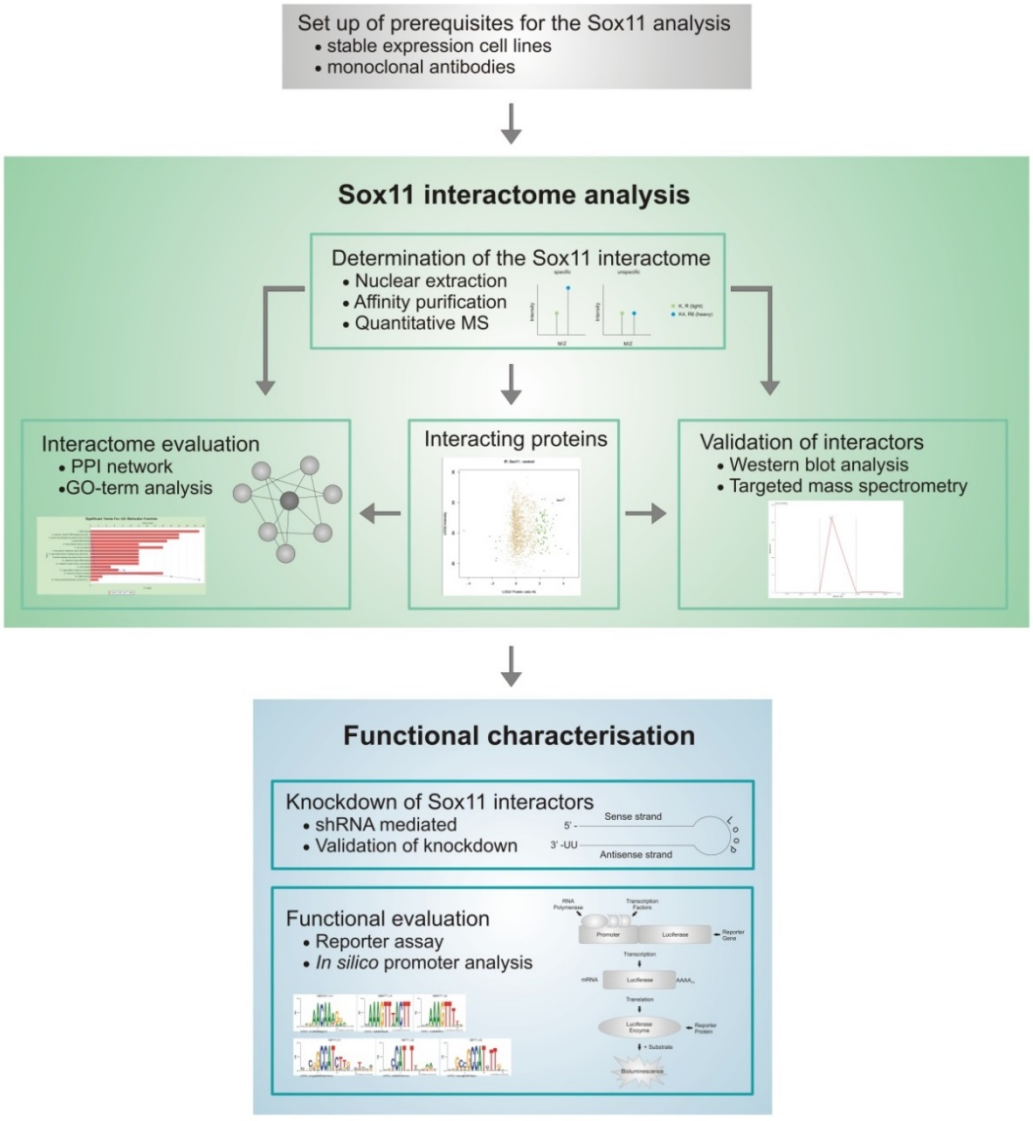

Figure 11:Experimental workflow
Basic prerequisites were established, before the Sox11 interactome analysis was performed. The Sox11 interactome was determined by affinity purification combined with SILAC and quantitative mass spectrometry. Thereafter, a protein-protein interaction network was build and the list of interacting proteins was subjected to GO-term analysis. The interactions were validated using western blot analysis and targeted mass spectrometry approaches, before selected interactors were characterised functionally. Therefore, reporter assays combined with shRNA-mediated knockdown of candidates, as well as *in silico* promoter analysis was applied.

4.2. Set up of prerequisites for the analysis of Sox11

4.2.1. Generation of stable Sox11 expression cell lines

Stable Sox11 expressing cell lines were established for the analysis of the Sox11 interactome on a relatively low expression level compared to transient transfection, resembling more the physiological conditions within cells. Furthermore, they should serve as a test system for the specificity and sensitivity of newly generated monoclonal antibodies recognising Sox11. To that end, Neuro2a cells, a mouse neuroblastoma cell line, that possesses minimal endogenous Sox11 expression and features good transfection efficiencies, were stably transfected with the (N)SF-TAP pDEST-Sox11 gateway expression vector. The selection of plasmid containing cells was carried out by the use of G418, taking advantage of the neomycin resistance of the pDEST vector, followed by monoclonal colony selection and expansion (see 3.2.1.5). 12 monoclonal cell lines were tested for stable Sox11 expression 4 ½ weeks post transfection (see figure 12). Therefore, nuclear extracts were prepared and 20µg lysate was subjected to SDS-PAGE combined with western blot analysis. A transient Sox11 transfected nuclear lysate was included as positive control. Sox11 expression was detected using a commercial monoclonal anti-Sox11 antibody (see table 5) whereas Gapdh western blot signals served as a loading control. All of the 12 tested clonal cell lines displayed clearly Sox11 expression at a size of 72kDa, with obtained signals significantly lower than the transient transfection control and a different bands pattern. Normalisation to the loading control Gapdh and quantification of the Sox11 signals revealed the highest expression combined with high signal purity for cell line number 2, which was continuingly cultured and applied for further experiments where stable Sox11 expression cell lines were used.

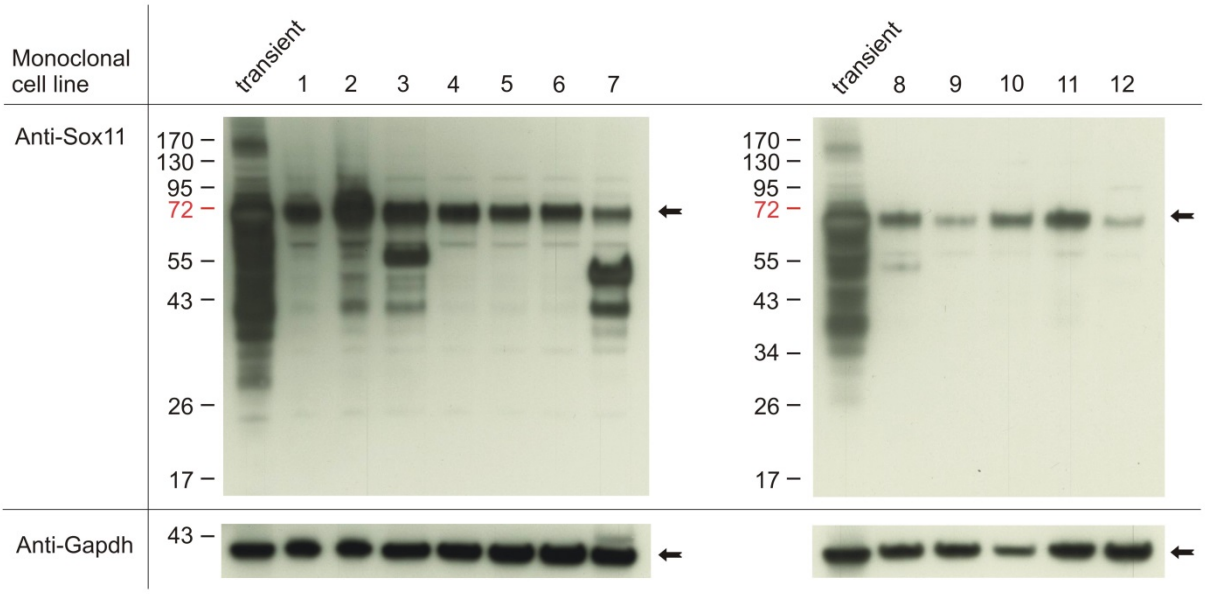

Figure 12:Monoclonal Sox11 stable expression Neuro2a cell lines
Western blot analysis was performed using 20µg nuclear extract for SDS-PAGE. Detection with commercial anti-Sox11 antibody revealed specific Sox11 signals with different intensities at 72kDa in 12 Sox11 stably expressing Neuro2a cell lines (see arrows). Transient Sox11 transfection served as positive control and anti-Gapdh immunoblotting (36kDa) was used as loading control for quantification.

4.2.2. Evaluation of monoclonal Sox11 antibodies

4.2.2.1. Establishment of monoclonal Sox11 antibodies

Sox11-recognising monoclonal antibodies were generated in house, as only polyclonal anti-Sox11 antibodies were commercially available. As a consequence, they differ in specificity and efficiency depending on the charge and display a couple of unspecific bands at high Sox11 expression levels upon transient transfection (see first lane in figure 12).

The monoclonal antibody production was carried out in house in the laboratory of Elisabeth Kremmer in the institute of laboratory immunology at the Helmholtz Zentrum München. The workflow for the generation of monoclonal antibodies was based on the achievements of Köhler and Milstein (Kohler et al., 1976, Kohler and Milstein, 1975). In principle, mice or rats were immunised with the antigen, followed by the extraction of antibody producing spleen B lymphocytes that were subsequently fused with myeloma cells. Each of the resulting hybridoma cells produced a single type of antibody, recognising a specific epitope that was present in the cell's supernatant. Two different strategies were applied, including peptide specific and protein specific antibody production in mice and rats. For the latter, a protein epitope signature tag of Sox11, short PrEST, was used as an antigen for immunisation. This

denotes a highly protein specific fragment, designed, that encompasses typically 50-150 amino acids, which is not part of transmembrane regions or signal peptides (Uhlen et al., 2010). The applied murine Sox11 PrEST had a defined length of 117 amino acids identical to the positions 189-301 of the Sox11 protein and was designed as mouse homologue to the human sequence according to the human protein atlas (http://www.proteinatlas.org) (see figure 14). It was cloned into a pETM30 vector and expressed in BL-21 *E.coli* using IPTG induction. Thereafter, cells were lysed and purified on a Ni-NTA column using the 6xHis tag (see 3.2.2.7 and 3.2.2.8). The applied IPTG concentrations as well as the induction time and lysis conditions were the parameters that had to be established (see figure 13).

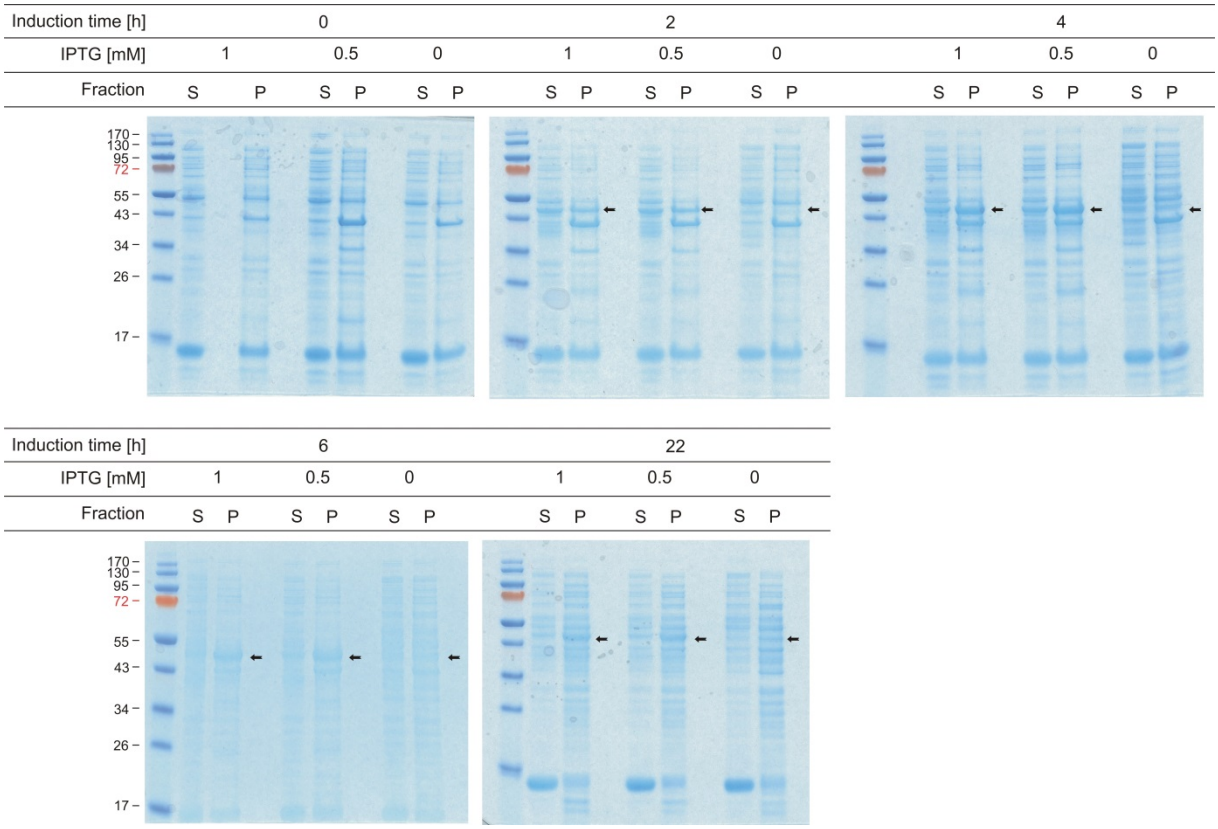

Figure 13:Establishment of induced Sox11 PrEST expression in BL-21 cells
Sox11 PrEST expression efficiency in BL-21 *E.coli* was assessed using SDS-PAGE of 10µg supernatant (S) or pellet (P) fraction combined with Coomassie staining. Different IPTG concentrations (0, 0.5 and 1mM) and induction times (0, 2, 4, 6 and 22h) were applied. The specific Sox11 PrEST band with a predicted size of 42kDa, indicating induced expression, is denoted with arrows at time points 2, 4, 6 and 22h.

The supernatant (S) contained soluble proteins, that were gained after lysis using lysis buffer without urea, followed by centrifugation. The pellet (P) was resuspended in lysis buffer containing 8M urea in order to solubilize the remaining proteins. The

expressed Sox11 PrEST (14kDa) linked to the His-GST tag (28kDa) was present at a molecular weight of about 42kDa on Coomassie stained SDS-gels run with 10µg lysate, in both IPTG induced samples but not in the control from 2h until 22h of induction time. The specific band was present more clearly in the pellet fraction (P) than in the supernatant (S), however the different IPTG concentrations didn't result in obvious expression changes. The estimated band representing the Sox11 PrEST was sliced out of the gel and subsequently digested using trypsin. The ensuing LC-MS/MS and Mascot/Scaffold analysis confirmed the presence of the desired protein fragment with a sequence coverage of 48% (see figure 14). Based on the outcome of the establishment of expression parameters, 0.5mM IPTG and 4h induction time were selected for further purifications, as the expression was best under these conditions. Moreover, the bacteria were lysed in lysis buffer comprising 8M urea to completely bring the Sox11 PrEST into solution.

Murine Sox11 PrEST sequence:

mdddedddeddelqlrpkpdaddddddepahshllppptqqqppqllrrysvakvpasp
tlssaaespegaslydevraggrlyysfknitkqqpppappalspassrcvstsss

Figure 14:Sequence coverage of Sox11 PrEST
The LC-MS/MS analysis of the sliced and tryptically digested protein band of the Sox11 PrEST revealed a sequence coverage of 48% by Mascot/Scaffold evaluation with the protein threshold set to 99%, the peptide threshold set to 80% and a selected minimum of 2 identified peptides.

The success of the subsequent Ni-NTA purification (see 3.2.2.8 and 3.2.2.9) was assessed on a Coomassie stained SDS-gel (see figure 15). The lysate input, flowthrough of the matrix and wash fraction 1 showed un-purified protein lysate, indicated by the presence of many non-specific protein bands. In contrast, elution steps 2-5, characterised by increasing Imidazole concentrations display elevated Sox11 PrEST concentrations with relatively high purity, certifying the successful clean-up of the expressed fragment via His-tag-mediated Ni-NTA purification. The elution steps 2-5 were pooled, dialysed against PBS to remove the toxic Imidazole and sent to E. Kremmer for immunisation and subsequent antibody production.

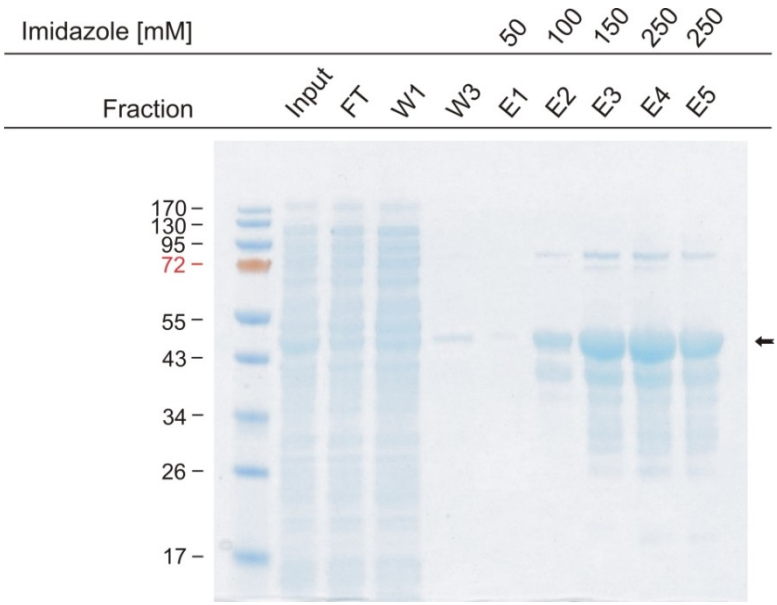

Figure 15:Ni-NTA purification of Sox11 PrEST
Purity of Sox11 PrEST was determined after Ni-NTA purification over His-tag by Coomassie stained SDS-gel of the different fractions input (lysate, 1µl)), flowthrough (FT, 1µl)), wash fraction 1 and 3 (W1 and W3, 15µl) and elution steps 1-5 (E1-E5, 2µl) from the step-wise elution with increasing imidazole concentrations (50-250mM). The appropriate Sox11 PrEST band is indicated with an arrow at approximately 42kDa.

4.2.2.2. Protein-specific monoclonal antibodies detect Sox11 efficiently in western blot analysis

The evaluation of monoclonal peptide-specific Sox11-recognising antibodies was performed using nuclear lysates of with (N)SF-TAP pDEST-Sox11 or empty vector control transiently transfected HEK-T cells and Neuro2a cells. SDS-PAGE and subsequent western blot analysis with peptide-derived anti-Sox11 antibodies from hybridoma supernatants at a dilution of 1:25 revealed Sox11-specific bands at approximately 75kDa (Sox11+SF-TAP tag) in HEK-T cells with over-expressed Sox11 (see figure 16). In the control conditions of both cell lines, as well as in the Sox11 over-expressing Neuro2a cells however, no bands were present. The two evaluated clones 1B9 and 2B9, shown in figure 16 are exemplified for all the tested hybridoma supernatants. Western blot analysis using an anti-FLAG antibody, recognising the SF-TAP tag though, displayed Sox11 over-expression in both cell lines. The Sox11 expression in the neuroblastoma cells was not as high as in HEK-T cells, due to the lower transfection ability of the cell line. Nevertheless, the Sox11 expression could not be reliably detected by the peptide specific anti-Sox11 antibodies and thus they all were classified as not suitable for the recognition of Sox11 in any further experiment.

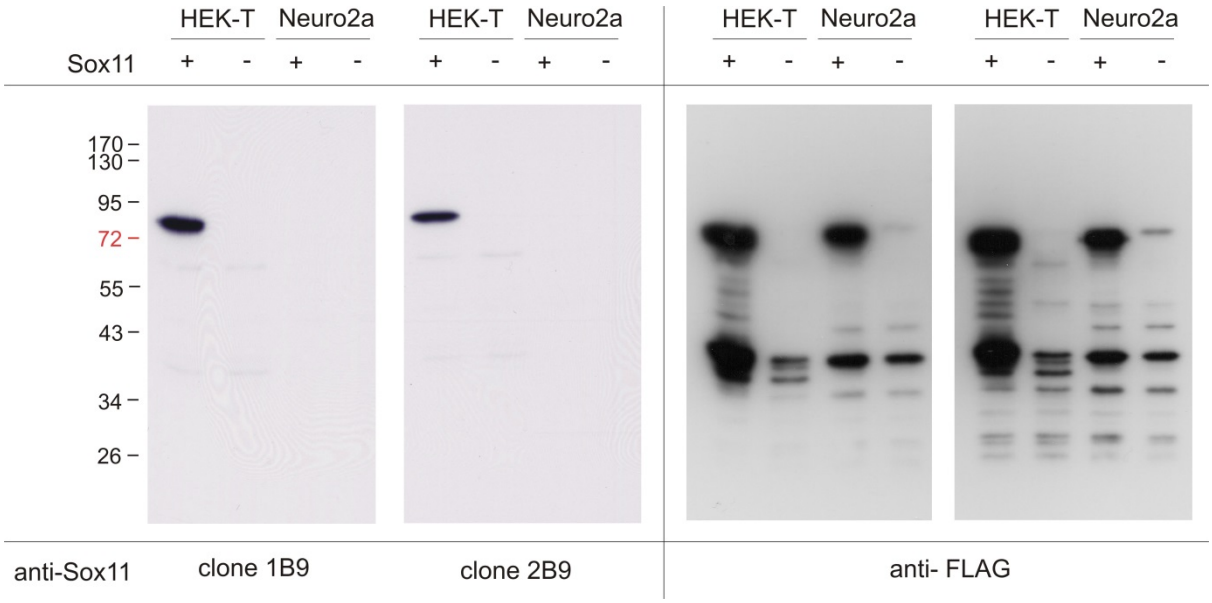

Figure 16:Peptide-specific monoclonal anti-Sox11 antibody evaluation
Peptide-specific Sox11-recognising antibodies were established on nuclear lysates of Sox11 over-expressing or empty vector transfected nuclear extracts of HEK-T and Neuro2a cells. 10µg lysate was analysed via SDS-PAGE combined with western blot analysis. Anti-Sox11 hybridoma supernatants clones 1B9 and 2B9 (1:25 in blocking buffer) displayed a Sox11-specific signal only in HEK-T cells. The control western blot with anti-FLAG antibody detecting the SF-TAP tag however confirmed Sox11 expression in both cell lines.

To overcome the existing lack of suitable Sox11-specific antibodies, the protein-specific monoclonal anti-Sox11 antibodies using the Sox11 PrEST as immunogen were generated and tested for Sox11 recognition and specificity. In a first screening they were applied in 1:10 dilutions in multiwell chambers on transiently Sox11 over-expressing nuclear lysate of HEK-T cells after performance of SDS-PAGE and subsequent western blotting (see exemplarily displayed clones in figure 17). Thereafter, subtype-specific HRP-coupled secondary antibodies were incubated on the membrane. A commercial anti-Sox11 antibody was used as positive control. Many of the hybridoma supernatants produced in rat detected Sox11 specifically at approximately 75kDa (see figure 17). The next step in the establishment procedure was the application of the antibody clones on stably Sox11 expressing Neuro2a cells, to check if they were also capable of detecting the markedly lower expression level of the transcription factor. This was also a test if the obstacles that the peptide-specific antibodies exhibited with the overexpression in the neuroblastoma cell line could be overcome with the new approach. The obtained Sox11 signal intensities were decreased compared to the transient over-expression of Sox11, nevertheless a lot of hybridoma supernatants displayed specific Sox11 bands at about 75kDa after they

were incubated on the membrane in a dilution of 1:10 (see exemplarily illustrated clones in figure 18).

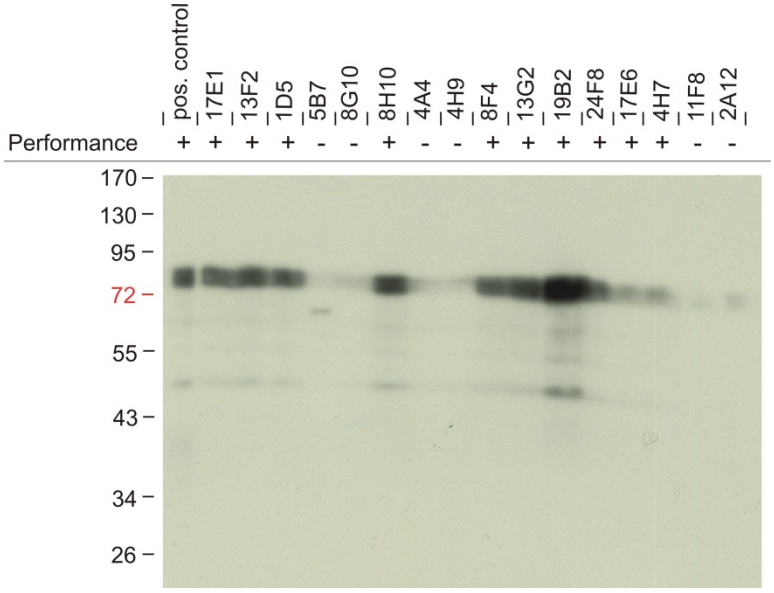

Figure 17:Screening of protein-specific antibodies in western blot analysis on Sox11 over-expression in HEK-T cells
The performance of hybridoma supernatants on western blot analysis was assessed using 150µg nuclear lysate of transiently Sox11 over-expressing HEK-T cells on SDS-PAGE with one-well gels. The antibodies were incubated on the membrane in a dilution of 1:10 in blocking solution. Subtype-specific secondary antibodies were applied and commercial anti-Sox11 antibody was used as positive control.

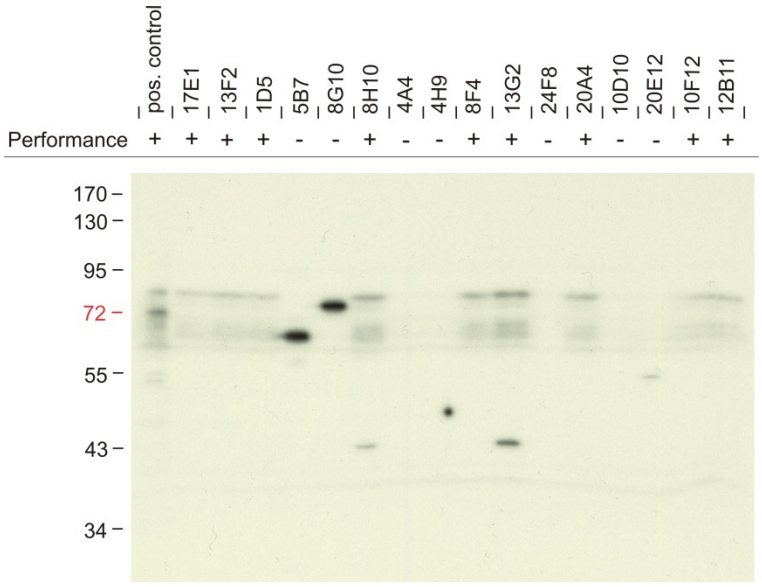

Figure 18:Screening of protein-specific antibodies in western blot analysis in stably Sox11 expressing Neuro2a cells
The performance of hybridoma supernatants on western blot analysis was assessed using 200µg nuclear lysate of stably Sox11 over-expressing Neuro2a cells on SDS-PAGE with one-well gels. The antibodies were incubated on the membrane in a dilution of 1:10 in blocking solution. Subtype-specific secondary antibodies were applied and commercial anti-Sox11 antibody was used as positive control.

As a third step, the recognition of the protein-specific antibodies of endogenously expressed Sox11 in Neuro2a cells was examined. Therefore, stable Sox11 transfected nuclear lysate was used as a positive control in addition to the non-transfected Neuro2a nuclear extracts. The application of most of the hybridoma supernatants in 1:10 dilutions resulted in specific signals for Sox11 in the stable expression lines, however none of the clones was able to detect the transcription factor on the very low endogenous expression level (see exemplarily illustrated clones in figure 19). In general, rat-derived hybridoma supernatants performed better than mouse antibodies.

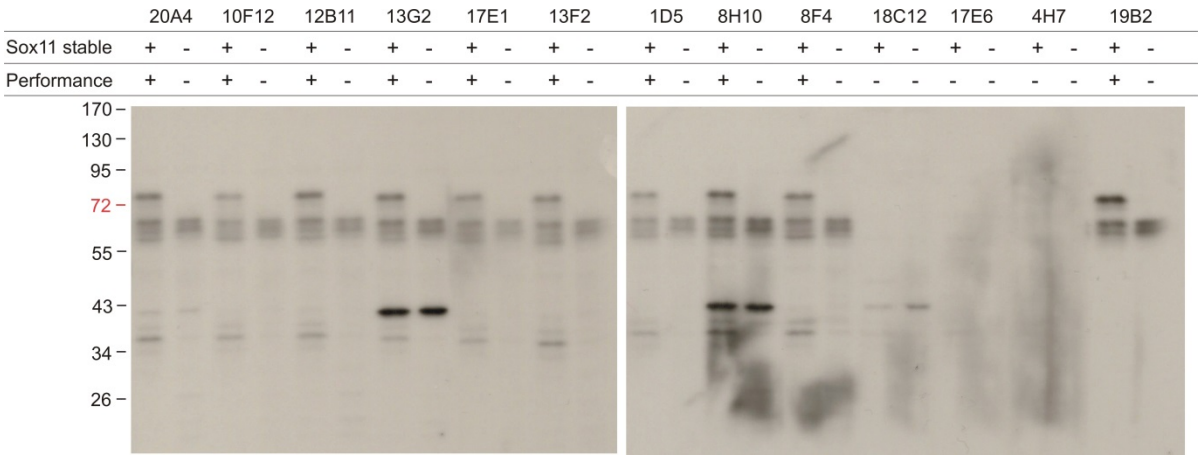

Figure 19:Screening of protein-specific antibodies in western blot analysis on endogenous level and in stably Sox11 expressing Neuro2a cells
The performance of hybridoma supernatants on western blot analysis was assessed using 200µg nuclear lysate of stably Sox11 over-expressing and non-transfected Neuro2a cells on SDS-PAGE with 15-well gels. The antibodies were incubated on the membrane in a dilution of 1:10 in blocking solution. Subtype-specific secondary antibodies were applied for detection.

The last check the generated protein-specific Sox11-recognising antibodies had to pass through was their capability of pulling down Sox11 in stable expression cell lines. To that end, co-immunoprecipitation was performed (see 3.2.5.1) with the hybridoma supernatants on nuclear extracts. This revealed the successful pull down of Sox11 when the complete eluate was subjected to SDS-PAGE and western blot analysis (see figure 20). Nevertheless, the enrichment of the bait protein was not very efficient, compared to the input of 10µg crude nuclear lysate. The detection was performed using the two isotype different hybridoma clones 13G2 and 19B2 that were identified as suitable for western blot analysis in the previous tests, as the specificity of the commercial antibody was not optimal. The beads alone served as a negative control and the immunoprecipitation was performed using the commercial

anti-Sox11 antibody as positive control. Furthermore, the tryptic proteolysis followed by LC-MS/MS analysis of the pull down assays could not detect any Sox11-specific peptides, due to the inefficient enrichment of the bait protein. In summary, many of the protein-specific anti-Sox11 antibodies are suitable for western blot analysis of moderate Sox11 levels (see table 10), but are not recommended for the application in co-immunoprecipitation assays.

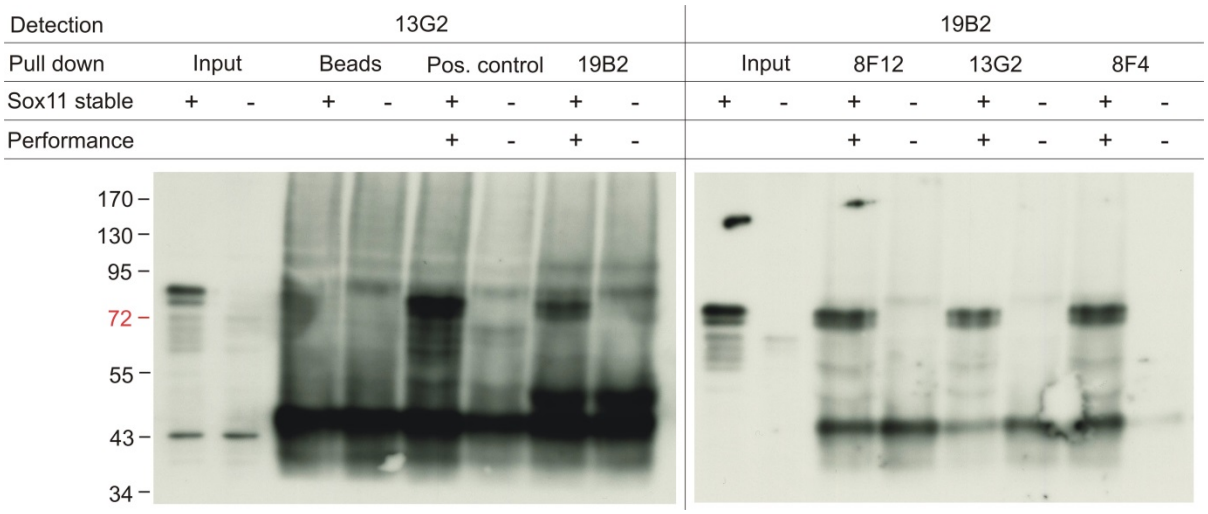

Figure 20:Screening of protein-specific antibodies in co- immunoprecipitation assays on endogenous level and in stably Sox11 expressing Neuro2a cells
The performance of hybridoma supernatants in pull down assays was assessed by incubation of 500µg nuclear lysate of stably Sox11 over-expressing and non-transfected Neuro2a cells with 1ml of hybridoma supernatant coupled to protein-G agarose. The complete eluate was applied to SDS-PAGE using 10-well gels. Commercial anti-Sox11antibody was used as positive control, beads alone served as negative control. The input consists of 10µg nuclear lysate. The detecting antibodies were incubated on the membrane in a dilution of 1:10 in blocking solution. Subtype-specific secondary antibodies were applied for detection.

Table 10: Protein-specific anti-Sox11 antibodies suitable for western blot analysis

antibody	IgG subtype	species
19B2	2a	rat
20A4	G1	rat
18C12	2a + 2b	rat
10F12	G1	rat
12B11	G1	rat
13G2	G1 + 2a + 2b + 2c	rat
17E1	G1	rat
17E6	2a	rat
13F2	G1 + 2a	rat
1D5	G1	rat
8H10	G1	rat
4H7	2a	rat
8F4	G1 + 2a + 2b	rat
1C9	2c	rat
4H6	G1	rat

4.3. Implementation of the Sox11 interactome

4.3.1. FLAG affinity purification efficiently precipitates transiently transfected Sox11 and its interactors

For a successful analysis of the Sox11 interactome in Neuro2a cells, nuclear extraction conditions as well as the method of choice for the affinity purification had to be established. The possibility of a co-immunoprecipitation assay on endogenous Sox11 level had already been excluded due to the lack of suitable antibodies for pull down assays even in the newly generated monoclonal antibodies. The affinity purification of stable Sox11 expression cell lines revealed only 5 identified peptides for the bait protein Sox11 after tandem mass spectrometric and Mascot/Scaffold analysis. With such a small number of bait peptides, the determination of the much less endogenously expressed interaction partners was not possible. On these grounds, the interactome analysis had to be established using transient over-expression of Sox11. Initially, the Strep affinity purification strategy was applied. The analysis of the pull downs by LC-MS/MS and western blot revealed an inhibitory effect of the high salt conditions of the nuclear extraction buffer C on the Strep affinity purification buffer system, resulting in a blocked SF-TAP tagged Sox11 binding to the Strep-Tactin matrix. The adjustment of the nuclear extraction conditions to half of the NaCl concentration in extraction buffer C resulted in a successful pull down of Sox11 (see figure 21).

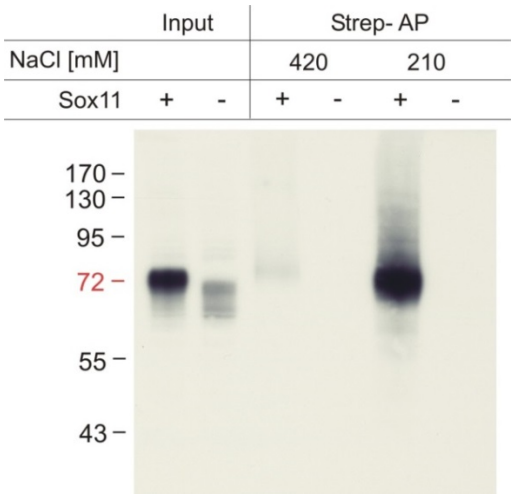

Figure 21:Strep affinity purification of transiently over-expressed Sox11 in Neuro2a
Strep affinity purification was performed on nuclear extracts of Sox11 over-expressing Neuro2a cells and empty vector control with different salt conditions (420mM and 210mM NaCl). The whole eluate and 10µg nuclear lysate (input) respectively was used for SDS-PAGE and western blot analysis. Detection was carried out by commercial Sox11 antibody.

Nonetheless, the search for specific interaction partners via quantitative mass spectrometry was not satisfying. Probably the release of proteins from the nucleus was not as efficient as with the double salt concentration. Furthermore, the Strep affinity purification may be not as suitable as FLAG affinity purification for the interactome analysis of moderately expressed interacting proteins. The binding of the FLAG tag causes less non-specific contaminants, which could cover the less abundant specific interactors in the analysis. As a consequence, FLAG affinity purification was performed on transiently Sox11 over-expressing nuclear lysates of Neuro2a cells. Mass spectrometry analysis revealed the best peptide identification rates and interaction partner list for the original extraction conditions including 420mM NaCl in nuclear extraction buffer C. This was confirmed by western blot analysis (see figure 22) as well as by quantitative mass spectrometry (see table 11).

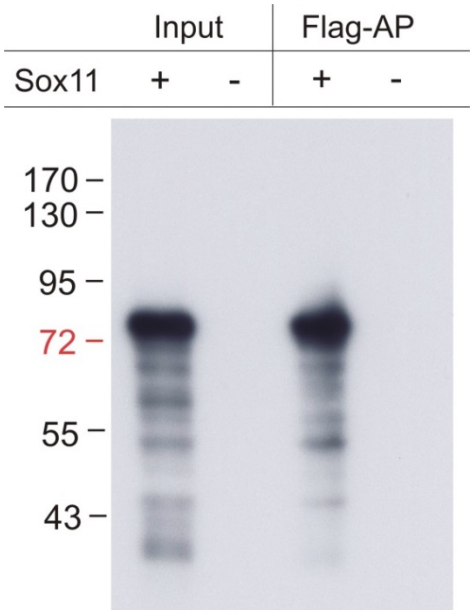

Figure 22:FLAG affinity purification of transiently over-expressed Sox11 in Neuro2a
FLAG affinity purification was performed on nuclear extracts of Sox11 over-expressing Neuro2a cells and empty vector control. 10µg nuclear lysate (input) and 2% of the AP eluate respectively was applied to SDS-PAGE and western blot analysis. Detection was carried out by the protein-specific stabilised antibody clone 19B2 in a dilution of 1:100.

The interactome analysis was implemented by 6 independent experiments using SILAC labelling, FLAG affinity purification of 5mg nuclear lysate under addition of benzonase, followed by precipitation of peptides, tryptic in-solution digestion combined with quantitative mass spectrometry. In 3 of the 6 performed experiments SILAC labelling was reversed to exclude label-dependent alterations of fold change. Data analysis using MaxQuant and R revealed a dataset of 1642 identified proteins,

of these 1609 were quantified and 66 proteins were determined to be significantly enriched (p≤0.05) in the Sox11 over-expressed fraction, detected by a minimum of 1 unique peptides per protein and present in at least one forward and one reverse experiment. The occurrence of comparatively few unspecific binding proteins presents a challenge to the statistical analysis, as the resulting distribution is not perfectly Gaussian. This is graphically elucidated by figure 23A and B, displaying the unspecific proteins as brown crosses and proteins specifically enriched in the Sox11 over-expressing fraction as green dots with a significance B of 0.05 (Cox and Mann, 2008). To overcome these limitations, a threshold which was set to a value of 2 was manually applied (see dotted lines in figure 23A). Quantified proteins above this level were referred to as significant, giving rise to an extended dataset of 164 interacting proteins, denoted as significant interactors of Sox11. The good correlation of significant hits in forward and reverse labelling experiments is displayed in figure 23B.

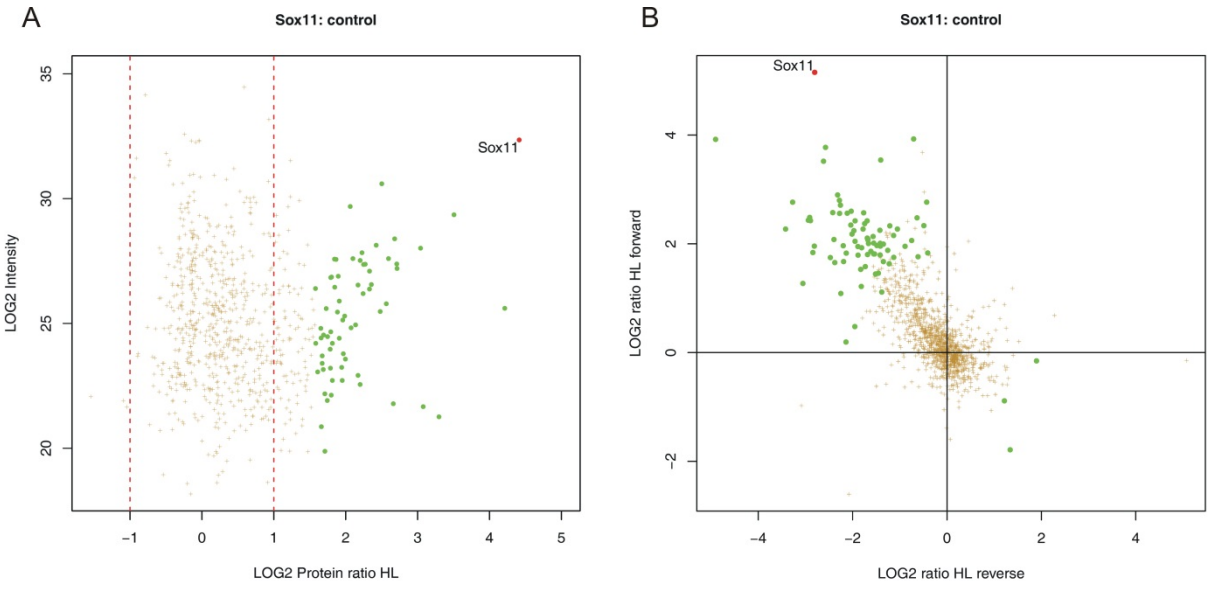

Figure 23:Scatter plot of the Sox11 interactome
Scatterplot of Sox11 interactome data after MaxQuant/R analysis from 6 independent experiments, including 3 reverse labellings. Brown crosses denote unspecific interacting proteins, green dots display proteins significantly enriched (p≤0.05) in the Sox11 over-expressing affinity purifications. Sox11 is highlighted as a red dot. Dotted lines depict manually set significance threshold value of 2. A) Log2 protein ratio HL (H: Sox11, L: control) is plotted against log2 intensity. B) Log2 ratio HL reverse (L: Sox11, H: control) is plotted against log2 ratio HL forward (H: Sox11, L: control).

The complete Sox11 interactome, comprised of 164 significant interaction partners, is illustrated graphically in a Sox11-centered network (see figure 24). The red connections also referred to as edges denote the experimentally identified interactions. The observed interactions between a subset of proteins are also complemented with previously identified interactions from protein interaction databases used by the Cytoscape plugin GeneMania, depicted by green edges (see the top of figure 24). This sub-network is displayed enlarged and more precisely described in figure 27. The entire list of Sox11 interacting proteins is listed in table 20, attached in the annex.

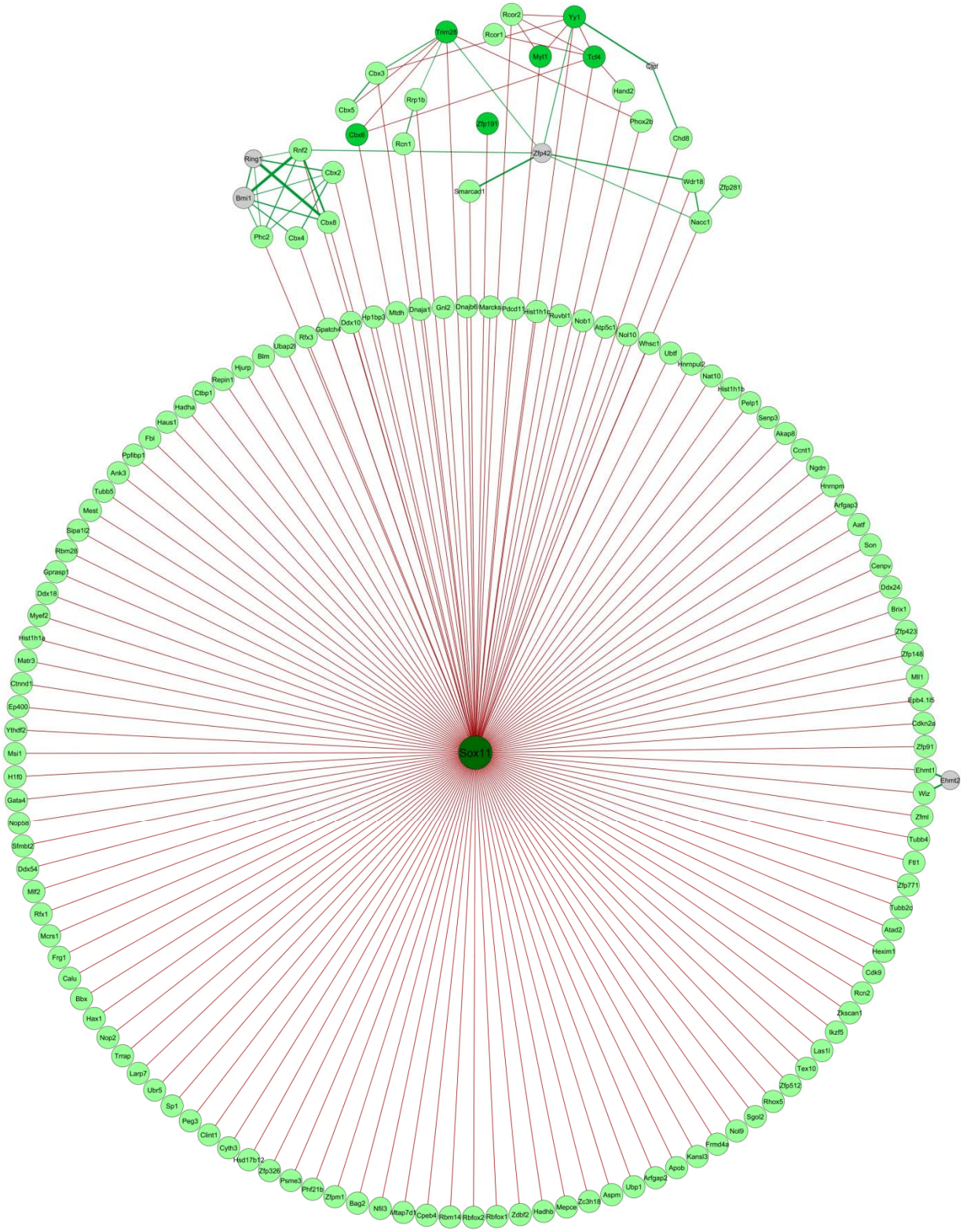

Figure 24:Sox11 interactome network
The complete Sox11 interactome network was built by combining the interactome dataset with information of mouse interaction databases used by the Cytoscape plugin GeneMania. Data were assessed from FLAG affinity purifications of Sox11 combined with pull downs of YY1, ZNF24, TRIM28, MYT1, TCF4 and CBX6 (dark and brilliant green nodes). Red edges connect newly identified interactions (bright green nodes) while connections that are previously described are linked by green edges. Grey nodes are included to connect identified proteins.

4.3.2. The Sox11 interactome is abundant in transcription factors and transcriptional modulators

The analysis of the Sox11 interactome revealed an enrichment of transcription factors and other proteins involved in regulation of transcriptional control. A subset of selected interaction partners, implicated in the regulation of gene expression is highlighted in the Sox11 interactome scatterplot in figure 25 (see also table 20). The transcriptional modulators include Transcription intermediary factor b (Tif1b, Trim28) which was detected by 27 unique peptides and a H/L ratio (Sox11/control) of 5.66 (see table 20). It belongs to the chromatin relaxation factors and controls the maintenance of pluripotency in mouse embryonic stem cells in a phosphorylation-dependent fashion (Seki et al., 2010). Likewise, Zinc finger protein 24 (Znf24, Zfp191) identified by 2 unique peptides and a H/L ratio of 3.16 is involved in the maintenance of neural cells during the multipotent progenitor stage as it prevents them from cell cycle exit and differentiation (Khalfallah et al., 2009). Furthermore, the multifunctional and ubiquitously expressed Yy1 transcription factor (Yy1), identified by 8 unique peptides and a H/L ratio of 5.91 which acts both as transcriptional activator and repressor (Shi et al., 1991), is part of the specific Sox11 interactome. Myelin transcription factor 1 (Myt1), which was detected by 7 unique peptides and a H/L ratio of 2.59 was recently found to be expressed in early developing mouse nervous tissues (Matsushita et al., 2014) and was previously shown to play a role in neuronal fate commitment in *Xenopus laevis* (Bellefroid et al., 1996). Haploinsufficiency of Transcription factor 4 (Tcf4), identified as specific interactor by 3 unique peptides and a H/L ratio of 3.75 is the major genetic cause of the Pitt-Hopkins Syndrome (Amiel et al., 2007, Zweier et al., 2007), which is characterised by intellectual disability, typical facial gestalt and hyperventilation (Pitt and Hopkins, 1978). A transcription factor belonging to the paired family of homeobox proteins Paired-like homeobox 2b (Phox2b), identified by 4 unique peptides and a H/L ratio of 3.46 as well as heart and Neural crest derivatives expressed 2 (Hand2), which is part of the basic helix-loop-helix family of transcription factors, identified by 2 unique peptides and a H/L ratio of 3.99 are found to play a role in the transcriptional regulation of specification and neurogenesis in in the autonomic nervous system (Rohrer, 2011). Also five chromobox proteins were identified with Cbx2 (detected by 2 unique peptides and a H/L ratio of 2.64) , Cbx3 (detected by 5 unique peptides and

a H/L ratio of 2.11), Cbx4 (detected by 8 unique peptides and a H/L ratio of 2.89), Cbx6 (detected by 2 unique peptides and a H/L ratio of 9.82), and Cbx8 (detected by 2 unique peptides and a H/L ratio of 3.27), that are part of the polycomb group of proteins (PcG) and modulate transcription epigenetically by the regulation of heterochromatin (Ma et al., 2014, Morey and Helin, 2010, Wotton and Merrill, 2007). Additionally, the chromodomain helicase DNA binding protein 8 (Chd8), identified by 7 unique peptides and a H/L ratio of 3.52 is part of the SNF2 family of proteins and is involved in transcriptional control as it plays a role in ATP-dependent chromatin remodelling (Marfella and Imbalzano, 2007).

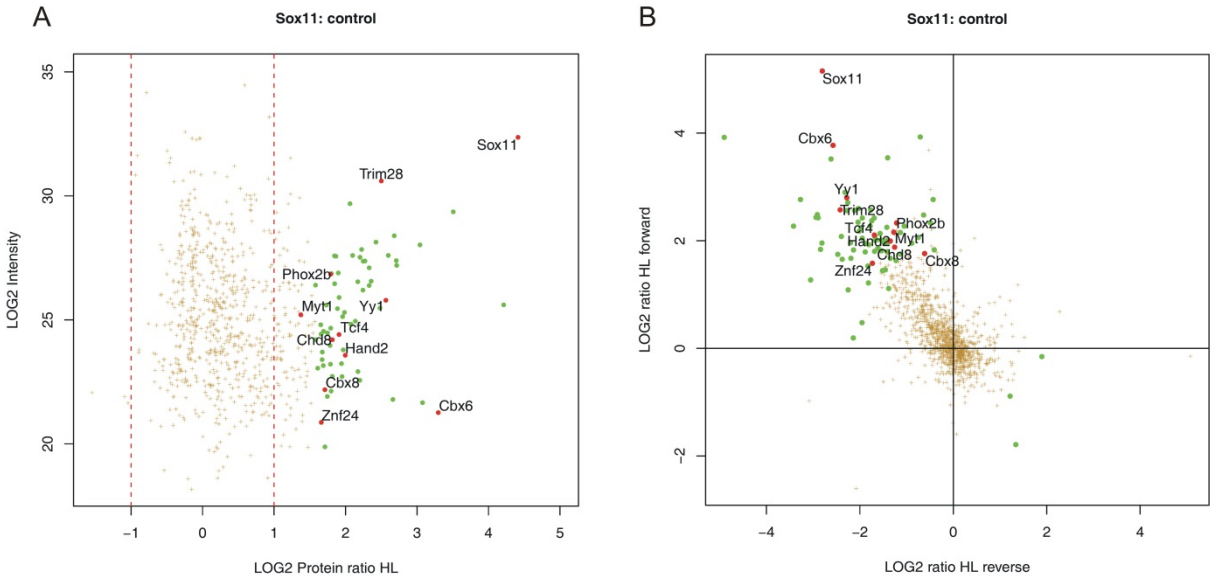

Figure 25:Scatterplot of the Sox11 interactome rich in transcriptional modulators
Scatterplot of Sox11 interactome data after MaxQuant/R analysis from 6 independent experiments, including 3 reverse labellings. Brown crosses denote unspecific interacting proteins, green dots display proteins significantly enriched ($p \leq 0.05$) in the Sox11 over-expressing affinity purifications. Sox11 and significant interacting proteins Trim28, Phox2b, Yy1, Myt1, Tcf4, Znf24, Cbx6, Cbx8, Phox2b and Chd8 are highlighted as red dots. Dotted lines depict manually set significance threshold value of 2. A) Log2 protein ratio HL (H: Sox11, L: control) is plotted against log2 intensity. B) Log2 ratio HL reverse (L: Sox11, H: control) is plotted against log2 ratio HL forward (H: Sox11, L: control).

Table 11: Subset of Sox11 interactors involved in transcriptional regulation

Accession number	Gene names	Unique peptides	Ratio H/L	Ratio forward	Ratio reverse	Significance A	Significance B
Q7M6Y2	Sox11	14	21.30	35.56	0.14	3.97E-07	2.86E-07
Q00899	Yy1	8	5.91	6.97	0.21	0.0026	0.0026
Q62318	Trim28	27	5.66	5.95	0.19	0.0033	0.0026
Q60722	Tcf4	3	3.75	4.30	0.31	0.0212	0.0212
O35690	Phox2b	4	3.46	5.03	0.43	0.0292	0.0240
Q91VN1	Znf24	2	3.16	3.00	0.30	0.0409	0.0420
Q8CFC2	Myt1	7	2.59	4.46	0.41	0.0795	0.0808
Q61039	Hand2	2	3.99	3.99	0.39	0.0166	0.0167
Q09XV5	Chd8	7	3.52	3.68	0.42	0.0274	0.0275
P30658	Cbx2	2	2.64	1.39	0.26	0.0755	0.0783
P23198	Cbx3	5	2.11	2.52	0.57	0.1437	0.1238
O55187	Cbx4	8	2.89	4.61	0.41	0.0559	0.0566
Q9DBY5	Cbx6	2	9.82	13.68	0.17	0.0001	0.0001
Q9QXV1	Cbx8	2	3.27	3.39	0.65	0.0361	0.0370

4.4. Validation of Sox11 interaction partners

4.4.1. Sox11 interacting proteins are efficiently confirmed by western blot analysis

Although the determination of the Sox11 interactome by quantitative mass spectrometry revealed a convincing list of specific interacting proteins, the results had to be validated by another method in order to confirm newly discovered interactions and increase the reliability of the interactome screen dataset. Consequently, eluates of FLAG affinity purifications as well as Sox11 or empty vector transfected nuclear lysates from Neuro2a cells were subjected to SDS-PAGE and subsequent western blot analysis. A subset of selected interactors, namely Trim28, Znf24, Yy1, Tcf4 and Phox2b was used for validation of the specific interaction with Sox11 (see figure 26). The signals obtained on nuclear extracts (input) of the Sox11 and the control condition revealed a stable expression of the five interacting proteins that was not altered upon Sox11 over-expression. Moreover, all of the interactors display a specific band in the Sox11 affinity purification, which is not present in the control fraction, thus confirming the efficient precipitation of Trim28, Znf24, Yy1, Tcf4 and Phox2b by Sox11, in addition to the mass spectrometry analysis on western blot level.

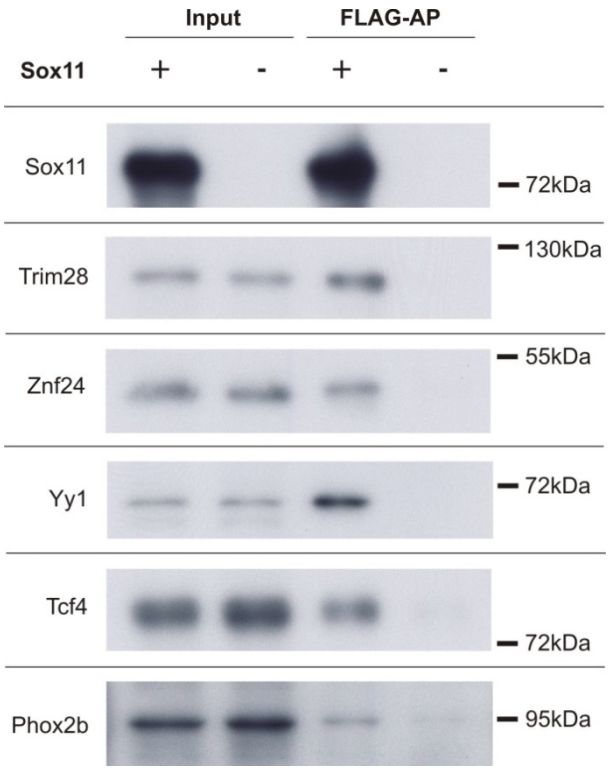

Figure 26: Western blot analysis of Sox11 interactors obtained by FLAG affinity purification
Western blotting of the Sox11 interactors Trim28, Znf24, Yy1, Tcf4 and Phox2b was performed using 10µg nuclear lysate of Sox11 over-expressing and empty vector control transfected cells as input and 2% (for Sox11 detection) or 10% (for interactor detection) of the FLAG affinity purification eluate, which was carried out using 5.5mg nuclear lysate. Sox11 was detected by stable clone 19B2, the interacting proteins by suitable commercial primary antibodies.

4.4.2. Sox11 interactors Myt1 and Yy1 are verified by targeted mass spectrometry

The neurogenesis-related Sox11 interactor Myt1 could not be validated by western blotting due to the lack of suitable antibodies for the transcription factor. Accordingly, a targeted mass spectrometry approach was established for Myt1 to confirm the identified interaction with Sox11. Yy1 was also included in the analysis in order to create an overlay with the western blot validation. For both proteins FLAG affinity purification eluates were measured using SIM scan methods on the Q Exactive mass spectrometer, integrating inclusion lists comprised of peptide-specific precursor masses and retention time windows. Data analysis via Skyline revealed peaks for every fragment ion displaying intensity over retention time. The automatically calculated peak area of the Sox11 affinity purification was divided by the control condition, resulting in Sox11 versus control ratios. For each protein 4 independent experiments were performed and subsequently one fragment ion per protein was

selected for quantification, which is depicted in table 12. The b7 ion KLEDATELVSK was used to evaluate Myt1 peak areas. The obtained ratios (6.11, 1.72 and 1.33) confirmed an enrichment of Myt1 in the Sox11 over-expressing affinity purification, in one experiment there was actually no fragment ion peak present in the control fraction, rendering quantification impossible. The assessment of Yy1 data revealed for the y5 ion FSLDFNLR even higher Sox11/control ratios (2942, 16.2, 14291.08), however there was also no peak detected in the control condition in 1 of 4 experiments, that's why it was excluded for quantification. Taken together, the specific interaction of Myt1 and Sox11 as well as Yy1 and Sox11 could be successfully verified by the application of a targeted mass spectrometric approach.

Table 12: Quantification of Myt1 and Yy1 by targeted mass spectrometry

Myt1 KLEDATELVSK b7

Experiment		1	2	3	4	Mean ratio	SEM
Peak area	Sox11	165637	64834	86411144	5588524544		
	Control	27099	0	50309104	4190584320		
Ratio	Sox11 vs. Control	6.11		1.72	1.33	**3.05**	1.53

Yy1 FSLDFNLR y5

Experiment		1	2	3	4	Mean ratio	SEM
Peak area	Sox11	7156138	7306518	15591569	8287518		
	Control	2432	434295	1091	0		
Ratio	Sox11 vs. Control	2942.49	16.82	14291.08		**5750.13**	4353.19

4.5. Evaluation of the Sox11 interactome

4.5.1. The Sox11 protein-protein interaction network

To evaluate the functional relationships between the observed interacting proteins and Sox11, a Sox11-centred protein-protein interaction network based on the dataset was established. Besides Sox11 TCF4, MYT1, TRIM28, ZNF24, YY1 and CBX6 (human cDNAs in (C)-SF-TAP pDEST Vector) served as baits for FLAG affinity purification to extend the network (see figure 27, nodes highlighted in brilliant green). The human constructs were used due to a better availability and high sequence homology to the murine cDNA. To establish the network end, we utilised Cytoscape

(Shannon et al., 2003) and acquired data to integrate previously described interactions from mouse databases applying the GeneMANIA plugin (Montojo et al., 2010). The mapping of our data revealed a dense merged network consisting of 29 nodes linked by 62 undirected interactions, referred to as edges (see figure 27). Closeness centrality analysis resulted in an average of 4.3 neighbours for each protein and revealed, as expected, Sox11 as the central protein of the network with the shortest distance to all other nodes, followed by Trim28, Yy1 and Tcf4. Sox11 also revealed the highest degree of connectivity as was uncovered by node degree distribution. Additionally, Trim28, Yy1 and Tcf4 as well as the polycomb repressive complex 1 (PRC1) components Rnf2, Phc2, Cbx2, Bmi1 and Ring1 were found to be highly connected. Green edges depict previously described interactions. Here, the wider the edges are, the stronger is the connection. Red edges represent the newly experimentally identified physical interactions in this study, while grey nodes act as link between co-precipitated proteins (bright green).

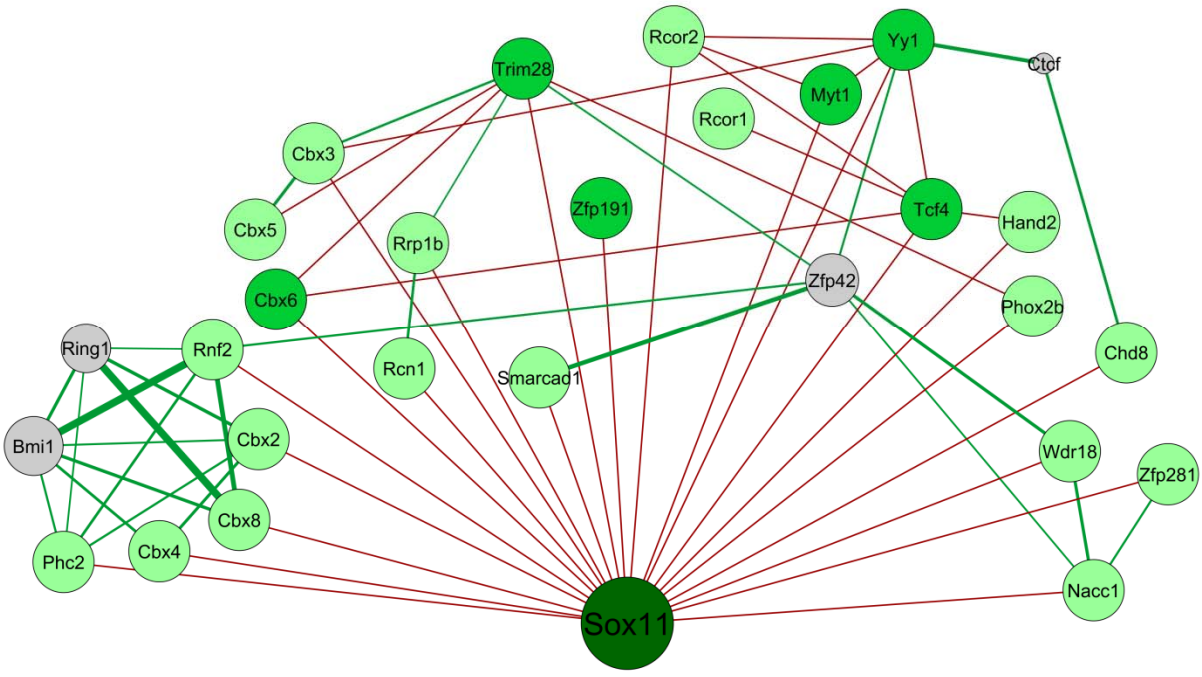

Figure 27:Sox11 protein-protein interaction network
The network was built by combining the interactome dataset with information of mouse interaction databases used by the Cytoscape plugin GeneMania allowing links by co-expression, shared protein domains, pathway and physical interactions, with at the minimum one experimental validation. Data were assessed from FLAG affinity purifications of Sox11, YY1, ZNF24, TRIM28, MYT1, TCF4 and CBX6 (dark and brilliant green nodes). Red edges connect newly identified interactions (bright green nodes) while connections that are previously described are linked by green edges. Grey nodes are included to connect identified proteins.

4.5.2. GO term analysis reveals enrichment of transcription regulatory activity

The list of the 164 significant Sox11 interacting proteins was subjected to GO term analysis using the ToppFun tool from the ToppGene software. The obtained proteins are enriched in molecular functions that are characteristic for transcription factors (see figure 28 3.-7. and 9.-13.) as well as for transcriptional modulators (see 3., 4., 8. and 16.) and regulation on translational level (see 1. and 2.).

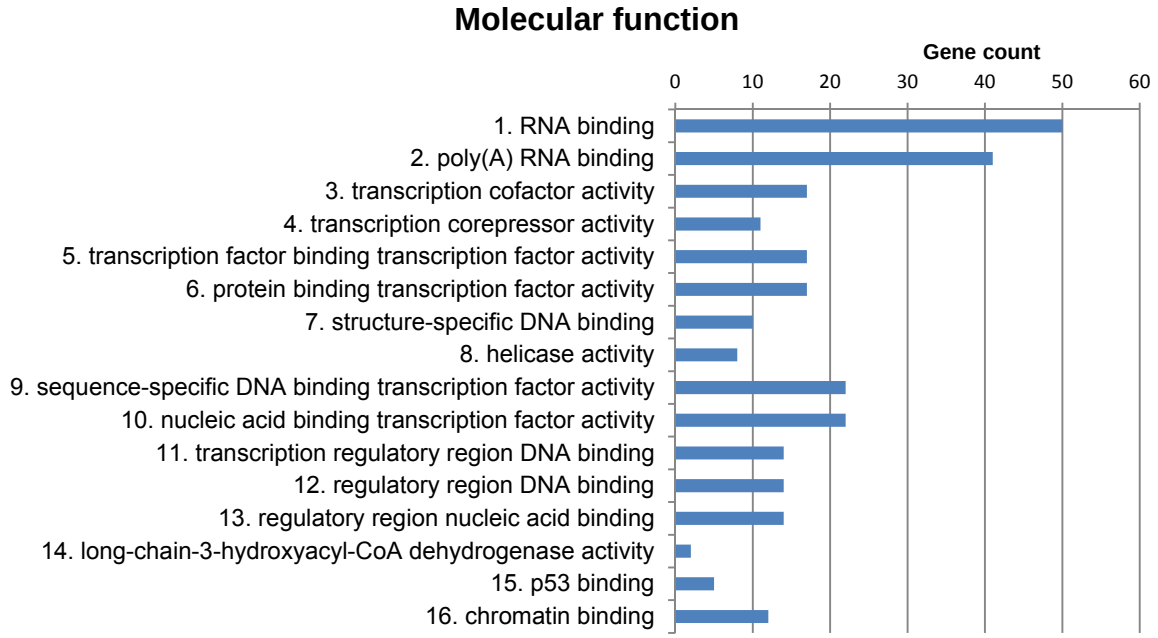

Figure 28:GO term analysis of enriched molecular functions
Molecular functions obtained by GO term analysis using ToppFun by ToppGene. The gene count displays the number of involved interacting proteins for each GO term. Significance was set to a value of 0.05 and data were corrected with Bonferroni for multiple testing.

The enriched biological processes identified in our dataset, revealed the role of the interactors in chromatin and chromosome organisation (see figure 29, 1. and 2.) and other processes linked to chromatin, histone and DNA modifications (13., 20., 22., 23., 33., 34.). Additionally, positive (17., 27) as well as negative (7., 8., 26) transcriptional regulation is overrepresented in our data analysis.

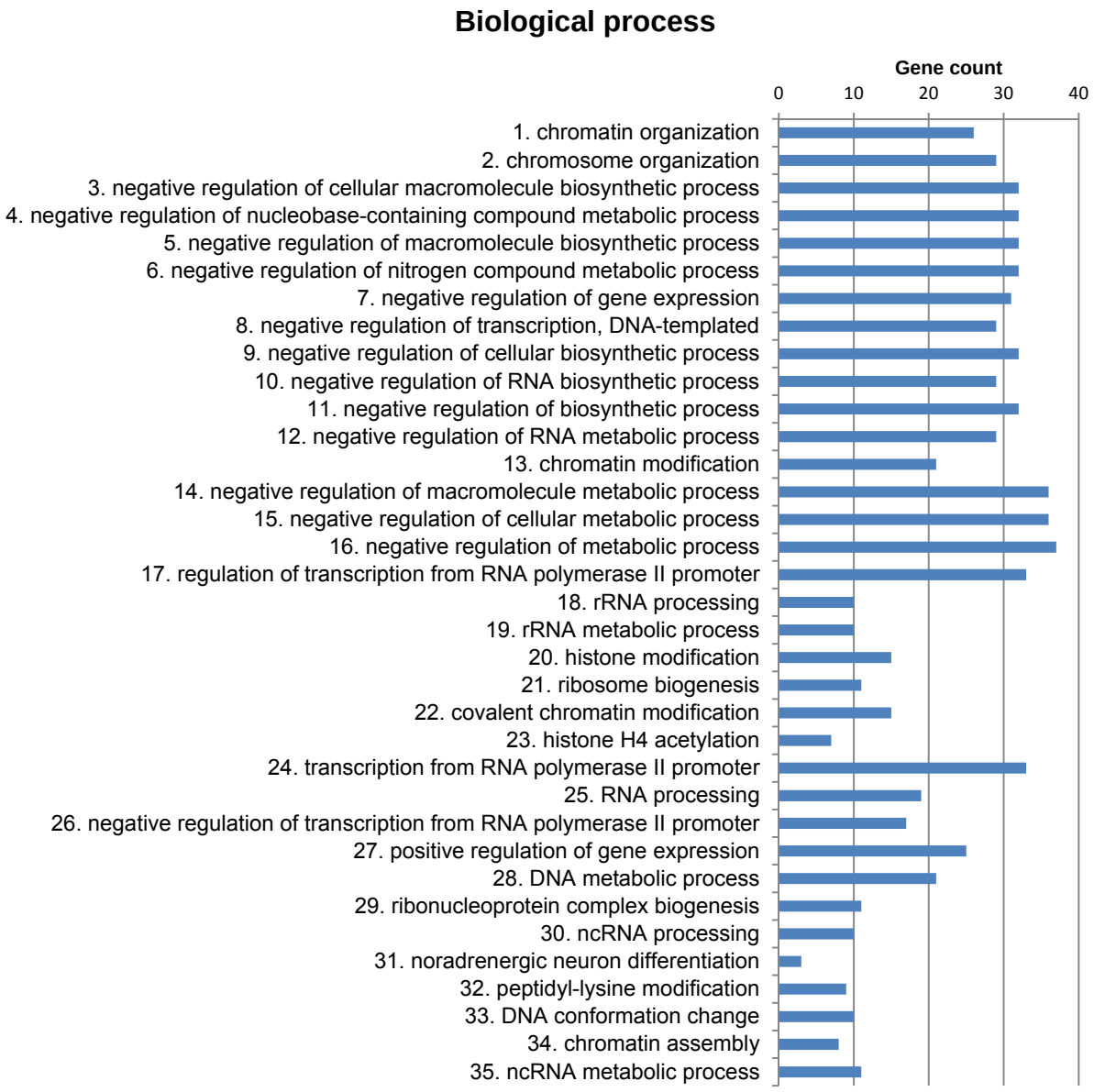

Figure 29:GO term analysis of enriched biological processes
Biological processes obtained by GO term analysis using ToppFun by ToppGene. The gene count displays the number of involved interacting proteins for each GO term. Significance was set to a value of 0.05 and data were corrected with Bonferroni for multiple testing.

The GO analysis cellular components generated 36 overrepresented terms in the interaction dataset (see figure 30). Herein, nuclear components related to chromosome, histone and chromatin modification and regulation complexes as well as transcription factor complexes are preponderant in the interactors list.

Altogether, our data reveals that the GO term analysis including molecular functions, biological processes and cellular components exhibits an accumulation of

transcription factors and proteins involved in the modulation of gene transcription in the specific Sox11 interactome dataset.

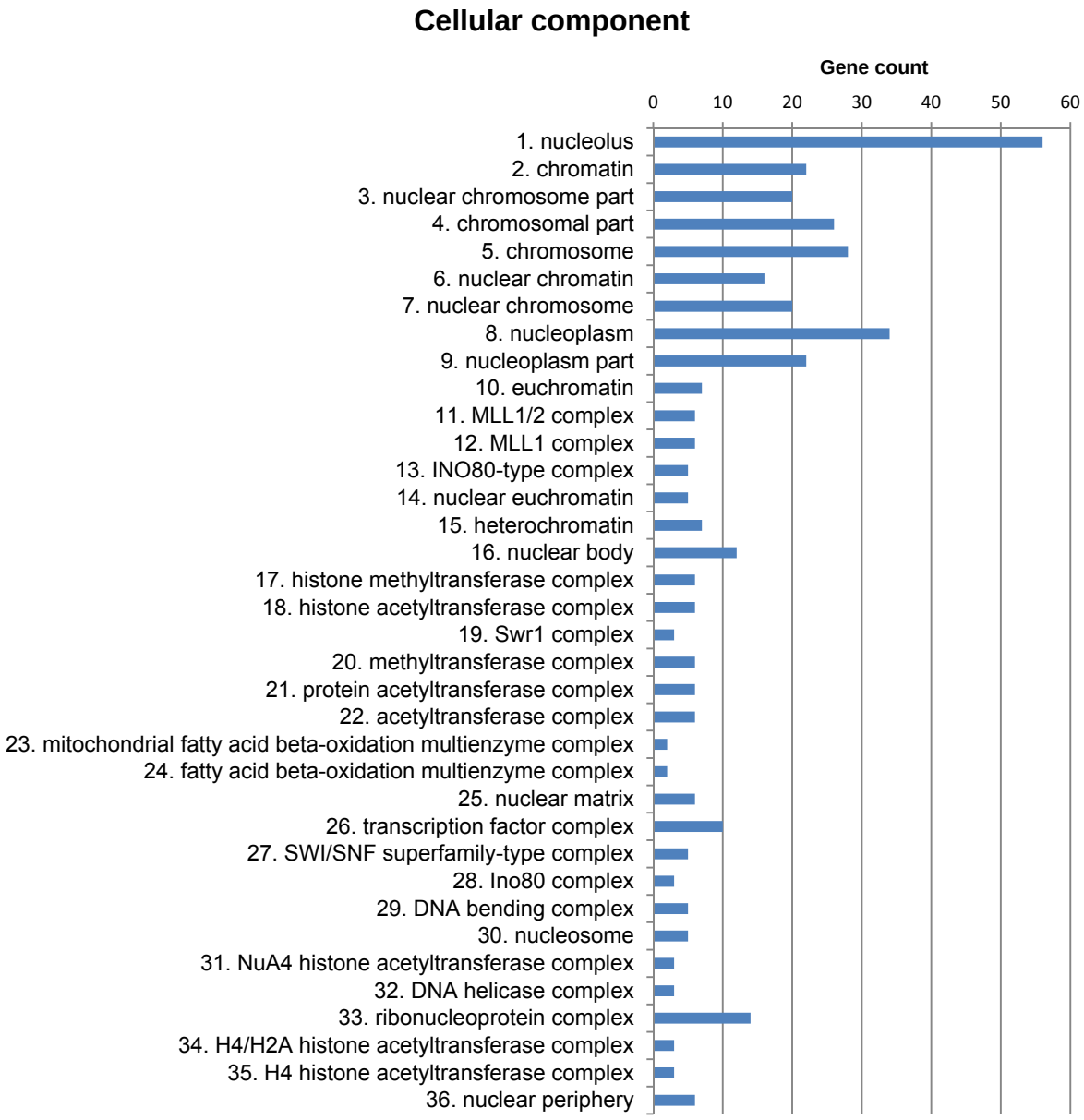

Figure 30:GO term analysis of enriched cellular components
Cellular components obtained by GO term analysis using ToppFun by ToppGene. The gene count displays the number of involved interacting proteins for each GO term. Significance was set to a value of 0.05 and data were corrected with Bonferroni for multiple testing.

4.6. Efficient shRNA-mediated knockdown of Sox11 interactors

Four transcription factors of the Sox11 interaction dataset were selected for a shRNA-dependent knockdown to allow their functional characterisation. Suitable oligonucleotides for shRNA constructs were purchased for the murine *Myt1*, *Tcf4*, *Yy1* and *Znf24*. The sequences were adapted from the mission shRNA information provided by Sigma Aldrich. The annealed and phosphorylated Oligonucleotides were cloned into the PWX1 Vector. The shRNA coding sequences were under the control of a murine U6 or human H1 promoter peculiarly adapted for shRNA-mediated knockdown, which was applied to the endogenous expressed proteins in Neuro2a cells.

4.6.1. Verification of knockdown efficiency on mRNA level

The efficiency of the shRNA-dependent knockdown had to be evaluated on mRNA level to check if the mRNA had been successfully degraded. This was achieved by quantitative Real-time PCR of cDNA generated from mRNA, isolated from Neuro2a cells that had been transfected with a knockdown plasmid. The analysis was carried out in 3 technical replicates of each sample. The normalisation to the reference gene *pyruvate dehydrogenase beta* (*Pdhb*) enabled relative quantification of the gene expression, and thus monitoring of the knockdown efficiency. The normalised relative expression compared to the empty vector transfected control condition was 34% for *Myt1*, 40% for *Tcf4*, 46% for *Yy1* and 58% for *Znf24* (see figure 31). This resulted in the best knockdown efficiency of 66% for *Myt1*, followed by 60% for *Tcf4*, 54% for *Yy1* and the lowest knockdown level was determined for *Znf24* with 42% efficiency compared to the control. Taken together, the shRNA-mediated knockdown decreased gene expression in all of the four transcription factors, with obtained knockdown efficiencies between 42 and 66%.

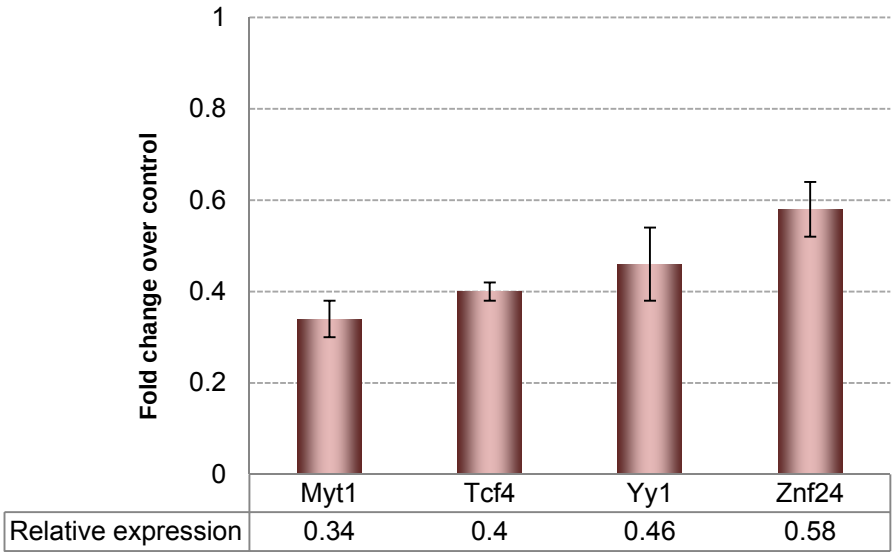

Figure 31:Relative expression on mRNA level following shRNA-mediated knockdown
ShRNA-mediated knockdown of *Myt1*, *Tcf4*, *Yy1* and *Znf24* was applied in Neuro2a cells. CDNA was synthesised from total RNA, isolated 48h after transfection. Relative expression on mRNA level was measured by quantitative RT-PCR using three technical replicates. Data were normalised to the expression of *Pdhb* as reference gene. Error bars depict the standard error of the mean.

4.6.2. Verification of knockdown efficiency on protein level

Additional to the evaluation on mRNA level, the knockdown level had to be assessed also on protein expression in order to validate the success of the shRNA-dependent knockdown of the four selected Sox11 interacting proteins on protein level. Therefore 2 different shRNA sequences under the control of the H1 or U6 promoter were tested for knockdown efficiency in Neuro2a cells for each of the candidate transcription factors. The transfected nuclear lysates were normalised to the expression of beta-Actin (Actb) on western blot as a loading control. Subsequent quantification compared to the empty vector control revealed knockdown efficiencies. Anti-GFP antibody was applied to monitor transfection rates of the individual plasmids (see figure 32). The best performing knockdown constructs were all under the control of the H1 promoter and are highlighted in bold in figure 32. The remaining relative expression after knockdown by the most efficient shRNAs is illustrated in figure 33. Myt1 displays a relative expression of 14% compared to the control condition, thus the knockdown is highly efficient with 86%. Tcf4 knockdown was even more successful exhibiting a relative expression level of 9%, hence a knockdown efficiency of 91%. The highest remaining relative expression was detected for Yy1 with 44% and a knockdown efficiency of 56%. Znf24 however, revealed 28% relative

expression compare to the control shRNA, according to a 72% efficient knockdown of the protein expression.

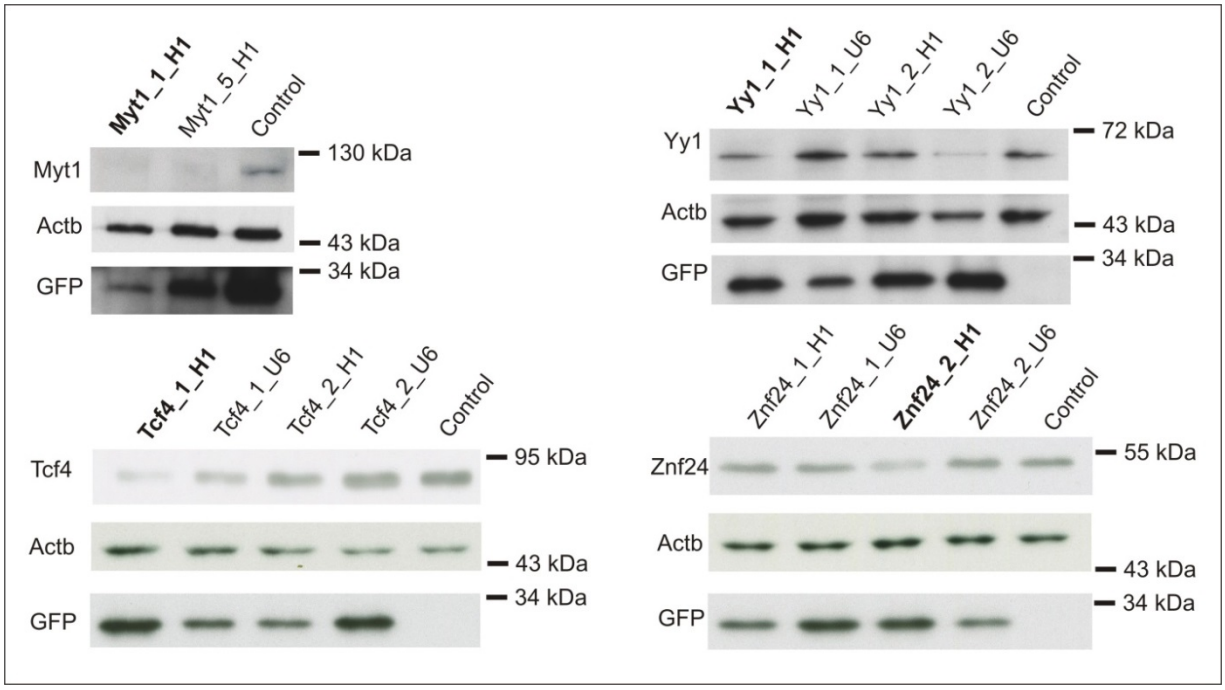

Figure 32:Western blot analysis of shRNA knockdown constructs
Western blot analysis was carried out for each protein using 10µg of cells nuclear lysates transfected with different shRNA constructs, isolated 48h post transfection for SDS-PAGE and compared to a unspecific shRNA control. Detection was achieved by using commercial antibodies. Anti-Actb antibody was used as a loading control and anti-GFP antibody was applied to monitor the efficiency of transfection.

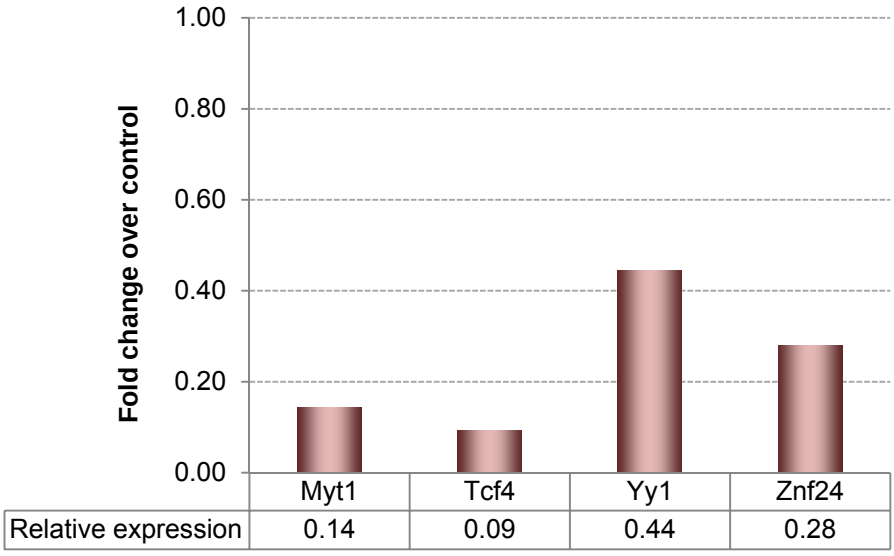

Figure 33: Relative expression on protein level following shRNA-mediated knockdown
ShRNA-mediated knockdown of Myt1, Tcf4, Yy1 and Znf24 was applied to Neuro2a cells. Nuclear lysates were isolated 48h after transfection. Relative expression on protein level was measured using SDS-PAGE coupled to western blot analysis. Data were normalised to the expression of Actb as reference protein. Displayed are the relative expressions of the best performing shRNA constructs.

4.7. Functional characterisation of candidate transcription factors and modulators

4.7.1. Reporter assays on Sox11 downstream promoters

For the functional evaluation, a selection of candidate transcription factors and transcriptional modulators of the Sox11 interactome dataset was chosen, that presumably play a role in the modulation of neurogenesis, neuronal differentiation and maturation as well as in the maintenance of the neural precursor cell properties. As Sox11 is involved in the promotion of neurogenesis and neuronal maturation, the candidate-dependent regulation of Sox11 downstream promoters was established to investigate their influence on these neuronal processes. To that end the effects of MYT1, TCF4, TIF1b, YY1, CBX6 and ZNF24 on the Sox11-regulated promoters of *Doublecortin* and *Stathmin1* were determined.

4.7.1.1. Dual luciferase assay on the human DCX promoter

The microtubule-associated protein Doublecortin (DCX) is considered as one of the earliest markers for immature neurons that are generated in neurogenic niches during adult neurogenesis (Brown et al., 2003). Recently, the *DCX* promoter has been shown to be activated by the SoxC proteins Sox11 and Sox4 in reporter assays using a DCX regulatory element coupled to luciferase (Mu et al., 2012). This previously identified 3.5 kb genomic region upstream of the human DCX ATG start codon which reliably induces expression of reporter genes and its activity overlaps with the endogenous expression of Doublecortin in neuronal precursors (Karl et al., 2005) we applied for dual luciferase assay. Herein, firefly luciferase serves as reporter gene and renilla luciferase as transfection control, enabling normalisation of changes in transfection efficiency. The assay was carried out by co-transfection of the transcription-regulating proteins MYT1, TCF4, TRIM28, YY1, CBX6 and ZNF24 together with the *DCX*-promoter/luciferase and the renilla luciferase constructs. Sox11 was applied as a positive control. The subsequently performed dual luciferase assay revealed a slight activation of the *DCX*-promoter by MYT1, CBX6 and ZNF24 with fold changes of 4.8, 4.1 and 2.1 over control (empty vector plus luciferase plasmids) compared to the strong 93.6 fold activation of Sox11 (see figure 34A) with a significance $p \leq 0.001$. This led to the assumption that there might be some

cooperative effect of Sox11 and its interacting proteins greater than the regulation of the factors alone. Consequently, the experiments were implemented under co-expression of each protein with Sox11 and the reporter constructs (see figure 34B), which resulted in the distinct 2.3 fold enhancement of *DCX* promoter activation by Myt1/Sox11 compared to Sox11 alone. Additionally, co-expression of Sox11 with TRIM28 and ZNF24 increased the ability of activating *DCX* with fold changes of 1.4 and 1.7 over Sox11. On the contrary, TCF4/Sox11 and YY1/Sox11 led to respectively a 1.4 and 1.2 fold decreased promoter activity. To validate these observations, a shRNA-mediated knockdown of Myt1, Tcf4, Yy1 and Znf24 was implemented in Neuro2a cells and the reporter assays were repeated applying co-expression of Sox11 with the knockdown constructs. A marked 1.66 fold decrease in the ability of promoter activation was detected for Myt1-KD/Sox11, as well as for Tcf4-KD/Sox11 (see figure 34C) compared to Sox11-dependent activation alone. In the case of Myt1 knockdown this decrease correlates with the elevated activation observed under over-expression suggesting a role for Myt1 in association with Sox11 during the progress of early neuronal differentiation. The decrease in activation observed by TCF4 knockdown didn't correlate with the increased activity under TCF4 over-expression. In contrast, Yy1-KD/Sox11 increased the expression of the reporter protein firefly luciferase 1.3 fold compared to Sox11 alone, thus confirming the inhibitory effect monitored by over-expressing YY1/Sox11.

Dual Luciferase Assay on *DCX*
A) Over-expression

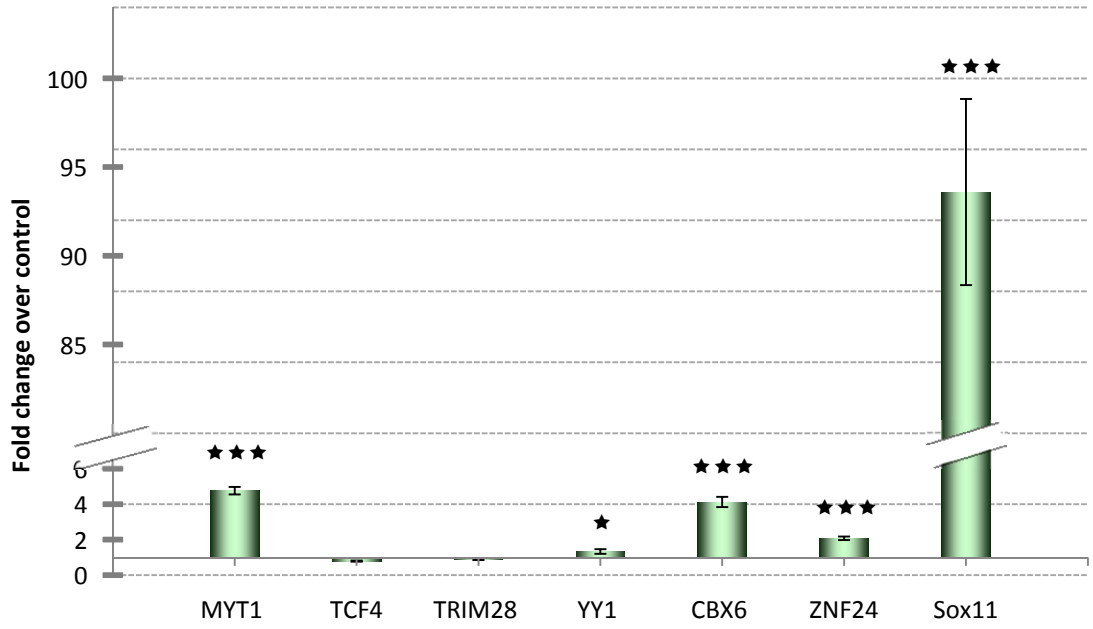

B) Co-expression with Sox11

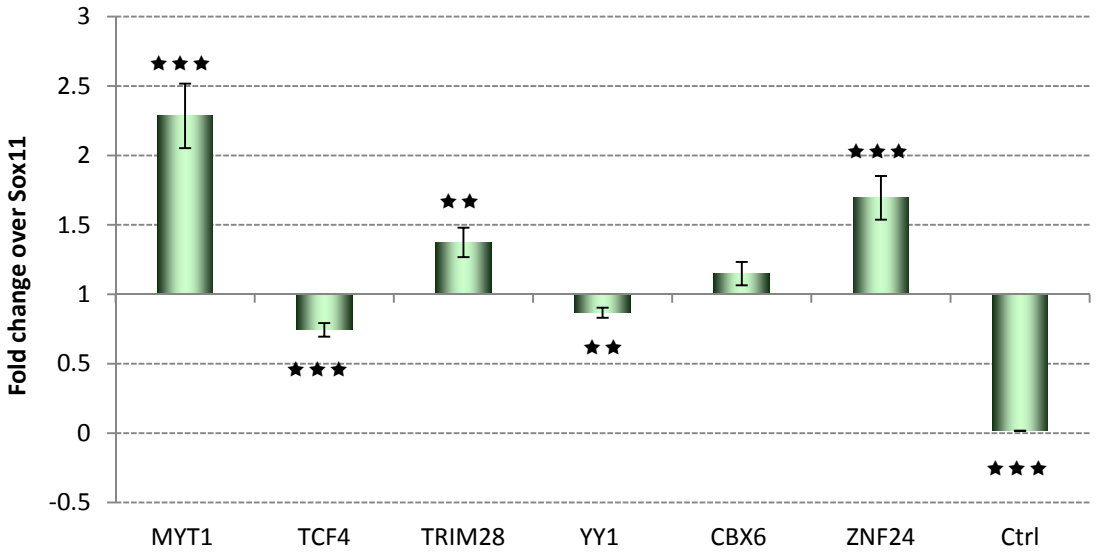

C) Knockdown + Over-expression of Sox11

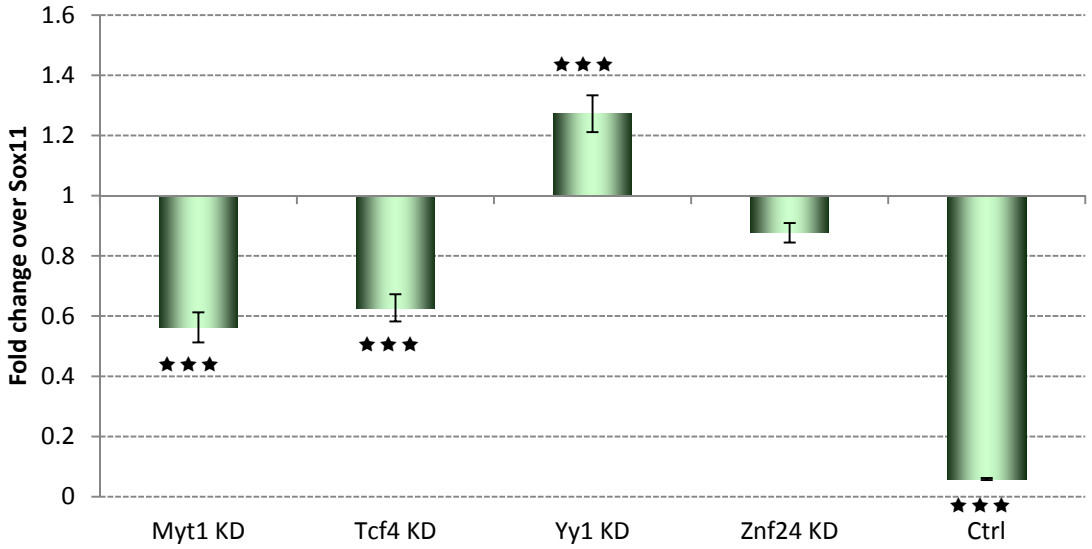

Figure 34:Dual luciferase assay on *DCX* promoter
Reporter assay on *DCX* regulatory element was performed using firefly luciferase as reporter protein and renilla luciferase as normalisation control to level out different transfection efficiencies. Sox11 over-expression served as positive control and empty vector plus luciferase plasmids as negative control (Ctrl). (A) MYT1, TCF4, TIF1b, YY1, CBX6, ZNF24 and empty vector control were over-expressed alone or (B) co-expressed with Sox11, promoter activity is shown by fold change of firefly versus renilla luciferase over control (A) and Sox11, respectively (B). Effects of shRNA-mediated knockdown of Myt1, Tcf4, Yy1 and Znf24 combined with over-expression of Sox11 on the promoters are illustrated as fold change over Sox11 (C). Significance value of the 3x3 biological replicates is indicated by stars (★ = p≤0.05, ★★ = p≤0.01, ★★★ = p≤0.001). Error bars denote the standard error of the mean.

4.7.1.2. Dual luciferase assay on the human STMN1 promoter

Next, we explored if cooperation of Sox11 with these transcription factors also modulates the expression of other Sox11 downstream targets. Thus the same experimental workflow was applied to the regulatory element of the human *Stathmin1 (STMN1)* gene which was recently identified as a putative direct transcriptional target of Sox11 (K. Doberauer, J. v. Wittgenstein, D.C. Lie, unpublished data). To this end, the human *STMN1* promoter was coupled to firefly luciferase as reporter gene. The over-expression of the interactors alone showed a decrease of activation for TCF4, TRIM28, YY1 and ZNF24 normalised to the control, pointing out a basal activity of the *STMN1* promoter construct, whereas Sox11 was found to regulate the promoter in a positive manner with a fold change of 2.8 compared to the control condition (see figure 35A). After the subsequent assay performing co-over-expression of each protein together with Sox11, a diminished promoter activity was observed for TCF4/Sox11, TRIM28/Sox11 and YY1/Sox11 by 1.3, 1.1 and 1.7 fold normalised to

Sox11-dependent regulation (see figure 35B). Here, MYT1/Sox11 showed only a slight shift of 1.1 fold towards activation. After knockdown of the proteins, this resulted in 2.3 fold decrease of Sox11-dependent promoter activity for Myt1 and in 1.4 fold increase of the *STMN1* promoter activation level for Yy1 (see figure 35C). These results were in line with the findings for the *DCX* regulatory element.

Dual luciferase assay on *STMN1*
A) Over-expression

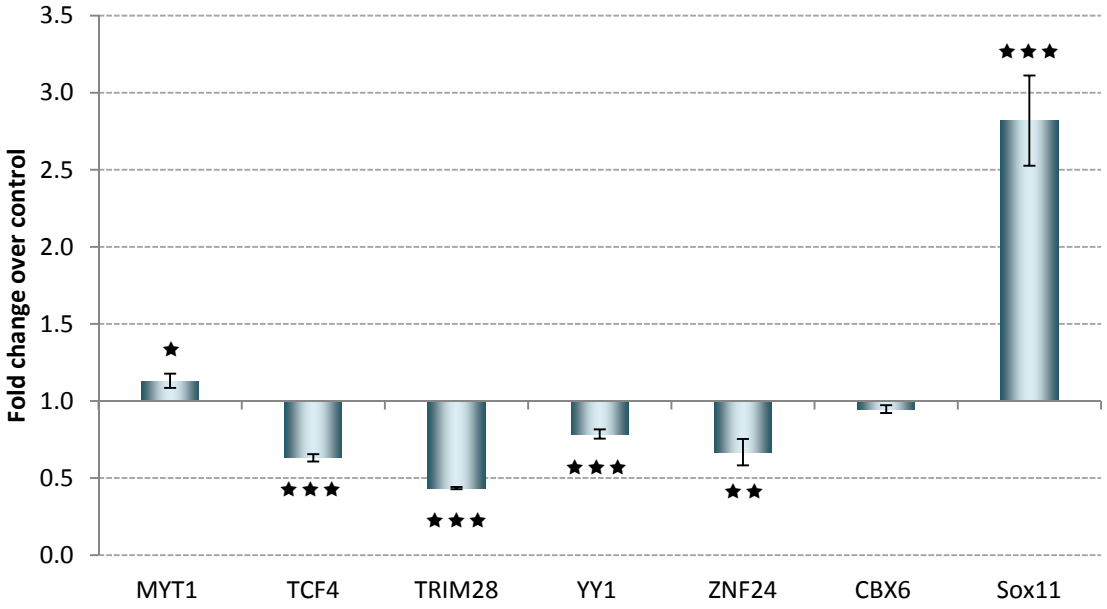

B) Co-expression with Sox11

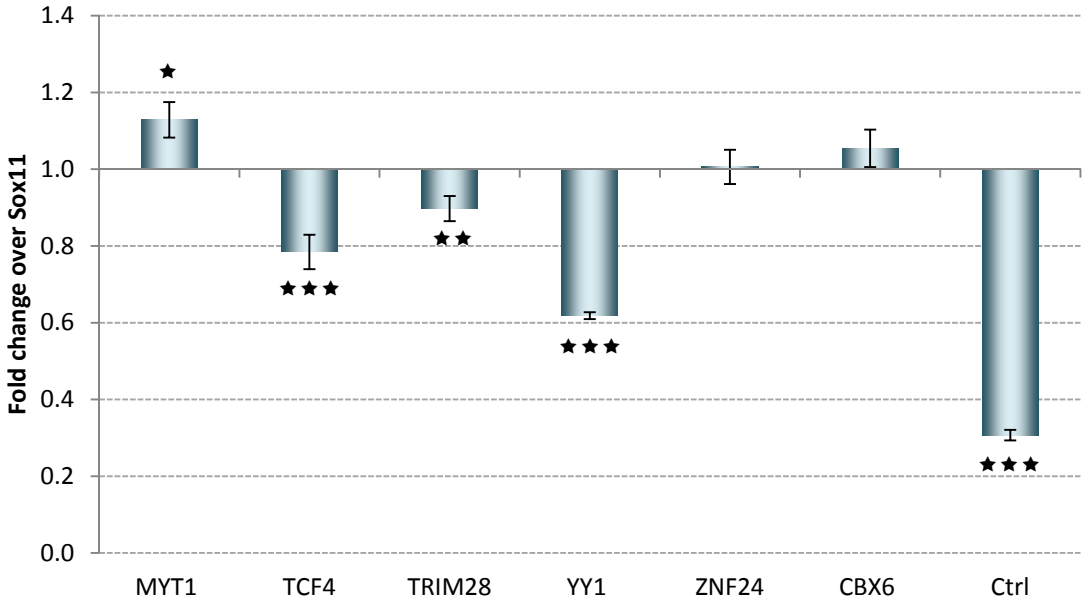

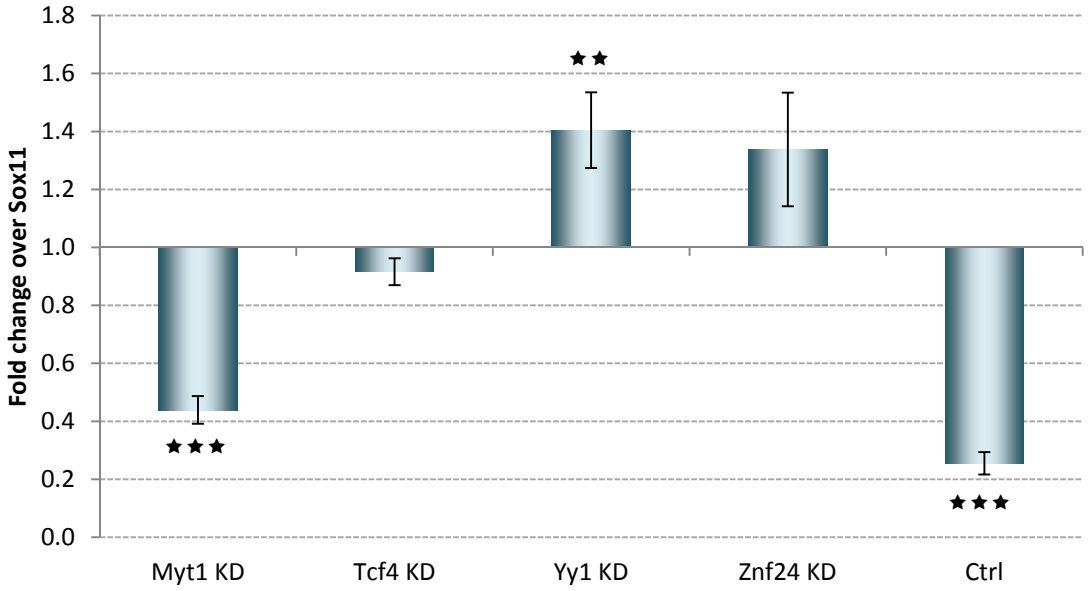

Figure 35:Dual luciferase assay on *STMN1* promoter
Reporter assay on *STMN1* regulatory element was performed using firefly luciferase as reporter protein and renilla luciferase as normalisation control to level out different transfection efficiencies. Sox11 over-expression served as positive control and empty vector plus luciferase plasmids as negative control (Ctrl). (A) MYT1, TCF4, TIF1b, YY1, CBX6, ZNF24 and empty vector control were over-expressed alone or (B) co-expressed with Sox11, promoter activity is shown by fold change of firefly versus renilla luciferase over control (A) and Sox11, respectively (B). Effects of shRNA-mediated knockdown of Myt1, Tcf4, Yy1 and Znf24 combined with over-expression of Sox11 on the promoters are illustrated as fold change over Sox11 (C). Significance value of the 3x3 biological replicates is indicated by stars (★ = p≤0.05, ★★ = p≤0.01, ★★★ = p≤0.001). Error bars denote the standard error of the mean.

4.7.2. *In silico* promoter analysis

4.7.2.1. Consensus sequences of transcription factors

The specific binding sites, where common transcription factors bind to DNA sequences were evaluated using the transcription factor database Matbase being part of the Genomatix Software. This analysis was performed for SOX11, MYT1 and YY1 and revealed specific consensus sequences for each transcription factor. According to the IUPAC nomenclature, the core sequence is illustrated in capital letters. Additionally, nucleotides with a conservation degree above 60% are depicted in bold. One binding site was available for SOX11, two were present for MYT1 and even three are recognised by YY1 (see figure 36). The transcription factor binds to the consensus sequence YY1.01 when it acts as activator, whereas it recognizes YY1.02 while exercising its repressive function.

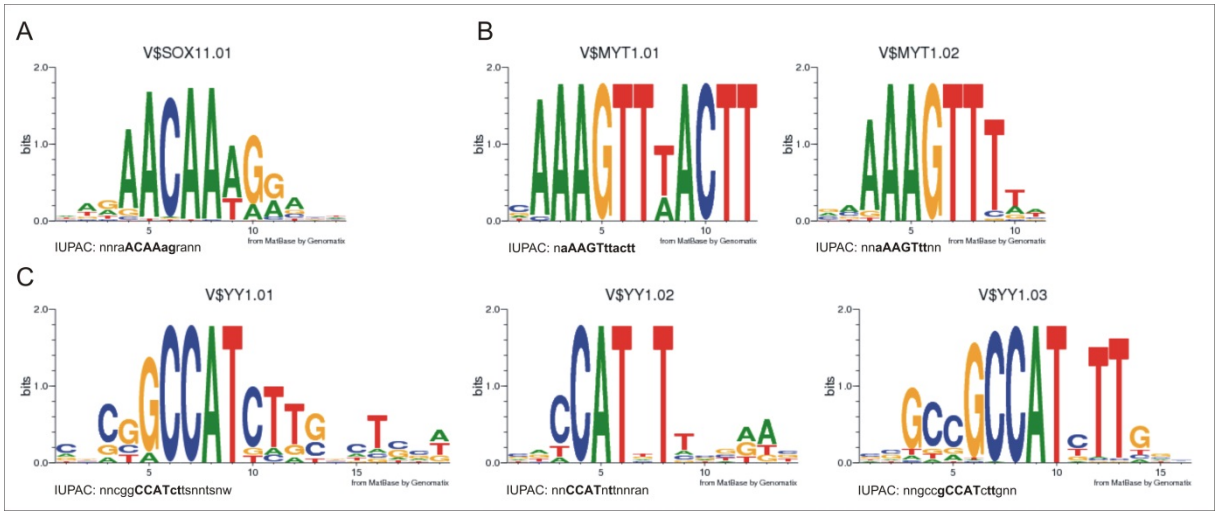

Figure 36:Consensus sequence logos of SOX11, MYT1 and YY1
Sequence logos for SOX11, MYT1 and YY1 were designed from Matbase by Genomatix showing the probable composition of nucleotides in specific transcription factor binding sites. Capital letters denote the core sequence (usually 4 nucleotides), depicted in bold are nucleotides with a degree of conservation above 60%. For SOX11 one consensus was identified, whereas MYT1 recognises two specific binding sites on the DNA and YY1 even three consensus sequences. Binding to V$YY1.01 allows YY1 to carry out its transcription activating function, while binding to V$YY1.02 is involved in YY1-dependent repression of promoter activity.

4.7.2.2. Transcription factor families with binding sites in DCX and Stmn1 promoters

The fragments of the human *DCX* and the *STMN1* promoter, which were used in the reporter assays as well as their mouse corresponding sequences, were analysed by means of the CommonTF tool coupled with the MatInspector tool from the Genomatix software. This aimed to the identification of consensus sequences for selected transcription factor families in the promoters regions. Both regulatory regions of *DCX* (see figure 37A) and *STMN1* (see figure 37B) in the organisms human and mouse were found to comprise a number of binding sites for the family of SOX (V$SORY) transcription factors, the MYT1 family (V$MYT1) as well as the YY1 (V$YY1F) family. The human *DCX* regulatory sequence includes several binding sites for members of the three families, whereas the mouse sequence only displays few binding regions. Within the human *STMN1* promoter sequence a small number of binding sites for the analysed families is present. In contrast to that, the mouse region reveals only binding potential for transcription factors of the SOX family. The availability of binding sites for the three transcription factor families serves as a starting point for the deeper analysis of specific consensus sites recognised by the individual family members SOX11, MYT1 and YY1.

Figure 37:SORY, MYT1 and YY1 family binding sites in *DCX* and *STMN1* promoter
The promoter sequences of human and mouse *DCX* (A) and *Stathmin1* (B) were analysed via the Common TF and MatInspector tool from Genomatix Software for the assessment of consensus sequences of transcription factor families. Both regulatory regions exhibit binding sites for the matrix families of the SOX proteins (V$SORY), the MYT1 family (V$MYT1) as well as the YY1 family of proteins (V$YY1).
Data were generated by Dr. Dietrich Trümbach, Institute for Developmental Genetics, Helmholtz Zentrum München.

4.7.2.3. Binding sites for SOX11, MYT1 and YY1 in DCX and STMN1 promoter

The assessment of specific binding sites for the transcription factors SOX11, MYT1 and YY1 in the regulatory regions of both *DCX* and *STMN1* was performed by means of the Common TFs and MatInspector tools from the Genomatix software. For SOX11 (see table 13) the analysis revealed 10 binding sites in the human *DCX* promoter and 2 in the corresponding murine region. In the *STMN1* promoter 4 SOX11 consensus sequences were present in the human and 2 sites in the murine promoter.

The search for specific binding sites resulted in 9 consensus sequences in the human and 7 in the murine *DCX* regulatory region for MYT1 (see table 13). The

STMN1 promoter however, exhibited only one binding site in the human and no MYT1-specific site in the murine sequence.

For YY1, The binding site analysis on the two promoter sequences resulted in one specific site in the human and 2 in the murine *DCX* promoter sequence (see table 13). Additionally, one binding site was detected for the transcription factor in the human *STMN1* promoter whereas no YY1-specific consensus sequence was present in the murine regulatory region of *Stmn1*.

Additional analysis of transcription factor modules present with SOX11 in the regulatory sequences of the two immature neuron markers revealed an over-representation of adjacent MYT1/SOX11 binding sites in the *DCX* and the *STMN1* promoter region (see table 14). Moreover, the transcription factor PHOX2B, that is part of the SOX11 interactome dataset, was found to be over-represented in the *DCX* promoter combined in a module with SOX11. Results are presented by calculated Z-score values (Kreyszig, 1979).

Table 13: SOX11, MYT1 and YY1 binding sites in *DCX* and *STMN1* promoters
Data were generated by Dr. Dietrich Trümbach, Institute for Developmental Genetics, Helmholtz Zentrum München.

	Matrix	human	mouse
DCX	V$MYT1.01	4	5
	V$MYT1.02	5	2
	V$SOX11.01	10	2
	V$YY1.01	1	0
	V$YY1.02	0	2
	V$YY1.03	0	0
STMN1	V$MYT1.02	1	0
	V$SOX11.01	4	2
	V$YY1.02	1	0

Table 14: Selected over-represented modules in human *DCX* and *STMN1* promoters
Data were generated by Dr. Dietrich Trümbach, Institute for Developmental Genetics, Helmholtz Zentrum München.

Promoter	Modules with V$SOX11.01	Matches	Z-Score
DCX	V$PHOX2B.01 V$SOX11.01	9	12.46
	V$MYT1.02 V$SOX11.01	2	2.32
STMN1	V$MYT1.02 V$SOX11.01	1	1.25

4.7.2.4. *Definition of models for the matrix families SORY/MYT1 and SORY/YY1*

By means of the Frameworker tool from the Genomatrix software, models for the combinations of transcription factor families SORY/MYT1 and SORY/YY1 were defined. For the analysis of the *DCX* promoter, the human and the mouse regulatory regions were used as input, due the conservation between the two species and the availability of consensus sequences for all three matrix families. The *STMN1* promoter, however, revealed only few binding sites for the evaluated transcription factors. Due to this fact, the *STMN1* analysis was carried out by the combination of human *STMN1* and *DCX* promoter sequences. This is enabled under the hypothesis of an estimated cooperative regulation of the two genes. Models, generated by Frameworker were defined and ranked according to several criteria, including the gap between the transcription factor binding sites, distance to the transcription start and matrix similarity. By using these standards, 11 models were found for SORY/MYT1 and 2 models for SORY/YY1 using the *DCX* promoter sequence (see table 15). For the combination of human *DCX* and *STMN1* promoter 2 models were generated for SORY/MYT1 (see table 16).

Table 15: Frameworker models of the human and mouse *DCX* promoter
Data were generated by Dr. Dietrich Trümbach, Institute for Developmental Genetics, Helmholtz Zentrum München.

Model	Element	Strand	Matrix similarity	Distance	Common to
D_SORY/MYT1-1	V$MYT1 V$SORY	- +	min. 0.76 min. 0.92	25 - 29 bp	3 matches in 2 seq. (100%), 3 non-overlapping
D_SORY/MYT1-2	V$MYT1 V$SORY	- +	min. 0.93 min. 0.88	50 - 59 bp	2 matches in 2 seq. (100%), 2 non-overlapping
D_SORY/MYT1-3	V$MYT1 V$SORY	- +	min. 0.94 min. 0.92	171 - 179 bp	2 matches in 2 seq. (100%), 2 non-overlapping
D_SORY/MYT1-4	V$MYT1 V$SORY	- +	min. 0.93 min. 0.94	46 - 54 bp	2 matches in 2 seq. (100%), 2 non-overlapping
D_SORY/MYT1-5	V$MYT1 V$SORY	- -	min. 0.96 min. 0.82	149 - 152 bp	2 matches in 2 seq. (100%), 2 non-overlapping
D_SORY/MYT1-6	V$MYT1 V$SORY	- -	min. 0.96 min. 0.82	152 - 161 bp	2 matches in 2 seq. (100%), 2 non-overlapping
D_SORY/MYT1-7	V$MYT1 V$SORY	+ +	min. 0.76 min. 0.92	69 - 77 bp	2 matches in 2 seq. (100%), 2 non-overlapping
D_SORY/MYT1-8	V$MYT1 V$SORY	+ +	min. 0.76 min. 0.88	77 - 82 bp	2 matches in 2 seq. (100%), 2 non-overlapping
D_SORY/MYT1-9	V$MYT1 V$SORY	+ +	min. 0.80 min. 0.94	135 - 140 bp	2 matches in 2 seq. (100%), 2 non-overlapping

D_SORY/MYT1-10	V$MYT1 V$SORY	+ -	min. 0.88 min. 0.83	140- 141 bp	2 matches in 2 seq. (100%), 2 non-overlapping
D_SORY/MYT1-11	V$MYT1 V$SORY	+ -	min. 0.76 min. 0.82	99- 100 bp	2 matches in 2 seq. (100%), 2 non-overlapping
D_SORY/YY1-1	V$SORY V$YY1F	- -	min. 0.88 min. 0.86	106- 106 bp	2 matches in 2 seq. (100%), 2 non-overlapping
D_SORY/YY1-2	V$SORY V$YY1F	- +	min. 0.97 min. 0.96	21- 25 bp	2 matches in 2 seq. (100%), 2 non-overlapping

Table 16: Frameworker models of the human *DCX* and *STMN1* promoter
Data were generated by Dr. Dietrich Trümbach, Institute for Developmental Genetics, Helmholtz Zentrum München.

Model	Element	Strand	Matrix similarity	Distance	Common to
DS_SORY/MYT1-1	V$MYT1 V$SORY	+ -	min. 0.93 min. 0.95	40 - 48 bp	2 matches in 2 seq. (100%), 2 non-overlapping
DS_SORY/MYT1-2	V$MYT1 V$SORY	+ -	min. 0.88 min. 0.94	141 - 144 bp	2 matches in 2 seq. (100%), 2 non-overlapping

4.7.2.5. Adjacent binding sites present in the *DCX* and *STMN1* promoter sequence

Although the generated models for the combinations of SORY/MYT1 and SORY/YY1 comprise different members from the selected transcription factor families, they exhibit a high similarity of recognised consensus sequences to the selected candidates, which could also enable their binding. Thus, these models are appropriate for the identification of SOX11-, MYT1- and YY1-specific binding sites on the two promoter sequences. By means of the Common TF and MatInspector tools from Genomatix adjacent binding sites were detected according to the defined models.

The human *DCX* promoter revealed two neighbouring binding sites for MYT1 and SOX11, according to the models D_SORY/MYT1-1, D_SORY/MYT1-11 and D_SORY/MYT1-4 (see table 17). In addition, adjacent binding sequences for YY1 and SOX11 were present in the murine *Dcx* promoter, corresponding to the model D_SORY/YY1-1. Within these 4 models that are illustrated in figure 38, the binding regions are highlighted (see figure 38A).

The search for binding sites in the human *STMN1* promoter resulted in one pair of adjacent consensus sequences that are recognized by MYT1 and SOX11, corresponding to the model DS_SORY/MYT1-1 (see table 18). The binding region is

illustrated in figure 38B. Interestingly, the *DCX*-based model D_SORY/MYT1-4 was also found in the *STMN1* sequence.

Table 17: Binding sites in *DCX* according to defined models
Data were generated by Dr. Dietrich Trümbach, Institute for Developmental Genetics, Helmholtz Zentrum München.

Model	Element	Position	Strand	Matrix similarity	Sequence	SORY in the model
human						
D_SORY/MYT1-11	V$SOX11.01 V$MYT1.02	330-354 436-448	- +	0.94 0.90	atacaACAAtggatgggataataaa aagAAGTtttaag	V$SOX30.01
D_SORY/MYT1-1	V$MYT1.01 V$SOX11.01	1361-1373 1384-1408	- +	0.76 0.91	acaAAGTagacta aaaaaACAAaaaaccagttgttgga	V$SOX4.01
D_SORY/MYT1-4	V$MYT1.02 V$SOX11.01	2607-2619 2668-2692	+ +	0.88 0.93	tacAAGTttgggg ccagaACAAtgaaaggtgtgcttcc	V$SOX12.01
murine						
D_SORY/YY1-1	V$YY1.02 V$SOX11.01	1365-1387 1383-1407	- -	0.95 0.94	cctggtCCATgtgctgagaatga agttaACAAagagactcatacctgg	V$HBP1.01

Table 18: Binding sites in *STMN1* according to defined models
Data were generated by Dr. Dietrich Trümbach, Institute for Developmental Genetics, Helmholtz Zentrum München.

Model	Element	Position	Strand	Matrix similarity	Sequence	SORY in the model
DS_SORY/MYT1-1	V$MYT1.02 V$SOX11.01	618-630 660-684	+ -	0.98 0.91	ccaAAGTttggaa cgagaACAAgggcagggcggagcag	V$SOX9.02 V$SOX9.02

For the generated models, detected in the DCX or *STMN1* promoters, Z-scores were calculated. Models were referred to as significant with Z-scores ≥ 1.96. According to that, the models D_SORY/MYT1-1, D_SORY/MYT1-11 and D_SORY/YY1-1, present in *DCX* as well as D_SORY/MYT1-4 and DS_SORY/MYT1-1, present in *DCX* and *STMN1* were significantly enriched in the corresponding promoter sequence (see table 19).

Table 19: Z-scores for detected models
Data were generated by Dr. Dietrich Trümbach, Institute for Developmental Genetics, Helmholtz Zentrum München.

Model	Promoter sequence	Hit	Z-score
D_SORY/MYT1-1	*DCX*	2	3.63
D_SORY/MYT1-4	*DCX*	1	0.54
D_SORY/MYT1-4	*DCX+STMN1*	2	2.23
D_SORY/MYT1-11	*DCX*	1	2.01
D_SORY/YY1-1	*DCX*	1	4.46
DS_SORY/MYT1-1	*STMN1*	1	1.42
DS_SORY/MYT1-1	*DCX+STMN1*	2	3.22

Figure 38:Models detected in *DCX* and *STMN1* promoters

The four models for *DCX* (A) and one model for *DCX/STMN1* (B), generated for the matrix families SORY/MYT1 and SORY/YY1 by Frameworker displayed adjacent binding sites within the human *DCX* (A) and *STMN1* (B) promoter. Corresponding binding regions are highlighted in red.

Data were generated by Dr. Dietrich Trümbach, Institute for Developmental Genetics, Helmholtz Zentrum München.

4.7.2.6. Genome-wide binding of defined models

The models for the transcription factor families SORY/MYT1 and SORY/YY1 that displayed binding sites in the *DCX* and *STMN1* promoter, respectively, were further analysed concerning their presence in all human promoters. The genome-wide binding was assayed by the ModelInspector tool from Genomatix. The obtained human promoters were subjected to Gene Ontology (GO) analysis. In particular, the models for the combined families SORY and MYT1 D_SORY/MYT1-1, D_SORY/MYT1-4 and DS_SORY/MYT1-1 displayed among others an enrichment of binding sites on promoters related to neuronal development (see figure 39). Within the model D_SORY/MYT1-1 15 biological processes, linked to brain, CNS and neuron development, generation and differentiation of neurons as well as ventricular zone neuroblast division (see figure 39A). NEUROD1, an important modulator of late neurogenesis downstream of SOX11 (Gao et al., 2009) is also enriched in this analysis. The model D_SORY/MYT1-4 was also found in 6 biological processes, related to neurogenesis, neuronal differentiation and development (see figure 39B). In this GO analysis, the *STMN1* gene was enriched in the genome-wide screening. In addition to neuronal development and differentiation, the model DS_SORY/MYT1-1 revealed different over-represented processes involved in neuroblast division and proliferation as well as neuron migration (see figure 39C).

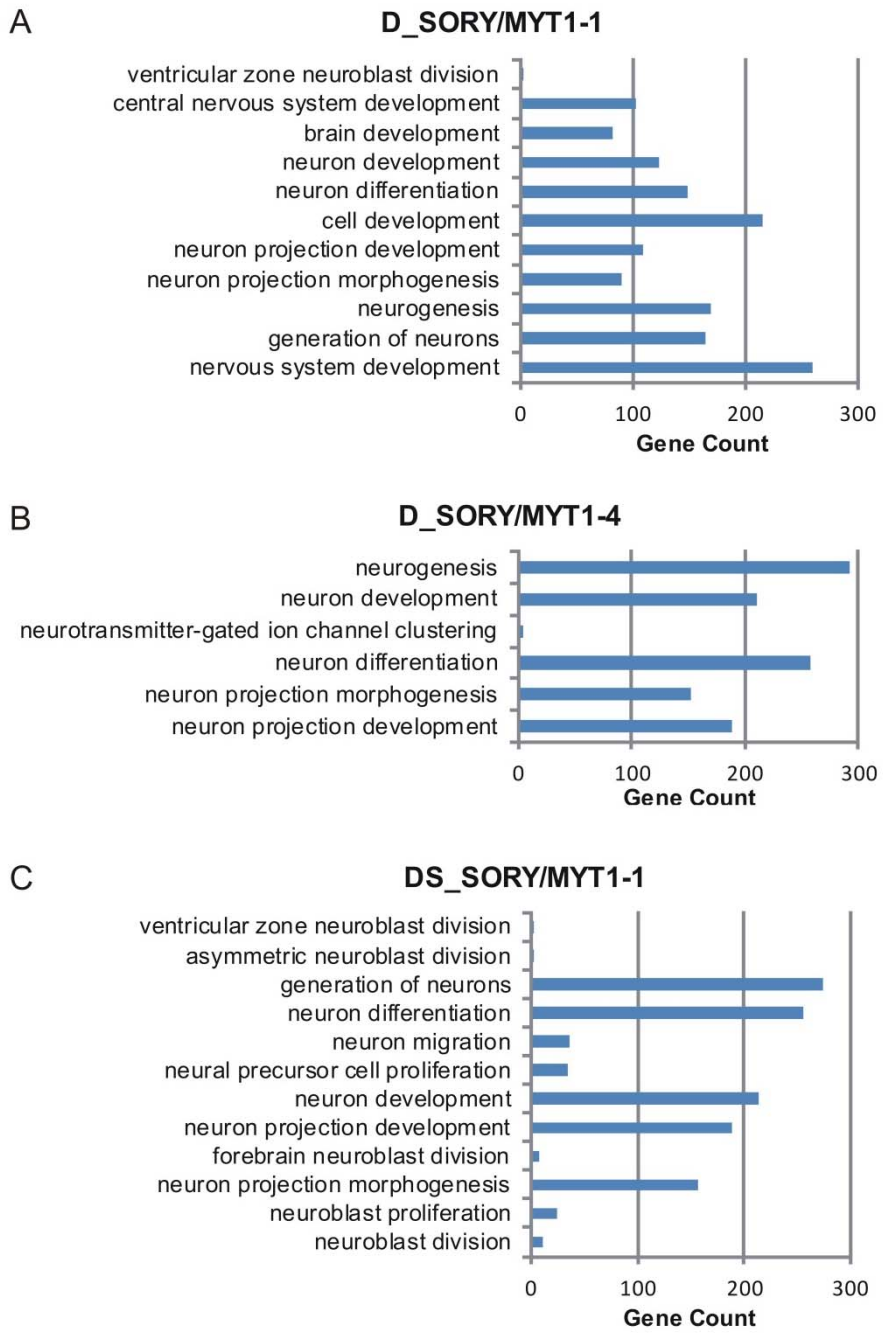

Figure 39:Enriched biological processes in genome-wide analysis of SORY/MYT1 models
Enriched biological processes and corresponding gene count of genes linked to neuron development from GO analysis in all human promoters of the models D_SORY/MYT1-1, D_SORY/MYT1-4 and DS_SORY/MYT1-1 with p≤0.01.

4.7.3. Expression pattern in the brain

4.7.3.1. Allen Brain Atlas expression data

The expression patterns of selected Sox11 interactors in the murine brain were assessed using data from the mouse brain of Allen Brain Atlas (http://mouse.brain-map.org/). For Myt1, Tcf4 and Cbx6 *in situ* hybridisations of sagittal mouse brain sections revealed expression in different brain regions, including the dentate gyrus of the hippocampal formation (see figure 40), where adult neurogenesis proceeds. The hybridisations for Trim28, Yy1 and Znf24 were very weak and thus didn't enable reliable expression analysis.

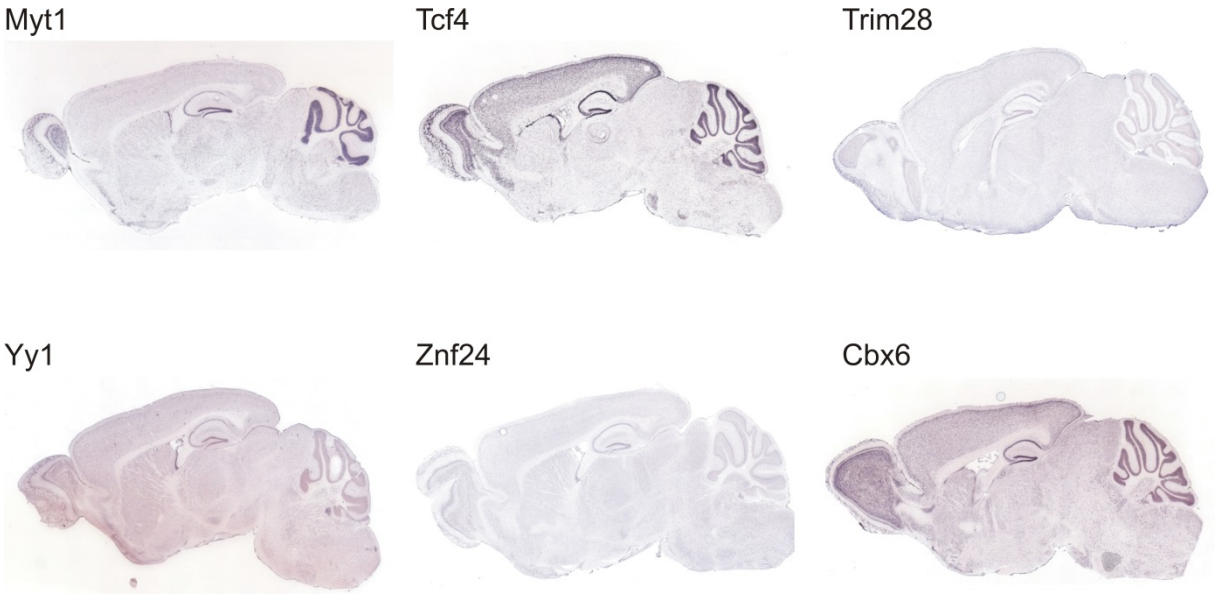

Figure 40:Expression in the mouse brain
Expression data for Myt1, Tcf4, Trim28, Yy1, Znf24 and Cbx6 were acquired from the mouse brain data of Allen Brain Atlas (http://mouse.brain-map.org/). *In situ* hybridisation was performed on sagittal sections of the mouse brain. Myt1, Tcf4 and Cbx6 display distinct expression in the hippocampal formation.

4.7.3.2. Expression in murine neuronal precursor cells

To evaluate the possibility of Sox11 interaction with the identified candidate transcription factors and regulators under native conditions, the protein expression level in murine brain cells was determined. Therefore, neuronal precursor cells (NPC) isolated from the dentate gyrus of the adult mouse brain, one of the niches where adult neurogenesis takes place, were examined. Western blot analysis of nuclear lysates from NPCs compared to Neuro2a cells (N2A) revealed endogenous expression of Sox11, Myt1, Yy1 and Znf24 in the murine brain cells (see figure 41). For Tcf4, several isoforms were described previously (Sepp et al., 2011). In Neuro2a cells, 2 isoforms were expressed, whereas exclusively the smaller isoform was detected in the neuronal precursor cells.

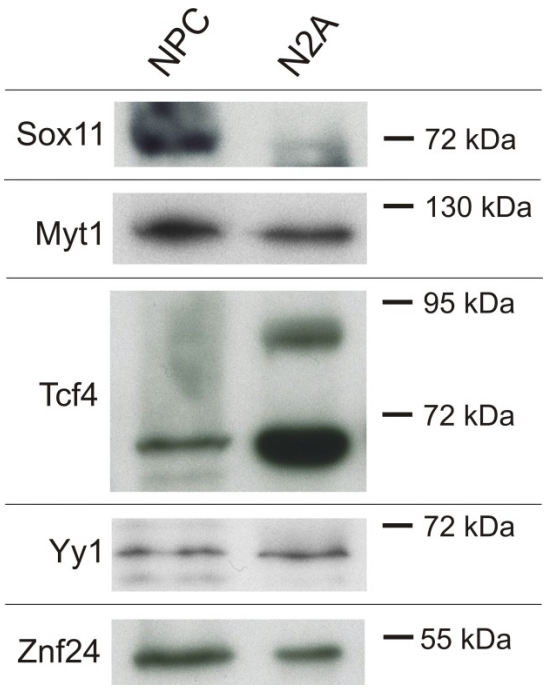

Figure 41:Protein expression in murine neuronal precursor cells and Neuro2a cells
Western blot analysis was carried out using 30µg nuclear extracts of murine neuronal precursor cells (NPC) and Neuro2a cells (N2A) for SDS-PAGE. Sox11 as well as Myt1, Tcf4, Yy1 and Znf24 were detected by commercial antibodies.

5. Discussion

5.1. Aptitude of different affinity purification strategies for Sox11 interactome analysis

The evaluation of different lysis conditions as well as the assessment of various immunoprecipitation and affinity purification methods followed by the final decision for the most promising strategy represents one of the most crucial parts in interactome analyses. From mass spectrometry based assays emerge analytical challenges relative to critical assessment of potentially identified interactors in furtherance of optimizing experimental conditions, while achieving an unbiased screening method revealing a reliable dataset. To that end, several parameters have to be considered for the unbiased evaluation. The first and probably most important issue one has to overcome is a sufficient enrichment level of the bait protein. The presence of an appropriate number of peptide identifications is crucial for the successful identification of interaction partners, as a considerable number of pulled down bait protein increases the probability of detecting endogenously low expressed interacting proteins. Furthermore, an appropriate dataset of identified co-purified proteins; and in case of quantitative approaches, the number of quantified proteins; are essential for the evaluation of different experimental and analytical parameters. Therefore, careful planning provides the possibility to unravel suboptimal experimental conditions that inhibit binding capacities, likewise inappropriate buffer conditions interfering with the purification system. Another important step in the assessment procedure of interactome analysis is the reproducibility of generated interaction data. There has to be an obvious overlap in interacting proteins when performing multiple biological and technical replicates. This is not only a matter of suitable purification methods or exact implementation of the workflow for each experiment, but can also be induced by the susceptibility of the highly sensitive mass spectrometers towards environmental contaminants and/or carryover of residual contaminations from previous runs. For interactome analysis, the expression level of the protein of interest could vary dramatically with transient transfection efficiency. Whereas, the endogenous expression is closer to the cell physiological conditions, this approach raises several challenges. First, one has to find a suitable cell line that expresses the protein on a certain level and second, co-immunoprecipitation of endogenous proteins requires

the availability of applicable antibodies. For the transcription factor SOX11, which we chose as bait for the interactome study, the selected neuroblastoma cell line Neuro2a exhibited a basal protein expression. Other, probably more beneficial cell lines for the investigation of neurogenesis-related regulatory processes like neuronal precursor cells isolated from neurogenic niches of adult mouse brains were excluded due to the dramatic loss of SOX11 expression after several passages in culture. Additionally, these cells present limitation with sufficient expansion to gain a suitable amount of nuclear lysates, which was required for an efficient immunoprecipitation assay. Commercially available anti-SOX11 antibodies were classified as not suitable for the pull down experiments due to inefficient enrichment of SOX11 combined with changing performance of polyclonal antibodies from different charges and high costs for the application in multiple experiments. However, one group performed in 2012 co-immunoprecipitations using a commercial anti-Sox11 purchased from Santa Cruz for pull down assays in mouse embryonic kidney cells on endogenous level. Hence, they were able to validate the interaction of SOX11 with WT1 (Wilm's tumor suppressor gene 1), a factor that regulates the *WNT4* gene, which is involved in nephrogenesis together with SOX11 in a synergistic fashion (Murugan et al., 2012). This could result from higher SOX11 expression levels in the applied cell system compared to the Neuro2a cells. Moreover, they only investigated the co-precipitation of one protein, therefore no complete interactome was determined. In this present study, the applied strategy to overcome the lack of appropriate anti-SOX11 antibodies was the production of peptide- as well as protein-based monoclonal antibodies in house using a SOX11-specific protein recombinant epitope signature tag (PrEST) for immunisation. It represents a unique SOX11 specific fragment comprised of 117 amino acids, designed by an antigen design software, which is not part of transmembrane regions or signal peptides (Uhlen et al., 2010). Extensive screenings revealed several antibodies suitable for western blot analysis, as illustrated in figures 17-19. However, they were not applicable in co-immunoprecipitation assays, displayed in figure 20. This effect could be caused by an impaired binding capacity of the antibodies to the natively folded protein compared to the denatured transcription factor in western blotting. Additionally, the basal endogenous expression level of SOX11 may not provide sufficient material for an efficient precipitation. Finally, the endogenous co-immunoprecipitation of SOX11 was not realisable given the circumstances. On that account, affinity purifications

were selected as the method of choice for the interactome screen. This strategy enables the use of tagged SOX11 constructs and thus circumvents the need for specific antibodies. A combined Strep FLAG tag (SF-TAP tag), comprised of a tandem Strep II and one single FLAG tag, suitable for highly efficient Strep FLAG tandem affinity purification (SF-TAP) as published before (Gloeckner et al., 2007) was fused to the N-terminus of the recombinant SOX11 expression construct via Gateway Cloning. Both parts of the two-step affinity purification strategy are also suitable for the performance as one-step purifications. The quantitative mass spectrometric approach applied for SOX11 interactome analysis using SILAC labelling was based on ratios quantification by comparing identified peptides of the experimental versus the control condition, leading to the discrimination of specific or unspecific identified binding partners. Consequently, a certain number of unspecific signals was required for a reliable interpretation of performed affinity purifications. As for the single-step Strep purification method in general, a relative high number of unspecific binding partners compared to the more pure FLAG affinity purifications was observed, this strategy was initially applied for the implementation of the SOX11 interactome. However, the presence of high salt concentrations in the nuclear extraction buffer C, which is needed to extract proteins efficiently from the nucleus, appeared to interfere with the buffer system of the Strep purification and inhibited binding of SOX11 to the Strep-Tactin matrix, as illustrated in figure 21. Reducing the NaCl concentration from 420mM to 210mM in the nuclear lysate preparation workflow led to a recovered binding capacity of the Strep II tag to the beads, but at the same time the quality of the obtained interaction partner list was not satisfying. This brought up the assumption of an incomplete extraction of nuclear proteins caused by the decreased salt concentration. The Strep purification method is suitable for the pull down of proteins from bacteria lysates as well as eukaryotic cytoplasmic proteins (Schmidt and Skerra, 2007), but it was not applied in many studies working with nuclear lysates, although one group claimed the robustness of Strep II–mediated purifications up to a NaCl concentration of 400mM in the reaction buffer concerning the efficiency of bait protein precipitation (Junttila et al., 2005). However, they did not mention the yield of interaction partner pull down, that were for sure much less expressed in relation to the protein of interest and were potentially not extracted to the same extend as usual under the high salt conditions. Another study implicating

the determination of the SOX2 interactome in embryonic stem cells reported the application of Strep pull down assays for the validation of interactors identified by FLAG affinity purification on western blot analysis (Gao et al., 2012). Here, the nuclear extraction was carried out using a kit where the salt concentration was not indicated. Furthermore, the Strep purification was performed in reaction buffers comprising solely 150mM NaCl. More frequently, FLAG affinity purifications were used for the analysis of nuclear protein complexes, like in an interactor screen of SOX2 in murine neural stem cells stably expressing SOX2 (Engelen et al., 2011). Consequently the FLAG one-step purification was applied for the Sox11 interactome analysis, where best performance was observed with the original nuclear extraction buffer conditions, comprising 420mM NaCl, as displayed in figure 22. In order to be closer to the physiological SOX11 level, stable SOX11 expression cell lines were included in the purification procedure, however the small number of detected peptides specific for SOX11 due to the low expression state rendered an interactome screen impossible. On that account, the FLAG pull down assays were conducted using transiently over-expressed SF-TAP tagged SOX11. The subsequent Methanol/Chloroform precipitation followed by in-solution tryptic digestion turned out to be the optimal sample preparation, as by the use of in-gel pre-fractionation peptide identification rates for the bait as well as for the interacting proteins decreased. This illustrated that the sample was rather pure than complex, which rendered a pre-separation unnecessary, as every redundant step results in sample loss. The implementation of 6 independent experiments, thereof 3 including reverse labelling and subsequent data analysis revealed a list of interactors either considered as specific or non-specific. The obtained high purity of the performed FLAG affinity purifications due to the high affinity of the FLAG tag to the matrix compared to the Strep tag (Gloeckner et al., 2007) led to a not exactly Gaussian distribution of the data, which were shifted towards the SOX11 condition, as illustrated in figure 22. That implies that the low abundance of unspecific binders which were needed to a certain extend for the quantification of specific signals and ratios calculations led to the assignment of genuine SOX11 interaction partners as not significantly enriched. To overcome this problem of data evaluation, a threshold was set manually, defining all proteins as significant interaction partners of SOX11 that revealed SOX11/control ratios above a value of 2.

5.2. Sox11 interactors are involved in transcriptional regulation and modulation of neurogenesis

The development-regulating transcription factor SOX11 is heavily involved in the regulation embryonic and adult neurogenesis. During this process, it plays a pivotal role in neural fate commitment of neuronal precursor cells. This is underlined by the distinct expression of SOX11 in neurogenic niches of the adult brain, limited to the early stage of immature neurons (Haslinger et al., 2009) and the absolute necessity of SOXC proteins for the efficient differentiation of murine neuronal precursor cells into neurons (Mu et al., 2012). In addition, it initiates the expression of neuron-specific proteins, like the cytoskeleton-associated early neuronal markers DCX (Haslinger et al., 2009, Mu et al., 2012), β-tubulin III (Bergsland et al., 2011, Bergsland et al., 2006), MAP2 (Hoser et al., 2008) and Drebrin (Song et al., 2008, Wang et al., 2010). The importance of SOX11 for a directed development and proper formation of the central nervous system is illustrated by the recent discovery of Sox11 deletions and mutations being associated with Coffin-Siris syndrome, a congenital disorder characterised by intellectual disability, growth deficiency, microcephaly, characteristic facial features and hypoplastic nails of the fifth fingers or toes (Lo-Castro et al., 2009, Tsurusaki et al., 2014). Furthermore, in the same study knockdown of SOX11 in zebrafish revealed brain malformations. Altogether these results point to SOX11 deletion and mutations being linked to the symptom of intellectual disability. Previous models for stem cell maintenance and neuronal differentiation laid the focus on the investigation of transcriptional core regulatory networks, determining the cellular expression profiles and identities by physical interactions and promotion of expression programs (Chen et al., 2008, Hobert, 2011). Thus, they were able to gain further insight into the integration of signalling pathways and identified targeted chromosomal regions by the determination of underlying regulatory networks. This present study aims to identify a core regulatory transcriptional network that contributes to the determination of early neuronal identity and provides further knowledge about the SOX11-dependent progress of neuronal fate commitment, differentiation and maturation during adult neurogenesis. The obtained SOX11-associated biochemical interactions serve as basis for the cooperation of different transcriptional modulators and transcription factors on the activation of neuronal gene programs. The current state of knowledge about the

interaction of SOX11 with other proteins is very sparse. Previously, SOX11 was found to cooperate with POU3f3 and POU3f2, two members of the neurogenesis-related POU-III class of transcription factors in reporter assays (Kuhlbrodt et al., 1998). Additionally, a transcriptional regulatory network, consisting of SOX11, the transcription factor Nuclear factor 1b (NFIB) and POU3F4, another member of the POU-III family was found to promote neurogenesis, underlining the relevance of SOX11 interaction with this family of transcription factors in vivo (Ninkovic et al., 2013). The present dataset of SOX11 interactors, which was acquired by FLAG affinity purifications combined with SILAC labelling and quantitative mass spectrometry is listed in table 20 and comprises mainly nuclear proteins. This confirms the efficiency of the nuclear extraction procedure and the low rate of cytoplasmic contaminations. The identified proteins can be divided into different subgroups according to their functions.

Among them, few proteins are involved in cytoskeleton organisation, ribosome biogenesis and vesicular trafficking. Both the nuclear transport and export of vesicles as well as ribosome formation are central nuclear processes. The proper synthesis of the ribosome enables in later steps the translation of mRNA in the cytoplasm. The enrichment of ribosome-associated proteins is underlined by the three hits rRNA processing, rRNA metabolic process and ribosome biogenesis in the GO analysis of biological processes for the interacting proteins in figure 29. The nucleus possesses its own filamental network, the so called nucleoskeleton that is located at the inner nuclear membrane and is involved in cellular signalling, but is also responsible for the maintanance of nuclear structure, the positioning and migration as well as preventing it from rupture (Wang et al., 2009, Wilson and Berk, 2010). Moreover the linkage of components of the cytoskeleton like microtubules, centrosomes, actin filaments, or intermediate filaments is mediated by the nuclear envelope bridging proteins KASH and SUN (Starr and Fridolfsson, 2010). Notably, nuclear migration is also an important step in neuronal migration and neurogenesis in both proliferative and post-mitotic phases. Interestingly, the cellular motility in neuronal precursor cells is dependent on the nuclear migration (Baye and Link, 2008). Furthermore, SOX11 is linked to the cytoskeleton, as it induces the expression of the cytoskeleton-associated proteins DCX (Haslinger et al., 2009, Mu et al., 2012), β-tubulin III (Bergsland et al., 2011, Bergsland et al., 2006), MAP2 (Hoser et al., 2008) and Drebrin (Song et al., 2008, Wang et al., 2010). These SOX11-regulated proteins are

involved in the process of neurogenesis, as exemplarily shown for DCX, which represents a microtubule stabilising protein, that is involved in early neuronal migration (des Portes et al., 1998, Francis et al., 1999). Although SOX11 is known to activate promoters of cytoskeletal proteins, no evidence was present from previous studies that point to the direct interaction of the transcription factor with members of this group of proteins.

However, the majority of SOX11 interacting proteins are referred to as RNA-binding. Both RNA- and poly(A)RNA-binding are the first two hits comprising the highest gene counts in the gene ontology for molecular function enrichment analysis in figure 28. RNA-binding proteins are considered as important regulatory factors in the cell as they are implicated in a variety of functions. There are proteins involved in the process of splicing, like the identified splicing regulator RBM4 (Lai et al., 2003), or RBM28, which is part of the spliceosomal snRNPs, forming the spliceosome together with pre-mRNA (Damianov et al., 2006). ZNF326 was identified to be part of the DBIRD complex, regulating alternative splicing events and transcript elongation through binding of RNA polymerase II (Close et al., 2012). Additionally, snRNA-stabilising proteins, playing a role in the splicing machinery, like MEPCE were identified (Jeronimo et al., 2007). With YTHDYF2 and ZC3H18 also RNA-binders responsible for mRNA stability and nuclear export after intron removal are present in the dataset (Chi et al., 2014, Wang et al., 2014). These proteins can also act as cofactors for the activation or repression of transcription. The determined SOX11 interactors RBM4, a corepressor and CoAA (RBM14), a coactivator are regulators of both alternative splicing and transcription, that are involved in the differentiation of neural stem cells and precursor cells (Auboeuf et al., 2004, Kar et al., 2006). The *trans* splicing of the two neighbouring genes during neural stem cell differentiation results in alternative variants that regulate the expression of the microtubule-associated protein Tau together with CoAA and RBM4 by balancing their splicing activities (Brooks et al., 2009). An interaction with SOX11 may lead to a recruitment of the two coregulators to SOX11 target genes in order to cooperately influence their expression and induce alternative splicing to produce the needed variants for the differentiation stages. Notably, transcription cofactor and corepressor activity include many SOX11 interactors in the overrepresented GO molecular functions. MSI1, another neuron-specific RNA-binding protein was identified. Due to its expression

restricted to neuronal precursor cells in both the embryonic and adult central nervous system, it exhibits a putative role in the self-renewal of neural stem cells or the progress of neuronal differentiation. (Sakakibara et al., 1996, Sakakibara and Okano, 1997). This resembles the expression pattern of SOX11 in neurogenic niches of the adult brain (Haslinger et al., 2009).

Furthermore, the interactome comprises a variety of modulators that influence transcription in an epigenetic manner. Amongst them are the DNA helicases CHD8 and SMARCAD, as illustrated by the SOX11 protein-protein interaction network inf figure 27. The DNA-binding and unwinding protein CHD8 is involved in neural development of neuronal precursor cells and is considered to be a strong risk factor for Autism Spectrum Disorder (ASD) (Sugathan et al., 2014). Interestingly, it interacts with another DNA helicase of the same family, CHD7 (Batsukh et al., 2010), which is a susceptibility gene for CHARGE syndrome, a congenital disorder characterised by choanal atresia and malformations of the heart, inner ear and retina, when it is mutated (Pagon et al., 1981, Vissers et al., 2004). Recently, CHD7 was found to physically interact with SOX2 in neural stem cells and was in addition identified as cofactor for SOX2. The two proteins regulate synergistically a set of common target genes associated with CHARGE syndrome or SOX2-dependent anophthalmia syndrome, a severe structural eye malformation (Engelen et al., 2011, Fantes et al., 2003). Recently, CHD7 was identified as an important driver of neurogenesis as it was able to activate the expression of SOX4 and SOX11 by chromatin remodelling of their promoters (Feng et al., 2013). The DNA helicase SMARCAD1 is involved in the formation of heterochromatin, by induction of histone methylation that is formed for proper DNA replication (Rowbotham et al., 2011). The terms helicase activity as well as chromatin binding are enriched in the GO molecular functions analysis for the SOX11 interactome dataset. Additionally, chromatin and chromosome organisation, chromatin modification and assembly are part of the enriched biological processes, pointing to the large group of epigenetic modulators in the Sox11 interacting proteins. Several histones were identified together with methyltransferases that act as coactivators like KMT2A (Nakamura et al., 2002) or corepressors of gene expression like WHSC1 (Garlisi et al., 2001) and EHMT1 (Ogawa et al., 2002) by histone methylation. Notably, mutations in *EHMT1* are linked to intellectual disability, similar to SOX11 (Kleefstra et al., 2012). The regulator KMT2A was recently found to modulate neural progenitor cell proliferation as well as neural and glial differentiation

(Huang et al., 2014). We identified as well FRG1, a regulator of methytransferases and the zinc finger protein WIZ, a linker between two methyltransferases that enables binding of a corepressor (Neguembor et al., 2013, Ueda et al., 2006). Another group of epigenetic chromatin remodellers are the acetyltransferases, which are represented by NAT10 and TRRAP leading to transcriptional activation (DeRan et al., 2008, Lv et al., 2003).

An additional important group of regulatory proteins are components of the polycomb group (PcG) complexes. These chromatin-modifying proteins are involved in the epigenetically controlled repression of gene expression programs. They play a crucial role in the regulation of many biological processes like cell cycle control, X-inactivation, cell fate commitment, maintenance of pluripotency in embryonic stem cells, cancer and other critical developmental mechanisms (Aloia et al., 2013, Muller and Verrijzer, 2009, Richly et al., 2011). The deletion of polycomb protein encoding genes led in mice to an impairment of ES cell formation (O'Carroll et al., 2001). Epigenetically regulatory proteins assemble to diverse protein complexes, however the two best characterised are the polycomb repressive complexes 1 (PRC1) and 2 (PRC2). PCR2 mediates trimethylation of lysine-27 (K27) of histone H3 via methyltransferase activity, catalysed by the component EZH2 (Margueron et al., 2008). The other mammalian complex-building proteins SUZ12 and EED support complex stability and ensure EZH2-mediated enzymatic activity (Margueron et al., 2009, Pasini et al., 2004). The active catalytic PRC2 compound EZH2 was identified in several runs of SOX11 FLAG affinity purifications, but was not considered as significant interactor, due to a weak or unstable binding to the bait during the purification step. Nevertheless, the association of SOX1 to the polycomb group of proteins is illustrated by the determined interaction of the transcription factor with components of the PRC1 complex. It is composed of the 5 polycomb proteins (Pc) CBX2, CBX4, CBX6, CBX7 and CBX8, the 3 polyhomeotics (PH) PHC1, PHC2 and PHC3, the 2 sex combs extra (SCE) RING1/RING1A and RING2/RING1B that are also known as RING and six posterior sex combs (PSC), which are termed as polycomb group ring fingers (PCGF) (Morey and Helin, 2010). The complex achieves its transcription repressive activity through CBX-mediated binding of K27 on histone H3 already trimethylated by PCR2 (Cao et al., 2002). Sox11 was found to interact with the CBX proteins CBX2, CBX4, CBX6 and CBX8, representing 4 of the 5

polycomb proteins of PRC1 essential for the recruitment and binding of the complex to the histone H3. They are displayed and connected in the SOX11 protein-protein interaction network in figure 27. The different domains of the polycomb proteins enable specific functions. The chromodomains mediate interaction with the histone H3 and thus promote stability of the complex and helps its recruitment to particular chromatin regions, whereas it was observed that the 5 CBX proteins enable binding to different methylated histone tails (Bernstein et al., 2006). Furthermore, they possess a C-terminal polycomb repressor box that mediates binding to other complex compounds like RING1B and is involved in transcriptional silencing (Bezsonova et al., 2009, Muller et al., 1995) as well as a DNA-binding domain (Senthilkumar and Mishra, 2009). Moreover the SCE protein RING1B (also known as RNF2), a gene regulating E3 ubiquitin ligase responsible for histone H2A monoubiquitination (Wang et al., 2004) and interacting with CBX proteins was identified. The polyhomeotic PHC2, that is involved in the transcriptional repression of Hox genes in embryonic development in cooperation with PHC1 (Isono et al., 2005) was also co-precipitated with SOX11. The absence of the remaining PRC1 components in the obtained interactome dataset could be based on obstacles with the experimental procedure or inefficient identification rates of low abundant peptides by mass spectrometry that are overlayed by high abundant peptides or contaminants from previous runs, resulting in impaired recognition of residual polycomb proteins. There is a link of the polycomb complex to neuronal differentiation, as the CBX proteins were co-precipitated with REST in embryonic stem cells and differentiating neurons and found to cooperatively act on the regulation of neuron-specific genes. (Ren and Kerppola, 2011). REST was initially characterised as repressor of neural genes in non-neural cells (Chong et al., 1995), but growing evidence suggests a role in silencing of neural genes and regulation of neural fate decisions during neuronal development (Ballas et al., 2005, Kuwabara et al., 2004) through interaction with Co-REST (Qureshi et al., 2010). The close homologue of Co-REST RCOR2 was part of the SOX11 interactome, as illustrated in figure 27. It plays a role in the maintenance of pluripotency in embryonic stem cells being a part of the LSD1 complex and substitutes for SOX2 in the reprogramming of somatic cells into iPS cells (Yang et al., 2011). The identified SOX11 interactor and transcriptional corepressor CTBP1 is also associated with the LSD1 complex (Shi et al., 2003). On the basis of these findings and the overrepresentation of chromatin modifying proteins, an interaction of SOX11

with chromatin remodellers like during neural fate commitment is a conceivable hypothesis. The abnormal spindle homolog, microcephaly associated protein (ASPM) that was found to interact with SOX11 is expressed in proliferating tissues and is responsible for the proper formation of the spindles during mitosis (Kouprina et al., 2005). Moreover, homozygous mutations of ASPM are the major cause of an autosomal recessive primary microcephaly (MCPH) through an incorrect regulation of mitotic spindle activity in neuronal precursor cells of the developing brain (Bond et al., 2002). Besides, proliferating progenitors of the adult brain express ASPM that ensures self-renewal properties and multipotency of the cells, prior commitment to neuronal fate and differentiation into neurons (Marinaro et al., 2011). Of special interest, we identified the interaction of SOX11 with tripartite motif containing 28 (TRIM28), also referred to as transcription intermediary factor β (TIF1b). TRIM28 acts as a gene control expression cofactor that binds to chromatin-modifying proteins and transcriptional repressors like KRAB domain containing zinc finger transcription factors. Furthermore, It is known to act as a scaffold for heterochromatin formation and the consequent repression of transcription by recruiting heterochromatin protein 1 (HP1), the histone methyltransferase SETDB1 and the histone deacetylase–containing complex NuRD (Sripathy et al., 2006, Urrutia, 2003). Additionally, the interaction of TRIM28 with HP1 was found to be essential for the course of differentiation in a modified embryonic carcinoma F9 cell line (Cammas et al., 2004). Another group identified TRIM28 as an important regulator in the maintenance of pluripotency in embryonic stem cells in a phosphorylation-dependent fashion (Seki et al., 2010). In these cells, the scaffold protein is phosphorylated at the C-terminal serine 824 (S824), which is known to activate chromatin relaxation (Ziv et al., 2006). The modification was found to be critical for the maintenance of pluripotency in mouse ES-cells, as the phosphorylation was present in the majority of pluripotent cells but not in most of the cells undergoing differentiation and absent in other somatic cell lines. Furthermore, the phosphorylation of S824 promotes the induction of iPS-cells from somatic cells, which implicated a shortened induction time in the generation of iPS cells. Moreover, the expression of pluripotency markers was increased compared to iPS cells comprising the non-phospholylated state of TRIM28. Notably, overexpression of TRIM28 in ES-cells resulted in a prolonged expression of pluripotency-specific transcription factor OCT3/4 and SSEA1, an embryonic stem cell

specific marker, pointing to an extension of the multipotent phase. In contrast, knockdown of the cofactor resulted in a reduced Nanog and SSEA1 expression, leading to the loss of pluripotency. When S824 is modified, TRIM28 localises to transcriptional active euchromatin, which suggests a phosphorylation-dependent contribution for TRIM28 in the activation of pluripotency markers. Additionally, it assembles to a complex with OCT3/4 and the components SMARCAD1, BRG-1 and BAF155 of the chromatin remodelling complex eBAF that is specific for ES-cells (Seki et al., 2010). These findings indicate that TRIM28 acts as a switch between the pluripotent stage of cells and induction of differentiation. According to the knowledge from these previous publications, an interaction of TRIM28 with SOX11 would be possible during the progression of neurogenesis at the step of neural fate determination. Potentially, C-terminally non-phosphorylated TRIM28 could serve as cofactor for SOX11-mediated regulation of early neuronal genes.

Another particularly interesting and important group of SOX11 interactors are the transcription factors, as reporter assays and *in silico* promoter analyses for adjacent binding sites can reveal synergetic cooperation with SOX11 on gene expression programs involved in neurogenesis. The Krüppel-like zinc finger transcription factor ZFP281 plays a role in the control of stemness in embryonic stem cells, as it is capable of activating and silencing several genes. It was shown to interact with OCT3/4, SOX2 and Nanog, three key regulators of pluripotency. Furthermore it exhibits binding sites in the promoters of the three transcription factors and was detected to activate Nanog expression (Wang et al., 2008). Furthermore the promoter of the zinc finger protein was identified as target of SOX4 in a chromatin immunoprecipitation screen in prostate cancer cells (Scharer et al., 2009). The SOX11 interactor NACC1, a BTB domain containing protein (Mackler et al., 2000) that acts as transcriptional corepressor also interacts with Nanog in an embryonic stem cell interaction screen, pointing to a role for the cofactor in the regulation of pluripotency (Wang et al., 2006). The transcription factor SP1, which was obtained in the SOX11 interactome study is capable of influencing transcription in a variety of cellular processes in both activating and repressing manner, also in combination with other transcription factors (Han et al., 2001, Infantino et al., 2011). Its activity is dependent on stimuli and can be altered by posttranslational modifications (Yang et al., 2001). Additionally, it is involved in the process of chromatin remodelling (Vicart et al., 2006, Zhang et al., 2006). The multifunctional transcription factor possesses

binding sites in the regulatory regions of SOX3, SOX14 and SOX18 and data point to an implication of SP1 in the basal activation of the SOX3 gene (Kovacevic-Grujicic et al., 2008, Kovacevic Grujicic N. et al., 2005). SOXB1 proteins like SOX3 are expressed in the neuronal precursor state during neurogenesis and join SOX2, which is implicated in the maintenance of pluripotency. As 95% of their target sites overlap, their functions seem to be at least in part redundant. Notably, the genome-wide binding profile of SOX3 in NPCs shows also a large overlap with the SOX11 binding sites in immature neurons (Bergsland et al., 2011), thus increasing the probability of a SOXB1 factor reactivation in later stages of neural fate commitment and mature neurons, where they exert other functions than in neuronal precursors. These observations were reported by other groups (Ferri et al., 2004, Malas et al., 2003). The assumption of a reappearance of SOX3 in later developmental stages would enable an implication of SOX11 as a cofactor in the activation of SOX3 downstream gene expression. In this way, the interacting transcription factors SOX11 and SP1 could cooperatively bind to the identified SP1 binding sites and activate the SOX3 promoter.

The identified SOX11 interacting protein ZNF423 belongs to the kruppel-like zinc finger family of transcription factors and was previously shown to be involved in the regulation of olfactory-receptor neuron differentiation by inhibition of the differentiation-promoting OLF-1/EBF transcription factors (Wang and Reed, 1993, Wang et al., 1997). It represses their activity by binding and preventing them from accessing specific promoter sites.(Tsai and Reed, 1997). Overexpression of ZNF423 in mature olfactory-receptor neurons resulted in reappearance of immature neuron markers, indicating a role for the transcription factor in the switch from differentiation to maturation (Cheng and Reed, 2007). The implication of SOX11 in neural fate decisions and neuronal maturation promotes the formation of new neurons in the dentate gyrus as well as in the olfactory bulb (Zhao et al., 2008). This functional and expression region overlap gives rise to a possible cooperation of SOX11 with the olfactory neuron development influencing zinc finger ZNF423. The paired-like homeobox 2b (PHOX2B), a transcription factor which is a member of the paired family of homeobox proteins was identified in the Sox11 interactome as well as heart and Neural crest derivatives expressed 2 (HAND2), which is part of the basic helix-loop-helix family of transcription factors. Peripheral ganglia of the autonomous

nervous system derive from neural crest cells. The transcription factor network of PHOX2B, HAND2 and GATA3 was initially identified as key regulators of early specification and differentiation of sympathetic neurons, but it was also found to be involved in later developmental stages of the peripheral nervous system like neurogenesis and maintaining subtype-dependent markers and features (Howard, 2005, Rohrer, 2011). The neural crest differentiation process into sympathetic ganglia is bone morphogenic protein (BMP)–dependent, thereby, a variety of transcription factors, namely PHOX2A, PHOX2B, ASCL1, INSM1, HAND2, GATA2/3, SOX4 and SOX11 are implicated (Howard et al., 2000, Tsarovina et al., 2008, Wildner et al., 2008). Knockdown of HAND2 and SOX11 led to a decreased number of precursor cells and immature sympathetic neurons (Hendershot et al., 2008, Potzner et al., 2010). PHOX2B was additionally found to be enriched in a module with SOX11 on the human *DCX* promoter, displayed in table 14, but the function of the transcription factor was not further assessed, as we concentrated on CNS-related neurogenesis in this study.

Notably, SOX11 interacts with TCF4, a transcription factor belonging to the class I basic helix-loop-helix (bHLH) family of proteins recognising Ephrussi-box (E-box) binding sites with the core consensus sequence CANNTG on DNA strands (Henthorn et al., 1990). Members of this group of transcriptional regulators form homodimers or heterodimers with class II bHLH transcription factors to enable binding to common DNA sequences and induce activation of gene expression (Murre et al., 1989). The ubiquitously expressed TCF4 is involved in many biological processes; in particular it plays an important role in neuron development. In the brain it is expressed in neurons whereas in the spinal cord it is restricted to oligodendrocytes, where it is implicated in their maturation process (Fu et al., 2009). The functional relation to CNS development is underlined by interactions of TCF4 with important regulators, like NEUROD2, a neurogenic bHLH protein among others involved in the activation of neurogenesis and survival of neurons (Farah et al., 2000, Olson et al., 2001). When assembling to a complex, TCF4 and NEUROD2 are able to induce neurogenesis (Ravanpay and Olson, 2008). The TCF4 gene encodes for two main isoforms, A and B, with B acting as a transcriptional repressor that silences for example the brain specific growth factor FGF1 (Liu et al., 1998), and with isoform A not displaying repressive functions (Skerjanc et al., 1996). Interestingly, heterozygous mutations or deletions of the *TCF4* gene have been identified as the main genetic cause for Pitt-

Hopkins Syndrome (Amiel et al., 2007, Brockschmidt et al., 2007, Zweier et al., 2007). This is a rare syndromic disease, first described in 1978 by Pitt and Hopkins, that is characterised by serious intellectual disability, developmental delay, absence of speech, distinct facial gestalt and hyperventilation coupled to apnoea (Marangi et al., 2011, Pitt and Hopkins, 1978, Takano et al., 2011). Additionally, genetic variations in the *TCF4* gene are associated with schizophrenia by genome wide association studies (Stefansson et al., 2009, Steinberg et al., 2011). Moreover, single nucleotide polymorphisms in *TCF4* are linked to Fuch's Corneal Dystrophy (Baratz et al., 2010, Li et al., 2011), a common eye disorder, hallmarked by the development of collagen-free regions in the cornea, potentially caused by cell death (Meek et al., 2003). The crucial role for TCF4 in brain development as well as the association of Transcription factor 4 with disorders characterised by intellectual disability could point to a cooperative interaction with Sox11 on neural target genes, as SOX11 was also recently linked to an intellectual disability disorder, the Coffin-Siris Syndrome (Tsurusaki et al., 2014).

5.3. Cooperation of SOX11 with other transcription factors on the regulation of neural genes

The potential cooperation of SOX11 with identified interactors from the interactome screening was examined in reporter assays. Therefore, the human promoter sequence of the well-established SOX11-activated early neuronal marker Doublecortin was used for the determination of regulating effects on the activity of the regulatory sequence. Furthermore, the human promoter of the putative SOX11 downstream target Stathmin1 was applied for the validation of observed activation or repressions on the DCX promoter and the transfer of the cooperation with SOX11 on other SOX11-regulated promoter regions was checked. Chosen for the reporter assays according to their functions related to neurogenesis were MYT1, TCF4, TRIM28, YY1, ZNF24 and CBX6. Only three of the selected transcription factors, MYT1, YY1 and ZNF24 displayed activity on the two SOX11-targeted promoters. As a consequence, their biological functions and relevance, as well as their synergetic effects with SOX11 are discussed in the next paragraph. The other three interactors TCF4, TRIM28 and CBX6 didn't show reliable effects on the two promoter sequences, as shown in figure 34 and 35. This observation might be the result of by

dose-dependent activities that were not levelled out as we used a standard DNA amount for each candidate. Otherwise, they might not affect one of these selected genes as these promoters are not the physiological targets. There is a variety of other possible genes they may cooperate with SOX11. Furthermore, a combination of potentially not yet known factors is required for the formation of a bigger complex that regulates gene expression. Nevertheless, significant effects on the regulation of the chosen SOX11-activated promoters DCX and Stathmin1 were observed for the three in the following described transcription factors MYT1, YY1 and ZNF24.

Of special interest is the identified interaction of SOX11 with Myelin transcription factor 1 (MYT1), as it was shown before to induce ectopic neurogenesis in *Xenopus laevis.* Under X-MYT1 inhibition, even normal neurogenesis was found to be impaired (Bellefroid et al., 1996). Deletion of the chromosomal region encompassing the *MYT1* gene locus was linked to intellectual disability (Kroepfl et al., 2008). Furthermore, the members of the NZF/MYT family are transiently expressed during the embryonic development of the mouse brain, pointing to an implication of the transcription factors in the control of neuron differentiation (Matsushita et al., 2014). Notably, MYT1L, a paralog of MYT1, was already successfully applied in several approaches to directly reprogram fibroblasts into functional neurons in different combinations with other transcription factors and microRNAs (Ambasudhan et al., 2011, Vierbuchen et al., 2010, Yoo et al., 2011). Another evidence to the relevance of MYT1 in the regulation of neuronal differentiation is proposed by the structural analysis of MYT1 double zinc finger-mediated DNA recognition, revealing potential binding sites in the regulatory sequences of proteins involved in neuron development including the basic helix-loop-helix (bHLH) transcription factors NEUROD and Neurogenin1 which are potent inducers of neuronal fate and SLC1A3, a glial high-affinity glutamate transporter that is involved in brain development and is associated with schizophrenia (Bertrand et al., 2002, Gamsjaeger et al., 2013, Gao et al., 2009, Hagiwara et al., 1996, Ma et al., 1996, Wilmsdorff et al., 2013, Yoo et al., 2011). These findings are consistent with our results, revealing the impact of MYT1 together with SOX11 on the activation of the immature neuron markers DCX and STMN1 in a synergetic fashion, illustrated in figure 34 and 35. This confirms their positive effect on neuronal differentiation. MYT1 is acting as a cofactor for SOX11, as the Myelin transcription factor 1 is not able to induce DCX and STMN1 expression on a high level by itself, however the SOX11-mediated activation is heavily enhanced by the

interaction with MYT1. The observation of their cooperative activation is supported by our results of the *in silico* promoter analysis for MYT1 and SOX11. The combination of both transcription factors is part of over-represented modules in both human *DCX* and *STMN1* promoters, illustrated in table 14. Moreover, 4 of 11 generated models for the MYT1 and SOX transcription factor families revealed adjacent binding sites within the *DCX* regulatory region and 1 of 2 models uncovered the presence of neighbouring binding sites in the *STMN1* promoter, as displayed in tables 15-18. In addition, the genome-wide distribution of the generated models in figure 39 displayed an enrichment of neurogenesis-related processes in the potential target genes, of the combination of the two transcription factors, like NEUROD1. This is further evidence for a synergistic action of MYT1 and SOX11 in the regulation of neuronal differentiation.

Another important specific interactor of SOX11 identified in the dataset is Yin Yang 1 (YY1), a transcription factor belonging to the GLI-kruppel class of zinc finger proteins. It was first discovered in 1991 and named after the Chinese words “Yin” and “Yang” for repression and activation transcriptional activities on the viral P5 promoter, that is repressed by the transcription factor in absence of the oncoprotein E1A and activated in the presence of E1A, determining the protein as a coactivator of YY1 (Shi et al., 1991). The ubiquitously expressed multifunctional protein is highly conserved between species and it is also known to interact with corepressors. Moreover, knockout studies showed that YY1 is indispensable for mouse embryogenesis, indicating a pivotal role for the transcription factor in development (Donohoe et al., 1999, Pisaneschi et al., 1994, Shi et al., 1997, Yang et al., 1996). Furthermore, YY1 is supposed to play an important role in the nervous system, as it is involved in the regulation of many genes implicated in neuronal development by both activation and repression (He et al., 2007, Kwon and Chung, 2003, Morgan et al., 2004, Yoo et al., 2001). In SH-SY5Y cells YY1 was found to activate transcription of the repressor element 1-silencing transcription factor (REST) (Jiang et al., 2008), which is involved in epigenetic silencing of neural genes during the switch from stem cells to neural progenitor cells. REST is an important repressor of genes responsible for neuronal differentiation and it is released together with its cofactors during neurogenesis in the step from the progenitor stage to immature neurons, leading to activation of neural genes (Ballas et al., 2005). A cofactor of REST, RCOR2 was actually present in our

SOX11 interactor screen, as well as several proteins belonging to the CBX-family of polycomb proteins, epigenetic regulatory factors, that are also found to interact with REST (Ren and Kerppola, 2011). In our promoter studies, we observed a massive decrease of SOX11-mediated activation of both early neuronal proteins *DCX* and *STMN1* regulatory regions under the influence of YY1. In contrast, the depletion of endogenous expressed YY1 increased the ability of SOX11 to activate both promoters. This cooperation between the two transcription factors is enabled by the presence of adjacent binding sites in the murine *DCX* promoter sequence, which was confirmed by 1 of the 2 generated models for the SOX11 and YY1 transcription families by *in silico* modelling, as displayed in tables 15 and 17. For the *STMN1* promoter, the analysis didn't reveal models for the detection of neighbouring binding regions. The previously reported repressive influence of YY1 on neurogenesis is in line with our hypothesis that includes YY1-dependent active repression of immature neuron markers like *DCX* and *STMN1* as a switch between the maintenance of neural cells as cycling progenitors and neuronal differentiation. A currently unknown stimulus towards neuronal maturation could induce a relief of repression by inhibition of YY1 binding to SOX11 and potentially induce interaction with a coactivator, which would enable SOX11 to push neuronal differentiation through positive regulation of neural promoters. The phenomenon of relief of repression was previously detected during the course of neuronal induction. In a reprogramming strategy from fibroblasts to neurons it was observed that the repression of a single microRNA regulating protein named PTB enables conversion of the cells into the neuronal lineage. The depletion of PTB reliefs the blocking of microRNA-dependent activity on different components of the REST complex, leading to a de-repression of multiple neuronal transcription factors and microRNAs (Xue et al., 2013). Furthermore, in Notch signalling, which is involved in various biological processes including progenitor proliferation, fate commitments and cell death (Gazave et al., 2009, Richards and Degnan, 2009) as well as adult neurogenesis (Imayoshi et al., 2010, Pierfelice et al., 2011) corepressor complexes block the transcription factor CSL which results in the inhibition of gene activation and an inactive Notch pathway. The exchange of corepressing proteins with coactivators induces CSL-mediated gene transcription and results in the activation of the Notch signalling pathway (Kopan and Ilagan, 2009).

Zink finger protein 24 (ZNF24 also referred to as ZFP191) was additionally identified as specific interactor in the SOX11 FLAG affinity purification dataset. It was first described in hematopoietic cells in the course of a screening for kruppel like zinc fingers and repressive activity on transcription was observed in yeast (Han et al., 1999). Later it was shown to bind the TCAT repeat motif in vitro, which is a microsatellite region in the tyrosine hydroxilase gene, implicating a role for ZNF24 in the central nervous system (Albanese et al., 2001). In mouse embryonic development ZNF24 was, among others, found to be expressed in the subventricular zone of the lateral ventricle and other proliferating regions of the brain (Khalfallah et al., 2008). The same group confirmed that neuronal precursor cells express ZNF24 and revealed that miss-expression of the transcription factor maintains neural cells as cycling progenitors whereas loss of function leads to exit of the cell cycle (Khalfallah et al., 2009). We detected a slight activation of the immature neuron marker DCX by ZNF24 in cooperation with SOX11, as illustrated in figure 34, which contradicts the previous data of analysing ZNF24 function. We found both transcription factors to be expressed in neuronal precursors in figure 41, allowing a possible interaction of ZNF24 and SOX11. As there is not much known about ZNF24's function, a further investigation of whether ZNF24 could exert a transcriptional activation to drive differentiation, as shown for DCX, in addition to its repressive function, dependent on its interaction partners.

Mutations in SOX11 have recently been causally associated with Coffin-Siris Syndrome, a congenital disorder characterised by intellectual disability (Tsurusaki et al., 2014). There is rising evidence from experimental studies and biochemical analyses that proteins encoded by genes linked to intellectual disability are connected in transcriptional networks controlling cellular processes and pathways, which are crucial for neuronal development and plasticity (Chelly et al., 2006, Inlow and Restifo, 2004). The fact that deletions or mutations in the genes encoding MYT1, TCF4, YY1 and ZNF24 have been linked to CNS malformation or intellectual disability syndromes (Amiel et al., 2007, Khalfallah et al., 2008, Kroepfl et al., 2008, Kwon and Chung, 2003), suggests that interference in the SOX11-centered transcriptional network possibly contributes to several cases of intellectual disability.

5.4. Perspectives

The determination of a variety of SOX11 interaction partners by the interactome screen and the subsequent functional characterisation of selected candidates provide new insight into the SOX11-centered transcriptional network implicated in the complex process of neuronal fate commitment and differentiation. The interactome comprises transcription factors and transcriptional modulators, which potentially contribute to the neuronal transcriptional core identity. However, a gain of information of this range raises new questions that have to be investigated with different functional approaches. Despite our effort to bring new knowledge about six selected candidates namely MYT1, TCF4, TRIM28, YY1, CBX6 and ZNF24, further characterization need to be carried out using different techniques. To this end, both gain and loss of function studies are in progress using neuronal precursor cells, isolated from the hippocampal dentate gyrus of the mouse brain. The impact of the over-expression and depletion respectively on the success of differentiation into neurons will be determined by the use of neuronal markers like DCX or βIII-tubulin. The co-expression with SOX11 could reveal new or validate already known cooperative effects. A similar approach led to the observation that virus-mediated over-expression of SOX11 promotes neurogenesis, as it increases the number of immature neurons in vitro, by monitoring the DCX expression as a marker for new-born neuronal cells, compared to control vector in murine neuronal precursors (Mu et al., 2012). For the three transcription factors MYT1, YY1 and ZNF24 this assay could confirm the identified activation or repression of the early neuronal markers DCX and STMN1 in a cellular model associated with neuronal differentiation. With reference the other transcriptional modulators, TCF4, TRIM28 and CBX6 that didn't show regulation of the two investigated promoters, the approach could unravel whether the gain or loss of function of the proteins influences generally neuronal differentiation in this model system. If they affect the process of differentiation, the effect of the regulating proteins on other genes implicated in neurogenesis should be further investigated with different promoters, which is also recommended for MYT1, YY1 and ZNF24. Therefore, the Genomatix software provides information about potential binding sites of single transcription factors or modelling with combinations. For MYT1 and SOX11, another interesting promoter revealed adjacent binding sites for the two transcription factors, namely *TCF3*, a bHLH transcription factor related to TCF4 and

known to be involved in the initiation of neurogenesis (Ravanpay and Olson, 2008). Also another bHLH protein implicated in late neuronal differentiation, NEUROD1 (Gao et al., 2009) is part of the potential target list for SOX11 and MYT1. Thus, promoter studies on *NEUROD1* could also reveal cooperation of the two transcription factors. For further investigation of the influence of MYT1, YY1 and ZNF24 on the *DCX* and *STMN1* regulation, chromatin immunoprecipitations would be the method of choice in order to obtain the specific binding sites in the regulatory sequence of the two early neuronal markers. Another possibility to assess the binding of a transcription factor to a specific DNA fragment would be an electrophoretic mobility shift assay. This not only reveals the binding activities, but also provides information about molecular stoichiometry and if recognition of the consensus sequence is mediated by monomers or multimers. Moreover, co-expression of the factors with SOX11 in the neurogenesis-active brain niches subgranular zone of the hippocampal dentate gyrus as well as the subventricular zone of the lateral ventricle and especially in neuronal precursor cells could be determined by immunohistochemical staining. This would confirm the observed expression in neuronal progenitors and their occurrence in the adult neurogenesis-specific brain regions at the same developmental stages. Eventually, an important step for future application of the candidate transcription factors in regenerative medicine would be the implementation of the transcriptional modulators in reprogramming assays of somatic cells into neurons as the current strategies and candidates need to be improved. SOX11 and MYT1L, paralog of MYT1 already successfully contributed to reprogramming studies (Ambasudhan et al., 2011, Liu et al., 2013). Based on the results of our study, the SOX11-centered transcriptional network provides a variety of potential candidates for the advance of reprogramming efforts of adult somatic cells into functional neurons in the future.

6. References

Ahn, S., Joyner, A.L., 2005. In vivo analysis of quiescent adult neural stem cells responding to Sonic hedgehog. Nature 437 (7060), 894-897.

Albanese, V., Biguet, N.F., Kiefer, H., Bayard, E., Mallet, J., Meloni, R., 2001. Quantitative effects on gene silencing by allelic variation at a tetranucleotide microsatellite. Hum Mol Genet 10 (17), 1785-1792.

Aloia, L., Di Stefano, B., Di Croce, L., 2013. Polycomb complexes in stem cells and embryonic development. Development 140 (12), 2525-2534.

Alonso, M., Viollet, C., Gabellec, M.M., Meas-Yedid, V., Olivo-Marin, J.C., Lledo, P.M., 2006. Olfactory discrimination learning increases the survival of adult-born neurons in the olfactory bulb. J Neurosci 26 (41), 10508-10513.

Alvarez-Buylla, A., Garcia-Verdugo, J.M., 2002. Neurogenesis in adult subventricular zone. J Neurosci 22 (3), 629-634.

Amat, J.A., Fields, K.L., Schubart, U.K., 1991. Distribution of phosphoprotein p19 in rat brain during ontogeny: stage-specific expression in neurons and glia. Brain Res Dev Brain Res 60 (2), 205-218.

Ambasudhan, R., Talantova, M., Coleman, R., Yuan, X., Zhu, S., Lipton, S.A., Ding, S., 2011. Direct reprogramming of adult human fibroblasts to functional neurons under defined conditions. Cell Stem Cell 9 (2), 113-118.

Amiel, J., Rio, M., de Pontual, L., Redon, R., Malan, V., Boddaert, N., Plouin, P., Carter, N.P., Lyonnet, S., Munnich, A., Colleaux, L., 2007. Mutations in TCF4, encoding a class I basic helix-loop-helix transcription factor, are responsible for Pitt-Hopkins syndrome, a severe epileptic encephalopathy associated with autonomic dysfunction. Am J Hum Genet 80 (5), 988-993.

Anton, E.S., Ghashghaei, H.T., Weber, J.L., McCann, C., Fischer, T.M., Cheung, I.D., Gassmann, M., Messing, A., Klein, R., Schwab, M.H., Lloyd, K.C., Lai, C., 2004. Receptor tyrosine kinase ErbB4 modulates neuroblast migration and placement in the adult forebrain. Nat Neurosci 7 (12), 1319-1328.

Arvidsson, A., Collin, T., Kirik, D., Kokaia, Z., Lindvall, O., 2002. Neuronal replacement from endogenous precursors in the adult brain after stroke. Nat Med 8 (9), 963-970.

Auboeuf, D., Dowhan, D.H., Li, X., Larkin, K., Ko, L., Berget, S.M., O'Malley, B.W., 2004. CoAA, a nuclear receptor coactivator protein at the interface of transcriptional coactivation and RNA splicing. Mol Cell Biol 24 (1), 442-453.

Bacigaluppi, M., Pluchino, S., Peruzzotti-Jametti, L., Kilic, E., Kilic, U., Salani, G., Brambilla, E., West, M.J., Comi, G., Martino, G., Hermann, D.M., 2009. Delayed post-ischaemic neuroprotection following systemic neural stem cell transplantation involves multiple mechanisms. Brain 132 (Pt 8), 2239-2251.

Ballas, N., Grunseich, C., Lu, D.D., Speh, J.C., Mandel, G., 2005. REST and its corepressors mediate plasticity of neuronal gene chromatin throughout neurogenesis. Cell 121 (4), 645-657.

Bannerman, D.M., Rawlins, J.N., McHugh, S.B., Deacon, R.M., Yee, B.K., Bast, T., Zhang, W.N., Pothuizen, H.H., Feldon, J., 2004. Regional dissociations within the hippocampus--memory and anxiety. Neurosci Biobehav Rev 28 (3), 273-283.

Baratz, K.H., Tosakulwong, N., Ryu, E., Brown, W.L., Branham, K., Chen, W., Tran, K.D., Schmid-Kubista, K.E., Heckenlively, J.R., Swaroop, A., Abecasis, G., Bailey, K.R., Edwards, A.O., 2010. E2-2 protein and Fuchs's corneal dystrophy. N Engl J Med 363 (11), 1016-1024.

Barth, P.G., 1987. Disorders of neuronal migration. Can J Neurol Sci 14 (1), 1-16.
Batsukh, T., Pieper, L., Koszucka, A.M., von Velsen, N., Hoyer-Fender, S., Elbracht, M., Bergman, J.E., Hoefsloot, L.H., Pauli, S., 2010. CHD8 interacts with CHD7, a protein which is mutated in CHARGE syndrome. Hum Mol Genet 19 (14), 2858-2866.
Baye, L.M., Link, B.A., 2008. Nuclear migration during retinal development. Brain Res 1192, 29-36.
Bellefroid, E.J., Bourguignon, C., Hollemann, T., Ma, Q., Anderson, D.J., Kintner, C., Pieler, T., 1996. X-MyT1, a Xenopus C2HC-type zinc finger protein with a regulatory function in neuronal differentiation. Cell 87 (7), 1191-1202.
Bendall, S.C., Hughes, C., Stewart, M.H., Doble, B., Bhatia, M., Lajoie, G.A., 2008. Prevention of amino acid conversion in SILAC experiments with embryonic stem cells. Mol Cell Proteomics 7 (9), 1587-1597.
Benlhabib, H., Herrera, J.E., 2006. Expression of the Op18 gene is maintained by the CCAAT-binding transcription factor NF-Y. Gene 377, 177-185.
Bergsland, M., Ramskold, D., Zaouter, C., Klum, S., Sandberg, R., Muhr, J., 2011. Sequentially acting Sox transcription factors in neural lineage development. Genes Dev 25 (23), 2453-2464.
Bergsland, M., Werme, M., Malewicz, M., Perlmann, T., Muhr, J., 2006. The establishment of neuronal properties is controlled by Sox4 and Sox11. Genes Dev 20 (24), 3475-3486.
Berninger, B., Costa, M.R., Koch, U., Schroeder, T., Sutor, B., Grothe, B., Gotz, M., 2007. Functional properties of neurons derived from in vitro reprogrammed postnatal astroglia. J Neurosci 27 (32), 8654-8664.
Bernstein, E., Duncan, E.M., Masui, O., Gil, J., Heard, E., Allis, C.D., 2006. Mouse polycomb proteins bind differentially to methylated histone H3 and RNA and are enriched in facultative heterochromatin. Mol Cell Biol 26 (7), 2560-2569.
Bertrand, N., Castro, D.S., Guillemot, F., 2002. Proneural genes and the specification of neural cell types. Nat Rev Neurosci 3 (7), 517-530.
Bezsonova, I., Walker, J.R., Bacik, J.P., Duan, S., Dhe-Paganon, S., Arrowsmith, C.H., 2009. Ring1B contains a ubiquitin-like docking module for interaction with Cbx proteins. Biochemistry 48 (44), 10542-10548.
Bhattaram, P., Penzo-Mendez, A., Sock, E., Colmenares, C., Kaneko, K.J., Vassilev, A., Depamphilis, M.L., Wegner, M., Lefebvre, V., 2010. Organogenesis relies on SoxC transcription factors for the survival of neural and mesenchymal progenitors. Nat Commun 1, 9.
Boekhoorn, K., van Dis, V., Goedknegt, E., Sobel, A., Lucassen, P.J., Hoogenraad, C.C., 2014. The microtubule destabilizing protein stathmin controls the transition from dividing neuronal precursors to postmitotic neurons during adult hippocampal neurogenesis. Dev Neurobiol.
Boldt, K., Gloeckner, C.J., Texier, Y., von Zweydorf, F., Ueffing, M., 2014. Applying SILAC for the Differential Analysis of Protein Complexes. Methods Mol Biol 1188, 177-190.
Bonaguidi, M.A., Wheeler, M.A., Shapiro, J.S., Stadel, R.P., Sun, G.J., Ming, G.L., Song, H., 2011. In vivo clonal analysis reveals self-renewing and multipotent adult neural stem cell characteristics. Cell 145 (7), 1142-1155.
Bond, J., Roberts, E., Mochida, G.H., Hampshire, D.J., Scott, S., Askham, J.M., Springell, K., Mahadevan, M., Crow, Y.J., Markham, A.F., Walsh, C.A., Woods, C.G., 2002. ASPM is a major determinant of cerebral cortical size. Nat Genet 32 (2), 316-320.

Bonfanti, L., Theodosis, D.T., 1994. Expression of polysialylated neural cell adhesion molecule by proliferating cells in the subependymal layer of the adult rat, in its rostral extension and in the olfactory bulb. Neuroscience 62 (1), 291-305.

Bowles, J., Schepers, G., Koopman, P., 2000. Phylogeny of the SOX family of developmental transcription factors based on sequence and structural indicators. Dev Biol 227 (2), 239-255.

Boyer, L.A., Lee, T.I., Cole, M.F., Johnstone, S.E., Levine, S.S., Zucker, J.P., Guenther, M.G., Kumar, R.M., Murray, H.L., Jenner, R.G., Gifford, D.K., Melton, D.A., Jaenisch, R., Young, R.A., 2005. Core transcriptional regulatory circuitry in human embryonic stem cells. Cell 122 (6), 947-956.

Bradford, M.M., 1976. A rapid and sensitive method for the quantitation of microgram quantities of protein utilizing the principle of protein-dye binding. Anal Biochem 72, 248-254.

Bredesen, D.E., Rao, R.V., Mehlen, P., 2006. Cell death in the nervous system. Nature 443 (7113), 796-802.

Brockschmidt, A., Todt, U., Ryu, S., Hoischen, A., Landwehr, C., Birnbaum, S., Frenck, W., Radlwimmer, B., Lichter, P., Engels, H., Driever, W., Kubisch, C., Weber, R.G., 2007. Severe mental retardation with breathing abnormalities (Pitt-Hopkins syndrome) is caused by haploinsufficiency of the neuronal bHLH transcription factor TCF4. Hum Mol Genet 16 (12), 1488-1494.

Bronstein, I., Fortin, J., Stanley, P.E., Stewart, G.S., Kricka, L.J., 1994. Chemiluminescent and bioluminescent reporter gene assays. Anal Biochem 219 (2), 169-181.

Brooks, Y.S., Wang, G., Yang, Z., Smith, K.K., Bieberich, E., Ko, L., 2009. Functional pre- mRNA trans-splicing of coactivator CoAA and corepressor RBM4 during stem/progenitor cell differentiation. J Biol Chem 284 (27), 18033-18046.

Brown, J.P., Couillard-Despres, S., Cooper-Kuhn, C.M., Winkler, J., Aigner, L., Kuhn, H.G., 2003. Transient expression of doublecortin during adult neurogenesis. J Comp Neurol 467 (1), 1-10.

Bruel-Jungerman, E., Laroche, S., Rampon, C., 2005. New neurons in the dentate gyrus are involved in the expression of enhanced long-term memory following environmental enrichment. Eur J Neurosci 21 (2), 513-521.

Bylund, M., Andersson, E., Novitch, B.G., Muhr, J., 2003. Vertebrate neurogenesis is counteracted by Sox1-3 activity. Nat Neurosci 6 (11), 1162-1168.

Caiazzo, M., Dell'Anno, M.T., Dvoretskova, E., Lazarevic, D., Taverna, S., Leo, D., Sotnikova, T.D., Menegon, A., Roncaglia, P., Colciago, G., Russo, G., Carninci, P., Pezzoli, G., Gainetdinov, R.R., Gustincich, S., Dityatev, A., Broccoli, V., 2011. Direct generation of functional dopaminergic neurons from mouse and human fibroblasts. Nature 476 (7359), 224-227.

Cammas, F., Herzog, M., Lerouge, T., Chambon, P., Losson, R., 2004. Association of the transcriptional corepressor TIF1beta with heterochromatin protein 1 (HP1): an essential role for progression through differentiation. Genes Dev 18 (17), 2147-2160.

Camoletto, P., Colesanti, A., Ozon, S., Sobel, A., Fasolo, A., 2001. Expression of stathmin and SCG10 proteins in the olfactory neurogenesis during development and after lesion in the adulthood. Brain Res Bull 54 (1), 19-28.

Cao, R., Wang, L., Wang, H., Xia, L., Erdjument-Bromage, H., Tempst, P., Jones, R.S., Zhang, Y., 2002. Role of histone H3 lysine 27 methylation in Polycomb-group silencing. Science 298 (5595), 1039-1043.

Chambers, S.M., Fasano, C.A., Papapetrou, E.P., Tomishima, M., Sadelain, M., Studer, L., 2009. Highly efficient neural conversion of human ES and iPS cells by dual inhibition of SMAD signaling. Nat Biotechnol 27 (3), 275-280.

Chelly, J., Khelfaoui, M., Francis, F., Cherif, B., Bienvenu, T., 2006. Genetics and pathophysiology of mental retardation. Eur J Hum Genet 14 (6), 701-713.

Chen, J., Bardes, E.E., Aronow, B.J., Jegga, A.G., 2009. ToppGene Suite for gene list enrichment analysis and candidate gene prioritization. Nucleic Acids Res 37 (Web Server issue), W305-311.

Chen, X., Xu, H., Yuan, P., Fang, F., Huss, M., Vega, V.B., Wong, E., Orlov, Y.L., Zhang, W., Jiang, J., Loh, Y.H., Yeo, H.C., Yeo, Z.X., Narang, V., Govindarajan, K.R., Leong, B., Shahab, A., Ruan, Y., Bourque, G., Sung, W.K., Clarke, N.D., Wei, C.L., Ng, H.H., 2008. Integration of external signaling pathways with the core transcriptional network in embryonic stem cells. Cell 133 (6), 1106-1117.

Cheng, L.E., Reed, R.R., 2007. Zfp423/OAZ participates in a developmental switch during olfactory neurogenesis. Neuron 54 (4), 547-557.

Cheung, M., Abu-Elmagd, M., Clevers, H., Scotting, P.J., 2000. Roles of Sox4 in central nervous system development. Brain Res Mol Brain Res 79 (1-2), 180-191.

Chi, B., Wang, K., Du, Y., Gui, B., Chang, X., Wang, L., Fan, J., Chen, S., Wu, X., Li, G., Cheng, H., 2014. A Sub-Element in PRE enhances nuclear export of intronless mRNAs by recruiting the TREX complex via ZC3H18. Nucleic Acids Res 42 (11), 7305-7318.

Chong, J.A., Tapia-Ramirez, J., Kim, S., Toledo-Aral, J.J., Zheng, Y., Boutros, M.C., Altshuller, Y.M., Frohman, M.A., Kraner, S.D., Mandel, G., 1995. REST: a mammalian silencer protein that restricts sodium channel gene expression to neurons. Cell 80 (6), 949-957.

Close, P., East, P., Dirac-Svejstrup, A.B., Hartmann, H., Heron, M., Maslen, S., Chariot, A., Soding, J., Skehel, M., Svejstrup, J.Q., 2012. DBIRD complex integrates alternative mRNA splicing with RNA polymerase II transcript elongation. Nature 484 (7394), 386-389.

Connor, F., Cary, P.D., Read, C.M., Preston, N.S., Driscoll, P.C., Denny, P., Crane-Robinson, C., Ashworth, A., 1994. DNA binding and bending properties of the post-meiotically expressed Sry-related protein Sox-5. Nucleic Acids Res 22 (16), 3339-3346.

Connor, F., Wright, E., Denny, P., Koopman, P., Ashworth, A., 1995. The Sry-related HMG box-containing gene Sox6 is expressed in the adult testis and developing nervous system of the mouse. Nucleic Acids Res 23 (17), 3365-3372.

Conover, J.C., Doetsch, F., Garcia-Verdugo, J.M., Gale, N.W., Yancopoulos, G.D., Alvarez-Buylla, A., 2000. Disruption of Eph/ephrin signaling affects migration and proliferation in the adult subventricular zone. Nat Neurosci 3 (11), 1091-1097.

Consiglio, A., Gritti, A., Dolcetta, D., Follenzi, A., Bordignon, C., Gage, F.H., Vescovi, A.L., Naldini, L., 2004. Robust in vivo gene transfer into adult mammalian neural stem cells by lentiviral vectors. Proc Natl Acad Sci U S A 101 (41), 14835-14840.

Cooper, O., Hargus, G., Deleidi, M., Blak, A., Osborn, T., Marlow, E., Lee, K., Levy, A., Perez-Torres, E., Yow, A., Isacson, O., 2010. Differentiation of human ES and Parkinson's disease iPS cells into ventral midbrain dopaminergic neurons

requires a high activity form of SHH, FGF8a and specific regionalization by retinoic acid. Mol Cell Neurosci 45 (3), 258-266.

Cox, J., Mann, M., 2008. MaxQuant enables high peptide identification rates, individualized p.p.b.-range mass accuracies and proteome-wide protein quantification. Nat Biotechnol 26 (12), 1367-1372.

Crooks, G.E., Hon, G., Chandonia, J.M., Brenner, S.E., 2004. WebLogo: a sequence logo generator. Genome Res 14 (6), 1188-1190.

Curmi, P.A., Gavet, O., Charbaut, E., Ozon, S., Lachkar-Colmerauer, S., Manceau, V., Siavoshian, S., Maucuer, A., Sobel, A., 1999. Stathmin and its phosphoprotein family: general properties, biochemical and functional interaction with tubulin. Cell Struct Funct 24 (5), 345-357.

Curtis, M.A., Kam, M., Nannmark, U., Anderson, M.F., Axell, M.Z., Wikkelso, C., Holtas, S., van Roon-Mom, W.M., Bjork-Eriksson, T., Nordborg, C., Frisen, J., Dragunow, M., Faull, R.L., Eriksson, P.S., 2007. Human neuroblasts migrate to the olfactory bulb via a lateral ventricular extension. Science 315 (5816), 1243-1249.

Damianov, A., Kann, M., Lane, W.S., Bindereif, A., 2006. Human RBM28 protein is a specific nucleolar component of the spliceosomal snRNPs. Biol Chem 387 (10-11), 1455-1460.

Davis, R.L., Weintraub, H., Lassar, A.B., 1987. Expression of a single transfected cDNA converts fibroblasts to myoblasts. Cell 51 (6), 987-1000.

Deisseroth, K., Singla, S., Toda, H., Monje, M., Palmer, T.D., Malenka, R.C., 2004. Excitation-neurogenesis coupling in adult neural stem/progenitor cells. Neuron 42 (4), 535-552.

DeRan, M., Pulvino, M., Greene, E., Su, C., Zhao, J., 2008. Transcriptional activation of histone genes requires NPAT-dependent recruitment of TRRAP-Tip60 complex to histone promoters during the G1/S phase transition. Mol Cell Biol 28 (1), 435-447.

des Portes, V., Francis, F., Pinard, J.M., Desguerre, I., Moutard, M.L., Snoeck, I., Meiners, L.C., Capron, F., Cusmai, R., Ricci, S., Motte, J., Echenne, B., Ponsot, G., Dulac, O., Chelly, J., Beldjord, C., 1998. doublecortin is the major gene causing X-linked subcortical laminar heterotopia (SCLH). Hum Mol Genet 7 (7), 1063-1070.

des Portes, V., Pinard, J.M., Billuart, P., Vinet, M.C., Koulakoff, A., Carrie, A., Gelot, A., Dupuis, E., Motte, J., Berwald-Netter, Y., Catala, M., Kahn, A., Beldjord, C., Chelly, J., 1998. A novel CNS gene required for neuronal migration and involved in X-linked subcortical laminar heterotopia and lissencephaly syndrome. Cell 92 (1), 51-61.

des Portes, V., Pinard, J.M., Smadja, D., Motte, J., Boespflug-Tanguy, O., Moutard, M.L., Desguerre, I., Billuart, P., Carrie, A., Bienvenu, T., Vinet, M.C., Bachner, L., Beldjord, C., Dulac, O., Kahn, A., Ponsot, G., Chelly, J., 1997. Dominant X linked subcortical laminar heterotopia and lissencephaly syndrome (XSCLH/LIS): evidence for the occurrence of mutation in males and mapping of a potential locus in Xq22. J Med Genet 34 (3), 177-183.

Doetsch, F., 2003. A niche for adult neural stem cells. Curr Opin Genet Dev 13 (5), 543-550.

Doetsch, F., Caille, I., Lim, D.A., Garcia-Verdugo, J.M., Alvarez-Buylla, A., 1999. Subventricular zone astrocytes are neural stem cells in the adult mammalian brain. Cell 97 (6), 703-716.

Doetsch, F., Petreanu, L., Caille, I., Garcia-Verdugo, J.M., Alvarez-Buylla, A., 2002. EGF converts transit-amplifying neurogenic precursors in the adult brain into multipotent stem cells. Neuron 36 (6), 1021-1034.

Donohoe, M.E., Zhang, X., McGinnis, L., Biggers, J., Li, E., Shi, Y., 1999. Targeted disruption of mouse Yin Yang 1 transcription factor results in peri-implantation lethality. Mol Cell Biol 19 (10), 7237-7244.

Dranovsky, A., Hen, R., 2006. Hippocampal neurogenesis: regulation by stress and antidepressants. Biol Psychiatry 59 (12), 1136-1143.

Duan, X., Chang, J.H., Ge, S., Faulkner, R.L., Kim, J.Y., Kitabatake, Y., Liu, X.B., Yang, C.H., Jordan, J.D., Ma, D.K., Liu, C.Y., Ganesan, S., Cheng, H.J., Ming, G.L., Lu, B., Song, H., 2007. Disrupted-In-Schizophrenia 1 regulates integration of newly generated neurons in the adult brain. Cell 130 (6), 1146-1158.

Duman, R.S., 2004. Depression: a case of neuronal life and death? Biol Psychiatry 56 (3), 140-145.

Duman, R.S., Monteggia, L.M., 2006. A neurotrophic model for stress-related mood disorders. Biol Psychiatry 59 (12), 1116-1127.

Dumitriu, B., Patrick, M.R., Petschek, J.P., Cherukuri, S., Klingmuller, U., Fox, P.L., Lefebvre, V., 2006. Sox6 cell-autonomously stimulates erythroid cell survival, proliferation, and terminal maturation and is thereby an important enhancer of definitive erythropoiesis during mouse development. Blood 108 (4), 1198-1207.

Dupret, D., Fabre, A., Dobrossy, M.D., Panatier, A., Rodriguez, J.J., Lamarque, S., Lemaire, V., Oliet, S.H., Piazza, P.V., Abrous, D.N., 2007. Spatial learning depends on both the addition and removal of new hippocampal neurons. PLoS Biol 5 (8), e214.

Dy, P., Penzo-Mendez, A., Wang, H., Pedraza, C.E., Macklin, W.B., Lefebvre, V., 2008. The three SoxC proteins--Sox4, Sox11 and Sox12--exhibit overlapping expression patterns and molecular properties. Nucleic Acids Res 36 (9), 3101-3117.

Ehm, O., Goritz, C., Covic, M., Schaffner, I., Schwarz, T.J., Karaca, E., Kempkes, B., Kremmer, E., Pfrieger, F.W., Espinosa, L., Bigas, A., Giachino, C., Taylor, V., Frisen, J., Lie, D.C., 2010. RBPJkappa-dependent signaling is essential for long-term maintenance of neural stem cells in the adult hippocampus. J Neurosci 30 (41), 13794-13807.

Encinas, J.M., Vaahtokari, A., Enikolopov, G., 2006. Fluoxetine targets early progenitor cells in the adult brain. Proc Natl Acad Sci U S A 103 (21), 8233-8238.

Engelen, E., Akinci, U., Bryne, J.C., Hou, J., Gontan, C., Moen, M., Szumska, D., Kockx, C., van Ijcken, W., Dekkers, D.H., Demmers, J., Rijkers, E.J., Bhattacharya, S., Philipsen, S., Pevny, L.H., Grosveld, F.G., Rottier, R.J., Lenhard, B., Poot, R.A., 2011. Sox2 cooperates with Chd7 to regulate genes that are mutated in human syndromes. Nat Genet 43 (6), 607-611.

Enwere, E., Shingo, T., Gregg, C., Fujikawa, H., Ohta, S., Weiss, S., 2004. Aging results in reduced epidermal growth factor receptor signaling, diminished olfactory neurogenesis, and deficits in fine olfactory discrimination. J Neurosci 24 (38), 8354-8365.

Eriksson, P.S., Perfilieva, E., Bjork-Eriksson, T., Alborn, A.M., Nordborg, C., Peterson, D.A., Gage, F.H., 1998. Neurogenesis in the adult human hippocampus. Nat Med 4 (11), 1313-1317.

Fantes, J., Ragge, N.K., Lynch, S.A., McGill, N.I., Collin, J.R., Howard-Peebles, P.N., Hayward, C., Vivian, A.J., Williamson, K., van Heyningen, V., FitzPatrick, D.R., 2003. Mutations in SOX2 cause anophthalmia. Nat Genet 33 (4), 461-463.

Farah, M.H., Olson, J.M., Sucic, H.B., Hume, R.I., Tapscott, S.J., Turner, D.L., 2000. Generation of neurons by transient expression of neural bHLH proteins in mammalian cells. Development 127 (4), 693-702.

Favaro, R., Valotta, M., Ferri, A.L., Latorre, E., Mariani, J., Giachino, C., Lancini, C., Tosetti, V., Ottolenghi, S., Taylor, V., Nicolis, S.K., 2009. Hippocampal development and neural stem cell maintenance require Sox2-dependent regulation of Shh. Nat Neurosci 12 (10), 1248-1256.

Feng, W., Khan, M.A., Bellvis, P., Zhu, Z., Bernhardt, O., Herold-Mende, C., Liu, H.K., 2013. The chromatin remodeler CHD7 regulates adult neurogenesis via activation of SoxC transcription factors. Cell Stem Cell 13 (1), 62-72.

Feng, W.J., Khan, M.A., Bellvis, P., Zhu, Z., Bernhardt, O., Herold-Mende, C., Liu, H.K., 2013. The Chromatin Remodeler CHD7 Regulates Adult Neurogenesis via Activation of SoxC Transcription Factors. Cell Stem Cell 13 (1), 62-72.

Fenn, J.B., Mann, M., Meng, C.K., Wong, S.F., Whitehouse, C.M., 1989. Electrospray ionization for mass spectrometry of large biomolecules. Science 246 (4926), 64-71.

Ferri, A.L., Cavallaro, M., Braida, D., Di Cristofano, A., Canta, A., Vezzani, A., Ottolenghi, S., Pandolfi, P.P., Sala, M., DeBiasi, S., Nicolis, S.K., 2004. Sox2 deficiency causes neurodegeneration and impaired neurogenesis in the adult mouse brain. Development 131 (15), 3805-3819.

Francis, F., Koulakoff, A., Boucher, D., Chafey, P., Schaar, B., Vinet, M.C., Friocourt, G., McDonnell, N., Reiner, O., Kahn, A., McConnell, S.K., Berwald-Netter, Y., Denoulet, P., Chelly, J., 1999. Doublecortin is a developmentally regulated, microtubule-associated protein expressed in migrating and differentiating neurons. Neuron 23 (2), 247-256.

Francois, M., Koopman, P., Beltrame, M., 2010. SoxF genes: Key players in the development of the cardio-vascular system. Int J Biochem Cell Biol 42 (3), 445-448.

Fu, H., Cai, J., Clevers, H., Fast, E., Gray, S., Greenberg, R., Jain, M.K., Ma, Q., Qiu, M., Rowitch, D.H., Taylor, C.M., Stiles, C.D., 2009. A genome-wide screen for spatially restricted expression patterns identifies transcription factors that regulate glial development. J Neurosci 29 (36), 11399-11408.

Fukuda, S., Kato, F., Tozuka, Y., Yamaguchi, M., Miyamoto, Y., Hisatsune, T., 2003. Two distinct subpopulations of nestin-positive cells in adult mouse dentate gyrus. J Neurosci 23 (28), 9357-9366.

Gage, F.H., 2000. Mammalian neural stem cells. Science 287 (5457), 1433-1438.

Gamsjaeger, R., O'Connell, M.R., Cubeddu, L., Shepherd, N.E., Lowry, J.A., Kwan, A.H., Vandevenne, M., Swanton, M.K., Matthews, J.M., Mackay, J.P., 2013. A structural analysis of DNA binding by myelin transcription factor 1 double zinc fingers. J Biol Chem 288 (49), 35180-35191.

Gao, Z., Cox, J.L., Gilmore, J.M., Ormsbee, B.D., Mallanna, S.K., Washburn, M.P., Rizzino, A., 2012. Determination of protein interactome of transcription factor Sox2 in embryonic stem cells engineered for inducible expression of four reprogramming factors. J Biol Chem 287 (14), 11384-11397.

Gao, Z., Ure, K., Ables, J.L., Lagace, D.C., Nave, K.A., Goebbels, S., Eisch, A.J., Hsieh, J., 2009. Neurod1 is essential for the survival and maturation of adult-born neurons. Nat Neurosci 12 (9), 1090-1092.

Gao, Z., Ure, K., Ding, P., Nashaat, M., Yuan, L., Ma, J., Hammer, R.E., Hsieh, J., 2011. The master negative regulator REST/NRSF controls adult neurogenesis by restraining the neurogenic program in quiescent stem cells. J Neurosci 31 (26), 9772-9786.

Garcia, A.D., Doan, N.B., Imura, T., Bush, T.G., Sofroniew, M.V., 2004. GFAP-expressing progenitors are the principal source of constitutive neurogenesis in adult mouse forebrain. Nat Neurosci 7 (11), 1233-1241.

Garlisi, C.G., Uss, A.S., Xiao, H., Tian, F., Sheridan, K.E., Wang, L., Motasim Billah, M., Egan, R.W., Stranick, K.S., Umland, S.P., 2001. A unique mRNA initiated within a middle intron of WHSC1/MMSET encodes a DNA binding protein that suppresses human IL-5 transcription. Am J Respir Cell Mol Biol 24 (1), 90-98.

Gaspar-Maia, A., Alajem, A., Polesso, F., Sridharan, R., Mason, M.J., Heidersbach, A., Ramalho-Santos, J., McManus, M.T., Plath, K., Meshorer, E., Ramalho-Santos, M., 2009. Chd1 regulates open chromatin and pluripotency of embryonic stem cells. Nature 460 (7257), 863-868.

Gazave, E., Lapebie, P., Richards, G.S., Brunet, F., Ereskovsky, A.V., Degnan, B.M., Borchiellini, C., Vervoort, M., Renard, E., 2009. Origin and evolution of the Notch signalling pathway: an overview from eukaryotic genomes. BMC Evol Biol 9, 249.

Ge, S., Yang, C.H., Hsu, K.S., Ming, G.L., Song, H., 2007. A critical period for enhanced synaptic plasticity in newly generated neurons of the adult brain. Neuron 54 (4), 559-566.

Gene Ontology, C., 2008. The Gene Ontology project in 2008. Nucleic Acids Res 36 (Database issue), D440-444.

Gheusi, G., Cremer, H., McLean, H., Chazal, G., Vincent, J.D., Lledo, P.M., 2000. Importance of newly generated neurons in the adult olfactory bulb for odor discrimination. Proc Natl Acad Sci U S A 97 (4), 1823-1828.

Gil-Perotin, S., Marin-Husstege, M., Li, J., Soriano-Navarro, M., Zindy, F., Roussel, M.F., Garcia-Verdugo, J.M., Casaccia-Bonnefil, P., 2006. Loss of p53 induces changes in the behavior of subventricular zone cells: implication for the genesis of glial tumors. J Neurosci 26 (4), 1107-1116.

Gloeckner, C.J., Boldt, K., Schumacher, A., Roepman, R., Ueffing, M., 2007. A novel tandem affinity purification strategy for the efficient isolation and characterisation of native protein complexes. Proteomics 7 (23), 4228-4234.

Gloeckner, C.J., Boldt, K., Ueffing, M., 2009. Strep/FLAG tandem affinity purification (SF-TAP) to study protein interactions. Curr Protoc Protein Sci Chapter 19, Unit19 20.

Gong, C., Wang, T.W., Huang, H.S., Parent, J.M., 2007. Reelin regulates neuronal progenitor migration in intact and epileptic hippocampus. J Neurosci 27 (8), 1803-1811.

Gould, E., Beylin, A., Tanapat, P., Reeves, A., Shors, T.J., 1999. Learning enhances adult neurogenesis in the hippocampal formation. Nat Neurosci 2 (3), 260-265.

Graham, V., Khudyakov, J., Ellis, P., Pevny, L., 2003. SOX2 functions to maintain neural progenitor identity. Neuron 39 (5), 749-765.

Grosschedl, R., Giese, K., Pagel, J., 1994. HMG domain proteins: architectural elements in the assembly of nucleoprotein structures. Trends Genet 10 (3), 94-100.

Gstaiger, M., Aebersold, R., 2009. Applying mass spectrometry-based proteomics to genetics, genomics and network biology. Nature Reviews Genetics 10 (9), 617-627.

Gubbay, J., Collignon, J., Koopman, P., Capel, B., Economou, A., Munsterberg, A., Vivian, N., Goodfellow, P., Lovell-Badge, R., 1990. A gene mapping to the sex-determining region of the mouse Y chromosome is a member of a novel family of embryonically expressed genes. Nature 346 (6281), 245-250.

Guenther, M.G., Levine, S.S., Boyer, L.A., Jaenisch, R., Young, R.A., 2007. A chromatin landmark and transcription initiation at most promoters in human cells. Cell 130 (1), 77-88.

Guo, Z., Zhang, L., Wu, Z., Chen, Y., Wang, F., Chen, G., 2014. In Vivo direct reprogramming of reactive glial cells into functional neurons after brain injury and in an Alzheimer's disease model. Cell Stem Cell 14 (2), 188-202.

Hack, M.A., Saghatelyan, A., de Chevigny, A., Pfeifer, A., Ashery-Padan, R., Lledo, P.M., Gotz, M., 2005. Neuronal fate determinants of adult olfactory bulb neurogenesis. Nat Neurosci 8 (7), 865-872.

Hacker, A., Capel, B., Goodfellow, P., Lovell-Badge, R., 1995. Expression of Sry, the mouse sex determining gene. Development 121 (6), 1603-1614.

Hagiwara, T., Tanaka, K., Takai, S., Maeno-Hikichi, Y., Mukainaka, Y., Wada, K., 1996. Genomic organization, promoter analysis, and chromosomal localization of the gene for the mouse glial high-affinity glutamate transporter Slc1a3. Genomics 33 (3), 508-515.

Han, B., Liu, N., Yang, X., Sun, H.B., Yang, Y.C., 2001. MRG1 expression in fibroblasts is regulated by Sp1/Sp3 and an Ets transcription factor. J Biol Chem 276 (11), 7937-7942.

Han, Z.G., Zhang, Q.H., Ye, M., Kan, L.X., Gu, B.W., He, K.L., Shi, S.L., Zhou, J., Fu, G., Mao, M., Chen, S.J., Yu, L., Chen, Z., 1999. Molecular cloning of six novel Kruppel-like zinc finger genes from hematopoietic cells and identification of a novel transregulatory domain KRNB. J Biol Chem 274 (50), 35741-35748.

Haslinger, A., Schwarz, T.J., Covic, M., Chichung Lie, D., 2009. Expression of Sox11 in adult neurogenic niches suggests a stage-specific role in adult neurogenesis. Eur J Neurosci 29 (11), 2103-2114.

He, Y., Dupree, J., Wang, J., Sandoval, J., Li, J., Liu, H., Shi, Y., Nave, K.A., Casaccia-Bonnefil, P., 2007. The transcription factor Yin Yang 1 is essential for oligodendrocyte progenitor differentiation. Neuron 55 (2), 217-230.

Heinrich, C., Blum, R., Gascon, S., Masserdotti, G., Tripathi, P., Sanchez, R., Tiedt, S., Schroeder, T., Gotz, M., Berninger, B., 2010. Directing astroglia from the cerebral cortex into subtype specific functional neurons. PLoS Biol 8 (5), e1000373.

Hendershot, T.J., Liu, H., Clouthier, D.E., Shepherd, I.T., Coppola, E., Studer, M., Firulli, A.B., Pittman, D.L., Howard, M.J., 2008. Conditional deletion of Hand2 reveals critical functions in neurogenesis and cell type-specific gene expression for development of neural crest-derived noradrenergic sympathetic ganglion neurons. Dev Biol 319 (2), 179-191.

Henthorn, P., McCarrick-Walmsley, R., Kadesch, T., 1990. Sequence of the cDNA encoding ITF-2, a positive-acting transcription factor. Nucleic Acids Res 18 (3), 678.

Hillman, C.H., Erickson, K.I., Kramer, A.F., 2008. Be smart, exercise your heart: exercise effects on brain and cognition. Nat Rev Neurosci 9 (1), 58-65.

Hobert, O., 2011. Regulation of terminal differentiation programs in the nervous system. Annu Rev Cell Dev Biol 27, 681-696.

Horesh, D., Sapir, T., Francis, F., Wolf, S.G., Caspi, M., Elbaum, M., Chelly, J., Reiner, O., 1999. Doublecortin, a stabilizer of microtubules. Hum Mol Genet 8 (9), 1599-1610.

Hoser, M., Potzner, M.R., Koch, J.M., Bosl, M.R., Wegner, M., Sock, E., 2008. Sox12 deletion in the mouse reveals nonreciprocal redundancy with the related Sox4 and Sox11 transcription factors. Mol Cell Biol 28 (15), 4675-4687.

Howard, M.J., 2005. Mechanisms and perspectives on differentiation of autonomic neurons. Dev Biol 277 (2), 271-286.

Howard, M.J., Stanke, M., Schneider, C., Wu, X., Rohrer, H., 2000. The transcription factor dHAND is a downstream effector of BMPs in sympathetic neuron specification. Development 127 (18), 4073-4081.

Hsieh, J., 2012. Orchestrating transcriptional control of adult neurogenesis. Genes Dev 26 (10), 1010-1021.

Hu, H., Tomasiewicz, H., Magnuson, T., Rutishauser, U., 1996. The role of polysialic acid in migration of olfactory bulb interneuron precursors in the subventricular zone. Neuron 16 (4), 735-743.

Huang, Y.C., Shih, H.Y., Lin, S.J., Chiu, C.C., Ma, T.L., Yeh, T.H., Cheng, Y.C., 2014. The epigenetic factor Kmt2a/Mll1 regulates neural progenitor proliferation and neuronal and glial differentiation. Dev Neurobiol.

Imayoshi, I., Sakamoto, M., Yamaguchi, M., Mori, K., Kageyama, R., 2010. Essential roles of Notch signaling in maintenance of neural stem cells in developing and adult brains. J Neurosci 30 (9), 3489-3498.

Infantino, V., Convertini, P., Iacobazzi, F., Pisano, I., Scarcia, P., Iacobazzi, V., 2011. Identification of a novel Sp1 splice variant as a strong transcriptional activator. Biochem Biophys Res Commun 412 (1), 86-91.

Inlow, J.K., Restifo, L.L., 2004. Molecular and comparative genetics of mental retardation. Genetics 166 (2), 835-881.

Iosif, R.E., Ekdahl, C.T., Ahlenius, H., Pronk, C.J., Bonde, S., Kokaia, Z., Jacobsen, S.E., Lindvall, O., 2006. Tumor necrosis factor receptor 1 is a negative regulator of progenitor proliferation in adult hippocampal neurogenesis. J Neurosci 26 (38), 9703-9712.

Isono, K., Fujimura, Y., Shinga, J., Yamaki, M., J, O.W., Takihara, Y., Murahashi, Y., Takada, Y., Mizutani-Koseki, Y., Koseki, H., 2005. Mammalian polyhomeotic homologues Phc2 and Phc1 act in synergy to mediate polycomb repression of Hox genes. Mol Cell Biol 25 (15), 6694-6706.

Jacques, T.S., Relvas, J.B., Nishimura, S., Pytela, R., Edwards, G.M., Streuli, C.H., ffrench-Constant, C., 1998. Neural precursor cell chain migration and division are regulated through different beta1 integrins. Development 125 (16), 3167-3177.

Jagasia, R., Steib, K., Englberger, E., Herold, S., Faus-Kessler, T., Saxe, M., Gage, F.H., Song, H., Lie, D.C., 2009. GABA-cAMP response element-binding protein signaling regulates maturation and survival of newly generated neurons in the adult hippocampus. J Neurosci 29 (25), 7966-7977.

Jaglin, X.H., Chelly, J., 2009. Tubulin-related cortical dysgeneses: microtubule dysfunction underlying neuronal migration defects. Trends Genet 25 (12), 555-566.

Jeronimo, C., Forget, D., Bouchard, A., Li, Q., Chua, G., Poitras, C., Therien, C., Bergeron, D., Bourassa, S., Greenblatt, J., Chabot, B., Poirier, G.G., Hughes, T.R., Blanchette, M., Price, D.H., Coulombe, B., 2007. Systematic analysis of

the protein interaction network for the human transcription machinery reveals the identity of the 7SK capping enzyme. Mol Cell 27 (2), 262-274.

Jessberger, S., Zhao, C., Toni, N., Clemenson, G.D., Jr., Li, Y., Gage, F.H., 2007. Seizure-associated, aberrant neurogenesis in adult rats characterized with retrovirus-mediated cell labeling. J Neurosci 27 (35), 9400-9407.

Jiang, L., Yao, M., Shi, J., Shen, P., Niu, G., Fei, J., 2008. Yin yang 1 directly regulates the transcription of RE-1 silencing transcription factor. J Neurosci Res 86 (6), 1209-1216.

Jin, K., Mao, X.O., Cottrell, B., Schilling, B., Xie, L., Row, R.H., Sun, Y., Peel, A., Childs, J., Gendeh, G., Gibson, B.W., Greenberg, D.A., 2004. Proteomic and immunochemical characterization of a role for stathmin in adult neurogenesis. FASEB J 18 (2), 287-299.

Jing, X., Wang, T., Huang, S., Glorioso, J.C., Albers, K.M., 2011. The transcription factor Sox11 promotes nerve regeneration through activation of the regeneration-associated gene Sprr1a. Exp Neurol.

Junttila, M.R., Saarinen, S., Schmidt, T., Kast, J., Westermarck, J., 2005. Single-step Strep-tag purification for the isolation and identification of protein complexes from mammalian cells. Proteomics 5 (5), 1199-1203.

Kamachi, Y., Uchikawa, M., Collignon, J., Lovell-Badge, R., Kondoh, H., 1998. Involvement of Sox1, 2 and 3 in the early and subsequent molecular events of lens induction. Development 125 (13), 2521-2532.

Kamachi, Y., Uchikawa, M., Kondoh, H., 2000. Pairing SOX off: with partners in the regulation of embryonic development. Trends Genet 16 (4), 182-187.

Kar, A., Havlioglu, N., Tarn, W.Y., Wu, J.Y., 2006. RBM4 interacts with an intronic element and stimulates tau exon 10 inclusion. J Biol Chem 281 (34), 24479-24488.

Karalay, O., Doberauer, K., Vadodaria, K.C., Knobloch, M., Berti, L., Miquelajauregui, A., Schwark, M., Jagasia, R., Taketo, M.M., Tarabykin, V., Lie, D.C., Jessberger, S., 2011. Prospero-related homeobox 1 gene (Prox1) is regulated by canonical Wnt signaling and has a stage-specific role in adult hippocampal neurogenesis. Proc Natl Acad Sci U S A 108 (14), 5807-5812.

Karl, C., Couillard-Despres, S., Prang, P., Munding, M., Kilb, W., Brigadski, T., Plotz, S., Mages, W., Luhmann, H., Winkler, J., Bogdahn, U., Aigner, L., 2005. Neuronal precursor-specific activity of a human doublecortin regulatory sequence. J Neurochem 92 (2), 264-282.

Kee, N., Teixeira, C.M., Wang, A.H., Frankland, P.W., 2007. Preferential incorporation of adult-generated granule cells into spatial memory networks in the dentate gyrus. Nat Neurosci 10 (3), 355-362.

Kent, J., Wheatley, S.C., Andrews, J.E., Sinclair, A.H., Koopman, P., 1996. A male-specific role for SOX9 in vertebrate sex determination. Development 122 (9), 2813-2822.

Khalfallah, O., Faucon-Biguet, N., Nardelli, J., Meloni, R., Mallet, J., 2008. Expression of the transcription factor Zfp191 during embryonic development in the mouse. Gene Expr Patterns 8 (3), 148-154.

Khalfallah, O., Ravassard, P., Lagache, C.S., Fligny, C., Serre, A., Bayard, E., Faucon-Biguet, N., Mallet, J., Meloni, R., Nardelli, J., 2009. Zinc finger protein 191 (ZNF191/Zfp191) is necessary to maintain neural cells as cycling progenitors. Stem Cells 27 (7), 1643-1653.

Kim, J., Schafer, J., Ming, G.L., 2006. New directions in neuroregeneration. Expert Opin Biol Ther 6 (8), 735-738.

Kippin, T.E., Martens, D.J., van der Kooy, D., 2005. p21 loss compromises the relative quiescence of forebrain stem cell proliferation leading to exhaustion of their proliferation capacity. Genes Dev 19 (6), 756-767.

Kleefstra, T., Kramer, J.M., Neveling, K., Willemsen, M.H., Koemans, T.S., Vissers, L.E., Wissink-Lindhout, W., Fenckova, M., van den Akker, W.M., Kasri, N.N., Nillesen, W.M., Prescott, T., Clark, R.D., Devriendt, K., van Reeuwijk, J., de Brouwer, A.P., Gilissen, C., Zhou, H., Brunner, H.G., Veltman, J.A., Schenck, A., van Bokhoven, H., 2012. Disruption of an EHMT1-associated chromatin-modification module causes intellectual disability. Am J Hum Genet 91 (1), 73-82.

Kohler, G., Howe, S.C., Milstein, C., 1976. Fusion between immunoglobulin-secreting and nonsecreting myeloma cell lines. Eur J Immunol 6 (4), 292-295.

Kohler, G., Milstein, C., 1975. Continuous cultures of fused cells secreting antibody of predefined specificity. Nature 256 (5517), 495-497.

Koopman, P., Munsterberg, A., Capel, B., Vivian, N., Lovell-Badge, R., 1990. Expression of a candidate sex-determining gene during mouse testis differentiation. Nature 348 (6300), 450-452.

Kopan, R., Ilagan, M.X., 2009. The canonical Notch signaling pathway: unfolding the activation mechanism. Cell 137 (2), 216-233.

Kouprina, N., Pavlicek, A., Collins, N.K., Nakano, M., Noskov, V.N., Ohzeki, J., Mochida, G.H., Risinger, J.I., Goldsmith, P., Gunsior, M., Solomon, G., Gersch, W., Kim, J.H., Barrett, J.C., Walsh, C.A., Jurka, J., Masumoto, H., Larionov, V., 2005. The microcephaly ASPM gene is expressed in proliferating tissues and encodes for a mitotic spindle protein. Hum Mol Genet 14 (15), 2155-2165.

Kovacevic-Grujicic, N., Mojsin, M., Djurovic, J., Petrovic, I., Stevanovic, M., 2008. Comparison of promoter regions of SOX3, SOX14 and SOX18 orthologs in mammals. DNA Sequence 19 (3), 185-194.

Kovacevic Grujicic N., Mojsin M., Krstic A., M., S., 2005. Functional characterization of the human SOX3 promoter: identification of

transcription factors implicated in basal promoter activity. Gene Expr Patterns 344, 287– 297.

Kreyszig, E., 1979. Applied Mathematics. John Wiley & Sons, Hoboken, NJ.

Kroepfl, T., Petek, E., Schwarzbraun, T., Kroisel, P.M., Plecko, B., 2008. Mental retardation in a girl with a subtelomeric deletion on chromosome 20q and complete deletion of the myelin transcription factor 1 gene (MYT1). Clin Genet 73 (5), 492-495.

Ku, M., Koche, R.P., Rheinbay, E., Mendenhall, E.M., Endoh, M., Mikkelsen, T.S., Presser, A., Nusbaum, C., Xie, X., Chi, A.S., Adli, M., Kasif, S., Ptaszek, L.M., Cowan, C.A., Lander, E.S., Koseki, H., Bernstein, B.E., 2008. Genomewide analysis of PRC1 and PRC2 occupancy identifies two classes of bivalent domains. PLoS Genet 4 (10), e1000242.

Kuhlbrodt, K., Herbarth, B., Sock, E., Enderich, J., Hermans-Borgmeyer, I., Wegner, M., 1998. Cooperative function of POU proteins and SOX proteins in glial cells. J Biol Chem 273 (26), 16050-16057.

Kuhlbrodt, K., Herbarth, B., Sock, E., Hermans-Borgmeyer, I., Wegner, M., 1998. Sox10, a novel transcriptional modulator in glial cells. J Neurosci 18 (1), 237-250.

Kuhn, H.G., Dickinson-Anson, H., Gage, F.H., 1996. Neurogenesis in the dentate gyrus of the adult rat: age-related decrease of neuronal progenitor proliferation. J Neurosci 16 (6), 2027-2033.

Kuhn, H.G., Winkler, J., Kempermann, G., Thal, L.J., Gage, F.H., 1997. Epidermal growth factor and fibroblast growth factor-2 have different effects on neural progenitors in the adult rat brain. J Neurosci 17 (15), 5820-5829.

Kuwabara, T., Hsieh, J., Muotri, A., Yeo, G., Warashina, M., Lie, D.C., Moore, L., Nakashima, K., Asashima, M., Gage, F.H., 2009. Wnt-mediated activation of NeuroD1 and retro-elements during adult neurogenesis. Nat Neurosci 12 (9), 1097-1105.

Kuwabara, T., Hsieh, J., Nakashima, K., Taira, K., Gage, F.H., 2004. A small modulatory dsRNA specifies the fate of adult neural stem cells. Cell 116 (6), 779-793.

Kwon, H.J., Chung, H.M., 2003. Yin Yang 1, a vertebrate polycomb group gene, regulates antero-posterior neural patterning. Biochem Biophys Res Commun 306 (4), 1008-1013.

Lai, M.C., Kuo, H.W., Chang, W.C., Tarn, W.Y., 2003. A novel splicing regulator shares a nuclear import pathway with SR proteins. EMBO J 22 (6), 1359-1369.

Landy, A., 1989. Dynamic, structural, and regulatory aspects of lambda site-specific recombination. Annu Rev Biochem 58, 913-949.

Laplagne, D.A., Kamienkowski, J.E., Esposito, M.S., Piatti, V.C., Zhao, C., Gage, F.H., Schinder, A.F., 2007. Similar GABAergic inputs in dentate granule cells born during embryonic and adult neurogenesis. Eur J Neurosci 25 (10), 2973-2981.

Lassar, A.B., Paterson, B.M., Weintraub, H., 1986. Transfection of a DNA locus that mediates the conversion of 10T1/2 fibroblasts to myoblasts. Cell 47 (5), 649-656.

Laudet, V., Stehelin, D., Clevers, H., 1993. Ancestry and diversity of the HMG box superfamily. Nucleic Acids Res 21 (10), 2493-2501.

Lavado, A., Lagutin, O.V., Chow, L.M., Baker, S.J., Oliver, G., 2010. Prox1 is required for granule cell maturation and intermediate progenitor maintenance during brain neurogenesis. PLoS Biol 8 (8).

Lee, A.K., Ahn, S.G., Yoon, J.H., Kim, S.A., 2011. Sox4 stimulates ss-catenin activity through induction of CK2. Oncol Rep 25 (2), 559-565.

Lefebvre, V., 2010. The SoxD transcription factors--Sox5, Sox6, and Sox13--are key cell fate modulators. Int J Biochem Cell Biol 42 (3), 429-432.

Li, G., Bien-Ly, N., Andrews-Zwilling, Y., Xu, Q., Bernardo, A., Ring, K., Halabisky, B., Deng, C., Mahley, R.W., Huang, Y., 2009. GABAergic interneuron dysfunction impairs hippocampal neurogenesis in adult apolipoprotein E4 knockin mice. Cell Stem Cell 5 (6), 634-645.

Li, X., Barkho, B.Z., Luo, Y., Smrt, R.D., Santistevan, N.J., Liu, C., Kuwabara, T., Gage, F.H., Zhao, X., 2008. Epigenetic regulation of the stem cell mitogen Fgf-2 by Mbd1 in adult neural stem/progenitor cells. J Biol Chem 283 (41), 27644-27652.

Li, Y.J., Minear, M.A., Rimmler, J., Zhao, B., Balajonda, E., Hauser, M.A., Allingham, R.R., Eghrari, A.O., Riazuddin, S.A., Katsanis, N., Gottsch, J.D., Gregory, S.G., Klintworth, G.K., Afshari, N.A., 2011. Replication of TCF4 through association and linkage studies in late-onset Fuchs endothelial corneal dystrophy. PLoS One 6 (4), e18044.

Liber, D., Domaschenz, R., Holmqvist, P.H., Mazzarella, L., Georgiou, A., Leleu, M., Fisher, A.G., Labosky, P.A., Dillon, N., 2010. Epigenetic priming of a pre-B cell-specific enhancer through binding of Sox2 and Foxd3 at the ESC stage. Cell Stem Cell 7 (1), 114-126.

Lie, D.C., Colamarino, S.A., Song, H.J., Desire, L., Mira, H., Consiglio, A., Lein, E.S., Jessberger, S., Lansford, H., Dearie, A.R., Gage, F.H., 2005. Wnt signalling regulates adult hippocampal neurogenesis. Nature 437 (7063), 1370-1375.

Lim, D.A., Huang, Y.C., Swigut, T., Mirick, A.L., Garcia-Verdugo, J.M., Wysocka, J., Ernst, P., Alvarez-Buylla, A., 2009. Chromatin remodelling factor Mll1 is essential for neurogenesis from postnatal neural stem cells. Nature 458 (7237), 529-533.

Lin, L., Lee, V.M., Wang, Y., Lin, J.S., Sock, E., Wegner, M., Lei, L., 2011. Sox11 regulates survival and axonal growth of embryonic sensory neurons. Dev Dyn 240 (1), 52-64.

Liu, M.L., Zang, T., Zou, Y., Chang, J.C., Gibson, J.R., Huber, K.M., Zhang, C.L., 2013. Small molecules enable neurogenin 2 to efficiently convert human fibroblasts into cholinergic neurons. Nat Commun 4, 2183.

Liu, Y., Ray, S.K., Yang, X.Q., Luntz-Leybman, V., Chiu, I.M., 1998. A splice variant of E2-2 basic helix-loop-helix protein represses the brain-specific fibroblast growth factor 1 promoter through the binding to an imperfect E-box. J Biol Chem 273 (30), 19269-19276.

Lo-Castro, A., Giana, G., Fichera, M., Castiglia, L., Grillo, L., Musumeci, S.A., Galasso, C., Curatolo, P., 2009. Deletion 2p25.2: a cryptic chromosome abnormality in a patient with autism and mental retardation detected using aCGH. Eur J Med Genet 52 (1), 67-70.

Lois, C., Garcia-Verdugo, J.M., Alvarez-Buylla, A., 1996. Chain migration of neuronal precursors. Science 271 (5251), 978-981.

Lugert, S., Basak, O., Knuckles, P., Haussler, U., Fabel, K., Gotz, M., Haas, C.A., Kempermann, G., Taylor, V., Giachino, C., 2010. Quiescent and active hippocampal neural stem cells with distinct morphologies respond selectively to physiological and pathological stimuli and aging. Cell Stem Cell 6 (5), 445-456.

Lujan, E., Chanda, S., Ahlenius, H., Sudhof, T.C., Wernig, M., 2012. Direct conversion of mouse fibroblasts to self-renewing, tripotent neural precursor cells. Proc Natl Acad Sci U S A 109 (7), 2527-2532.

Lv, J., Liu, H., Wang, Q., Tang, Z., Hou, L., Zhang, B., 2003. Molecular cloning of a novel human gene encoding histone acetyltransferase-like protein involved in transcriptional activation of hTERT. Biochem Biophys Res Commun 311 (2), 506-513.

Ma, Q., Kintner, C., Anderson, D.J., 1996. Identification of neurogenin, a vertebrate neuronal determination gene. Cell 87 (1), 43-52.

Ma, R.G., Zhang, Y., Sun, T.T., Cheng, B., 2014. Epigenetic regulation by polycomb group complexes: focus on roles of CBX proteins. J Zhejiang Univ Sci B 15 (5), 412-428.

Mackler, S.A., Korutla, L., Cha, X.Y., Koebbe, M.J., Fournier, K.M., Bowers, M.S., Kalivas, P.W., 2000. NAC-1 is a brain POZ/BTB protein that can prevent cocaine-induced sensitization in the rat. J Neurosci 20 (16), 6210-6217.

Malas, S., Postlethwaite, M., Ekonomou, A., Whalley, B., Nishiguchi, S., Wood, H., Meldrum, B., Constanti, A., Episkopou, V., 2003. Sox1-deficient mice suffer

from epilepsy associated with abnormal ventral forebrain development and olfactory cortex hyperexcitability. Neuroscience 119 (2), 421-432.

Manganas, L.N., Zhang, X., Li, Y., Hazel, R.D., Smith, S.D., Wagshul, M.E., Henn, F., Benveniste, H., Djuric, P.M., Enikolopov, G., Maletic-Savatic, M., 2007. Magnetic resonance spectroscopy identifies neural progenitor cells in the live human brain. Science 318 (5852), 980-985.

Mann, M., Hendrickson, R.C., Pandey, A., 2001. Analysis of proteins and proteomes by mass spectrometry. Annu Rev Biochem 70, 437-473.

Marangi, G., Ricciardi, S., Orteschi, D., Lattante, S., Murdolo, M., Dallapiccola, B., Biscione, C., Lecce, R., Chiurazzi, P., Romano, C., Greco, D., Pettinato, R., Sorge, G., Pantaleoni, C., Alfei, E., Toldo, I., Magnani, C., Bonanni, P., Martinez, F., Serra, G., Battaglia, D., Lettori, D., Vasco, G., Baroncini, A., Daolio, C., Zollino, M., 2011. The Pitt-Hopkins syndrome: report of 16 new patients and clinical diagnostic criteria. Am J Med Genet A 155A (7), 1536-1545.

Marfella, C.G., Imbalzano, A.N., 2007. The Chd family of chromatin remodelers. Mutat Res 618 (1-2), 30-40.

Margueron, R., Justin, N., Ohno, K., Sharpe, M.L., Son, J., Drury, W.J., 3rd, Voigt, P., Martin, S.R., Taylor, W.R., De Marco, V., Pirrotta, V., Reinberg, D., Gamblin, S.J., 2009. Role of the polycomb protein EED in the propagation of repressive histone marks. Nature 461 (7265), 762-767.

Margueron, R., Li, G., Sarma, K., Blais, A., Zavadil, J., Woodcock, C.L., Dynlacht, B.D., Reinberg, D., 2008. Ezh1 and Ezh2 maintain repressive chromatin through different mechanisms. Mol Cell 32 (4), 503-518.

Marin-Burgin, A., Mongiat, L.A., Pardi, M.B., Schinder, A.F., 2012. Unique processing during a period of high excitation/inhibition balance in adult-born neurons. Science 335 (6073), 1238-1242.

Marinaro, C., Butti, E., Bergamaschi, A., Papale, A., Furlan, R., Comi, G., Martino, G., Muzio, L., 2011. In vivo fate analysis reveals the multipotent and self-renewal features of embryonic AspM expressing cells. PLoS One 6 (4), e19419.

Martinowich, K., Hattori, D., Wu, H., Fouse, S., He, F., Hu, Y., Fan, G.P., Sun, Y.E., 2003. DNA methylation-related chromatin remodeling in activity-dependent Bdnf gene regulation. Science 302 (5646), 890-893.

Matsushita, F., Kameyama, T., Kadokawa, Y., Marunouchi, T., 2014. Spatiotemporal expression pattern of Myt/NZF family zinc finger transcription factors during mouse nervous system development. Dev Dyn 243 (4), 588-600.

McEwen, B.S., 2001. Plasticity of the hippocampus: adaptation to chronic stress and allostatic load. Ann N Y Acad Sci 933, 265-277.

Meek, K.M., Leonard, D.W., Connon, C.J., Dennis, S., Khan, S., 2003. Transparency, swelling and scarring in the corneal stroma. Eye (Lond) 17 (8), 927-936.

Merkle, F.T., Mirzadeh, Z., Alvarez-Buylla, A., 2007. Mosaic organization of neural stem cells in the adult brain. Science 317 (5836), 381-384.

Meshorer, E., Yellajoshula, D., George, E., Scambler, P.J., Brown, D.T., Misteli, T., 2006. Hyperdynamic plasticity of chromatin proteins in pluripotent embryonic stem cells. Dev Cell 10 (1), 105-116.

Meyer, T.S., Lamberts, B.L., 1965. Use of coomassie brilliant blue R250 for the electrophoresis of microgram quantities of parotid saliva proteins on acrylamide-gel strips. Biochim Biophys Acta 107 (1), 144-145.

Michalski, A., Damoc, E., Hauschild, J.P., Lange, O., Wieghaus, A., Makarov, A., Nagaraj, N., Cox, J., Mann, M., Horning, S., 2011. Mass spectrometry-based proteomics using Q Exactive, a high-performance benchtop quadrupole Orbitrap mass spectrometer. Mol Cell Proteomics 10 (9), M111 011015.

Mikkelsen, T.S., Ku, M., Jaffe, D.B., Issac, B., Lieberman, E., Giannoukos, G., Alvarez, P., Brockman, W., Kim, T.K., Koche, R.P., Lee, W., Mendenhall, E., O'Donovan, A., Presser, A., Russ, C., Xie, X., Meissner, A., Wernig, M., Jaenisch, R., Nusbaum, C., Lander, E.S., Bernstein, B.E., 2007. Genome-wide maps of chromatin state in pluripotent and lineage-committed cells. Nature 448 (7153), 553-560.

Miller, J.A., Nathanson, J., Franjic, D., Shim, S., Dalley, R.A., Shapouri, S., Smith, K.A., Sunkin, S.M., Bernard, A., Bennett, J.L., Lee, C.K., Hawrylycz, M.J., Jones, A.R., Amaral, D.G., Sestan, N., Gage, F.H., Lein, E.S., 2013. Conserved molecular signatures of neurogenesis in the hippocampal subgranular zone of rodents and primates. Development 140 (22), 4633-4644.

Ming, G.L., Song, H., 2011. Adult neurogenesis in the mammalian brain: significant answers and significant questions. Neuron 70 (4), 687-702.

Mohn, F., Weber, M., Rebhan, M., Roloff, T.C., Richter, J., Stadler, M.B., Bibel, M., Schubeler, D., 2008. Lineage-specific polycomb targets and de novo DNA methylation define restriction and potential of neuronal progenitors. Molecular Cell 30 (6), 755-766.

Molofsky, A.V., He, S., Bydon, M., Morrison, S.J., Pardal, R., 2005. Bmi-1 promotes neural stem cell self-renewal and neural development but not mouse growth and survival by repressing the p16Ink4a and p19Arf senescence pathways. Genes Dev 19 (12), 1432-1437.

Molofsky, A.V., Slutsky, S.G., Joseph, N.M., He, S., Pardal, R., Krishnamurthy, J., Sharpless, N.E., Morrison, S.J., 2006. Increasing p16INK4a expression decreases forebrain progenitors and neurogenesis during ageing. Nature 443 (7110), 448-452.

Montojo, J., Zuberi, K., Rodriguez, H., Kazi, F., Wright, G., Donaldson, S.L., Morris, Q., Bader, G.D., 2010. GeneMANIA Cytoscape plugin: fast gene function predictions on the desktop. Bioinformatics 26 (22), 2927-2928.

Morais da Silva, S., Hacker, A., Harley, V., Goodfellow, P., Swain, A., Lovell-Badge, R., 1996. Sox9 expression during gonadal development implies a conserved role for the gene in testis differentiation in mammals and birds. Nat Genet 14 (1), 62-68.

Morey, L., Helin, K., 2010. Polycomb group protein-mediated repression of transcription. Trends Biochem Sci 35 (6), 323-332.

Morgan, M.J., Woltering, J.M., In der Rieden, P.M., Durston, A.J., Thiery, J.P., 2004. YY1 regulates the neural crest-associated slug gene in Xenopus laevis. J Biol Chem 279 (45), 46826-46834.

Morrison, S.J., Spradling, A.C., 2008. Stem cells and niches: mechanisms that promote stem cell maintenance throughout life. Cell 132 (4), 598-611.

Mu, L., Berti, L., Masserdotti, G., Covic, M., Michaelidis, T.M., Doberauer, K., Merz, K., Rehfeld, F., Haslinger, A., Wegner, M., Sock, E., Lefebvre, V., Couillard-Despres, S., Aigner, L., Berninger, B., Lie, D.C., 2012. SoxC transcription factors are required for neuronal differentiation in adult hippocampal neurogenesis. J Neurosci 32 (9), 3067-3080.

Muller, J., Gaunt, S., Lawrence, P.A., 1995. Function of the Polycomb protein is conserved in mice and flies. Development 121 (9), 2847-2852.

Muller, J., Verrijzer, P., 2009. Biochemical mechanisms of gene regulation by polycomb group protein complexes. Curr Opin Genet Dev 19 (2), 150-158.

Muotri, A.R., Chu, V.T., Marchetto, M.C., Deng, W., Moran, J.V., Gage, F.H., 2005. Somatic mosaicism in neuronal precursor cells mediated by L1 retrotransposition. Nature 435 (7044), 903-910.

Murre, C., McCaw, P.S., Vaessin, H., Caudy, M., Jan, L.Y., Jan, Y.N., Cabrera, C.V., Buskin, J.N., Hauschka, S.D., Lassar, A.B., et al., 1989. Interactions between heterologous helix-loop-helix proteins generate complexes that bind specifically to a common DNA sequence. Cell 58 (3), 537-544.

Murugan, S., Shan, J., Kuhl, S.J., Tata, A., Pietila, I., Kuhl, M., Vainio, S.J., 2012. WT1 and Sox11 regulate synergistically the promoter of the Wnt4 gene that encodes a critical signal for nephrogenesis. Exp Cell Res 318 (10), 1134-1145.

Nacher, J., McEwen, B.S., 2006. The role of N-methyl-D-asparate receptors in neurogenesis. Hippocampus 16 (3), 267-270.

Nakamura, T., Mori, T., Tada, S., Krajewski, W., Rozovskaia, T., Wassell, R., Dubois, G., Mazo, A., Croce, C.M., Canaani, E., 2002. ALL-1 is a histone methyltransferase that assembles a supercomplex of proteins involved in transcriptional regulation. Mol Cell 10 (5), 1119-1128.

Neguembor, M.V., Xynos, A., Onorati, M.C., Caccia, R., Bortolanza, S., Godio, C., Pistoni, M., Corona, D.F., Schotta, G., Gabellini, D., 2013. FSHD muscular dystrophy region gene 1 binds Suv4-20h1 histone methyltransferase and impairs myogenesis. J Mol Cell Biol 5 (5), 294-307.

Nerlov, C., Graf, T., 1998. PU.1 induces myeloid lineage commitment in multipotent hematopoietic progenitors. Genes Dev 12 (15), 2403-2412.

Ninkovic, J., Steiner-Mezzadri, A., Jawerka, M., Akinci, U., Masserdotti, G., Petricca, S., Fischer, J., von Holst, A., Beckers, J., Lie, C.D., Petrik, D., Miller, E., Tang, J., Wu, J., Lefebvre, V., Demmers, J., Eisch, A., Metzger, D., Crabtree, G., Irmler, M., Poot, R., Gotz, M., 2013. The BAF complex interacts with Pax6 in adult neural progenitors to establish a neurogenic cross-regulatory transcriptional network. Cell Stem Cell 13 (4), 403-418.

Nishiguchi, S., Wood, H., Kondoh, H., Lovell-Badge, R., Episkopou, V., 1998. Sox1 directly regulates the gamma-crystallin genes and is essential for lens development in mice. Genes Dev 12 (6), 776-781.

Niv, F., Keiner, S., Krishna, Witte, O.W., Lie, D.C., Redecker, C., 2012. Aberrant neurogenesis after stroke: a retroviral cell labeling study. Stroke 43 (9), 2468-2475.

O'Carroll, D., Erhardt, S., Pagani, M., Barton, S.C., Surani, M.A., Jenuwein, T., 2001. The polycomb-group gene Ezh2 is required for early mouse development. Mol Cell Biol 21 (13), 4330-4336.

Ogawa, H., Ishiguro, K., Gaubatz, S., Livingston, D.M., Nakatani, Y., 2002. A complex with chromatin modifiers that occupies E2F- and Myc-responsive genes in G0 cells. Science 296 (5570), 1132-1136.

Olsen, J.V., de Godoy, L.M., Li, G., Macek, B., Mortensen, P., Pesch, R., Makarov, A., Lange, O., Horning, S., Mann, M., 2005. Parts per million mass accuracy on an Orbitrap mass spectrometer via lock mass injection into a C-trap. Mol Cell Proteomics 4 (12), 2010-2021.

Olsen, J.V., Schwartz, J.C., Griep-Raming, J., Nielsen, M.L., Damoc, E., Denisov, E., Lange, O., Remes, P., Taylor, D., Splendore, M., Wouters, E.R., Senko, M., Makarov, A., Mann, M., Horning, S., 2009. A dual pressure linear ion trap

Orbitrap instrument with very high sequencing speed. Mol Cell Proteomics 8 (12), 2759-2769.
Olson, J.M., Asakura, A., Snider, L., Hawkes, R., Strand, A., Stoeck, J., Hallahan, A., Pritchard, J., Tapscott, S.J., 2001. NeuroD2 is necessary for development and survival of central nervous system neurons. Dev Biol 234 (1), 174-187.
Ong, S.E., Blagoev, B., Kratchmarova, I., Kristensen, D.B., Steen, H., Pandey, A., Mann, M., 2002. Stable isotope labeling by amino acids in cell culture, SILAC, as a simple and accurate approach to expression proteomics. Mol Cell Proteomics 1 (5), 376-386.
Ozen, I., Galichet, C., Watts, C., Parras, C., Guillemot, F., Raineteau, O., 2007. Proliferating neuronal progenitors in the postnatal hippocampus transiently express the proneural gene Ngn2. Eur J Neurosci 25 (9), 2591-2603.
Pagon, R.A., Graham, J.M., Jr., Zonana, J., Yong, S.L., 1981. Coloboma, congenital heart disease, and choanal atresia with multiple anomalies: CHARGE association. J Pediatr 99 (2), 223-227.
Paik, J.H., Ding, Z., Narurkar, R., Ramkissoon, S., Muller, F., Kamoun, W.S., Chae, S.S., Zheng, H., Ying, H., Mahoney, J., Hiller, D., Jiang, S., Protopopov, A., Wong, W.H., Chin, L., Ligon, K.L., DePinho, R.A., 2009. FoxOs cooperatively regulate diverse pathways governing neural stem cell homeostasis. Cell Stem Cell 5 (5), 540-553.
Palmer, T.D., Takahashi, J., Gage, F.H., 1997. The adult rat hippocampus contains primordial neural stem cells. Mol Cell Neurosci 8 (6), 389-404.
Pang, Z.P., Yang, N., Vierbuchen, T., Ostermeier, A., Fuentes, D.R., Yang, T.Q., Citri, A., Sebastiano, V., Marro, S., Sudhof, T.C., Wernig, M., 2011. Induction of human neuronal cells by defined transcription factors. Nature 476 (7359), 220-223.
Pasini, D., Bracken, A.P., Jensen, M.R., Lazzerini Denchi, E., Helin, K., 2004. Suz12 is essential for mouse development and for EZH2 histone methyltransferase activity. EMBO J 23 (20), 4061-4071.
Petreanu, L., Alvarez-Buylla, A., 2002. Maturation and death of adult-born olfactory bulb granule neurons: role of olfaction. J Neurosci 22 (14), 6106-6113.
Pfaffl, M.W., 2001. A new mathematical model for relative quantification in real-time RT-PCR. Nucleic Acids Res 29 (9), e45.
Pfisterer, U., Kirkeby, A., Torper, O., Wood, J., Nelander, J., Dufour, A., Bjorklund, A., Lindvall, O., Jakobsson, J., Parmar, M., 2011. Direct conversion of human fibroblasts to dopaminergic neurons. Proc Natl Acad Sci U S A 108 (25), 10343-10348.
Pierfelice, T., Alberi, L., Gaiano, N., 2011. Notch in the vertebrate nervous system: an old dog with new tricks. Neuron 69 (5), 840-855.
Pinard, J.M., Motte, J., Chiron, C., Brian, R., Andermann, E., Dulac, O., 1994. Subcortical laminar heterotopia and lissencephaly in two families: a single X linked dominant gene. J Neurol Neurosurg Psychiatry 57 (8), 914-920.
Pingault, V., Bondurand, N., Kuhlbrodt, K., Goerich, D.E., Prehu, M.O., Puliti, A., Herbarth, B., Hermans-Borgmeyer, I., Legius, E., Matthijs, G., Amiel, J., Lyonnet, S., Ceccherini, I., Romeo, G., Smith, J.C., Read, A.P., Wegner, M., Goossens, M., 1998. SOX10 mutations in patients with Waardenburg-Hirschsprung disease. Nat Genet 18 (2), 171-173.
Pisaneschi, G., Ceccotti, S., Falchetti, M.L., Fiumicino, S., Carnevali, F., Beccari, E., 1994. Characterization of FIII/YY1, a Xenopus laevis conserved zinc-finger

protein binding to the first exon of L1 and L14 ribosomal protein genes. Biochem Biophys Res Commun 205 (2), 1236-1242.
Pitt, D., Hopkins, I., 1978. A syndrome of mental retardation, wide mouth and intermittent overbreathing. Aust Paediatr J 14 (3), 182-184.
Pluchino, S., Cossetti, C., 2013. How stem cells speak with host immune cells in inflammatory brain diseases. Glia 61 (9), 1379-1401.
Pomp, O., Brokhman, I., Ziegler, L., Almog, M., Korngreen, A., Tavian, M., Goldstein, R.S., 2008. PA6-induced human embryonic stem cell-derived neurospheres: a new source of human peripheral sensory neurons and neural crest cells. Brain Res 1230, 50-60.
Potzner, M.R., Tsarovina, K., Binder, E., Penzo-Mendez, A., Lefebvre, V., Rohrer, H., Wegner, M., Sock, E., 2010. Sequential requirement of Sox4 and Sox11 during development of the sympathetic nervous system. Development 137 (5), 775-784.
Poulain, F.E., Sobel, A., 2010. The microtubule network and neuronal morphogenesis: Dynamic and coordinated orchestration through multiple players. Mol Cell Neurosci 43 (1), 15-32.
Price, D.L., Struble, R.G., Whitehouse, P.J., Kitt, C.A., Cork, L.C., Walker, L.C., Casanova, M.F., 1986. Alzheimer's disease: a multisystem disorder. Res Publ Assoc Res Nerv Ment Dis 64, 209-214.
Qureshi, I.A., Gokhan, S., Mehler, M.F., 2010. REST and CoREST are transcriptional and epigenetic regulators of seminal neural fate decisions. Cell Cycle 9 (22), 4477-4486.
Rappsilber, J., Ishihama, Y., Mann, M., 2003. Stop and go extraction tips for matrix-assisted laser desorption/ionization, nanoelectrospray, and LC/MS sample pretreatment in proteomics. Anal Chem 75 (3), 663-670.
Ravanpay, A.C., Olson, J.M., 2008. E protein dosage influences brain development more than family member identity. J Neurosci Res 86 (7), 1472-1481.
Ren, X., Kerppola, T.K., 2011. REST interacts with Cbx proteins and regulates polycomb repressive complex 1 occupancy at RE1 elements. Mol Cell Biol 31 (10), 2100-2110.
Richards, G.S., Degnan, B.M., 2009. The dawn of developmental signaling in the metazoa. Cold Spring Harb Symp Quant Biol 74, 81-90.
Richly, H., Aloia, L., Di Croce, L., 2011. Roles of the Polycomb group proteins in stem cells and cancer. Cell Death Dis 2, e204.
Rochefort, C., Gheusi, G., Vincent, J.D., Lledo, P.M., 2002. Enriched odor exposure increases the number of newborn neurons in the adult olfactory bulb and improves odor memory. J Neurosci 22 (7), 2679-2689.
Rohrer, H., 2011. Transcriptional control of differentiation and neurogenesis in autonomic ganglia. Eur J Neurosci 34 (10), 1563-1573.
Rolls, A., Shechter, R., London, A., Ziv, Y., Ronen, A., Levy, R., Schwartz, M., 2007. Toll-like receptors modulate adult hippocampal neurogenesis. Nat Cell Biol 9 (9), 1081-1088.
Rowbotham, S.P., Barki, L., Neves-Costa, A., Santos, F., Dean, W., Hawkes, N., Choudhary, P., Will, W.R., Webster, J., Oxley, D., Green, C.M., Varga-Weisz, P., Mermoud, J.E., 2011. Maintenance of silent chromatin through replication requires SWI/SNF-like chromatin remodeler SMARCAD1. Mol Cell 42 (3), 285-296.
Roybon, L., Mastracci, T.L., Ribeiro, D., Sussel, L., Brundin, P., Li, J.Y., 2010. GABAergic differentiation induced by Mash1 is compromised by the bHLH

proteins Neurogenin2, NeuroD1, and NeuroD2. Cereb Cortex 20 (5), 1234-1244.

Saghatelyan, A., Roux, P., Migliore, M., Rochefort, C., Desmaisons, D., Charneau, P., Shepherd, G.M., Lledo, P.M., 2005. Activity-dependent adjustments of the inhibitory network in the olfactory bulb following early postnatal deprivation. Neuron 46 (1), 103-116.

Sakakibara, S., Imai, T., Hamaguchi, K., Okabe, M., Aruga, J., Nakajima, K., Yasutomi, D., Nagata, T., Kurihara, Y., Uesugi, S., Miyata, T., Ogawa, M., Mikoshiba, K., Okano, H., 1996. Mouse-Musashi-1, a neural RNA-binding protein highly enriched in the mammalian CNS stem cell. Dev Biol 176 (2), 230-242.

Sakakibara, S., Okano, H., 1997. Expression of neural RNA-binding proteins in the postnatal CNS: implications of their roles in neuronal and glial cell development. J Neurosci 17 (21), 8300-8312.

Sandberg, M., Kallstrom, M., Muhr, J., 2005. Sox21 promotes the progression of vertebrate neurogenesis. Nat Neurosci 8 (8), 995-1001.

Schagger, H., von Jagow, G., 1987. Tricine-sodium dodecyl sulfate-polyacrylamide gel electrophoresis for the separation of proteins in the range from 1 to 100 kDa. Anal Biochem 166 (2), 368-379.

Scharer, C.D., McCabe, C.D., Ali-Seyed, M., Berger, M.F., Bulyk, M.L., Moreno, C.S., 2009. Genome-wide promoter analysis of the SOX4 transcriptional network in prostate cancer cells. Cancer Res 69 (2), 709-717.

Schepers, G.E., Teasdale, R.D., Koopman, P., 2002. Twenty pairs of sox: extent, homology, and nomenclature of the mouse and human sox transcription factor gene families. Dev Cell 3 (2), 167-170.

Schilham, M.W., Moerer, P., Cumano, A., Clevers, H.C., 1997. Sox-4 facilitates thymocyte differentiation. Eur J Immunol 27 (5), 1292-1295.

Schlierf, B., Ludwig, A., Klenovsek, K., Wegner, M., 2002. Cooperative binding of Sox10 to DNA: requirements and consequences. Nucleic Acids Res 30 (24), 5509-5516.

Schmidt-Hieber, C., Jonas, P., Bischofberger, J., 2004. Enhanced synaptic plasticity in newly generated granule cells of the adult hippocampus. Nature 429 (6988), 184-187.

Schmidt, T.G., Skerra, A., 2007. The Strep-tag system for one-step purification and high-affinity detection or capturing of proteins. Nat Protoc 2 (6), 1528-1535.

Schneider, T.D., Stephens, R.M., 1990. Sequence logos: a new way to display consensus sequences. Nucleic Acids Res 18 (20), 6097-6100.

Scigelova, M., Makarov, A., 2006. Orbitrap mass analyzer--overview and applications in proteomics. Proteomics 6 Suppl 2, 16-21.

Scobie, K.N., Hall, B.J., Wilke, S.A., Klemenhagen, K.C., Fujii-Kuriyama, Y., Ghosh, A., Hen, R., Sahay, A., 2009. Kruppel-like factor 9 is necessary for late-phase neuronal maturation in the developing dentate gyrus and during adult hippocampal neurogenesis. J Neurosci 29 (31), 9875-9887.

Seki, Y., Kurisaki, A., Watanabe-Susaki, K., Nakajima, Y., Nakanishi, M., Arai, Y., Shiota, K., Sugino, H., Asashima, M., 2010. TIF1beta regulates the pluripotency of embryonic stem cells in a phosphorylation-dependent manner. Proc Natl Acad Sci U S A 107 (24), 10926-10931.

Senthilkumar, R., Mishra, R.K., 2009. Novel motifs distinguish multiple homologues of Polycomb in vertebrates: expansion and diversification of the epigenetic toolkit. Bmc Genomics 10.

Seo, S., Lim, J.W., Yellajoshyula, D., Chang, L.W., Kroll, K.L., 2007. Neurogenin and NeuroD direct transcriptional targets and their regulatory enhancers. EMBO J 26 (24), 5093-5108.

Sepp, M., Kannike, K., Eesmaa, A., Urb, M., Timmusk, T., 2011. Functional diversity of human basic helix-loop-helix transcription factor TCF4 isoforms generated by alternative 5' exon usage and splicing. PLoS One 6 (7), e22138.

Shannon, P., Markiel, A., Ozier, O., Baliga, N.S., Wang, J.T., Ramage, D., Amin, N., Schwikowski, B., Ideker, T., 2003. Cytoscape: a software environment for integrated models of biomolecular interaction networks. Genome Res 13 (11), 2498-2504.

Shen, L., Nam, H.S., Song, P., Moore, H., Anderson, S.A., 2006. FoxG1 haploinsufficiency results in impaired neurogenesis in the postnatal hippocampus and contextual memory deficits. Hippocampus 16 (10), 875-890.

Shi, Y., Chichung Lie, D., Taupin, P., Nakashima, K., Ray, J., Yu, R.T., Gage, F.H., Evans, R.M., 2004. Expression and function of orphan nuclear receptor TLX in adult neural stem cells. Nature 427 (6969), 78-83.

Shi, Y., Lee, J.S., Galvin, K.M., 1997. Everything you have ever wanted to know about Yin Yang 1. Biochim Biophys Acta 1332 (2), F49-66.

Shi, Y., Seto, E., Chang, L.S., Shenk, T., 1991. Transcriptional repression by YY1, a human GLI-Kruppel-related protein, and relief of repression by adenovirus E1A protein. Cell 67 (2), 377-388.

Shi, Y.J., Sawada, J., Sui, G.C., Affar, E.B., Whetstine, J.R., Lan, F., Ogawa, H., Luke, M.P.S., Nakatani, Y., Shi, Y., 2003. Coordinated histone modifications mediated by a CtBP co-repressor complex. Nature 422 (6933), 735-738.

Shimozaki, K., Zhang, C.L., Suh, H., Denli, A.M., Evans, R.M., Gage, F.H., 2011. Sex determining region Y-box 2 (SOX2) regulation of nuclear receptor tailless (TLX) transcription in adult neural stem cells. J Biol Chem.

Sinner, D., Kordich, J.J., Spence, J.R., Opoka, R., Rankin, S., Lin, S.C., Jonatan, D., Zorn, A.M., Wells, J.M., 2007. Sox17 and Sox4 differentially regulate beta-catenin/T-cell factor activity and proliferation of colon carcinoma cells. Mol Cell Biol 27 (22), 7802-7815.

Skerjanc, I.S., Truong, J., Filion, P., McBurney, M.W., 1996. A splice variant of the ITF-2 transcript encodes a transcription factor that inhibits MyoD activity. J Biol Chem 271 (7), 3555-3561.

Smale, S.T., 2010. Pioneer factors in embryonic stem cells and differentiation. Curr Opin Genet Dev 20 (5), 519-526.

Smith, W.C., Harland, R.M., 1992. Expression cloning of noggin, a new dorsalizing factor localized to the Spemann organizer in Xenopus embryos. Cell 70 (5), 829-840.

Smits, P., Li, P., Mandel, J., Zhang, Z., Deng, J.M., Behringer, R.R., de Crombrugghe, B., Lefebvre, V., 2001. The transcription factors L-Sox5 and Sox6 are essential for cartilage formation. Dev Cell 1 (2), 277-290.

Sock, E., Rettig, S.D., Enderich, J., Bosl, M.R., Tamm, E.R., Wegner, M., 2004. Gene targeting reveals a widespread role for the high-mobility-group transcription factor Sox11 in tissue remodeling. Mol Cell Biol 24 (15), 6635-6644.

Son, E.Y., Ichida, J.K., Wainger, B.J., Toma, J.S., Rafuse, V.F., Woolf, C.J., Eggan, K., 2011. Conversion of mouse and human fibroblasts into functional spinal motor neurons. Cell Stem Cell 9 (3), 205-218.

Song, H., Stevens, C.F., Gage, F.H., 2002. Astroglia induce neurogenesis from adult neural stem cells. Nature 417 (6884), 39-44.

Song, M., Kojima, N., Hanamura, K., Sekino, Y., Inoue, H.K., Mikuni, M., Shirao, T., 2008. Expression of drebrin E in migrating neuroblasts in adult rat brain: coincidence between drebrin E disappearance from cell body and cessation of migration. Neuroscience 152 (3), 670-682.

Southard-Smith, E.M., Kos, L., Pavan, W.J., 1998. Sox10 mutation disrupts neural crest development in Dom Hirschsprung mouse model. Nat Genet 18 (1), 60-64.

Spalding, K.L., Bergmann, O., Alkass, K., Bernard, S., Salehpour, M., Huttner, H.B., Bostrom, E., Westerlund, I., Vial, C., Buchholz, B.A., Possnert, G., Mash, D.C., Druid, H., Frisen, J., 2013. Dynamics of hippocampal neurogenesis in adult humans. Cell 153 (6), 1219-1227.

Sripathy, S.P., Stevens, J., Schultz, D.C., 2006. The KAP1 corepressor functions to coordinate the assembly of de novo HP1-demarcated microenvironments of heterochromatin required for KRAB zinc finger protein-mediated transcriptional repression. Mol Cell Biol 26 (22), 8623-8638.

Starr, D.A., Fridolfsson, H.N., 2010. Interactions between nuclei and the cytoskeleton are mediated by SUN-KASH nuclear-envelope bridges. Annu Rev Cell Dev Biol 26, 421-444.

Stefansson, H., Ophoff, R.A., Steinberg, S., Andreassen, O.A., Cichon, S., Rujescu, D., Werge, T., Pietilainen, O.P., Mors, O., Mortensen, P.B., Sigurdsson, E., Gustafsson, O., Nyegaard, M., Tuulio-Henriksson, A., Ingason, A., Hansen, T., Suvisaari, J., Lonnqvist, J., Paunio, T., Borglum, A.D., Hartmann, A., Fink-Jensen, A., Nordentoft, M., Hougaard, D., Norgaard-Pedersen, B., Bottcher, Y., Olesen, J., Breuer, R., Moller, H.J., Giegling, I., Rasmussen, H.B., Timm, S., Mattheisen, M., Bitter, I., Rethelyi, J.M., Magnusdottir, B.B., Sigmundsson, T., Olason, P., Masson, G., Gulcher, J.R., Haraldsson, M., Fossdal, R., Thorgeirsson, T.E., Thorsteinsdottir, U., Ruggeri, M., Tosato, S., Franke, B., Strengman, E., Kiemeney, L.A., Genetic, R., Outcome in, P., Melle, I., Djurovic, S., Abramova, L., Kaleda, V., Sanjuan, J., de Frutos, R., Bramon, E., Vassos, E., Fraser, G., Ettinger, U., Picchioni, M., Walker, N., Toulopoulou, T., Need, A.C., Ge, D., Yoon, J.L., Shianna, K.V., Freimer, N.B., Cantor, R.M., Murray, R., Kong, A., Golimbet, V., Carracedo, A., Arango, C., Costas, J., Jonsson, E.G., Terenius, L., Agartz, I., Petursson, H., Nothen, M.M., Rietschel, M., Matthews, P.M., Muglia, P., Peltonen, L., St Clair, D., Goldstein, D.B., Stefansson, K., Collier, D.A., 2009. Common variants conferring risk of schizophrenia. Nature 460 (7256), 744-747.

Steinberg, S., de Jong, S., Irish Schizophrenia Genomics, C., Andreassen, O.A., Werge, T., Borglum, A.D., Mors, O., Mortensen, P.B., Gustafsson, O., Costas, J., Pietilainen, O.P., Demontis, D., Papiol, S., Huttenlocher, J., Mattheisen, M., Breuer, R., Vassos, E., Giegling, I., Fraser, G., Walker, N., Tuulio-Henriksson, A., Suvisaari, J., Lonnqvist, J., Paunio, T., Agartz, I., Melle, I., Djurovic, S., Strengman, E., Group, Jurgens, G., Glenthoj, B., Terenius, L., Hougaard, D.M., Orntoft, T., Wiuf, C., Didriksen, M., Hollegaard, M.V., Nordentoft, M., van Winkel, R., Kenis, G., Abramova, L., Kaleda, V., Arrojo, M., Sanjuan, J., Arango, C., Sperling, S., Rossner, M., Ribolsi, M., Magni, V., Siracusano, A., Christiansen, C., Kiemeney, L.A., Veldink, J., van den Berg, L., Ingason, A., Muglia, P., Murray, R., Nothen, M.M., Sigurdsson, E., Petursson, H., Thorsteinsdottir, U., Kong, A., Rubino, I.A., De Hert, M., Rethelyi, J.M., Bitter, I., Jonsson, E.G., Golimbet, V., Carracedo, A., Ehrenreich, H., Craddock, N., Owen, M.J., O'Donovan, M.C., Wellcome Trust Case Control, C., Ruggeri, M.,

Tosato, S., Peltonen, L., Ophoff, R.A., Collier, D.A., St Clair, D., Rietschel, M., Cichon, S., Stefansson, H., Rujescu, D., Stefansson, K., 2011. Common variants at VRK2 and TCF4 conferring risk of schizophrenia. Hum Mol Genet 20 (20), 4076-4081.

Steiner, B., Klempin, F., Wang, L., Kott, M., Kettenmann, H., Kempermann, G., 2006. Type-2 cells as link between glial and neuronal lineage in adult hippocampal neurogenesis. Glia 54 (8), 805-814.

Sugathan, A., Biagioli, M., Golzio, C., Erdin, S., Blumenthal, I., Manavalan, P., Ragavendran, A., Brand, H., Lucente, D., Miles, J., Sheridan, S.D., Stortchevoi, A., Kellis, M., Haggarty, S.J., Katsanis, N., Gusella, J.F., Talkowski, M.E., 2014. CHD8 regulates neurodevelopmental pathways associated with autism spectrum disorder in neural progenitors. Proc Natl Acad Sci U S A.

Suh, H., Consiglio, A., Ray, J., Sawai, T., D'Amour, K.A., Gage, F.H., 2007. In vivo fate analysis reveals the multipotent and self-renewal capacities of Sox2+ neural stem cells in the adult hippocampus. Cell Stem Cell 1 (5), 515-528.

Sun, B., Halabisky, B., Zhou, Y., Palop, J.J., Yu, G., Mucke, L., Gan, L., 2009. Imbalance between GABAergic and Glutamatergic Transmission Impairs Adult Neurogenesis in an Animal Model of Alzheimer's Disease. Cell Stem Cell 5 (6), 624-633.

Sun, J., Sun, J., Ming, G.L., Song, H., 2011. Epigenetic regulation of neurogenesis in the adult mammalian brain. Eur J Neurosci 33 (6), 1087-1093.

Szulwach, K.E., Li, X.K., Smrt, R.D., Li, Y.J., Luo, Y.P., Lin, L., Santistevan, N.J., Li, W.D., Zhao, X.Y., Jin, P., 2010. Cross talk between microRNA and epigenetic regulation in adult neurogenesis. Journal of Cell Biology 189 (1), 127-U181.

Takahashi, K., Yamanaka, S., 2006. Induction of pluripotent stem cells from mouse embryonic and adult fibroblast cultures by defined factors. Cell 126 (4), 663-676.

Takano, K., Tan, W.H., Irons, M.B., Jones, J.R., Schwartz, C.E., 2011. Pitt-Hopkins syndrome should be in the differential diagnosis for males presenting with an ATR-X phenotype. Clin Genet 80 (6), 600-601.

Takemoto, T., Uchikawa, M., Yoshida, M., Bell, D.M., Lovell-Badge, R., Papaioannou, V.E., Kondoh, H., 2011. Tbx6-dependent Sox2 regulation determines neural or mesodermal fate in axial stem cells. Nature 470 (7334), 394-398.

Taranova, O.V., Magness, S.T., Fagan, B.M., Wu, Y., Surzenko, N., Hutton, S.R., Pevny, L.H., 2006. SOX2 is a dose-dependent regulator of retinal neural progenitor competence. Genes Dev 20 (9), 1187-1202.

Tashiro, A., Makino, H., Gage, F.H., 2007. Experience-specific functional modification of the dentate gyrus through adult neurogenesis: a critical period during an immature stage. J Neurosci 27 (12), 3252-3259.

Taylor, S.M., Jones, P.A., 1979. Multiple new phenotypes induced in 10T1/2 and 3T3 cells treated with 5-azacytidine. Cell 17 (4), 771-779.

Thein, D.C., Thalhammer, J.M., Hartwig, A.C., Crenshaw, E.B., 3rd, Lefebvre, V., Wegner, M., Sock, E., 2010. The closely related transcription factors Sox4 and Sox11 function as survival factors during spinal cord development. J Neurochem 115 (1), 131-141.

Thomson, M., Liu, S.J., Zou, L.N., Smith, Z., Meissner, A., Ramanathan, S., 2011. Pluripotency factors in embryonic stem cells regulate differentiation into germ layers. Cell 145 (6), 875-889.

Thored, P., Wood, J., Arvidsson, A., Cammenga, J., Kokaia, Z., Lindvall, O., 2007. Long-term neuroblast migration along blood vessels in an area with transient angiogenesis and increased vascularization after stroke. Stroke 38 (11), 3032-3039.

Torper, O., Pfisterer, U., Wolf, D.A., Pereira, M., Lau, S., Jakobsson, J., Bjorklund, A., Grealish, S., Parmar, M., 2013. Generation of induced neurons via direct conversion in vivo. Proc Natl Acad Sci U S A 110 (17), 7038-7043.

Towbin, H., Staehelin, T., Gordon, J., 1979. Electrophoretic transfer of proteins from polyacrylamide gels to nitrocellulose sheets: procedure and some applications. Proc Natl Acad Sci U S A 76 (9), 4350-4354.

Tozuka, Y., Fukuda, S., Namba, T., Seki, T., Hisatsune, T., 2005. GABAergic excitation promotes neuronal differentiation in adult hippocampal progenitor cells. Neuron 47 (6), 803-815.

Tsai, R.Y., Reed, R.R., 1997. Cloning and functional characterization of Roaz, a zinc finger protein that interacts with O/E-1 to regulate gene expression: implications for olfactory neuronal development. J Neurosci 17 (11), 4159-4169.

Tsarovina, K., Schellenberger, J., Schneider, C., Rohrer, H., 2008. Progenitor cell maintenance and neurogenesis in sympathetic ganglia involves Notch signaling. Mol Cell Neurosci 37 (1), 20-31.

Tsurusaki, Y., Koshimizu, E., Ohashi, H., Phadke, S., Kou, I., Shiina, M., Suzuki, T., Okamoto, N., Imamura, S., Yamashita, M., Watanabe, S., Yoshiura, K., Kodera, H., Miyatake, S., Nakashima, M., Saitsu, H., Ogata, K., Ikegawa, S., Miyake, N., Matsumoto, N., 2014. De novo SOX11 mutations cause Coffin-Siris syndrome. Nat Commun 5, 4011.

Tyanova, S., Mann, M., Cox, J., 2014. MaxQuant for In-Depth Analysis of Large SILAC Datasets. Methods Mol Biol 1188, 351-364.

Ueda, J., Tachibana, M., Ikura, T., Shinkai, Y., 2006. Zinc finger protein Wiz links G9a/GLP histone methyltransferases to the co-repressor molecule CtBP. J Biol Chem 281 (29), 20120-20128.

Uhlen, M., Oksvold, P., Fagerberg, L., Lundberg, E., Jonasson, K., Forsberg, M., Zwahlen, M., Kampf, C., Wester, K., Hober, S., Wernerus, H., Bjorling, L., Ponten, F., 2010. Towards a knowledge-based Human Protein Atlas. Nat Biotechnol 28 (12), 1248-1250.

Urbanek, P., Wang, Z.Q., Fetka, I., Wagner, E.F., Busslinger, M., 1994. Complete block of early B cell differentiation and altered patterning of the posterior midbrain in mice lacking Pax5/BSAP. Cell 79 (5), 901-912.

Urrutia, R., 2003. KRAB-containing zinc-finger repressor proteins. Genome Biol 4 (10), 231.

Uy, B.R., Simoes-Costa, M., Koo, D.E., Sauka-Spengler, T., Bronner, M.E., 2014. Evolutionarily conserved role for SoxC genes in neural crest specification and neuronal differentiation. Dev Biol.

van de Wetering, M., Clevers, H., 1992. Sequence-specific interaction of the HMG box proteins TCF-1 and SRY occurs within the minor groove of a Watson-Crick double helix. EMBO J 11 (8), 3039-3044.

van Praag, H., Kempermann, G., Gage, F.H., 1999. Running increases cell proliferation and neurogenesis in the adult mouse dentate gyrus. Nat Neurosci 2 (3), 266-270.

Verret, L., Jankowsky, J.L., Xu, G.M., Borchelt, D.R., Rampon, C., 2007. Alzheimer's-type amyloidosis in transgenic mice impairs survival of newborn neurons derived from adult hippocampal neurogenesis. J Neurosci 27 (25), 6771-6780.

Vicart, A., Lefebvre, T., Imbert, J., Fernandez, A., Kahn-Perles, B., 2006. Increased chromatin association of Sp1 in interphase cells by PP2A-mediated dephosphorylations. J Mol Biol 364 (5), 897-908.

Videbech, P., Ravnkilde, B., 2004. Hippocampal volume and depression: a meta-analysis of MRI studies. Am J Psychiatry 161 (11), 1957-1966.

Vierbuchen, T., Ostermeier, A., Pang, Z.P., Kokubu, Y., Sudhof, T.C., Wernig, M., 2010. Direct conversion of fibroblasts to functional neurons by defined factors. Nature 463 (7284), 1035-1041.

Vissers, L.E., van Ravenswaaij, C.M., Admiraal, R., Hurst, J.A., de Vries, B.B., Janssen, I.M., van der Vliet, W.A., Huys, E.H., de Jong, P.J., Hamel, B.C., Schoenmakers, E.F., Brunner, H.G., Veltman, J.A., van Kessel, A.G., 2004. Mutations in a new member of the chromodomain gene family cause CHARGE syndrome. Nat Genet 36 (9), 955-957.

Wagner, T., Wirth, J., Meyer, J., Zabel, B., Held, M., Zimmer, J., Pasantes, J., Bricarelli, F.D., Keutel, J., Hustert, E., Wolf, U., Tommerup, N., Schempp, W., Scherer, G., 1994. Autosomal sex reversal and campomelic dysplasia are caused by mutations in and around the SRY-related gene SOX9. Cell 79 (6), 1111-1120.

Walter, C., Murphy, B.L., Pun, R.Y., Spieles-Engemann, A.L., Danzer, S.C., 2007. Pilocarpine-induced seizures cause selective time-dependent changes to adult-generated hippocampal dentate granule cells. J Neurosci 27 (28), 7541-7552.

Wang, H., Wang, L., Erdjument-Bromage, H., Vidal, M., Tempst, P., Jones, R.S., Zhang, Y., 2004. Role of histone H2A ubiquitination in Polycomb silencing. Nature 431 (7010), 873-878.

Wang, J., Rao, S., Chu, J., Shen, X., Levasseur, D.N., Theunissen, T.W., Orkin, S.H., 2006. A protein interaction network for pluripotency of embryonic stem cells. Nature 444 (7117), 364-368.

Wang, M.M., Reed, R.R., 1993. Molecular cloning of the olfactory neuronal transcription factor Olf-1 by genetic selection in yeast. Nature 364 (6433), 121-126.

Wang, N., Tytell, J.D., Ingber, D.E., 2009. Mechanotransduction at a distance: mechanically coupling the extracellular matrix with the nucleus. Nat Rev Mol Cell Biol 10 (1), 75-82.

Wang, S.S., Tsai, R.Y., Reed, R.R., 1997. The characterization of the Olf-1/EBF-like HLH transcription factor family: implications in olfactory gene regulation and neuronal development. J Neurosci 17 (11), 4149-4158.

Wang, T.W., Stromberg, G.P., Whitney, J.T., Brower, N.W., Klymkowsky, M.W., Parent, J.M., 2006. Sox3 expression identifies neural progenitors in persistent neonatal and adult mouse forebrain germinative zones. J Comp Neurol 497 (1), 88-100.

Wang, X., Bjorklund, S., Wasik, A.M., Grandien, A., Andersson, P., Kimby, E., Dahlman-Wright, K., Zhao, C., Christensson, B., Sander, B., 2010. Gene expression profiling and chromatin immunoprecipitation identify DBN1, SETMAR and HIG2 as direct targets of SOX11 in mantle cell lymphoma. PLoS One 5 (11), e14085.

Wang, X., Lu, Z., Gomez, A., Hon, G.C., Yue, Y., Han, D., Fu, Y., Parisien, M., Dai, Q., Jia, G., Ren, B., Pan, T., He, C., 2014. N6-methyladenosine-dependent regulation of messenger RNA stability. Nature 505 (7481), 117-120.

Wang, Z., Oron, E., Nelson, B., Razis, S., Ivanova, N., 2012. Distinct lineage specification roles for NANOG, OCT4, and SOX2 in human embryonic stem cells. Cell Stem Cell 10 (4), 440-454.

Wang, Z.X., Teh, C.H.L., Chan, C.M.Y., Chu, C., Rossbach, M., Kunarso, G., Allapitchay, T.B., Wong, K.Y., Stanton, L.W., 2008. The Transcription Factor Zfp281 Controls Embryonic Stem Cell Pluripotency by Direct Activation and Repression of Target Genes. Stem Cells 26 (11), 2791-2799.

Wegner, M., 1999. From head to toes: the multiple facets of Sox proteins. Nucleic Acids Res 27 (6), 1409-1420.

Wessel, D., Flugge, U.I., 1984. A method for the quantitative recovery of protein in dilute solution in the presence of detergents and lipids. Anal Biochem 138 (1), 141-143.

Wildner, H., Gierl, M.S., Strehle, M., Pla, P., Birchmeier, C., 2008. Insm1 (IA-1) is a crucial component of the transcriptional network that controls differentiation of the sympatho-adrenal lineage. Development 135 (3), 473-481.

Wilmsdorff, M.V., Blaich, C., Zink, M., Treutlein, J., Bauer, M., Schulze, T., Schneider-Axmann, T., Gruber, O., Rietschel, M., Schmitt, A., Falkai, P., 2013. Gene expression of glutamate transporters SLC1A1, SLC1A3 and SLC1A6 in the cerebellar subregions of elderly schizophrenia patients and effects of antipsychotic treatment. World J Biol Psychiatry 14 (7), 490-499.

Wilson, K.L., Berk, J.M., 2010. The nuclear envelope at a glance. J Cell Sci 123 (Pt 12), 1973-1978.

Winner, B., Rockenstein, E., Lie, D.C., Aigner, R., Mante, M., Bogdahn, U., Couillard-Despres, S., Masliah, E., Winkler, J., 2008. Mutant alpha-synuclein exacerbates age-related decrease of neurogenesis. Neurobiol Aging 29 (6), 913-925.

Wotton, D., Merrill, J.C., 2007. Pc2 and SUMOylation. Biochem Soc Trans 35 (Pt 6), 1401-1404.

Wu, W., Wong, K., Chen, J., Jiang, Z., Dupuis, S., Wu, J.Y., Rao, Y., 1999. Directional guidance of neuronal migration in the olfactory system by the protein Slit. Nature 400 (6742), 331-336.

Xie, H., Ye, M., Feng, R., Graf, T., 2004. Stepwise reprogramming of B cells into macrophages. Cell 117 (5), 663-676.

Xue, Y., Ouyang, K., Huang, J., Zhou, Y., Ouyang, H., Li, H., Wang, G., Wu, Q., Wei, C., Bi, Y., Jiang, L., Cai, Z., Sun, H., Zhang, K., Zhang, Y., Chen, J., Fu, X.D., 2013. Direct conversion of fibroblasts to neurons by reprogramming PTB-regulated microRNA circuits. Cell 152 (1-2), 82-96.

Yamamizu, K., Schlessinger, D., Ko, M.S., 2014. SOX9 accelerates ESC differentiation to three germ layer lineages by repressing SOX2 expression through P21 (WAF1/CIP1). Development 141 (22), 4254-4266.

Yang, P., Wang, Y.X., Chen, J.Y., Li, H., Kang, L., Zhang, Y., Chen, S., Zhu, B., Gao, S.R., 2011. RCOR2 Is a Subunit of the LSD1 Complex That Regulates ESC Property and Substitutes for SOX2 in Reprogramming Somatic Cells to Pluripotency. Stem Cells 29 (5), 791-801.

Yang, W.M., Inouye, C., Zeng, Y., Bearss, D., Seto, E., 1996. Transcriptional repression by YY1 is mediated by interaction with a mammalian homolog of

the yeast global regulator RPD3. Proc Natl Acad Sci U S A 93 (23), 12845-12850.

Yang, X., Su, K., Roos, M.D., Chang, Q., Paterson, A.J., Kudlow, J.E., 2001. O-linkage of N-acetylglucosamine to Sp1 activation domain inhibits its transcriptional capability. Proc Natl Acad Sci U S A 98 (12), 6611-6616.

Yates, J.R., Cociorva, D., Liao, L.J., Zabrouskov, V., 2006. Performance of a linear ion trap-orbitrap hybrid for peptide analysis. Analytical Chemistry 78 (2), 493-500.

Yates, J.R., Ruse, C.I., Nakorchevsky, A., 2009. Proteomics by mass spectrometry: approaches, advances, and applications. Annu Rev Biomed Eng 11, 49-79.

Yi, Z., Cohen-Barak, O., Hagiwara, N., Kingsley, P.D., Fuchs, D.A., Erickson, D.T., Epner, E.M., Palis, J., Brilliant, M.H., 2006. Sox6 directly silences epsilon globin expression in definitive erythropoiesis. PLoS Genet 2 (2), e14.

Yocum, A.K., Chinnaiyan, A.M., 2009. Current affairs in quantitative targeted proteomics: multiple reaction monitoring-mass spectrometry. Brief Funct Genomic Proteomic 8 (2), 145-157.

Yoo, A.S., Sun, A.X., Li, L., Shcheglovitov, A., Portmann, T., Li, Y., Lee-Messer, C., Dolmetsch, R.E., Tsien, R.W., Crabtree, G.R., 2011. MicroRNA-mediated conversion of human fibroblasts to neurons. Nature 476 (7359), 228-231.

Yoo, J., Jeong, M.J., Lee, S.S., Lee, K.I., Kwon, B.M., Park, Y.M., Han, M.Y., 2001. Negative regulation of YY1 transcription factor on the dynamin I gene promoter. Biochem Biophys Res Commun 283 (2), 340-343.

Yu, Y.Q., Gilar, M., Lee, P.J., Bouvier, E.S., Gebler, J.C., 2003. Enzyme-friendly, mass spectrometry-compatible surfactant for in-solution enzymatic digestion of proteins. Anal Chem 75 (21), 6023-6028.

Zhang, Y., Liao, M., Dufau, M.L., 2006. Phosphatidylinositol 3-kinase/protein kinase Czeta-induced phosphorylation of Sp1 and p107 repressor release have a critical role in histone deacetylase inhibitor-mediated derepression [corrected] of transcription of the luteinizing hormone receptor gene. Mol Cell Biol 26 (18), 6748-6761.

Zhao, C., Deng, W., Gage, F.H., 2008. Mechanisms and functional implications of adult neurogenesis. Cell 132 (4), 645-660.

Zhao, C., Teng, E.M., Summers, R.G., Jr., Ming, G.L., Gage, F.H., 2006. Distinct morphological stages of dentate granule neuron maturation in the adult mouse hippocampus. J Neurosci 26 (1), 3-11.

Zhao, M., Li, D., Shimazu, K., Zhou, Y.X., Lu, B., Deng, C.X., 2007. Fibroblast growth factor receptor-1 is required for long-term potentiation, memory consolidation, and neurogenesis. Biol Psychiatry 62 (5), 381-390.

Zhao, S., Chai, X., Frotscher, M., 2007. Balance between neurogenesis and gliogenesis in the adult hippocampus: role for reelin. Dev Neurosci 29 (1-2), 84-90.

Ziv, Y., Bielopolski, D., Galanty, Y., Lukas, C., Taya, Y., Schultz, D.C., Lukas, J., Bekker-Jensen, S., Bartek, J., Shiloh, Y., 2006. Chromatin relaxation in response to DNA double-strand breaks is modulated by a novel ATM- and KAP-1 dependent pathway. Nat Cell Biol 8 (8), 870-876.

Zweier, C., Peippo, M.M., Hoyer, J., Sousa, S., Bottani, A., Clayton-Smith, J., Reardon, W., Saraiva, J., Cabral, A., Gohring, I., Devriendt, K., de Ravel, T., Bijlsma, E.K., Hennekam, R.C., Orrico, A., Cohen, M., Dreweke, A., Reis, A., Nurnberg, P., Rauch, A., 2007. Haploinsufficiency of TCF4 causes syndromal

mental retardation with intermittent hyperventilation (Pitt-Hopkins syndrome). Am J Hum Genet 80 (5), 994-1001.

7. Annex

Table 20: Significant SOX11 interactors

Accession number	Gene names	Unique peptides	Ratio H/L	Ratio forward	Ratio reverse	Significance A	Significance B
Q7M6Y2	Sox11	14	21.30	35.56	0.14	3.97E-07	2.86E-07
Q64364	Cdkn2a	4	18.53	15.17	0.03	1.28E-06	1.07E-06
Q8CDM1	Atad2	33	11.37	11.46	0.16	5.12E-05	3.81E-05
Q9DBY5	Cbx6	2	9.82	13.68	0.17	0.0001	0.0001
Q8BU00	Ikzf5	2	8.43	15.23	0.61	0.0004	0.0003
A2BE28	Las1l	16	8.23	6.80	0.10	0.0004	0.0003
Q9EP97	Senp3	13	6.56	5.60	0.13	0.0015	0.0012
Q8BP92	Rcn2	12	6.54	5.41	0.13	0.0015	0.0012
Q9DBD5	Pelp1	16	6.41	5.38	0.13	0.0017	0.0013
Q8BGS3	Zkscan1	3	6.33	11.64	0.38	0.0018	0.0018
Q99J95	Cdk9	11	6.05	3.89	0.14	0.0023	0.0018
Q00899	Yy1	8	5.91	6.97	0.21	0.0026	0.0026
Q62318	Trim28	27	5.66	5.95	0.19	0.0033	0.0026
Q8R409	Hexim1	6	5.58	5.58	0.64	0.0035	0.0035
Q4VBE8	Wdr18	11	5.37	5.89	0.21	0.0043	0.0034
E9Q414	Apob	2	5.17	0.51	0.12	0.0052	0.0051
Q8BGS1	Epb41l5	13	5.13	5.91	0.23	0.0054	0.0043
Q3TZX8	Nol9	10	5.03	6.06	0.24	0.0059	0.0046
Q8BIE6	Frmd4a	11	5.03	7.47	0.20	0.0059	0.0047
Q7TSY8	Sgol2	25	4.83	6.54	0.21	0.0071	0.0057
Q9QWV9	Ccnt1	18	4.75	4.23	0.19	0.0077	0.0061
Q62511	Zfp91	10	4.73	4.73	0.25	0.0078	0.0062
Q69Z99	Znf512	13	4.68	5.94	0.29	0.0083	0.0066
Q9DBR0	Akap8	14	4.60	5.09	0.24	0.0089	0.0071
Q8VE92	Rbm4b;Rbm4	4	4.59	3.90	0.22	0.0090	0.0089
P55200	Kmt2a	5	4.51	4.76	0.37	0.0098	0.0097
Q3URQ0	Tex10	14	4.51	5.18	0.30	0.0098	0.0078
P52651	Rhox5	5	4.40	3.56	0.23	0.0109	0.0108
Q0P678	Zc3h18	10	4.29	4.53	0.25	0.0122	0.0098
Q99LI5	Znf281	9	4.21	5.36	0.26	0.0131	0.0130
Q9D0E1	Hnrnpm	34	4.17	3.15	0.19	0.0137	0.0110
Q61039	Hand2	2	3.99	3.99	0.39	0.0166	0.0167
Q8K3A9	Mepce	8	3.96	4.39	0.34	0.0171	0.0170
Q9DB96	Ngdn	3	3.91	4.21	0.31	0.0180	0.0180
Q9JKX4	Aatf	7	3.88	3.19	0.22	0.0185	0.0185
Q7TSZ8	Nacc1	2	3.86	4.13	0.26	0.0189	0.0191
Q811S7	Ubp1	4	3.84	3.87	0.27	0.0193	0.0195
Q99K28	Arfgap2	7	3.76	5.36	0.31	0.0212	0.0212
Q60722	Tcf4	3	3.75	4.30	0.31	0.0212	0.0212

Q9Z148	Ehmt2	12	3.72	4.25	0.31	0.0219	0.0178
Q9D8S3	Arfgap3	9	3.70	4.84	0.29	0.0226	0.0226
Q8CJ27	Aspm	34	3.64	3.36	0.18	0.0239	0.0195
Q5DW34	Ehmt1	15	3.60	4.02	0.32	0.0252	0.0206
Q8C2Q3	Rbm14	12	3.59	3.80	0.29	0.0253	0.0206
Q9R0L7	Akap8l	2	3.53	3.53	1.11	0.0271	0.0276
Q09XV5	Chd8	7	3.52	3.68	0.42	0.0274	0.0275
Q9QWH1	Phc2	2	3.51	3.51	0.34	0.0276	0.0281
Q9CQJ4	Rnf2	10	3.49	4.04	0.34	0.0284	0.0233
Q9CXS4	Cenpv	4	3.48	3.56	0.75	0.0286	0.0292
Q9QX47	Son	7	3.46	3.46	0.27	0.0291	0.0292
O35690	Phox2b	4	3.46	5.03	0.43	0.0292	0.0240
Q5SS00	Zdbf2	7	3.45	4.83	0.48	0.0295	0.0301
Q99JY0	Hadhb	4	3.44	3.87	0.54	0.0299	0.0300
Q8BP71	Rbfox2;Rbfox1	4	3.36	3.92	0.36	0.0327	0.0329
Q8C966	Phf21b	3	3.35	3.64	0.33	0.0330	0.0337
P61290	Psme3	8	3.32	3.49	0.31	0.0343	0.0345
Q9DCA5	Brix1	2	3.27	3.89	0.38	0.0359	0.0368
Q9QXV1	Cbx8	2	3.27	3.39	0.65	0.0361	0.0370
O70503	Hsd17b12	5	3.23	3.37	0.46	0.0378	0.0381
O08967	Cyth3	3	3.22	2.89	0.28	0.0381	0.0391
Q7TN98	Cpeb4	2	3.19	3.19	0.39	0.0395	0.0398
O08750	Nfil3	3	3.19	5.05	0.71	0.0396	0.0407
Q91VN1	Znf24	2	3.16	3.00	0.30	0.0409	0.0420
Q9ESV0	Ddx24	6	3.15	3.15	0.39	0.0412	0.0416
Q91YN9	Bag2	6	3.15	3.15	0.63	0.0416	0.0420
O35615	Zfpm1	11	3.10	4.13	1.37	0.0436	0.0440
Q80TP3	Ubr5	7	3.05	4.57	0.43	0.0463	0.0476
Q04692	Smarcad1	7	2.99	2.99	0.34	0.0495	0.0500
Q05CL8	Larp7	13	2.99	2.33	0.28	0.0499	0.0415
Q80YV3	Trrap	13	2.97	3.28	0.44	0.0510	0.0515
Q9R0G7	Zeb2	11	2.93	2.93	0.29	0.0531	0.0538
Q99KN9	Clint1	5	2.92	3.20	0.52	0.0542	0.0549
O55187	Cbx4	8	2.89	4.61	0.41	0.0559	0.0566
Q3URU2	Peg3	15	2.88	4.02	0.37	0.0563	0.0569
O89090	Sp1	2	2.87	2.92	0.38	0.0574	0.0581
Q99KX1	Mlf2	2	2.86	3.10	0.43	0.0577	0.0596
Q9DBC7	Prkar1a	6	2.81	2.31	0.34	0.0611	0.0619
Q8K4L0	Ddx54	10	2.80	2.87	0.37	0.0621	0.0630
Q99L90	Mcrs1	2	2.78	1.14	0.23	0.0636	0.0658
Q9D6Z1	Nop56	21	2.77	2.62	0.34	0.0643	0.0539
P48377	Rfx1	2	2.77	4.45	0.46	0.0644	0.0667
Q08369	Gata4	2	2.75	2.75	0.36	0.0657	0.0680
P10922	H1f0	3	2.72	2.72	0.35	0.0679	0.0703

Q5DTW2	Sfmbt2	6	2.71	3.34	0.38	0.0689	0.0699
Q9QYH6	Maged1	2	2.71	3.47	0.37	0.0689	0.0714
Q9EST3	Eif4enif1	5	2.71	5.33	0.56	0.0691	0.0716
Q9DBE9	Ftsj3	3	2.70	3.51	0.50	0.0700	0.0726
Q6DFW4	Nop58	15	2.68	2.58	0.36	0.0716	0.0602
P30658	Cbx2	2	2.64	1.39	0.26	0.0755	0.0783
Q8VBW5	Bbx	5	2.63	4.35	0.42	0.0756	0.0767
Q922K7	Nop2	7	2.63	3.42	0.38	0.0759	0.0771
O35387	Hax1	2	2.63	2.16	0.38	0.0762	0.0790
O88286	Wiz	15	2.61	2.84	0.42	0.0774	0.0653
Q8CFC2	Myt1	7	2.59	4.46	0.41	0.0795	0.0808
Q9CXK8	Nip7	2	2.58	3.04	0.44	0.0805	0.0835
Q9Z2X1	Hnrnpf	13	2.56	3.01	0.53	0.0826	0.0698
O35887	Calu	11	2.55	2.91	0.46	0.0832	0.0703
P97376	Frg1	8	2.54	2.30	0.38	0.0850	0.0864
Q05186	Rcn1	2	2.54	2.54	0.41	0.0851	0.0884
Q61624	Znf148	6	2.53	2.19	0.35	0.0852	0.0866
Q80TE4	Sipa1l2	14	2.53	2.57	0.40	0.0856	0.0724
Q9CYH6	Rrs1	2	2.50	2.55	0.45	0.0884	0.0919
Q8CGC6	Rbm28	3	2.50	3.27	0.51	0.0884	0.0919
Q9WV92	Epb41l3	2	2.47	1.69	0.31	0.0917	0.0953
A2AJI0	Map7d1	7	2.47	2.47	0.41	0.0926	0.0942
Q5U4C1	Gprasp1	4	2.45	2.45	0.49	0.0944	0.0983
O88291	Znf326	6	2.45	2.26	0.41	0.0949	0.0966
Q6A065	Cep170	17	2.44	2.56	0.43	0.0958	0.0814
Q8C8U0	Ppfibp1	3	2.41	2.83	0.50	0.0991	0.1032
G5E8K5	Ank3	4	2.38	2.95	0.76	0.1033	0.1076
Q99NH0	Ankrd17	8	2.35	2.35	0.54	0.1061	0.1081
Q8BJ90	Znf771	2	2.35	2.82	0.53	0.1067	0.1112
P99024	Tubb5	3	2.35	3.11	0.47	0.1070	0.0912
P68372	Tubb4b;Tubb4a	4	2.35	3.03	0.52	0.1071	0.0913
Q07646	Mest	2	2.34	2.89	0.52	0.1079	0.1125
P30999	Ctnnd1	10	2.34	2.26	0.41	0.1083	0.1103
Q8CHI8	Ep400	3	2.33	1.80	0.37	0.1092	0.1139
Q91YT7	Ythdf2	8	2.33	1.76	0.39	0.1095	0.0934
Q61464	Znf638	7	2.32	2.51	0.61	0.1108	0.1129
Q61474	Msi1	5	2.32	2.39	0.47	0.1111	0.1132
Q80TS5	Znf423	4	2.31	2.53	0.69	0.1116	0.1164
Q8K363	Ddx18	12	2.31	2.37	0.44	0.1120	0.0957
Q8C854	Myef2	10	2.31	2.23	0.42	0.1121	0.0957
P43275	Hist1h1a	5	2.30	2.65	0.47	0.1129	0.0965
Q8K310	Matr3	27	2.30	2.58	0.54	0.1141	0.0975
Q80X50	Ubap2l	14	2.28	2.19	0.42	0.1170	0.1001
P48381	Rfx3	3	2.27	2.98	0.64	0.1184	0.1235
Q99MY8	Ash1l	3	2.26	2.17	0.43	0.1195	0.1247

Q3TFK5	Gpatch4	3	2.25	2.25	0.55	0.1202	0.1254
Q80Y44	Ddx10	2	2.24	3.85	1.00	0.1224	0.1278
Q3TEA8	Hp1bp3	8	2.24	2.70	0.47	0.1224	0.1248
A2RSY1	Kansl3	2	2.24	1.68	0.44	0.1227	0.1280
Q80WJ7	Mtdh	8	2.23	2.42	0.49	0.1243	0.1268
P63037	Dnaja1	10	2.22	2.12	0.43	0.1248	0.1070
Q9WTQ5	Akap12	12	2.22	2.31	0.47	0.1250	0.1275
Q99LH1	Gnl2	4	2.20	2.39	0.65	0.1280	0.1336
P35550	Fbl	9	2.20	2.19	0.45	0.1292	0.1109
Q8BHX1	Haus1	2	2.19	1.45	0.34	0.1296	0.1353
Q8BMS1	Hadha	6	2.19	4.17	0.60	0.1306	0.1332
O88712	Ctbp1	5	2.18	2.35	0.50	0.1312	0.1127
Q99M87	Dnaja3	7	2.18	3.21	0.60	0.1312	0.1339
Q91YK2	Rrp1b	4	2.15	2.15	0.75	0.1367	0.1429
Q5U4E2	Repin1	3	2.14	2.24	0.53	0.1377	0.1439
Q6PG16	Hjurp	2	2.14	3.15	0.81	0.1380	0.1442
O88700	Blm	3	2.14	1.80	0.45	0.1387	0.1449
Q8C796	Rcor2	5	2.14	2.14	0.48	0.1392	0.1420
Q5RJG1	Nol10	6	2.13	2.85	0.54	0.1406	0.1469
Q8BVE8	Whsc1	4	2.12	2.84	0.71	0.1414	0.1443
Q9QYJ0	Dnaja2	11	2.11	2.20	0.49	0.1429	0.1232
P23198	Cbx3	5	2.11	2.52	0.57	0.1437	0.1238
Q00PI9	Hnrnpul2	11	2.11	2.11	0.43	0.1444	0.1245
P25976	Ubtf	5	2.10	2.46	0.58	0.1454	0.1485
Q9JMC3	Dnaja4	2	2.10	1.80	0.42	0.1458	0.1524
P43276	Hist1h1b	10	2.10	2.33	0.57	0.1459	0.1259
Q8K224	Nat10	8	2.09	2.04	0.47	0.1465	0.1496
Q9CYA6	Zcchc8	2	2.07	1.82	0.45	0.1514	0.1584
P26645	Marcks	2	2.06	2.06	0.50	0.1525	0.1594
O54946	Dnajb6	5	2.06	2.06	0.53	0.1529	0.1561
P15864	Hist1h1c	4	2.05	2.51	0.57	0.1548	0.1339
Q9WTX8	Mad1l1	6	2.05	2.46	0.61	0.1552	0.1586
Q6NS46	Pdcd11	4	2.05	2.67	0.58	0.1553	0.1624
Q8BW10	Nob1	6	2.05	2.05	0.52	0.1556	0.1589
P60122	Ruvbl1	16	2.03	2.06	0.50	0.1583	0.1370
P29391	Ftl1;Ftl2	6	2.02	1.94	0.46	0.1610	0.1645
Q91VR2	Atp5c1	6	2.00	2.27	0.58	0.1647	0.1683

7.1. Abbreviations

aa	amino acid(s)
ADP	adenosine 5’-diphosphate
AP	affinity purification
APS	ammonium peroxodisulfate
ATP	adenosine 5’-triphosphate
B	group B homology domain
bHLH	basic helix-loop-helix
bp	base pair
BSA	bovine serum albumin
cc	coil-coil domain
cDNA	complementary DNA
CHIP	chromatin immunoprecipitation
CID	collision induced dissociation
CNS	central nervous system
co-IP	co-immunoprecipitation
Cp	crossing point
Da	dalton (molecular mass)
D	dimerisation domain
dATP	2'-deoxyadenosine 5'-triphosphate
ddH_2O	ultra-pure water
DG	dentate gyrus
dH_2O	deionised water
DMEM	Dulbecco's modified Eagle medium
DMSO	dimethylsulfoxid
DNA	deoxyribonucleic acid
dNTP	2’-deoxynucleotide 5’-triphosphate
dsDNA	double-stranded DNA
DTT	dithiothreitol
ECL	enhanced chemiluminescence
ER	endoplasmic reticulum
ES cell	embryonic stem cell
ESI	electrospray ionisation
FBS	fetal bovine serum
FT	flowthrough
GFP	green fluorescent protein
GO	gene ontology
N2A	Neuro2a
NP-40	nonident P-40
NPC	neural precursor cell
NSC	neural stem cell
nt	nucleotide(s)
OB	olfactory bulb
OD	optical density
ORF	open reading frame
P	pellet
p.a.	pro analysis (reagent-grade)
PBS	phosphate-buffered saline
PcG	polycomb
PCR	polymerase chain reaction
PEI	polyethylenimine
PNK	T4 polynucleotide kinase
PNS	peripheral nervous system
Pol II	RNA polymerase II
Pol III	RNA polymerase III
PPI	protein-protein interaction
PRC1	polycomb repressive complex 1
PRC2	polycomb repressive complex 1
PrEST	protein recombinant epitope signature tag
PVDF	polyvinylidene difluoride
R	relative expression
RMS	rostral migratory stream
RNA	ribonucleic acid
rRNA	ribosomal RNA
RT	room temperature
S	supernatant
SDS	sodium dodecyl sulfate
SDS-PAGE	SDS-polyacrylamide electrophoresis
SF-TAP	Strep/Flag tandem affinity purification
SGZ	subgranular zone
Shh	sonic hedgehog
shRNA	short hairpin RNA
SILAC	stable isotope labelling of amino acids in cell culture
SIM	selected ion monitoring
SNP	single nucleotide polymorphism

H3K27me3	H3 lysine 27 tri-methylation
H3K4me3	H3 lysine 4 tri-methylation
HCD	higher-energy collisional dissociation
HF	high fidelity
HMG box	high mobility group box
HP	hippocampal formation
HPLC	high performance liquid chromatography
HRP	horseradish peroxidase
ICM	inner cell mass
IgG	immunoglobulin G
IP	immunoprecipitation
iPS cell	induced pluripotent stem cell
K2	protein-protein interaction domain
kb	kilo base
kDa	kilo Dalton
LC-MS/MS	liquid chromatography-tandem mass spectrometry
LTQ	linear quadrupole ion trap
m/*z*	mass to charge ratio
mAb	monoclonal antibody
miRNA	microRNA
MRM	multiple reaction monitoring
mRNA	messenger RNA
MS	mass spectrometry
MS/MS	tandem MS
SOX	SRY-related HMG box
SRM	selected reaction monitoring
ssDNA	single stranded DNA
StageTips	stop and go extraction tips
SVZ	subventricular zone
TA	trans-activation domain
Taq	Thermus aquaticus
TBS	tris-buffered saline
TBS-T	TBS-Tween
TE	trophoectoderm
TEMED	N,N,N',N'-tetramethylethylene-diamine
TF	transcription factor
TFA	trifluoroacetic acid
TH	tyrosine hydroxylase
TLR	toll-like receptor
T_m	melting temperature
TR	trans-repression domain
TrxG	trithorax
U	unit (enzymatic activity)
UV	ultraviolet
v/v	volume per volume
w/v	weight per volume

Amino acids:

Alanine	A	Leucine	L
Arginine	R	Lysine	K
Asparagine	N	Methionine	M
Aspartic acid	D	Phenylalanine	F
Cysteine	C	Proline	P
Glutamic acid	E	Serine	S
Glutamine	Q	Threonine	T
Glycine	G	Tryptophan	W
Histidine	H	Tyrosine	Y
Isoleucine	I	Valine	V

Purine and pyrimidine bases:

A	adenine
C	cytosine
G	guanine
T	thymine
U	uracil

7.2. Figure Index

7.3. Table Index

7.4. Acknowledgements/Danksagung

Abschließend möchte ich mich bei allen bedanken, die mich unterstützt und zum Gelingen dieser Arbeit beigetragen haben.

An erster Stelle gilt mein Dank Dr. Johannes Gloeckner, der die Betreuung meiner Arbeit übernommen hat. Die Kombination aus häufigen Besprechungen, die mir immer neue hilfreiche Denkanstöße und Feedback gaben und gleichzeitig die Freiheit, selbstständig zu arbeiten und Probleme anzugehen, ermöglichte es mir, diese Arbeit erfolgreich durchzuführen und mir eine eigene und selbstständige Herangehensweise an wissenschaftliche Themen anzueignen. Dafür, dass er mich an seinem immensen Wissen hat teilhaben lassen und immer ein offenes Ohr für meine Probleme und Nöte hatte, möchte ich mich herzlich bedanken.

Ich bedanke mich herzlich bei Prof. Dr. Marius Ueffing für die Möglichkeit, diese Arbeit in seiner Abteilung anzufertigen, sowie für seine Tätigkeit als Prüfer und Gutachter meiner Arbeit. Seine konstruktiven Vorschläge bei meinen Vorträgen und Postern waren immer sehr hilfreich.

Prof. Dr. Olaf Rieß danke ich im Besonderen für seine Bereiterklärung, als Gutachter diese Arbeit seitens der mathematisch-naturwissenschaftlichen Fakultät zu betreuen.

Auch Prof. Dr. Chichung Lie, der als Experte der SOX11-Thematik immer ein hilfsbereiter Ansprechpartner für mich war und das Projekt durch zahlreiche konstruktive Diskussionen und Ideen entscheidend vorangebracht hat, gilt mein besonderer Dank. Außerdem möchte ich ihm und seinen Mitarbeitern für die zur Verfügung gestellten Konstrukte, Protokolle usw. danken.

Bei Prof. Dr. Hans-Georg Rammensee und JProf. Dr. Robert Lukowski bedanke ich mich herzlich für ihre Tätigkeit als Prüfer meiner Arbeit.

Dr. Andrea Meixner gilt mein besonderer Dank, da sie immer ein offenes Ohr für meine Probleme aller Art hatte und sich immer sehr engagiert hat, um diese mit mir zusammen zu lösen. Außerdem hat sie mich durch das Korrekturlesen der Arbeit besonders unterstützt. Vielen Dank für deine unermüdliche Hilfe im Labor, liebe Andrea!

Ich möchte mich auch bei Dr. Mohammed Ali Jarboui herzlich bedanken, vor allem für seine Hilfe im Erstellen und die Einführung in die Welt der Protein-Interaktions-Netzwerke, sowie das Korrekturlesen der Arbeit.

Den „Masse-Mädels“ Nicola Horn, Yasmin Wissinger, Franziska Klose und natürlich Jennifer Ott danke ich für ihren unermüdlichen Einsatz, meine Proben zu laden und sonstige Probleme bezüglich der Massenspektrometer mit mir zu lösen.

Auch Dr. Karsten Boldt danke ich für konstruktive Kritik und Vorschläge bezüglich des Projekts und Tipps für das Angehen von massenspektrometrischen Fragestellungen.

Bei Dr. Tina Beyer möchte ich mich ebenfalls für ihre Hilfestellung in der qRT-PCR Thematik bedanken und für alle anderen hilfreichen Tipps im letzten Abschnitt der Arbeit.

Zudem möchte ich mich bei allen Kollegen des medizinischen Proteomzentrums für die nette Arbeitsatmosphäre, Hilfsbereitschaft, sowie die guten Gespräche und Diskussionen bedanken.

Bei Jenni, Nicola, Yasmin und Andrea bedanke ich mich außerdem für ihre Freundschaft. Durch die angeregten Gespräche mit euch wurden zahlreiche Mittagspausen bereichert. Auch im nicht immer einfachen Laborarbeitsalltag habt ihr mich immer unterstützt und aufgebaut!

Zum Schluss möchte ich mich noch bei meinen Freunden und meiner Familie bedanken, die mich all die Jahre immer unterstützt und motiviert haben.
Besonders danke ich meinem Mann Norbert, der meine Freude geteilt, geduldig meine Launen ertragen und mich immer wieder aufgebaut und neu bestärkt hat.
Ein großes Dankeschön geht an meine Eltern, die mir das Studium ermöglicht haben, immer an mich und meine Fähigkeiten geglaubt haben und alle Höhen und Tiefen mit mir mitgemacht haben.